EXTRACTION OPTIMISATION FOR AND HYGROSCOPIC BEHAVIOUR OF FLAX FIBRES IN COMPOSITE APPLICATIONS

Kevin HENDRICKX

Supervisors:

prof. dr. ir. Jan Ivens
prof. dr. ir. Aart Willem Van Vuure
prof. dr. ir. Wim Thielemans

Members of the Examination Committee:

prof. dr. ir. Ignace Verpoest
prof. dr. ir. Toon Goedemé
prof. dr. ing. Jo Van Caneghem
prof. dr. ir. Joris Van Acker (Universiteit Gent)
dr. ir. Vincent Placet (FEMTO-ST)
ir. Jan Sijnave (Algemeen Belgisch Vlasverbond)

Dissertation presented in partial fulfilment of the requirements for the degree of Doctor of Engineering Technology

May 2019

© 2019 Kevin HENDRICKX
Uitgegeven in eigen beheer, Kevin HENDRICKX, Jan De Nayerlaan 5,
2860 Sint-Katelijne-Waver

Alle rechten voorbehouden. Niets uit deze uitgave mag worden vermenigvuldigd en/of openbaar gemaakt worden door middel van druk, fotokopie, microfilm, elektronisch of op welke andere wijze ook zonder voorafgaandelijke schriftelijke toestemming van de uitgever.

All rights reserved. No part of the publication may be reproduced in any form by print, photoprint, microfilm, electronic or any other means without written permission from the publisher.

“Books must follow sciences, and not sciences books.”
- Francis Bacon

Dankwoord

Welkom in, waarschijnlijk het enige stuk tekst in dit doctoraat dat u zal lezen, het dankwoord. Op voorhand mijn excuses voor mijn vooringenomenheid mocht dat niet zo zijn, maar het is nu eenmaal een publiek geheim dat dit het stuk is dat de meeste lezers onder ogen komt.

Jan, jij bent de eerste waartoe ik mij in dit dankwoord wil richten. Als promotor was jij een echte multitasker, waarbij je je jouw facultaire, en later campus-, verantwoordelijkheden succesvol combineerde met de begeleiding van je onderzoekers. Onze discussies hebben vaak geleid tot nieuwe ideeën, en hielpen me verder wanneer ik geen uitweg zag. Bedankt voor het vertrouwen en de vrijheid die je mij de afgelopen vier jaar hebt gegeven. Het heeft mij toegelaten om mij te ontwikkelen tot de onderzoeker die ik nu ben.

Aart en Wim, ook jullie bedankt, als co-promotoren kon ik steeds rekenen op jullie advies. Wim, eveneens bedankt voor de experimenten die ik mocht uitvoeren in Kortrijk.

De leden van mijn begeleidings- en examencommissie wil ik bedanken voor hun inbreng. Hun waardevolle inbreng heeft een belangrijke bijdrage geleverd aan de algemene kwaliteit van dit doctoraat.

Stijn, Caroline, Wim, Marnix, Bert, Pascal, Joris, Nele, Jan en Griet, bedankt dat ik met jullie 2,5 jaar mocht samenwerken in het FlaxPreComp consortium onder de vleugels van SIM. We hebben ons allen ingespannen om in een zeer korte tijd, een maximaal resultaat neer te zetten. Laten we hopen dat dit in de nabije toekomst zijn vruchten afwerpt! Het was een enorm boeiende periode waar ik met plezier op terugkijk.

Een doctoraat is gelukkig geen 4 jaar eenzame opsluiting. Het was een plezier om dit onderzoek te kunnen doen in de Composite Materials Group in MTM. Bedankt allemaal om deze periode zo boeiend te maken in alle opzichten. Het is onmogelijk om hier een exhaustieve lijst van namen in te voegen voor iedereen die op zijn manier heeft bijgedragen aan dit doctoraat. Toch licht ik er graag enkele personen uit.

Delphine jij was mijn *partner in crime* tijdens deze 4 jaar. Alles wat we realiseerden, zowel op wetenschappelijk als op minder wetenschappelijke gebied, verliep altijd vlot. Jouw optimisme en enthousiasme zal me altijd bijblijven. Ik ben fier op wat we in deze periode samen hebben gerealiseerd.

Yentl, Marina, Dieter en Gilles, bedankt voor de vele babbels in deze periode in, wat wellicht het bureau met de meeste vensters in heel MTM moet zijn. Yentl, jij was erbij vanaf het begin. Het was een voorrecht te zien hoe je grotere en kleinere doch doelgerichte stappen dichterbij je einddoel kwam; ZAP'er worden! Veel geluk tijdens je verdere carrière!

Mahoor, Farida, Katleen, Man, Jun, Yoran, Oksana, Morissa, Rafael, Francisco, Pedro, thanks for the talks and fun we had the last years during the many activities that were organized in the group.

Jana, bedankt voor de samenwerking. Om één of andere reden belandden we ook steeds op dezelfde congressen. Het was altijd aangenaam om deze met jou te beleven. Chris, bedankt om me te introduceren op campus De Nayer en de practica die ik daar mocht geven. Je hebt een grote passie voor het bijbrengen van kennis aan de studenten tijdens de practica materiaalkunde en hiervoor bewonder ik je enorm.

Aan alle administratief en technisch van het departement, bedankt om alle apparatuur steeds piekfijn in orde te houden, te helpen bij tijdrovende experimenten, lokalen te reserveren, lunch klaar te zetten en nog zoveel meer… Kris, Bart, Manuël en Marc, jullie stonden steeds klaar met technisch advies rond de vele set-ups en machines, bedankt!

Quinten en Dana, bedankt voor jullie onvoorwaardelijke vriendschap. Er zijn weinig mensen waarop je altijd kan terugvallen, maar jullie behoren tot deze selecte groep. Bedankt dat ik bij jullie mijn gedachten kon verzetten en dat ik eens niet hoefde te praten over mijn doctoraat.

Aan mijn ouders, broer en zus, bedankt voor jullie steun en bereidheid om te luisteren naar mijn verhalen. Bedankt om mij de mogelijkheid te geven om dit te kunnen doen en om mij te vormen als persoon
.
Als laatste een grote dankjewel aan Gwendolyn, mijn vrouw, mijn betere helft, de liefde van mijn leven. Vier jaar geleden zijn we samen begonnen aan dit verhaal. Een verbouwing, een huwelijk en nog heel wat avonturen later zijn we nu hier beland. Gwendolyn, ik ben blij dat ik deze reis samen met jou mocht maken. Bij jou vind ik altijd een luisterend oor, een troostende schouder of een eenvoudige lach. Ik ben gelukkig en fier dat ik jou mijn vrouw mag noemen. Op naar onze toekomst!

Kevin

Abstract

Flax fibres (*Linum Usitatissimum*) combine excellent mechanical properties with a very low density. In terms of specific stiffness they can compete with E-glass fibres. This is why they are currently used in lightweight applications such as composites. However, there are two main factors inhibiting their breakthrough in this market:

- The cost of flax fibres compared to glass fibres remains high due to the energy and labour-intensive production process of the fibres and limited fibre yield.
- Flax fibres are sensitive to moisture absorption. This makes composite producers are wary to use these fibres in their applications as they are worried about the implication of this absorption on the short- and long-term composite properties. This raises the question on the durability of these materials, especially in conditions where cyclic variations of relative humidity are expected.

This dissertation therefore aims to identify the critical parameters and fibre characteristic needed to obtain fibres which can be used in composites and reveal the effects of moisture during static and dynamic hygroscopic loading.

It was found that fibre fineness has a large influence on the transverse composite properties. In the current production process, this parameter is controlled in part by the degree of retting of the stems but largely by scutching and hackling. For coarse fibres, even a mild combing operation is sufficient to drastically increase transverse performance of the composites. The degree of retting impacts the longitudinal tensile response of the composites. A higher degree of retting lowers the modulus of the fibres, except in the initial elastic response region. The fibre variety nor the purity have a direct effect on the mechanical performance of the fibres.

In the second part of this thesis kinetic and equilibrium parameters of the moisture absorption and desorption process were collected and connected to the microstructure of the fibre and composites. It was established that the diffusion behaviour of flax fibres both *in*- and *ex*-composite was Fickian in absorption. During desorption, deviations from this behaviour were found when equilibrating to extremely low relative humidity. The diffusion coefficients were found to be dependent on the moisture concentration of the fibres. Furthermore, the longitudinal and transverse mechanical properties of flax fibre composites decrease as their moisture content increases. An exception is the longitudinal tensile strength which increases, due to the plasticizing effect of water. To link these observations to the microstructure, the fibres were chemically modified aiming at altering their moisture behaviour. From this a theory is proposed which describes the diffusion process in technical flax fibres.

Finally, the effect of hygroscopic fatigue of the composites was examined. After very few cycles, flax fibres composites show extensive debonding and technical fibre splitting. These damage modes severely impact transverse performance of the composites.

Samenvatting

Vlasvezels (*Linum Usitatissimum*) combineren uitstekende mechanische eigenschappen met een zeer lage dichtheid. In termen van specifieke stijfheid kunnen ze concurreren met E-glasvezels. Daarom worden ze momenteel gebruikt in lichtgewichttoepassingen zoals composieten. Er zijn echter twee belangrijke factoren die hun doorbraak in deze markt belemmeren:

- De kosten van vlasvezels in vergelijking met glasvezels blijven hoog vanwege het energie- en arbeidsintensieve productieproces van de vezels en de beperkte vezelopbrengst.
- Vlasvezels zijn gevoelig voor vochtopname. Hierdoor zijn producenten van composieten op hun hoede om deze vezels in hun toepassingen te gebruiken, omdat zij zich zorgen maken over de implicatie van deze absorptie voor de composieteigenschappen op korte en lange termijn. Dit stelt de duurzaamheid van deze materialen in vraag, vooral in omstandigheden waarin cyclische variaties van relatieve vochtigheid worden verwacht.

Deze dissertatie heeft daarom tot doel de kritische parameters en vezelkarakteristiek te identificeren die nodig zijn om vezels te verkrijgen die in composieten kunnen worden gebruikt. Daarnaast zullen de effecten van vocht tijdens statische en dynamische hygroscopische belasting worden onthuld.

Vezelfijnheid heeft een grote invloed heeft op de transversale composieteigenschappen. In het huidige productieproces wordt deze parameter gedeeltelijk beheerst door rotingsgraad van de stengels, maar grotendeels door zwingelen en hekelen. Voor ruwe vezels volstaat zelfs een milde kambewerking om de transversale eigenschappen van de composieten drastisch te verhogen. De rotingsgraad beïnvloedt de longitudinale trekrespons van de composieten. Een hogere rotingsgraad verlaagt de modulus van de vezels, behalve in het initiële elastische responsgebied. De vezelvariëteit noch de zuiverheid hebben een direct effect op de mechanische prestaties van de vezels.

In het tweede deel van dit proefschrift werden kinetische en evenwichtsparameters van het vochtabsorptie- en desorptieproces verzameld en verbonden met de microstructuur van de vezel en composieten. Er werd vastgesteld dat het diffusiegedrag van vlasvezels zowel *in*- als *ex*- composiet Fickiaans was. Tijdens desorptie werden afwijkingen van dit gedrag gevonden bij het equilibreren tot extreem lage relatieve vochtigheid. De diffusiecoëfficiënten blijken afhankelijk te zijn van de vochtconcentratie in de vezels. Bovendien nemen de longitudinale en transversale mechanische eigenschappen van vlasvezelcomposieten af naarmate hun vochtgehalte toeneemt. Een uitzondering hierop is de treksterkte in de lengterichting die toeneemt, vanwege het weekmakend effect van water. Om deze

waarnemingen te koppelen aan de microstructuur, werden de vezels chemisch gemodificeerd met het doel hun vochtgedrag te veranderen. Hieruit wordt een theorie voorgesteld die het diffusieproces in technische vlasvezels beschrijft.

Ten slotte werd het effect van hygroscopische vermoeiing van de composieten onderzocht. Na weinig cycli vertonen vlasvezelcomposieten reeds een uitgebreide vezel-matrixonthechting en splitsing van de technische vezels. Deze schademodi hebben een grote invloed op de transversale performantie van de composieten.

Table of Contents

Dankwoord i

Abstract iii

Samenvatting v

Table of Contents vii

List of Figures x

List of Tables xiv

Chapter 1 General context 3

Chapter 2 Introduction 9

2.1. Microstructure of flax straw and fibres 9

2.2. Extraction of flax fibres 10

2.3. Moisture in flax fibres and their composites 14

2.4. Conclusion 17

Chapter 3 Problem statement 23

3.1. Main objectives and hypothesis 23

3.2. Outline of the dissertation 23

Chapter 4 Relationships between the extraction process, fibre and composite properties 27

4.1. Digital image correlation as a strain measurement technique for fibre tensile tests 27

4.1.1. Introduction 27

4.1.2. Materials & Methods 30

4.1.3. Results and discussion 36

4.1.4. Conclusions 43

4.2. The influence of flax fibre fineness and purity on the mechanical performance of the technical fibres and their composites 47

4.2.1. Introduction 47

4.2.2. Materials and methods 48

4.2.3. Transverse properties 53
4.2.4. Results and discussion 53
4.2.5. Conclusions 70
4.3. Influence of flax fibre variety, retting conditions and processing on the composite properties..... 74
4.3.1. Introduction 74
4.3.2. Materials and methods 76
4.3.3. Results and discussion 78
4.3.4. Conclusions 88
Chapter 5 The behaviour of flax fibres and their composites in humid environments 95
5.1. Kinetic and equilibrium hygroscopic behaviour of flax fibres and their composites 95
5.1.1. Introduction 95
5.1.2. Materials and methods 96
5.1.3. Results and discussion 99
5.1.4. Conclusions 118
5.2. Decreasing the moisture sensitivity of flax fibres through crosslinking treatments..... 124
5.2.1. Introduction 124
5.2.2. Materials & Methods 125
5.2.3. Matrix material 125
5.2.4. Results & Discussion 128
5.2.5. Conclusions 138
Chapter 6 Impact of cyclic humidity variations on the composite properties 145
6.1. Development and progression of damage in flax fibre reinforced composites under cyclic hygroscopic loading 145
6.1.1. Introduction 145
6.1.2. Materials & Methods 146
6.1.3. Results & Discussion 150

6.1.4. Conclusions 165
Chapter 7 General conclusions..... 171
7.1. Fineness and purity..... 171
7.2. Variety and retting..... 173
7.3. Insights in moisture diffusion in flax fibres and their composites..... 173
7.4. Impact of hygroscopic fatigue on the composite properties.. 175
7.5. Scientific and industrial impact of the research 175
7.6. Future outlook 177
Curriculum vitae..... 181

List of Figures

Figure 2-1: Schematic representation of a cross section of a flax stem. The fibres are localized in bundles on the outer perimeter of the stem. A micrograph reveals the different biological tissues which can be found in the stem. [1,2] 9
Figure 2-2: The hierarchical structure of flax fibers accompanied by the unit operations of the extraction process which transform the structure of the fibres. [3] 10
Figure 2-3: Traditional scheme to extract flax fibres from the plant. The masses indicate the average yield after each operation, assuming that 1000 kg of straw flax was used as the feed. Losses of water-soluble components during retting exist but are not shown here. Some "inferior" losses such as dust, dirt, and moisture loss of the fibres have been disregarded as well. [8–11] 11
Figure 2-4: Typical cross-sectional view of a flax fibre scutching turbine. The number of arms is variable as well as their angular orientation [27]. (Adapted by [1] from [9]) 12
Figure 2-5: Relative environmental impact indicators of scutched fibres compared to the value of hackled flax fibres. [28] 13
Figure 2-6: Effect of liquid water on the fibre, fibre-matrix interface and matrix during absorption ((a), (b) and (c)) and desorption (d). [56] 16
Figure 4-1: Sandpaper frames and fiber preparation for the fibre tests. The frame is folded to increase fibre gripping during the test. Indirect strain measurement does not require optical flags to be attached to the fibre whereas direct strain measurement relies on these optical flags to measure the strain. 32
Figure 4-2: Schematic representation of the indirect methods to determine fibre modulus. 35
Figure 4-3: Linear regression of the measured data via method 1 for the determination of the fibre modulus. 37
Figure 4-4: Linear regression and extrapolation of the measured data to infinite gauge length ($1/l0$=0) via method 2 for the determination of the fibre modulus. 37
Figure 4-5: Rational extrapolation of the measured data via the method 3 for the determination of the fibre modulus. 38
Figure 4-6: The evolution of the bias on E_f in relation to the number of iterations in the Monte Carlo simulation for the different methods. 40
Figure 4-7: Traditional extraction chain for flax fibres. 47
Figure 4-8: Different combs used to increase the fineness of the fibres. 49
Figure 4-9: Schematic illustration of the fibre diameter algorithm. The diameter is calculated for every pixel found on the axial centerline of the fibre. 51
Figure 4-10: Correlation of fineness values obtained with the gravimetric method and airflow. (R^2=0.26) 54
Figure 4-11: Relative frequency histogram of the gravimetric fibre diameters. 55
Figure 4-12: Technical flax fibre used in the automated image analysis showing fibre splitting and irregular geometry 55
Figure 4-13: Relationship between the gravimetric fibre diameter and optical fibre width. (R^2=0.93) 56
Figure 4-14: Fibre diameter distribution determined with the optical method for batches: (a) 4, (b) 4C1, (c) 4C2 and (d) 4C3. The data was fitted to the lognormal distribution. .. 58
Figure 4-15: Stress-strain behaviour of 47 scutched technical fibres. 59

Figure 4-16: Evolution of the tangent modulus with increasing strain for a representative scutched technical fibre. 60
Figure 4-17: A negative correlation exists between fibre diameter and fibre strength for fibres of batch 4. (Correlation coefficient = -0.71) 62
Figure 4-18: Stress-strain curves resulting from tensile tests on six composite samples ... 63
Figure 4-19: (a) Longitudinal back-calculated fibre modulus of the unidirectional composites calculated in the region between 0% and 0.1% strain. (b) Longitudinal back-calculated fibre strength of the unidirectional composites. 64
Figure 4-20: (a) Evolution of longitudinal back-calculated fibre modulus of the unidirectional composites, calculated in the region between 0% and 0.1% strain for decreasing fibre diameter, due to different levels of combing. (b) Evolution of longitudinal back-calculated fibre strength of the unidirectional composites for decreasing fibre diameter. 66
Figure 4-21: (a) Transverse flexural composite modulus of the unidirectional composites. (b) Transverse flexural composite strength of the unidirectional composites. 67
Figure 4-22: (a) Evolution of transverse composite modulus for decreasing fibre diameter (R^2 = 0.86). (b) Evolution of transverse composite strength for decreasing fibre diameter (R^2 = 0.98). 69
Figure 4-23: Relative frequency histogram of fibre fineness for scutched Amina and Vesta flax fibres. 79
Figure 4-24: Normalized tangent modulus of Amina and Vesta fibres in the composites as a function of strain. 81
Figure 4-25: Back-calculated fibre (a) stiffness and (b) strength from the composites containing scutched fibres with different degrees of retting. 82
Figure 4-26: Three distinct types of tensile behaviour displayed by elementary flax fibres. (Reprinted from [6] with permission from Elsevier.) 83
Figure 4-27: Evolution of normalized tangent modulus of the Amina flax fibre composites with tensile strain. 84
Figure 4-28: Back-calculated fibre (a) stiffness and (b) strength from the composites containing Amina flax fibres that underwent different processing steps. The broken, scutched and hackled fibres were dew retted. 88
Figure 5-1: Moisture content of an initially dry elementary flax fibre as a function of time when brought into contact with an atmosphere at 20°C and 40% RH measured using DVS. The data was fitted using the analytical solution to Fick's second law for perfect, infinitely long cylinders (R^2=99.9%). 100
Figure 5-2: Diffusion coefficient as a function of moisture content in the elementary and technical fibres as measured by DVS. 101
Figure 5-3: Schematic representation of the absorption process at (a) low and (b) intermediate and (c) high relative humidity. Water molecules interact with the hydroxyl functional groups of the biopolymers in the fibre. IZ = immobile zone, MZ = mobile zone; at high water content, water molecules start to aggregate. 103
Figure 5-4: Absorption and desorption isotherms for elementary and technical flax fibres. The isotherms of elementary and technical fibres are nearly identical both in absorption and desorption. 104
Figure 5-5: Schematic of the proposed diffusion process in technical flax fibres. (a) A technical flax fibre which has not reached its equilibrium moisture content. (b) Fast diffusion step, with water molecules diffusing mainly along the middle lamellae. (c) Slow diffusion step, with water diffusing into the cell wall matrix of the elementary fibres. The arrows indicate the main pathways for moisture diffusion. 105

Figure 5-6: Moisture loss of an initially saturated elementary flax fibre at 20°C and 30% RH as a function of time when brought into contact with an atmosphere of 20°C and 0% RH. The data was fitted (a) using the analytical solution to Fick's second law for perfect, infinitely long cylinders (R^2=86%) and (b) using the model according to Carter and Kibler (R^2=99.9%) [60]. 107
Figure 5-7: Diffusion coefficient as a function of moisture content in the elementary fibres for both absorption and desorption calculated using Fick's law. (*Fitted value according to Fick's law with R^2<0.9) 109
Figure 5-8: Schematic of the stages in the desorption process. The zone where Langmuir diffusion occurs in the fibre is shown in dark grey. This type of diffusion is initiated when the moisture concentration in that zone drops below a critical moisture content (M_{crit}). As the zone expands, the diffusion coefficient lowers significantly. (M=moisture content of the fibre, d=distance from the fibre centre)..... 110
Figure 5-9: Chemical structure of the fluorescent dye, rhodamine 6G. 111
Figure 5-10: Fluorescence microscopy on a flax stem brought into contact with water containing rhodamine 6G (a) immediately after application of the drop, (b) after 20 s has passed and (c) image subtraction of (a) and (b). 112
Figure 5-11: Back-calculated moisture content of the flax fibres in a unidirectional composite as a function of the relative humidity. Both absorption and desorption processes are shown. 114
Figure 5-12: Evolution of unidirectional composite modulus and strength with relative humidity for (a) longitudinal and (b) transverse loading conditions. 117
Figure 5-13: Chemical structure of the reagents used to treat the fibres: (a) benzaldehyde (BEN), (b) 1,2,7,8-diepoxyoctane (DEO), (c) benzene-1,4-dicarboxaldehyde (TER) and (d) 1,5-pentanedial (GLU). 128
Figure 5-14: DVS isotherms of the untreated and treated flax fibres in (a) absorption and (b) desorption. (c) The hysteresis calculated as the difference of the absorption and desorption isotherms. The color codes are consistent throughout the text. 131
Figure 5-15: (a) Schematic representation of the absorption process at (a) low relative humidity in an untreated fibre and (b) at low relative humidity in a crosslinked fibre. In the latter case the crosslinks (solid line) force the backbone biopolymer chains further apart and prevent other hydroxyl groups from interacting. 132
Figure 5-16: Diffusion coefficients as a function of moisture content in the untreated and treated fibres..... 134
Figure 5-17: Back-calculated fibre (a) stiffness and (b) strength from tensile tests performed on the composites for the different treatments. (c) The failure strain of the composites. 135
Figure 5-18: (a) Evolution of the back-calculated fibre tangent modulus at saturation and (b) evolution of this tangent modulus by normalizing to the initial stiffness. 137
Figure 6-1: Scheme of the hygroscopic cycle, repeated ten times. The diffusion coefficient and EMC were monitored at regular intervals during each cycle. Damage inspection and mechanical testing was performed every other cycle..... 147
Figure 6-2: EMC of the composites throughout the cycles, after each absorption half-cycle. Dotted lines indicate the average EMC value throughout the cycles. 151
Figure 6-3: Representative cross-sections captured using µ-CT after 0, 1, 3, 5 and 10 hygroscopic cycles, shown in (a), (b), (c), (d) and (e), respectively. All samples are scanned in oven dry condition. To increase clarity, certain parts of the image were enlarged. 153
Figure 6-4: µ-CT damage visualization of two composite specimens with a different polymer matrix. After 10 cycles both fibre-fibre debonding and fibre-matrix debonding has

developed in the epoxy composite. In contrast, the flax-PP sample only shows fibre-matrix debonding. 154
Figure 6-5: (a) Increase of void content with increasing cycle number for the composites. (b) Impact of void content on the transverse diffusion coefficient. The dotted regression lines are only added to highlight the upward trend and do not necessarily reflect the effective relationship between damage content and diffusion coefficient. 155
Figure 6-6: (a) Transverse flexural stiffness and (b) transverse flexural strength of the composites with increasing cycle number. (cycle 0 = reference oven-dry state) 157
Figure 6-7: (a) Back-calculated longitudinal tensile stiffness and (b) back-calculated longitudinal tensile strength of the composites with increasing cycle number. (cycle 0 = reference oven-dry state) 159
Figure 6-8: Normalized moisture content and hygroscopic strain during moisture sorption of a unidirectional composite specimen as a function of the absorption time. 160
Figure 6-9: Full field strain map in the y-direction of (a) the neat epoxy resin and (b) of a unidirectional flax-epoxy sample. 161
Figure 6-10: Determination of the CHE of (a) neat epoxy and (b) the unidirectional composite (R^2=0.993, R^2=0.994, R^2=0.874 for β_m, β_T and β_L fits respectively) 162

List of Tables

Table 2-1: Chemical composition of flax fibres. Water and water-soluble substances are not taken into account. [30,35–40] 15
Table 4-1: Mechanical properties of flax and bamboo technical fibres. [a]weakest test length – strongest test length 28
Table 4-2: Results of fibre tensile tests on steel fibres using the different methods to determine the fibre Young's modulus. 36
Table 4-3: Input parameters for the Monte Carlo simulation. 39
Table 4-4: RMSE of the different methods after 10 000 Monte Carlo iterations..... 40
Table 4-5: Tensile modulus, strength and strain to failure of the fibres using direct strain measurement 41
Table 4-6: Risks and mitigation during fibre testing of selected physical parameters 43
Table 4-7: Average (arithmetic) and 95th percentile values of the diameters of unrefined and refined fibres in the different batches. The parameters which provide the best fit of the lognormal distribution to the data are also shown. 59
Table 4-8: Tensile modulus and strength of fibres originating from batches 4 and 4C1... 61
Table 4-9: Back-calculated longitudinal fibre properties for all batches of scutched and uncombed flax fibres. 65
Table 4-10: Evolution of the fibre purity with each combing operation (decreasing fibre diameter). *The purity of the batch after the last combing operation was assumed to be 100%. Hence, no standard deviation on the result can be provided. 70
Table 4-11: Longitudinal stiffness and strength of the Amina and Vesta fibres in the composite. 79
Table 5-1: Evolution of the diffusion coefficient and EMC for each RH increment of elementary flax fibres during DVS. 101
Table 5-2: Kinetic parameters determined via Fick's law and the Carter and Kibler model for the desorption of elementary flax fibres when dried from saturation at 40%RH to their fully dry state at 20°C. 109
Table 5-3: Experimentally observed through the thickness diffusion coefficients for the different RH levels, after several stepwise 30%RH increases (0% to 30%, 30% to 60% and 60% to 90%RH) Also, the predicted values using Hashin's formula based on the measured values of D_f (technical fibre) and D_m are given 116
Table 5-4: Mechanical properties of the matrix system. 125
Table 5-5: Relative mass increase of the fibres after the treatment and the yield of the reaction, assuming the fibre is composed entirely of anhydroglucose unit based polymers. 129
Table 6-1: Input parameters, necessary for back-calculation of the fibre's CHE. 164

Chapter 1

General context

Chapter 1 General context

As of 2015, every new vehicle that is sold in the European Union should consist of at least 95 wt% reusable materials and at least 85 wt% recyclable materials (End of Life Vehicles Directive 2000/53/EC) [1]. Besides these stringent requirements on the materials used, the vehicle's CO_2 emission also cannot surpass 130 g/km. In 2020, restrictions will become even more severe with an emission limit of 95 g/km. Similar trends can be observed on a global scale with the United States (Corporate Average Fuel Economy (CAFE) legislation [2]) and China limiting diesel car CO_2 emissions to 115 g/km by 2025 and 135 g/km in 2020, respectively [3].

Translating these requirements into "engineering" properties, the automotive sector is continuously looking for materials that are easily recyclable/reusable while also being lightweight and at the lowest possible cost. Moreover, minimum values of certain mechanical properties for a specific part are almost always superimposed on the former restrictions. The material class which offers the most potential to meet these requirements is fibre reinforced polymers or polymer composites. Indeed, when fibres are embedded in a polymer, the mechanical behaviour of the resulting material is greatly enhanced when compared to the neat polymer for only a marginal increase in the part's mass. These considerations have caused an exponential growth in the use of composites in the automotive industry. While in 2010 only 14% of a vehicle's total mass could be attributed to plastics and composites, this is projected to become 23% in 2020, making it the strongest growing material class in the industry [3]. The example of the automotive industry explains why composites are gaining importance. However, the argumentation can be extended to several other markets, such as aviation, aerospace and construction. Due to their wide availability, relatively low cost, and excellent mechanical properties, glass and carbon fibres nowadays account for 99%, by volume, of the fibres that are used in composites. Despite their advantages, the energy required to produce these fibres is high, making the recycling and reuse of these materials absolutely vital. Moreover, carbon fibre production still requires petroleum based raw materials. Unfortunately, reuse nor recycling of these fibres is straightforward, especially in combination with thermoset resins where the matrix generally needs to pyrolyzed to recuperate the fibres. The reuse and recycling of the fibres generally makes them shorter, creating difficulties to properly align the fibres.

Natural fibres, such as flax, provide an elegant solution to these end of life difficulties. Not only do they exhibit excellent mechanical properties, e.g. a stiffness value comparable to those of glass fibres, they are nearly twice as light, enabling an even larger mass reduction of composite parts. Furthermore, they possess several properties which are difficult to find in synthetic fibres such as non-abrasiveness, thermal and acoustic insulation, and vibrational damping. Flax

is characterized by its low environmental impact, as each part of the plant is used, virtually no fertilization is needed to grow the plants, and it simultaneously absorbs CO_2. When these fibres are combined with a fully biobased matrix, a "near zero environmental impact" material could be produced. Subsequent recycling by shredding the composite and using it (e.g. in injection molding) prolonges the economic life of the material and contributes to a circular economy. Finally, at the end of the material's economic lifecycle(s), energy recuperation by incineration/biodegradation is possible.

Up to now, however, the market penetration of flax fibre composites remains low despite extensive studies on their mechanical behaviour in quasi-static, impact, and fatigue loading, as well as data on their damage tolerance. Hesitance of the industry towards the incorporation of these fibres in composites is related to several issues which still remain. Firstly, and most importantly, the cost of the fibres compared to glass fibres, remains too high and is extremely variable. Historically, the extraction process of flax fibres was developed and optimized for non-technical applications, such as clothing and furniture. Thus, in contrast to synthetic fibres, flax fibre cost is mainly determined by the highly variable demand in the non-technical fibre market. Furthermore, the extraction process itself has remained unchanged for the last centuries, apart from the mechanisation of some manual processes. Despite the automation efforts a significant amount of manual labour remains part of the process and surprisingly, to date, it has not been verified whether the flax fibres need to run through the entire traditional extraction process before they can be used in composites. In addition, the influence of the unit operations, which are included in the process, on the final composite properties is presently not sufficiently clear. Secondly, the behaviour of flax fibre composites in humid environments is not well understood. It has been long established that flax fibres absorb moisture from the environment and that their mechanical properties depend on the moisture content in the fibre. However, insights into the absorption process and the mechanisms which are responsible for this degradation is lacking. Without clear understanding, proposing targeted solutions to counteract the degradation is next to impossible.

In conclusion, flax fibre composites are extremely promising materials that have the potential to enable part of the global shift towards a circular economy. Their breakthrough is prevented by two main factors being the cost of the commercially available preforms and the lack of understanding regarding the impact of moisture on the properties of these materials. Hence, there is a need for a revision of the current extraction process, which determines the cost of the fibres, supplemented with a detailed analysis on the kinetic and equilibrium processes associated with moisture absorption.

References

[1] Directive 2000/53/EC of the European Parliament and of the Council. 2000.
[2] Automobile fuel economy (U.S. House of Representatives). 2010.
[3] JEC Group. Overview of the global composites market, at the crossroads. Paris: JEC Group; 2017.

Chapter 2

Introduction

Chapter 2 Introduction

2.1. Microstructure of flax straw and fibres

Flax fibres are the structural cells in the flax plant *Linum Usitatissimum L*. The overall goal of the extraction process is to separate these biological structures from the rest of the plant and to obtain separate fibre entities. Figure 2-1 shows a cross section of a mature flax stem immediately after harvesting. Flax fibres, also called cells or elementary flax fibres, are localized in bundles, or technical flax fibres, at the outer perimeter of the cylindrical stem and are to be separated from the inner woody core tissues (cambium, primary xylem and secondary xylem) during extraction.

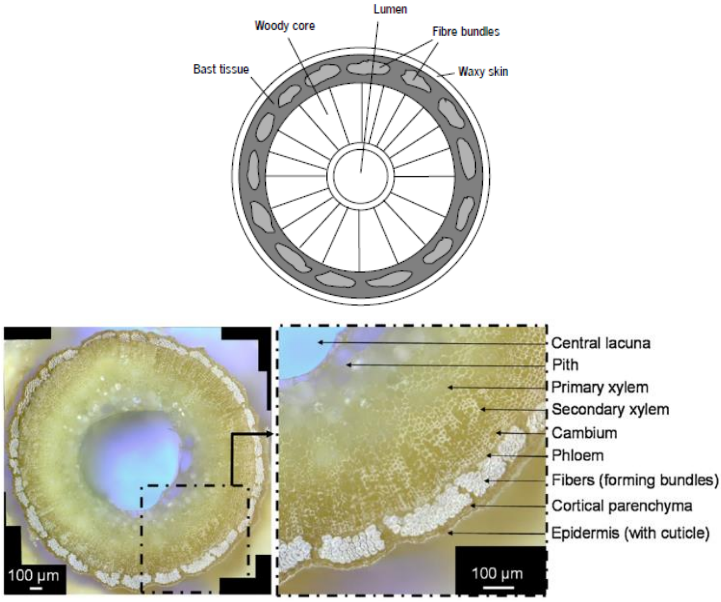

Figure 2-1: Schematic representation of a cross section of a flax stem. The fibres are localized in bundles on the outer perimeter of the stem. A micrograph reveals the different biological tissues which can be found in the stem. [1,2]

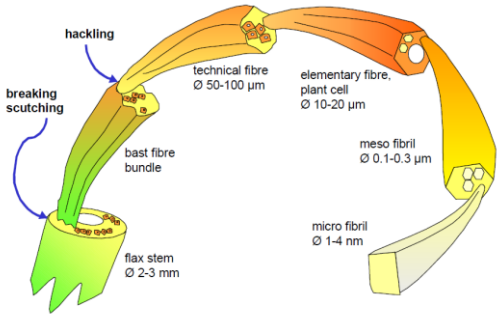

Figure 2-2: The hierarchical structure of flax fibers accompanied by the unit operations of the extraction process which transform the structure of the fibres. [3]

In a technical flax fibre, as shown in Figure 2-2, the elementary fibres are connected through a thin layer, approximately 500 nm thick [4,5]. This interphase layer, known as the middle lamella, maintains the cohesion within the technical fibre. However, being mainly composed of pectins, the mechanical properties of this layer are intrinsically low compared to the elementary fibres themselves, which are mainly composed of crystalline cellulose [4–7]. Charlet *et al.* have shown that the average shear modulus and shear strength of this interphase is equal to 18.7 kPa and 2.9 MPa, respectively. These low values are important as it allows the fibres to be gradually refined during the extraction process by failure of the middle lamellae.

2.2. Extraction of flax fibres

In the traditional extraction scheme of flax fibres, summarized in Figure 2-3, the plants, called straws or straw flax, are pulled out of the soil, maintaining the roots and seeds. The total length of the plant reaches 1 to 1.5 m depending on the weather conditions. Immediately afterwards, dedicated harvesting machinery removes and subsequently separates the linseeds and the chaff from the stems, a process called rippling.

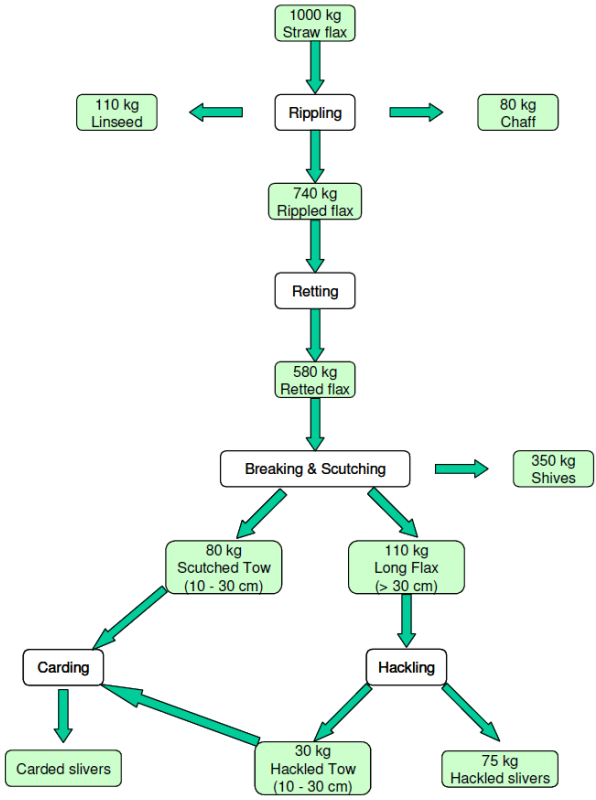

Figure 2-3: Traditional scheme to extract flax fibres from the plant. The masses indicate the average yield after each operation, assuming that 1000 kg of straw flax was used as the feed. Losses of water-soluble components during retting exist but are not shown here. Some "inferior" losses such as dust, dirt, and moisture loss of the fibres have been disregarded as well. [8–11]

After rippling, the stems are left on the field for several weeks and turned every few days. During dew retting, different bacteria and fungi colonize the fibres which subsequently produce enzymes such as pectinases, hemicellulases, cellulases, and laccases which degrade the polysaccharides in the stem [12–15]. In particular, the secretion of pectinases is pronounced in optimal conditions. This facilitates the separation of the fibres from the cambium in later extraction stages and weakens the middle lamellae, decreasing the size of the fibre bundles [16,17]. Unfortunately, the process is heavily influenced by weather conditions, such as the amount of rainfall, temperature, and even wind [9,18,19]. Hence, the flax stems require different residence times on the field, varying from 2 to 5 weeks [9].

When retting is complete, the fibres are collected in bales and sent to mechanical extraction lines [20]. In the previous extraction steps the fibres were only minimally mechanically stressed. Also note that up to this point there are no fibre

losses as they are still contained in rather intact stem structures. Furthermore, the extracted chaff and linseed are not considered as waste, as they are used in various applications [21,22]. In a first mechanical unit operation, the flax stems are broken between serrated rollers. The process causes the xylem tissue or shives to break into smaller sections and loosen from the fibrous layers.

Next, the broken stems are grabbed by two rubber belts approximately at the stem's middle section, producing two overhanging parts of the stem. The overhanging parts enter a turbine where blunt steel knives are attached to rotating arms which strike the broken stems, removing the weakly adhering woody particles. In a subsequent operation, the location where the stems were initially grabbed is changed by a second belt system which grabs the stems at a different location. This ensures that all parts of the stem have undergone scutching. The rotation speed of the turbine can range between 160 to 245 rpm depending on the degree of retting of the stems [23]. It has been established that increased rotational speeds, and thus an increased number of fibre beatings, is required for stems which have been retted insufficiently [24], yet at the detriment of reduced fibre yield. Finally, during scutching, in addition to the removal of shives, the refinement of the fibres starts by failure of the weakest fibre interphases.

In the next step, called hackling, the fibres are passed over a combing field mounted with steel pins [25]. As the pin spacing decreases, passage of the coarser technical fibres is prevented, forcing them to separate into smaller entities [26]. Furthermore, hackling causes the fibres to disentangle and align with the combing direction. Finally, stretching and doubling produce what is known as sliver and can be further processed into yarns and other preforms both technical and non-technical.

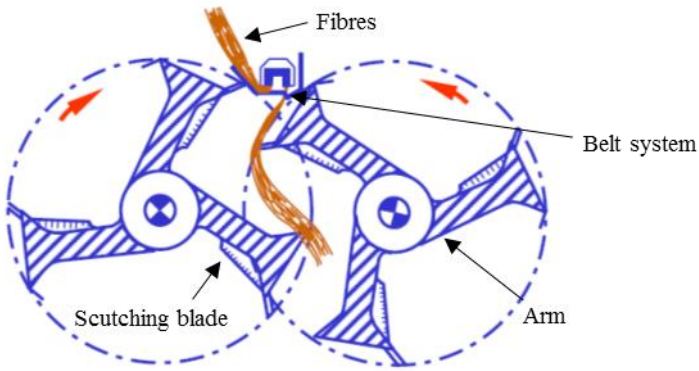

Figure 2-4: Typical cross-sectional view of a flax fibre scutching turbine. The number of arms is variable as well as their angular orientation [27]. (Adapted by [1] from [9])

Considering the data presented in Figure 2-3, the extent of processing decreases the overall yield of long fibres. Indeed, during scutching, 42% of the fibres in the

material are “lost” in the form of shorter (10 – 30 cm) fibres in the scutching turbine. The loss of fibrous material can be due to two factors. Firstly, the interphase in a specific fibre could fail completely, effectively splitting off part of the technical fibre. Secondly, fibre entanglement could lead to a buildup in tensile stresses in the flax fibres. These tensile stresses may be significant and lead to tensile failure of some technical fibres. Shorter fibres may be recuperated and be aligned using a carding machine from which a carded sliver may be obtained. Usually, this secondary sliver is considered to be of a lower quality for non-technical applications due to coarseness of the fibres and the higher amount of impurities.

Similarly, during hackling, merely 70% of the fibres survive the hackling step as long fibres. The remainder is separated as short fibres due to the same mechanisms as stated above for scutching, though hackled tow has higher purity.

From the above discussion it is clear that scutching and hackling decrease the yield of long (> 30 cm) flax fibres. Taking the harvested flax straw as a reference, the long fibre yield after hackling is only 7.5%. From this perspective, the yield could be increased to 11% when hackling is not performed, and the extraction process is interrupted after scutching.

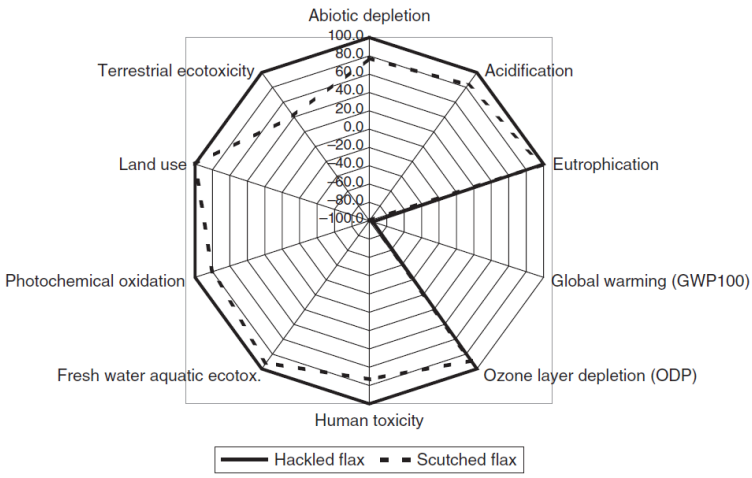

Figure 2-5: Relative environmental impact indicators of scutched fibres compared to the value of hackled flax fibres. [28]

Furthermore, each unit operation that is performed on the fibres increases the energy use and manual labour, hence, increasing the production costs. Moreover, the producers will attribute most of the costs to the long flax fibres for which the yield is decreased, increasing their cost even further. Baley *et al.* compared the environmental impact of scutched fibres to that of hackled fibers over their life cycle [28]. It was established that both scutching and hackling adversely affect the environmental impact of the fibres. However, hackling does so more than

scutching. Indeed, the energy required for hackling reaches 0.55 kWh/kg compared to 0.116 kWh/kg for scutching. The embodied energy of the fibres thereby increases from 4.4 MJ/kg to 11.6 MJ/kg. Finally, Figure 2-5 shows that hackling also adversely affects all other environmental impact indicators in a negative manner. For example, terrestrial ecotoxicity rises by 30%, photochemical oxidation and acidification both increase by 20%.

The discussion above raises the question whether hackled slivers should be considered the final product of the extraction. If hackled fibres could be replaced by scutched fibres, there is a significant potential to decrease both the environmental impact and cost of the resulting preforms. Historically, hackling was introduced to reduce the technical fibre diameter so that yarn spinning was facilitated [9,11]. However, spinning is no absolute requirement to produce reinforcing architectures for composites, as exemplified by a unidirectional configuration [29].

In summary, the extraction process of flax fibres is oriented and optimized towards the non-technical market. Yet, the difference between what is considered a high-quality fibre for composites and for non-technical applications remains to be investigated. Hence, there is a need to define measurable quality parameters for flax fibres for composites and to investigate the effect of the different unit operations in the extraction process on the final fibre quality.

2.3. Moisture in flax fibres and their composites

Flax fibres are composed of various polysaccharides (cellulose, hemicellulose, pectin) and lignin, making them prone to water sorption. The approximate mass fractions of the different constituents are shown in Table 2-1. Between 60% and 80% of the fibre mass, is crystalline matter. This crystalline matter are crystalline regions of cellulose known as microfibrils. These microfibrils are discontinuous as they contain “dislocated”, i.e. amorphous sections, where amorphous cellulose is present. [30,31]. Moreover, cellulose is the only semi-crystalline constituent in the fibre, the other polysaccharides are unable to crystallize [32]. It has been established that water molecules cannot penetrate into the microfibrils during moisture absorption of the fibres [33,34].

Constituent	Mass fraction (%)
Cellulose	65-85
Hemicellulose	15-22.4
Pectin	1-2.3
Lignin	2-5
Waxes and other components	1.5-2

Table 2-1: Chemical composition of flax fibres. Water and water-soluble substances are not taken into account. [30,35–40]

This leaves approximately between 35% and 15% of the fibre mass that is susceptible to moisture sorption. In particular hemicellulose, being the second most abundant biopolymer in the fibre, was identified as the main storage for moisture during sorption [41,42]. At the origin of the sorption process lie the hydroxyl functionalities which are present on all polysaccharides and lignin. However, the contribution of lignin to water sorption is rather low as it does not contain as many hydroxyl groups as the other biopolymers. Water molecules can interact with these hydroxyl groups forming hydrogen bonds [32,43].
When these fibres are embedded in a polymer to produce a composite, several moisture related effects are developed:

- The moisture that is absorbed by the fibres will cause the moisture content, and thus the mass, of the composite to increase when compared to the neat polymer [44,45].
- Diffusion of moisture in natural fibre composite materials is usually significantly faster than what is observed in synthetic fibre composites [43,46–48].
- Moisture causes the fibres to expand, generating stresses at the fibre-matrix interface [45,49,50]. Eventually these stresses can lead to internal damage in the composites, such as fibre-matrix debonding, especially when moisture is absorbed and desorbed cyclically [45].
- The mechanical properties of the fibres might be affected by water sorption. Célino *et al.* reviewed the results of different studies on the effect of moisture on the mechanical properties but was not able to reach a conclusion. Indeed, literature data exist that report stiffness and strength of natural fibres increasing, decreasing, or remaining unchanged with the evolution of moisture content in the fibres [44,51–54].

Most of the studies mentioned above examine the case where a flax fibre composite is in direct contact with liquid water. Figure 2-6 illustrates the phenomena that occur during sorption in this case. First, the fibres swell, generating the aforementioned interface stresses which lead to the formation of

micro cracks in the matrix and possibly fibre- matrix debonding. Next, the capillaries produced by the debonding as well as the matrix capillaries will be filled with liquid water. Subsequently, water soluble compounds will be extracted from the fibres, with the amount depending on the contact time [55,56].

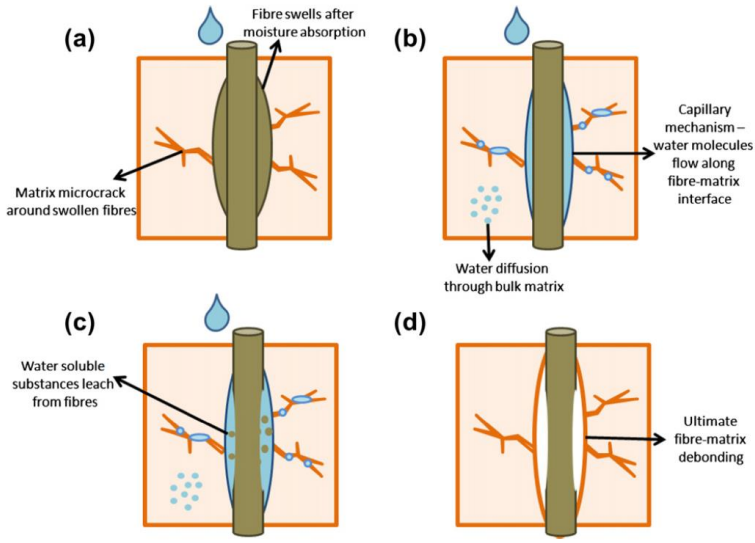

Figure 2-6: Effect of liquid water on the fibre, fibre-matrix interface and matrix during absorption ((a), (b) and (c)) and desorption (d). [56]

It is clear that the mechanism by which moisture enters the fibre is severely affected by the presence of liquid water, leading to difficulties in interpretation of the results, such as diffusion coefficients. Moreover, most composite parts in service do not experience extended periods of time where they are in contact with liquid water. Studies that replace the liquid water with water vapour are therefore more appropriate to evaluate the fibre and composite behaviour in moist conditions [30,47,52].

In the literature there is a fundamental lack of understanding of the absorption and desorption process itself. For example, to the best of the author's knowledge, it is not known how the moisture is spatially distributed within the fibre during the absorption phase. Nonetheless, this is important as it can reveal regions of preferential sorption which impact the absorption rate and hence the diffusion coefficient of the fibres and composites.

The above discussion justifies a thorough characterization of the absorption and desorption behaviour of elementary and technical flax fibres as well as their composites. A thorough understanding will facilitate future efforts to counteract or adapt to moisture absorption in flax fibres and other natural fibre composites. Finally, the collected parameters can aid in the modelling of the absorption process and interfacial stresses.

2.4. Conclusion

Two main factors preventing the breakthrough of flax fibre composites have been identified and illustrated in this chapter.

Firstly, the extraction process of flax fibres has remained unchanged for centuries and is entirely adapted to achieve the optimal fibre quality for non-technical applications. Fibre quality requirements can, however, be significantly different for composite applications. Therefore, several objective quality parameters for the fibres will need to be identified, parameters that have a predictive nature towards the properties of the composites. Finally, a revision of the necessary unit operations in the current extraction process is necessary. In particular, it was shown that hackling is a preferred candidate for elimination due to its significant influence on the environmental impact and cost of the fibres.

Secondly, a fundamental understanding of the moisture sorption process in flax fibres is lacking. This not only prevents focussed research on counteracting or adapting to this moisture ingress, it also does not allow the absorption process from being modelled effectively. The latter would increase the understanding even further and increase the predictability of the mechanical and durability behaviour of composite parts in real applications.

Finally, most studies on the moisture absorption of flax fibres and their composites have been carried out in the presence of liquid water which is not representative of their actual use. It was therefore advised to shift attention to more realistic scenarios where the composite is in contact with water vapour, controlled by the relative humidity of the surrounding air.

References

[1] Bos HL. The potential of flax fibres as reinforcement for composite materials. Technische Universiteit Eindhoven, 2004.

[2] Goudenhooft C, Bourmaud A, Baley C. Varietal selection of flax over time: Evolution of plant architecture related to influence on the mechanical properties of fibers. Ind Crops Prod 2017;97:56–64. doi:10.1016/J.INDCROP.2016.11.062.

[3] Bos HL, Van Den Oever MJA, Peters OCJJ. Tensile and compressive properties of flax fibres for natural fibre reinforced composites. J Mater Sci 2002;37:1683–92. doi:10.1023/A:1014925621252.

[4] Morvan C, Andème-Onzighi C, Girault R, Himmelsbach DS, Driouich A, Akin DE. Building flax fibres: more than one brick in the walls. Plant Physiol Biochem 2003;41:935–44. doi:10.1016/j.plaphy.2003.07.001.

[5] Charlet K, Béakou A. Mechanical properties of interfaces within a flax bundle – Part I: Experimental analysis. Int J Adhes Adhes 2011;31:875–81. doi:10.1016/j.ijadhadh.2011.08.008.

[6] Beakou A, Charlet K. Mechanical properties of interfaces within a flax bundle—Part II: Numerical analysis. Int J Adhes Adhes 2013;43:54–9. doi:10.1016/j.ijadhadh.2013.01.013.

[7] Charlet K, Beakou A. Interfaces within flax fibre bundle: Experimental characterization and numerical modelling. J Compos Mater 2013;48:3263–9. doi:10.1177/0021998313508871.

[8] van Dam JEG, Van Vilsteren GET, Zomers FHA, Shannon WB, Hamilton IT. Increased Application of Domestically Produced Plant Fibres in Textiles, Pulp and Paper Production, and Composite Materials. Wageningen: Agro-industrial research division; 1994.

[9] Dewilde B. 20 eeuwen vlas in Vlaanderen. 1st ed. Terra - Lannoo; 1984.

[10] Van De Weyenberg I. Flax fibres as a reinforcement for epoxy composites. KU Leuven, 2005.

[11] van Sumere CF, Sharma HSS. The Biology and processing of flax. 1992.

[12] Rosemberg JA, De França FP. Importance of galacturonic Acid in controlling the retting of flax. Appl Microbiol 1967;15:484–6.

[13] Henriksson G, Akin DE, Hanlin RT, Rodriguez C, Archibald DD, Rigsby LL, et al. Identification and Retting Efficiencies of Fungi Isolated from Dew-Retted Flax in the United States and Europe. vol. 63. 1997.

[14] BROWN AE, SHARMA HSS. Production of polysaccharide-degrading enzymes by saprophytic fungi from glyphosate-treated flax and their involvement in retting. Ann Appl Biol 1984;105:65–74. doi:10.1111/j.1744-7348.1984.tb02803.x.

[15] Akin DE. Linen Most Useful: Perspectives on Structure, Chemistry, and Enzymes for Retting Flax. ISRN Biotechnol 2013;2013:1–23. doi:10.5402/2013/186534.

[16] Akin DE, Foulk JA, Dodd RB, McAlister DD. Enzyme-retting of flax and characterization of processed fibers. J Biotechnol 2001;89:193–203. doi:10.1016/S0168-1656(01)00298-X.

[17] Akin DE, Henriksson G, Evans JD, Adamsen APS, Foulk JA, Dodd RB. Progress in Enzyme-Retting of Flax. J Nat Fibers 2004;1:21–47. doi:10.1300/J395v01n01_03.

[18] Pallesen BE. The quality of combine-harvested fibre flax for industrials purposes depends on the degree of retting. Ind Crops Prod 1996;5:65–78. doi:10.1016/0926-6690(95)00049-6.

[19] Easson DL, Molloy RM. A study of the plant, fibre and seed development in flax and linseed (Linum usitatissimum) grown at a range of seed rates. J Agric Sci 2000;135:S0021859699008400. doi:10.1017/S0021859699008400.

[20] Müssig J. Industrial Applications of Natural Fibres. Chichester, UK: John Wiley & Sons, Ltd; 2010. doi:10.1002/9780470660324.

[21] Komlajeva L, Adamovics A. EVALUATION OF FLAX (LINUM USITATISSIMUM L.) QUALITY PARAMETERS FOR BIOENERGY PRODUCTION. n.d.
[22] Kurt Çömlekçi G, Ulutan S. Encapsulation of linseed oil and linseed oil based alkyd resin by urea formaldehyde shell for self-healing systems. Prog Org Coatings 2018;121:190–200. doi:10.1016/J.PORGCOAT.2018.04.027.
[23] Bourmaud A, Beaugrand J, Shah DU, Placet V, Baley C. Towards the design of high-performance plant fibre composites. Prog Mater Sci 2018;97:347–408. doi:10.1016/J.PMATSCI.2018.05.005.
[24] Schünke U, Schwalen N. Objektive Qualitätsbestimmung von Faserlein. Melliand Text n.d.;3:168–9.
[25] Salmon-Minotte J. Flax. In: FRANCK RR, editor. Bast Other Plant Fibres, 2005.
[26] Coroller G, Lefeuvre A, Le Duigou A, Bourmaud A, Ausias G, Gaudry T, et al. Effect of flax fibres individualisation on tensile failure of flax/epoxy unidirectional composite. Compos Part A Appl Sci Manuf 2013;51:62–70. doi:10.1016/j.compositesa.2013.03.018.
[27] Depoortere NV. Trommel voor zwingelturbine. 2007/0318, 2009.
[28] Le Duigou A, Davies P, Baley C. Environmental impact analysis of the production of flax fibres to be used as composite material reinforcement. J Biobased Mater Bioenergy 2011;5:153–65. doi:10.1166/jbmb.2011.1116.
[29] Khalfallah M, Abbès B, Abbès F, Guo YQ, Marcel V, Duval a., et al. Innovative flax tapes reinforced Acrodur biocomposites: A new alternative for automotive applications. Mater Des 2014;64:116–26. doi:10.1016/j.matdes.2014.07.029.
[30] Dittenber DB, Gangarao HVS. Critical review of recent publications on use of natural composites in infrastructure. Compos Part A Appl Sci Manuf 2012;43:1419–29. doi:10.1016/j.compositesa.2011.11.019.
[31] Lewin M. Handbook of fiber chemistry. CRC/Taylor & Francis; 2007.
[32] Célino A, Fréour S, Jacquemin F, Casari P. The hygroscopic behavior of plant fibers: a review. Front Chem 2013;1:43. doi:10.3389/fchem.2013.00043.
[33] Nakamura K, Hatakeyama T, Hatakeyama H. Studies on Bound Water of Cellulose by Differential Scanning Calorimetry. Text Res J 1981;51:607–13. doi:10.1177/004051758105100909.
[34] Nelson RA. The determination of moisture transitions in cellulosic materials using differential scanning calorimetry. J Appl Polym Sci 1977;21:645–54. doi:10.1002/app.1977.070210306.
[35] Bledzki AK, Gassan J. Einfluß von haftvermittlern auf das feuchteverhalten naturfaserverstärkter kunststoffe. Angew Makromol Chemie 1996;236:129–38. doi:10.1002/apmc.1996.052360110.
[36] Bledzki A. Composites reinforced with cellulose based fibres. Prog Polym Sci 1999;24:221–74. doi:10.1016/S0079-6700(98)00018-5.
[37] Müssig J. Untersuchung der Eignung heimischer Pflanzenfasern für die Herstellung von naturfaserverstärkten Duroplasten-vom Anbau zum Verbundwerkstoff. VDI-Verlag; 2001.
[38] Day A, Ruel K, Neutelings G, Crônier D, David H, Hawkins S, et al. Lignification in the flax stem: Evidence for an unusual lignin in bast fibers. Planta 2005;222:234–45. doi:10.1007/s00425-005-1537-1.
[39] De Rosa IM, Kenny JM, Puglia D, Santulli C, Sarasini F. Morphological, thermal and mechanical characterization of okra (Abelmoschus esculentus) fibres as potential reinforcement in polymer composites. Compos Sci Technol 2010;70:116–22. doi:10.1016/J.COMPSCITECH.2009.09.013.
[40] Faruk O, Bledzki AK, Fink H-P, Sain M. Progress Report on Natural Fiber Reinforced Composites. Macromol Mater Eng 2014;299:9–26. doi:10.1002/mame.201300008.

[41] Davies GC, Bruce DM. Effect of Environmental Relative Humidity and Damage on the Tensile Properties of Flax and Nettle Fibers. Text Res J 1998;68:623–9. doi:10.1177/004051759806800901.

[42] Pejic BM, Kostic MM, Skundric PD, Praskalo JZ. The effects of hemicelluloses and lignin removal on water uptake behavior of hemp fibers. Bioresour Technol 2008;99:7152–9. doi:10.1016/j.biortech.2007.12.073.

[43] Célino A, Fréour S, Jacquemin F, Casari P. Characterization and modeling of the moisture diffusion behavior of natural fibers. J Appl Polym Sci 2013;130:297–306. doi:10.1002/app.39148.

[44] Assarar M, Scida D, El Mahi a., Poilâne C, Ayad R. Influence of water ageing on mechanical properties and damage events of two reinforced composite materials: Flax–fibres and glass–fibres. Mater Des 2011;32:788–95. doi:10.1016/j.matdes.2010.07.024.

[45] Dhakal H, Zhang Z, Richardson M. Effect of water absorption on the mechanical properties of hemp fibre reinforced unsaturated polyester composites. Compos Sci Technol 2007;67:1674–83. doi:10.1016/j.compscitech.2006.06.019.

[46] Le Duigou A, Davies P, Baley C. Exploring durability of interfaces in flax fibre/epoxy micro-composites. Compos Part A Appl Sci Manuf 2013;48:121–8. doi:10.1016/j.compositesa.2013.01.010.

[47] Alix S, Philippe E, Bessadok A, Lebrun L, Morvan C, Marais S. Effect of chemical treatments on water sorption and mechanical properties of flax fibres. Bioresour Technol 2009;100:4742–9. doi:10.1016/j.biortech.2009.04.067.

[48] Alix S, Lebrun L, Morvan C, Marais S. Study of water behaviour of chemically treated flax fibres-based composites: A way to approach the hydric interface. Compos Sci Technol 2011;71:893–9. doi:10.1016/j.compscitech.2011.02.004.

[49] Bismarck A, Aranberri-Askargorta I, Springer J, Lampke T, Wielage B, Stamboulis A, et al. Surface characterization of flax, hemp and cellulose fibers; Surface properties and the water uptake behavior. Polym Compos 2002;23:872–94. doi:10.1002/pc.10485.

[50] le Duigou A, Merotte J, Bourmaud A, Davies P, Belhouli K, Baley C. Hygroscopic expansion: A key point to describe natural fibre/polymer matrix interface bond strength. Compos Sci Technol 2017;151:228–33. doi:10.1016/J.COMPSCITECH.2017.08.028.

[51] Van Voorn B, Smit HHG, Sinke RJ, De Klerk B. Natural fibre reinforced sheet moulding compound. Compos - Part A Appl Sci Manuf 2001;32:1271–9. doi:10.1016/S1359-835X(01)00085-9.

[52] Berges M, Léger R, Placet V, Person V, Corn S, Gabrion X, et al. Influence of moisture uptake on the static, cyclic and dynamic behaviour of unidirectional flax fibre-reinforced epoxy laminates. Compos Part A Appl Sci Manuf 2016;88:165–77. doi:10.1016/j.compositesa.2016.05.029.

[53] Placet V, Cisse O, Boubakar ML. Influence of environmental relative humidity on the tensile and rotational behaviour of hemp fibres. J Mater Sci 2012;47:3435–46. doi:10.1007/s10853-011-6191-3.

[54] Stamboulis A. Environmental durability of flax fibres and their composites based on polypropylene matrix. Appl Compos Mater 2000;7:273–94. doi:10.1023/A:1026581922221.

[55] Newman RH. Auto-accelerative water damage in an epoxy composite reinforced with plain-weave flax fabric. Compos Part A Appl Sci Manuf 2009;40:1615–20. doi:10.1016/j.compositesa.2009.07.010.

[56] Azwa ZN, Yousif BF, Manalo AC, Karunasena W. A review on the degradability of polymeric composites based on natural fibres. Mater Des 2013;47:424–42. doi:10.1016/j.matdes.2012.11.025.

Chapter 3

Problem statement

Chapter 3 Problem statement

3.1. Main objectives and hypothesis

The potential of flax fibres in composite applications is enormous. Their high specific mechanical properties, such as specific stiffness and strength allow for light designs of structural parts. Flax fibre composites also exhibit excellent fatigue properties while their environmental impact is much lower than for synthetic fibres. Two principle factors, however, are preventing the breakthrough of flax fibres in the composite industry. Firstly, and most importantly, the cost of flax fibres compared to glass fibres currently is still too high. This parameter is mainly linked to the energy intensive, hence costly, production process of the fibres which is made even worse by the limited fibre yield. Moreover, several operations in the fibre extraction chain still require transportation or manual labour. The second factor preventing their breakthrough is the inherent moisture sensitivity of the fibres. As flax fibres absorb moisture, composite manufacturers and end users are worried about the implication on the resulting short- and long-term composite properties. This raises the question on the durability of these materials, especially in conditions where cyclic variations of relative humidity are expected.

The two main objectives of this study are:

- to understand the impact of the fibre extraction operations on the physical and mechanical properties of the fibres and of their composites.
- to characterize the moisture absorption and desorption behaviour both under static and cyclic relative humidity levels and to establish the influence of moisture on the mechanical properties of the composites.

It is hypothesized that not every operation in the extraction process is required to obtain fibres which can be used in composites. Furthermore, the microstructure of the fibre is expected to control the moisture absorption and desorption process. The following chapters will contain research data to evaluate the above stated hypotheses.

3.2. Outline of the dissertation

In **chapter 2** the reader is briefly introduced to flax, flax fibres and the extraction process which is required to obtain the fibres. The traditional processing operations are described, and their necessity is critically assessed in view of their use in non-technical and technical textile applications. In the final part the moisture absorption in flax fibres and their composites is outlined. Moreover, the chapter illustrates several issues and shortcomings of data in literature related to the moisture sensitivity.

Chapter 4 focusses on the first objective of this study, namely understanding the extraction process. In first instance, a method is presented to accurately and reliably determine the properties of single fibres using optical strain measurement. This method development was important as it was subsequently used in the evaluation of single fibre properties of technical flax fibres. Next, the influence of flax fibre fineness and purity on the mechanical properties of fibres and composites is discussed. Finally, the chapter illustrates the importance of retting and flax fibre variety.

In the subsequent **chapter 5**, essential information is gathered regarding the parameters linked to the absorption and desorption of moisture in fibres and composites. Furthermore, the influence of a specific class of crosslinking treatments on this characteristic is determined.

The final results chapter, **chapter 6**, discusses the impact of cyclic absorption and desorption of moisture on the composite properties. This is done to approach the conditions as they would occur in structural applications.

In the final part of the dissertation, **chapter 7**, several scientific conclusions are formulated as well as their impact on current industrial practices. An outlook is presented on future research topics too deepen and broaden the results of this study.

Chapter 4

Relationships between the extraction process, fibre and composite properties

Chapter 4 Relationships between the extraction process, fibre and composite properties

4.1. Digital image correlation as a strain measurement technique for fibre tensile tests

D. Depuydt*, K. Hendrickx*, W. Biesmans, J. Ivens, A.W. Van Vuure, Digital image correlation as a strain measurement technique for fibre tensile tests, Compos. Part A: Appl. Sci. Manuf. 99 (2017) 76–83

* These authors contributed equally

4.1.1. Introduction

Fibre tensile tests are a way to determine the fibre's mechanical properties. It is the preferred method when limited material is available, in material development stage. The fibre's tensile properties are needed to perform micromechanical analyses and mechanical modelling of these materials and their composites. For synthetic fibres, the fibre properties are often provided by the manufacturers. However, when testing new materials, and especially from natural resources, datasheets are often not available.

Natural fibres are becoming increasingly important as a reinforcing fibre in composite materials. Therefore, the need for consistent fibre properties increases. Additionally, fibre manufacturers, or cultivators in the case of natural fibres, should be able to rely on fibre properties to measure the quality of the produced material. Unfortunately, the literature reveals a large range of the measured natural fibre properties, as can be seen in Table 4-1. A part of this variation can be attributed to the inherent variability in plant materials, but this is unlikely to be a complete explanation. There is a need for a consistent fibre testing method where the scatter is only a function of the material variability and not of the testing setup. Summerscales et al. [1] provide a checklist for the material related data and testing conditions that always should be reported in order to compare the experimental data with literature.

Table 4-1: Mechanical properties of flax and bamboo technical fibres. [a]weakest test length – strongest test length

Young's modulus (GPa)	Strength (MPa)	Failure strain (%)	Comment	Ref.
Flax				
31 ± 12	305 ± 120	1.3 ± 0.4	Gauge 75mm, 1mm/min, green flax	[4]
32 ± 12	310 ± 120	1.1 ± 0.4	Gauge 75mm, 1mm/min, retted flax	[4]
Bamboo				
33.37	639 ± 175 - 813 ± 94[a]	2.0 ± 0.6 - 2.9 ± 0.7[a]	Gauge 5,15,25,35 mm 1mm/min, steam explosion	[9]
43	775 ± 103 - 860 ± 119[a]	1.7 ± 0.2 - 1.9 ± 0.3[a]	Gauge 5,10,25,40 mm 1mm/min, mechanical extraction	[16]
35.91	503	1.4	Mechanical extraction	[20]
19.67	341	1.73	Chemical extraction	[20]
35.9 ± 13.1	441 ± 220	1.3	1mm/min, steam explosion	[21]

There are a few problems when testing natural fibres, that can lead to a wide range of results [2, 3]. Firstly, the literature does not always clearly state whether tests are performed on an *elementary* fibre (a single plant cell) or a *technical* fibre (a bundle of *elementary* fibres). It is well recognised that *elementary* fibres have higher stiffness and strength compared to *technical* fibres [4]. Secondly, when testing *technical* fibres at very short gauge lengths, *elementary* fibres can get gripped from end to end. The short gauge length reduces the probability of finding a weak location and reduces the effects of the weak inter-*elementary* fibre middle lamellae [3]. Besides the problems mentioned above, some other test related influencing factors are known: the strain rate (viscoelastic behaviour of the fibres), the environmental conditions (hygroscopic behaviour of natural fibres) and the gripping method (gripping of frame or fibre) should therefore always be reported [5, 6].

Haag et al. [2] summed up the previous issues, and added the importance of the determination of the cross sectional area. Via different optical techniques such as flatbed scanner, light microscopy and laser-based analysis they determined, from the projected diameter, the cross-section of the fibre. Furthermore, the authors tried different calculations to determine the cross-sectional area, assuming either a circular or an elliptical shape. It was seen that the scatter induced by the different calculation methods, resulted in a large variation which is partly responsible for the high scatter on the natural fibre properties. Thomason et al. [7] embedded *technical* flax and sisal fibres after tensile testing, and traced the contour of the fibre to determine the cross sectional. This method revealed a large difference between 'projected diameter techniques' and true diameter determination. In this research a gravimetric method was used, for the determination of fibre diameter, as is outlined in Defoirdt et al. [9]. It is believed that this method to determine the cross-section is user independent and can lead to a reduced spread on the fibre properties of natural fibres, avoiding the struggle of assuming a cross-sectional geometry of the irregular fibre and avoiding numerous measurements for each fibre.

A final influencing factor, which is normally not addressed, is the importance of a correct strain measurement method, and this is investigated in this paper. The strain in a fibre tensile test is often measured indirectly via the grip displacement, due to the difficulties in measuring it in a direct manner. To compensate for the system compliance, ASTM C1557-14 [8] prescribes a procedure to perform the data reduction. Defoirdt et al. [9] have developed an alternative procedure to correct the strain values to calculate the fibre properties[1]. However, for both methods it is necessary to test at least at 3 different gauge lengths. Hence, the method requires a significant number of fibres. It remains to investigate whether the correction on the strain for system compliance covers all the effects occurring during a tensile test. Fuentes et al. [10] developed a technique to measure local *technical* fibre properties by applying a speckle pattern on the fibre itself. The

analysed length hereby is a few millimetres, therefore giving insight in the local behaviour of the fibre. With the strain mapping it was also possible to indicate movements of *elementary* fibres.
In this research, a novel method is presented for direct measurement of strain during single fibre tensile testing. The new technique is compared to the existing methods, including the different ways of data reduction for tensile fibre tests. Cold drawn steel, a material with known properties, is used to assess the accuracy of each method. Finally, two types of natural fibres, bamboo and flax are characterised by the new technique.

4.1.2. Materials & Methods

4.1.2.1. Steel fibres

Cold drawn stainless steel (type 316L) fibres with a Young's modulus of 193 GPa and a diameter of 30 µm were supplied by NV Bekaert SA. The continuous steel fibres are produced in a bundle drawing process in which steel wires are embedded in a copper matrix and subsequently cold drawn to reduce the bundle diameter. After this process the copper matrix is removed electrochemically. The cross-sectional area of the fibres after drawing has a constant value but has a polygonal appearance [11]. Optical microscopy showed that the fibre diameter did not vary along the fibre length. The average cross sectional area of the fibre (A) was calculated by equation 1.

$$A = \frac{m}{\rho l} \qquad (1)$$

In the above equation m is the fibre mass, ρ is the fibre density and l is the fibre length. The fibre mass was determined with an analytical balance (Mettler AT 261 DeltaRange, Mettler Toledo) accurate to 10^{-5} g. The density of the steel fibres was 7.8 g/cm³.

4.1.2.2. Flax

Technical flax fibres (*Linum usitatissimum L.*) were sampled from FlaxTape 200, a unidirectional flax fibre tape for composite applications with an areal density of 200 g/m², supplied by Lineo NV. The tape consists out of scutched and aligned *technical* fibres, originating from different harvests to average out variations in the fibre properties. The density of the fibres was determined using a gas pycnometer, Beckman model 930, in which helium gas at a pressure of 0.5 bar was used as the displacement medium. Prior to the density measurement, the fibres were cut to a length of 1 cm and vacuum dried for 19 hours at 60°C. The short fibre length ensured that the lumen were accessibly to the helium gas during pycnometry. The measured density, i.e. cell wall bulk density, was 1.47 ± 0.01 g/cm³. For the tensile tests, the fibres were cut to a length of 10 cm, dried for 24 hours at 60°C and subsequently conditioned at 50% relative humidity (RH) and 21°C for at least 24

hours. In the latter condition, the mass of the fibres was measured to calculate the average cross-sectional area using equation 1.

4.1.2.3. Bamboo

Bamboo fibres (*Guadua angustifolia Kunth*) were sourced from Columbia, the Coffee Region, at 1300 meters above sea level with an annual average temperature of 23 °C and an annual average precipitation of 2200 mm and a relative humidity of 80% according to the environmental authorities of the region [12]. From the bamboo culms, which have an average culm diameter of 11 cm and a height of 20-23 meter, fibres were fully mechanically extracted from the middle part of the culm using an in house developed technique [12]. The density and average cross-sectional area of the fibres was determined following the same procedure and the same specimen preparation as for the flax fibres. The measured density was 1.36 ± 0.02 g/cm³.

4.1.2.4. Fibre tensile test set-up

To compare the different existing methods, steel fibres with known Young's modulus were chosen to experimentally determine the fibre modulus. The fibre was glued onto abrasive paper (PS11A grain 1000, Klingspor) frame using a double-sided glue roller (Permanent Pritt glue roller, Henkel). Although, this method of gripping may lead to premature failure of the fibre due to damage and thus lower the measured strength, it is irrelevant to determine the fibre modulus due to the defect insensitiveness of this latter property. Figure 4-1 shows the frame dimensions for a test gauge length of 50 mm and the position of the fibre in this frame. The frame facilitates sample mounting and fibre alignment in the grips, whereas the abrasive paper minimises fibre slippage during the test.
Tensile tests were performed on an Instron 5943 equipped with a 100 N load cell according to the ASTM C1557-14 [8] standard in a conditioned environment at 50% RH and 21°C. The frame was pneumatically gripped with a gripping force of 200 N. A pre-load of 0.01 N was applied to the fibre to straighten it. Fibre straightness is critical when the strain is to be derived from the crosshead displacement. Furthermore, the upper grip is connected to the load cell with a ball joint which ensures the alignment of the fibre in the first stages of the test. The crosshead displacement rate was chosen according to the ASTM C1557-14 standard, which suggests to achieve fracture within 30 seconds of testing [8]. For the investigated fibres, this translates to a crosshead displacement rate of 1.5 mm/min.

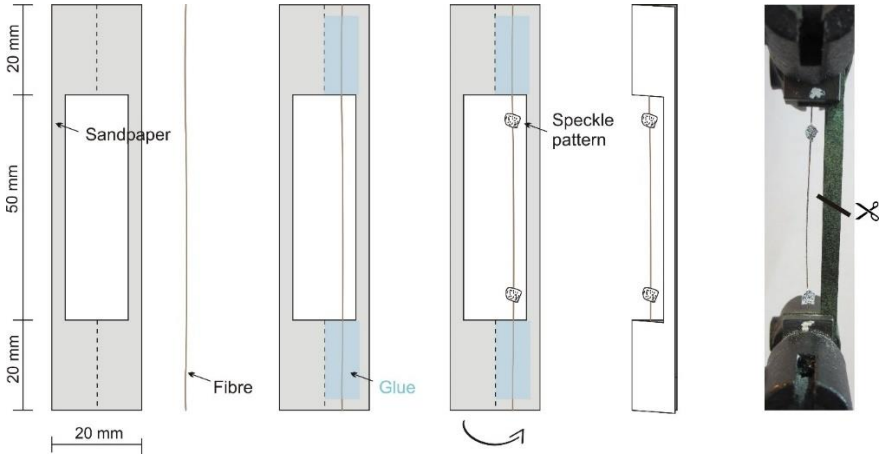

Figure 4-1: Sandpaper frames and fiber preparation for the fibre tests. The frame is folded to increase fibre gripping during the test. Indirect strain measurement does not require optical flags to be attached to the fibre whereas direct strain measurement relies on these optical flags to measure the strain.

4.1.2.5. Indirect strain measurement

In indirect strain measurement, the crosshead displacement is assumed equal to the axial extension of the fibre. When indirect strain measurement is used, the measured deformation can be partly due to the deformation of the test machine and slippage of the sample in the grips. To correct for the deformation of the test machine, samples with different gauge lengths are needed. Four different gauge lengths were used in this study: 10 mm, 20 mm, 35 mm and 50 mm. For the respective gauge lengths, 17, 20, 20 and 22 steel fibres were successfully tested.

4.1.2.6. Direct strain measurement

A method was developed to optically measure the fibre strain. The technique requires some additional modifications to the samples and the test set-up. The specimens were attached to an abrasive frame as outlined above. Additionally, two optical flags with an approximate diameter of 3 mm were attached to the fibre surface using white correction fluid (correction pen Tipp-Ex, Bic World). On these white flags a black speckle pattern was applied with spray paint, as shown in Figure 4-1.

The gauge length was fixed to 50 mm to manipulate the fibres easily, 22 steel fibres were successfully tested. This method requires only one gauge length to be tested since deformations due to slippage between fibre and grips are not registered. Moving to shorter or longer gauge lengths will increase or decrease the strength respectively but leave stiffness unaffected for synthetic fibres. In natural fibres also the stiffness can be affected when the gauge length becomes so small,

that at least one *elementary* fibre is gripped from end to end, this results in an increase in the stiffness [3]. In this research 24 bamboo fibres and 18 flax fibres were successfully tested.
Rotations or movements in the plane of the sand paper do not affect the strain measurement as in the case of indirect strain measurement. The out-of-plane motion (forward and backward fibre movement relative to the camera) does affect the strain measurement significantly and care should be taken to limit this movement during the test [2].
For the registration of the images during tensile testing, a digital camera (*Limess messtechnik & software GmbH,* Krefeld, Germany) with a spatial resolution of 96 dpi, equipped with a Componon-S 2.8/50 lens (Schneider Kreuznach, Bad Kreuznach, Germany), were used. The distance between sample and camera was 1 m. Samples were illuminated frontally with a 350 W halogen lamp. Subsequent images and force registration were taken during the test with an interval of 150 ms using acquisition software (LimShot, *Limess messtechnik & software GmbH,* Krefeld, Germany).

4.1.2.7. Data reduction

The accuracy of a tensile test depends on the accuracy of the force and strain measurement during the test. When the strain of the fibre is indirectly measured via the crosshead displacement a correction for the system compliance is made to deduce the fibre strain and fibre stiffness. Three different methods were applied to correct for the system compliance. The fourth method is based on direct strain measurement and does not require this correction.

- Method 1: Method as described in ASTM C1557-14 [8],
- Method 2: Method as described by Defoirdt et al. [9][1],
- Method 3: Modification of method 2
- Method 4: Digital image correlation

For all methods, the strain range for which the modulus of the fibres was calculated was 0 to 0.1%. This is a stricter requirement than set fort by ASTM C1557-14 which proposes a strain region between 0 and 0.3%. However, flax fibres already exhibit nonlinear behaviour in this region, justifying the restriction. Finally, it was assumed that all fibres deform homogeneously and elastically in this region.

a. Method 1: Data reduction according to ASTM C1557-14 [8]

In ASTM C1557-14 [8], the method to determine the fibre modulus takes into account the deformation of the test set-up. The crosshead displacement resulting from this increase in deformation per unit of force (F) is designated as the system compliance (C_s). The system compliance is assumed to be constant for a given test apparatus, gripping system and fibre type. Consequently, C_sF is the part of the total

crosshead displacement (ΔL) that is not attributable to fibre deformation. Considering the previous, equation 2 is valid which expresses the total crosshead displacement as the sum of fibre elongation (Δl_f) and set-up elongation (C_sF).

$$\Delta L = \Delta l_f + C_s F \tag{2}$$

Dividing equation 2 with the applied force and applying Hooke's law to replace the fibre elongation, equation 3 is obtained in which l_0 is the initial gauge length and E_f is the fibre Young's Modulus.

$$\frac{\Delta L}{F} = \frac{l_0}{AE_f} + C_s \tag{3}$$

This proves the linear relation between $\frac{\Delta L}{F}$ and $\frac{l_0}{A}$. Let $\frac{\Delta L}{F}$ be the inverse of the slope taken in the linear part of the measured force-displacement curve then the slope of the linear regression line of $\frac{\Delta L}{F}$ versus $\frac{l_0}{A}$ for different gauge lengths equals $1/E_f$. The method is graphically illustrated in Figure 4-2. In order to apply this method, tests on different $\frac{l_0}{A}$ ratios are necessary. ASTM C1557-14 suggests testing at least 3 different gauge lengths [8].

b. Method 2: Data reduction according to Defoirdt et al. [9]

An alternative method to perform the data reduction to obtain the fibre modulus has been proposed by Defoirdt et al. [9]. For each sample the apparent fibre modulus is calculated as defined in equation 4.

$$E_{app} = \frac{F l_0}{A\Delta L} \tag{4}$$

$$\lim_{l_0 \to \infty} \Delta L = \Delta l_f \tag{5}$$

At infinite gauge length, equation 2 transforms into equation 5, where ΔL equals Δl_f as C_sF becomes negligibly small. The regression line of E_{app} versus $\frac{1}{l_0}$ intersects the y-axis at E_f. The method is illustrated in Figure 4-2, where E_{app} is the stiffness found as the slope in the linear part of the stress-strain curve, derived from the measured force and displacement of the machine. Apart from a constant system compliance it also assumes the existence of a linear relationship between E_{app} and $\frac{1}{l_0}$.

c. Method 3: Modification to the data reduction by Defoirdt et al. [9]

By following the substitutions outlined below, equation 7 is obtained which reveals that the true relationship between E_{app} and $\frac{1}{l_0}$ is a rational function.

$$E_{app} = \frac{F l_0}{A\Delta L} = \frac{l_0 F}{A(\Delta l_f + C_s F)} \tag{6}$$

Combining equation 6 with $F = \frac{E_f \Delta l_f A}{l_0}$ and dividing by Δl_f

$$E_{app} = \frac{E_f}{1 + C_s E_f A \frac{1}{l_0}} \quad (7)$$

Finding E_f is identical to the unmodified method except that nonlinear least-squares fitting must be performed to fit the data to the rational function. The Levenberg-Marquardt algorithm [13, 14] was used to fit the experimental data to $E_{app} = \frac{A}{1+B*\left(\frac{1}{l_0}\right)}$ with A and B free variables. The optimized A value equals the effective fibre modulus E_f. The method is schematically represented in Figure 4-2.

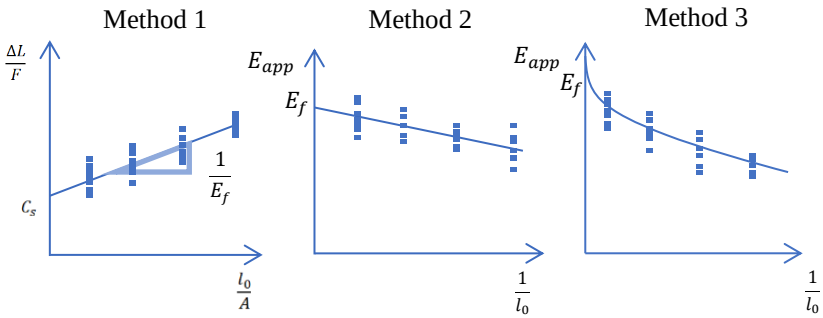

Figure 4-2: Schematic representation of the indirect methods to determine fibre modulus.

d. Method 4: Digital image correlation

Images were processed with Vic 2D 2009 (*Correlated Solutions*, Columbia, USA) correlation software to determine the pixel displacement of both optical flags. The subset window and step size were set to 15 and 3 pixels, respectively. Finally, the relative displacement of the optical flags was calculated and the fibre strain, based on the relative pixel displacements, was extracted.

4.1.2.8. Statistical analysis

To determine whether the sample data has been drawn from a normally distributed population, a Shapiro-Wilk test is performed. The null hypothesis for the test is that the data are normally distributed. For a chosen alpha level of 0.05, the null hypothesis is rejected when the p-value is less than 0.05. For normally distributed data, the results are summarized using the mean ± standard deviation notation.
To detect significant differences between group means, one sample, two-sided t-tests were performed. It was assumed that the population mean of the steel fibres was known and equal to 193 GPa. 95% confidence intervals of methods 1 to 3 were constructed according to the methods described in [15]. The 95 % confidence interval for the developed method was based on the t- statistic. To compare the sensitivity of the estimated modulus to random variations in the measured sample values, a Monte Carlo simulation was run for all three testing methods.

4.1.3. Results and discussion

4.1.3.1. Determination of the fibre modulus using indirect strain measurement

The results for the modulus of the steel fibres, according to the three different methods, are presented in Table 4-2, whereas Figure 4-3 to Figure 4-5 indicate how the results were obtained.

	E (GPa)	95% confidence interval	
Method 1	147 ± 4	141	155
Method 2	140 ± 2	135	144
Method 3	150 ± 4	142	157

Table 4-2: Results of fibre tensile tests on steel fibres using the different methods to determine the fibre Young's modulus.

The modulus for the steel fibre obtained via Method 1 (Figure 4-3) is 147 ± 4 GPa and via Method 2 (Figure 4-4) 140 ± 2 GPa. Both methods show only a minor spread on the results, reflected in their low standard deviation. However, the estimate of the Young's modulus is poor, since the real fibre modulus (193 GPa) is significantly different from the test result ($p=10^{-64}$). In paragraph 4.1.2.7.c the assumption of a linear relation between the apparent stiffness E_{app} and the inverse of the gauge length ($\frac{1}{l_0}$) was rejected and has been demonstrated to follow a rational relationship. Figure 4-5 shows the fit of this rational function to the experimental data. The predicted fibre stiffness based on method 3 is 150 ± 4 GPa, which is 7.3% larger than for method 2. Though the accuracy increases, this value still underestimates the effective stiffness of the steel fibres by as much as 25%.

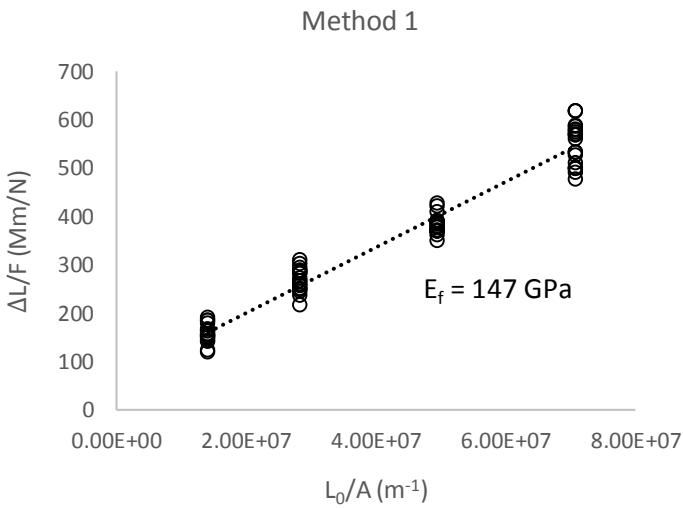

Figure 4-3: Linear regression of the measured data via method 1 for the determination of the fibre modulus.

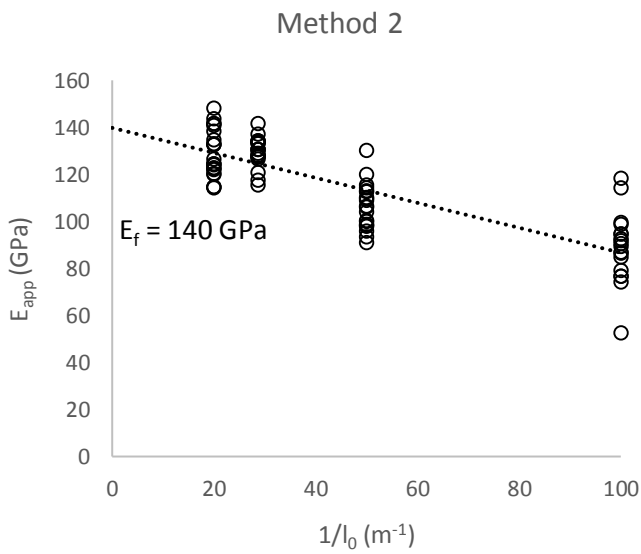

Figure 4-4: Linear regression and extrapolation of the measured data to infinite gauge length ($\frac{1}{l_0}$=0) via method 2 for the determination of the fibre modulus.

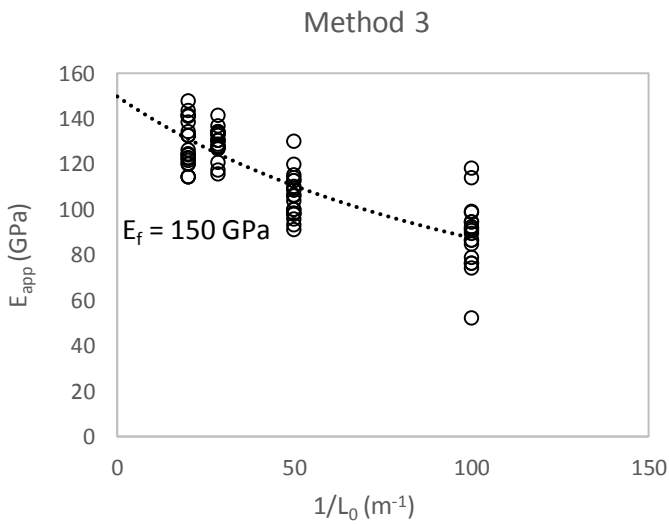

Figure 4-5: Rational extrapolation of the measured data via the method 3 for the determination of the fibre modulus.

It must be concluded that neither method 1, nor method 2 or 3 is able to adequately correct the measured strain values and obtain a correct value for the Young's Modulus. This is caused by the assumption of a constant system compliance. The system compliance was created as a constant that corrects for the elastic deformations of the machine parts. However, it does not correct for slippage that can occur between fibre and frame or between frame and grip. It could be argued that a different sample preparation method would lead to a decreased contribution of slippage to the total deformation. Indeed, this might be correct, but slippage effects are generally too small to detect visually, requiring advanced techniques to correct for the previous, generating an additional disadvantage of the indirect method. The crosshead displacement attributable to slippage is unpredictable and is not necessarily a function of the applied force. Therefore, equation 2 no longer holds rendering all indirect strain methods invalid. The increase in crosshead displacement not attributable to fibre elongation, generated by this effect can lead to a significant underestimation of the fibre modulus. This effect is especially pronounced for very stiff fibres where the material elongation is small. Here, a small increase in crosshead displacement attributable to slippage can lead to an extremely high relative error on the material elongation and hence on the fibre stiffness. It is therefore advised to use very long fibres (>50 mm) if this technique is considered.

Considering the challenge it would be to take slippage effects into account, the authors hypothesise that the solution must be found in an alternative, direct strain measurement method.

4.1.3.2. Sensitivity analysis

To compare the sensitivity of the estimated modulus to random variations in the measured sample values, a Monte Carlo simulation was run for all three testing methods. In this simulation, fixed, experimentally obtained values were chosen for the parameters depicted in Table 4-3. From these values and by using equation 2, the average F/ΔL was calculated for each gauge length.

E_f (GPa)	193			
A (m²)	7 E-10			
C_s (m/N)	64.5 E-06			
Number of samples per gauge length	17			
l_0 (mm)	10	20	35	50
Average $\frac{F}{\Delta L}$ (N/m)	6288.34	3755.95	2618.14	1823.81
Stdev $\frac{F}{\Delta L}$ (N/m)	1054.08	342.51	127.07	144.54

Table 4-3: Input parameters for the Monte Carlo simulation.

Gaussian noise was added to the simulated values F/ΔL, modeling random variations in the measured samples. This way, a simulated set of 17 samples is created for each gauge length. The standard deviations of the Gaussian noise were chosen equal to the experimentally determined standard deviations for each gauge length. To justify the generation of Gaussian distributed data a Shapiro-Wilk normality test was performed on the experimental data of ΔL/F and F/ΔL. It was concluded that both data series originate from a normally distributed population (α=0.05). From the generated samples, the modulus was calculated according to the different methods. This process was repeated 10 000 times.

To evaluate the accuracy of the different methods, the root-mean-square error (RMSE) was calculated from equation 8. In this equation, E_i represents the fibre modulus that is calculated in each iteration of the Monte Carlo simulation. By comparing the RMSE for the different methods in Table 4-4, it can be seen that method 2 is the most sensitive to variations of the force-displacement data.

N=10000	Method 1	Method 2	Method 3
RMSE	0.0344	0.0880	0.0303
RB	0.0061	-0.0867	0.0012

Table 4-4: RMSE of the different methods after 10 000 Monte Carlo iterations.

To explain this difference, a second indicator, the relative bias (RB), was calculated according to equation 9. For high iteration numbers, the bias on the modulus should converge to zero.

$$\mathrm{RMSE} = \sqrt{\frac{\sum_{i=1}^{n}\left(E_i - E_f\right)^2}{n}} \tag{8}$$

$$\mathrm{RB} = \frac{\frac{\sum_{i=1}^{n}(E_i - E_f)}{n}}{E_f} \tag{9}$$

Figure 4-6 shows the relation of the bias to the number of Monte Carlo iterations. It can be seen that method 2 is constantly underestimating the stiffness by around 8%, which explains the high RMSE for this method. Method 1 and method 3 both have a negligible bias and an equally low RMSE, from which we can conclude that the methods are equally accurate in the estimation of the fibre modulus.

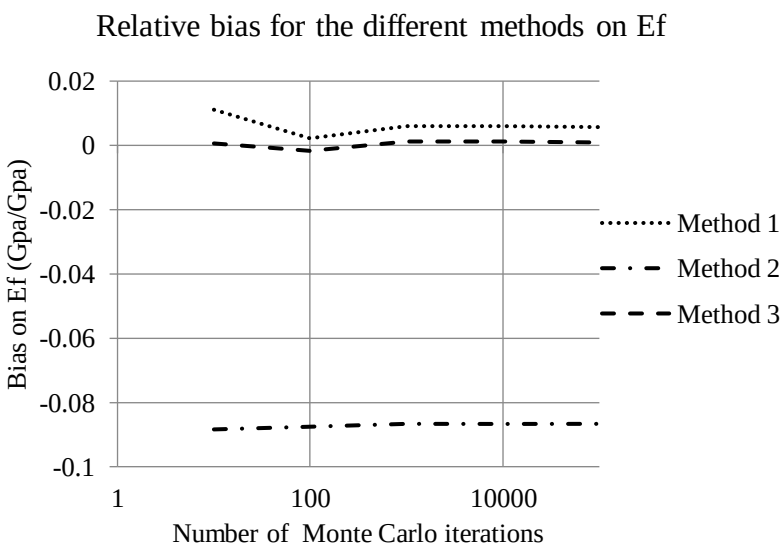

Figure 4-6: The evolution of the bias on E_f in relation to the number of iterations in the Monte Carlo simulation for the different methods.

4.1.3.3. Determination of the fibre modulus using direct strain measurement

The steel fibre modulus obtained by digital image correlation is 187 ± 12 GPa, as listed in Table 4-5.

Fibre	E modulus (GPa)	Tensile strength (MPa)	Strain to failure (%)
Steel	187 ± 12	1564 ± 141	0.98 ± 0.09
Bamboo	52 ± 7	658 ± 135	1.33 ± 0.20
Flax	40 ± 11	643 ± 247	1.64 ± 0.32

Table 4-5: Tensile modulus, strength and strain to failure of the fibres using direct strain measurement

Even though the actual modulus (193 GPa) falls within the confidence interval of the test result, a larger variability is found in comparison with the previous three methods. However, the bias on the result is significantly lower. Comparing the relative bias on the results of Table 4-4, 21%-26%, with the relative standard deviation found in the digital image correlation experiment, 6%, it becomes clear that the relative bias on method 1-3 is bigger than the relative standard deviation found in the digital image correlation method. However possible routes to further decrease the variability of the method are described in Table 4-6. The proposed technique is promising although further optimization is required to decrease the standard deviation on the mean. In this case, digital image correlation is the preferred method for the determination of the strain and stiffness.

The mechanical properties of *technical* bamboo and flax fibres were measured using digital image correlation. For the bamboo *technical* fibre, a modulus of 51.8 ± 6.8 GPa was measured with an average failure strain of 1.33 ± 0.20 %. The stiffness exceeds the values measured in literature [16], due to the improved measurement of the fibre strain. Flax *technical* fibre modulus was determined to be 40 ± 11 GPa with a strain to failure of 1.64 ± 0.32 %. This result corresponds well with data found in literature for *technical* flax fibres [4, 17]. It is assumed that the gauge length (50 mm) ensures that no elementary fibre spans the clamp to clamp length. Note that the stiffness of individual technical flax fibres is much lower than compared to their value in composites (+/- 60 GPa). This is likely caused by sliding of the elementary fibres in the technical fibre upon tensile loading. In composites, this is prevented as the matrix surrounds most of the elementary fibres. However, the values in the previous references should be interpreted with caution as they utilise method 1 to calculate the fibre stiffness. Note that this stiffness value is not representative for the behaviour of flax fibres in composite materials where the behaviour of *elementary* fibres dominates the composite stiffness instead of the *technical* fibres. This has been extensively discussed in Shah et al. [3].

4.1.3.4. Opportunities in direct strain measurement on fibres

Direct strain measurement is especially valuable when testing natural fibres. A large portion of the natural fibres has not been screened for their potential use as a reinforcing fibre in composites. Using the conventional indirect strain methods, testing a new fibre requires large amounts of fibres and is time consuming [18][4]. Moreover, extracting the fibres from the plants can be difficult. ASTM C1557 advises to use at least 3 different gauge lengths. Using the presented method there is no need to vary the gauge length of the fibres, therefore three times fewer samples are required.

In conjunction with this, the usefulness of testing single *technical* natural fibres is sometimes questioned. Indeed, certain natural fibres, such as *technical* flax fibres, underperform in single fibre tests relative to their performance in composites. This is explained by additional deformation modes which exist due to the microstructure of the fibres. The most prominent are relative sliding of elementary fibres within the technical fibre and reorientation of cellulose microfibrils within the elementary fibres. Nevertheless, fibre testing can serve to first screening tool and to investigate potential extraction issues.

Optical strain measurement allows to measure local strains directly on the fibre surface [10]. It has been shown that appropriate speckle patterns can be produced, even at the micro-scale [19][5]. This technique is promising to produce full-field strain maps of the fibres during deformation and to investigate features such as defects.

As discussed in previous sections, during optical strain registration some environmental or experimental parameters may influence the test result. A summary of the most important factors, together with possible mitigations, is given in Table 4-6.

Physical parameter	Risk	Mitigation
Out-of-plane movement	When the fibre moves towards or away from the camera, the registered pixel movement is under- or overestimated, respectively [22].	1. Limit the out-of-plane movement of the fibre by choosing a ball joint connection of 1 grip. 2. Correct using a single camera by rotating or using a region of interest as described in [22, 23] 3. Eliminate by using a stereo 2D set-up with 2 cameras to measure the out-of-plane movement [24].

Out-of-plane movement	The optical flags can be considered as 2D flags. Rotation of the flags may occur during the test.	Prevent twisting the fibre during sample preparation.
Lighting conditions	The lighting conditions change during the test.	1. Use a light source with a constant and diffuse illuminance [25, 26]. Increasing the illuminance leads to a lower exposure time which decreases noise. 2. If lightning changes cannot be prevented, use a robust correlation algorithm [27].
Optical flags	The attachment of the optical flags can give rise to stress concentrations during fibre loading, especially when the material used to create the optical flag has a high stiffness compared to the fibre. The measured stiffness would be largely unaltered but the fibre may fail prematurely, hence the apparent fibre strength and strain to failure is lower.	To prevent stress concentrations, the flag material stiffness should be as low as possible. When attaching flags to fibres that have high strains to failure the flags may detach or crack during the test. To avoid this, use a flag material with a high failure strain.
Gauge length	The length in pixels of the fibre's gauge length is insufficient, lowering the accuracy of the correlation.	Although DIC measurements have sub-pixel resolution it is advisable that the gauge length in the images is longer than 50 pixels.

Table 4-6: Risks and mitigation during fibre testing of selected physical parameters

4.1.4. Conclusions

Measuring mechanical properties of fibres is crucial to gain more insight in the composite mechanics. Although standardized, the current measurement and especially data reduction methods are prone to significant error. According to the data reduction method proposed by ASTM C1557-14 [8] the modulus of 316L steel fibres was underestimated by 25%. This was due to an amount of crosshead displacement that did not result in fibre deformation. Instead, the additional displacement could be caused by slippage between fibre and frame and/or between frame and grip.

Indirect strain measurement is therefore not advised to determine the fibre's modulus and strain to failure since slippage is difficult to detect during or after the test. Hence, the results produced with this method when slippage occurs should be considered invalid, even when the standard deviation on the method would be small. Direct strain measurement based on digital image correlation eliminates the effect of slippage because the deformation of the fibre is registered optically. Using this direct method, the measured mean stiffness is highly accurate. The measured stiffness of the above-mentioned fibres was not statistically different from the effective fibre stiffness. However, the spread on the result was increased compared to the indirect measurement methods. Indeed, two-dimensional optical strain measurement is sensitive to lighting conditions and out-of-plane fibre motion. The latter problem could possibly be eliminated by moving towards stereo-2D optical strain measurement, leaving direct strain measurement as the preferred method in determining the fibre tensile modulus.

Direct strain measurement offers the advantage of reducing the number of tests compared to indirect techniques, all requiring tests at different gauge lengths. This creates a significant opportunity for the evaluation of natural fibre properties where material scarcity and extraction difficulties often prevent the use of an indirect method.

References

[1] Summerscales J, Le Duigou A, Baley C. A checklist for the description of plant/vegetal/bast natural fibre reinforced composites. ICCM 20th Internation Conference on Composite Materials. Copenhagen2015.
[2] Haag K, Mussig J. Scatter in tensile properties of flax fibre bundles: influence of determination and calculation of the cross-sectional area. Journal of Materials Science. 2016;51(17):7907-17.
[3] Shah DU, Nag RK, Clifford MJ. Why do we observe significant differences between measured and 'back-calculated' properties of natural fibres? Cellulose. 2016;23(3):1481-90.
[4] Alix S, Lebrun L, Marais S, Philippe E, Bourmaud A, Baley C, Morvan C. Pectinase treatments on technical fibres of flax: Effects on water sorption and mechanical properties. Carbohydrate Polymers. 2012;87(1):177-85.
[5] Kim JH, Heckert NA, Leigh SD, Kobayashi H, McDonough WG, Rice KD, Holmes GA. Effects of fiber gripping methods on the single fiber tensile test: I. Non-parametric statistical analysis. Journal of Materials Science. 2013;48(10):3623-37.
[6] Kim JH, Heckert NA, Mates SP, Seppala JE, McDonough WG, Davis CS, Rice KD, Holmes GA. Effect of fiber gripping method on the single fiber tensile test: II. Comparison of fiber gripping materials and loading rates. Journal of Materials Science. 2015;50(5):2049-60.
[7] Thomason JL, Carruthers J, Kelly J, Johnson G. Fibre cross-section determination and variability in sisal and flax and its effects on fibre performance characterisation. Composites Science and Technology. 2011;71(7):1008-15.
[8] ASTM C1557-14, Standard Test Method for Tensile Strength and Young's Modulus of Fibers, ASTM International, West Conshohocken, PA, 2014, www.astm.org
[9] Defoirdt N, Biswas S, De Vriese L, Tran LQN, Van Acker J, Ahsan Q, Gorbatikh L, Van Vuure A, Verpoest I. Assessment of the tensile properties of coir, bamboo and jute fibre. Composites Part a-Applied Science and Manufacturing. 2010;41(5):588-95.
[10] Fuentes CA, Willekens P, Hendrikx N, Lemmens B, Claeys J, Croughs J, Dupont-Gillain C, Seveno D, Van Vuure A. Microstructure and mechanical properties of hemp technical fibres for composite applications by micro computed tomography and digital image correlation. ECCM17 17th European Conference on Composite Materials. Munich, Germany2016.
[11] Callens MG, Gorbatikh L, Verpoest I. Ductile steel fibre composites with brittle and ductile matrices. Composites Part A: Applied Science and Manufacturing. 2014;61:235-44.
[12] Trujillo E. Polymer composite materials based on bamboo fibers. In: Leuven K, editor. Leuven2014.
[13] Levenberg K. A Method for the Solution of Certain Non-Linear Problems in Least Squares. Quarterly of Applied Mathematics. 1944;2:164-8.
[14] Marquardt DW. An Algorithm for Least-Squares Estimation of Nonlinear Parameters. SIAM Journal on Applied Mathematics. 1963;11(2):431-41.
[15] Pomerantsev AL. Confidence intervals for nonlinear regression extrapolation. Chemometrics and Intelligent Laboratory Systems. 1999;49(1):41-8.
[16] Osorio L, Trujillo E, Van Vuure AW, Verpoest I. Morphological aspects and mechanical properties of single bamboo fibers and flexural characterization of

bamboo/epoxy composites. Journal of Reinforced Plastics and Composites. 2011;30(5):396-408.
[17] Bos HL, Van den Oever MJA, Peters O. Tensile and compressive properties of flax fibres for natural fibre reinforced composites. Journal of Materials Science. 2002;37(8):1683-92.
[18] Lefeuvre A, Bourmaud A, Lebrun L, Morvan C, Baley C. A study of the yearly reproducibility of flax fiber tensile properties. Industrial Crops and Products. 2013;50:400-7.
[19] Mehdikhani M, Aravand M, Sabuncuoglu B, Callens MG, Lomov SV, Gorbatikh L. Full-field strain measurements at the micro-scale in fiber-reinforced composites using digital image correlation. Composite Structures. 2016;140:192-201.
[20] Rao KMM, Rao KM. Extraction and tensile properties of natural fibers: Vakka, date and bamboo. Composite Structures. 2007;77(3):288-95.
[21] Okubo K, Fujii T, Yamamoto Y. Development of bamboo-based polymer composites and their mechanical properties. Composites Part a-Applied Science and Manufacturing. 2004;35(3):377-83.
[22] Wittevrongel L, Badaloni M, Balcaen R, Lava P, Debruyne D. Evaluation of Methodologies for Compensation of Out of Plane Motions in a 2D Digital Image Correlation Setup. Strain. 2015;51(5):357-69.
[23] Tay CJ, Quan C, Huang YH, Fu Y. Digital image correlation for whole field out-of-plane displacement measurement using a single camera. Optics Communications. 2005;251(1-3):23-36.
[24] Badaloni M. Optimization and design of tests for material characterization using simulated experiments. In: KU Leuven FoES, editor.2016.
[25] Pan B, Lu Z, Xie H. Mean intensity gradient: An effective global parameter for quality assessment of the speckle patterns used in digital image correlation. Optics and Lasers in Engineering. 2010;48(4):469-77.
[26] Hua T, Xie HM, Wang SM, Hu ZX, Chen PW, Zhang QM. Evaluation of the quality of a speckle pattern in the digital image correlation method by mean subset fluctuation. Optics and Laser Technology. 2011;43(1):9-13.
[27] Pan B, Qian KM, Xie HM, Asundi A. Two-dimensional digital image correlation for in-plane displacement and strain measurement: a review. Measurement Science and Technology. 2009;20(6).

4.2. The influence of flax fibre fineness and purity on the mechanical performance of the technical fibres and their composites

Kevin Hendrickx, Ramona R. Sitohang, Wim Thielemans,
Aart Willem Van Vuure, Jan Ivens

4.2.1. Introduction

The historical use of flax fibres in non-technical textiles has led to an elaborate process to extract the fibres from the plant [1,2]. Flax fibre producers typically follow the extraction chain shown in Figure 4-7.

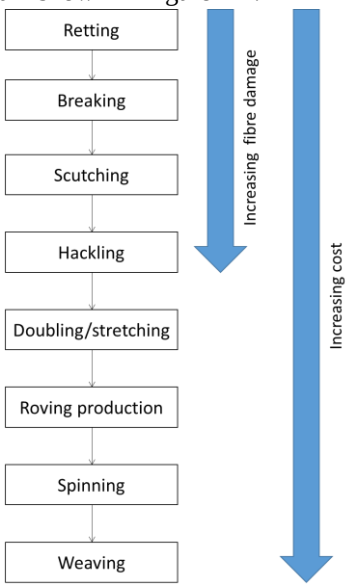

Figure 4-7: Traditional extraction chain for flax fibres.

Retting is the first step in the extraction of the fibres and starts immediately after pulling the flax stems from the field. Several forms of retting exist such as water, dew, and enzymatic retting. Presently, dew retting, also known as field retting, has the lowest production costs and is the dominant process despite the fact that it results in a lower and inconsistent fibre quality [3]. During retting, microbial and fungal processes partially degrade the pectins and other cementing compounds that bind the fibres to other tissues of the plant stem [4]. The activity of these microorganisms, and thus the extent of degradation, is highly dependent on temperature and the amount of humidity (morning dew and rainfall). Currently, there are no methods in place to quantify this degradation. This implies that the stems only proceed to the subsequent breaking step after an experience-based yet subjective assessment by the harvester.

Before decortication can start, the non-fibrous parts of the stem called shives are broken between serrated rollers to maximize their removal. For flax, the

decortication step, referred to as scutching, is executed using turbines wherein steel plates repeatedly beat the fibres [5]. The semi-clean fibres are collected at the end of the turbine from where they proceed to the hackler.
Steel pins parallelize the scutched fibres in the hackling process by combing them. As the fibres move through the machine, the pin spacing of the combs decreases, leading to fibre refinement by reducing their diameter. After hackling, the fibres are considered clean and have their maximum fineness. Further processing aims at preparing the hackled flax to be spun into yarns which can in their turn be processed to weaves.
Each step in the previous process is designed to maximize the final quality of the textile that is produced in terms of purity, homogeneity, smoothness, and yarn strength. However, the quality requirements for non-technical textiles are very different from textiles to be used in composites. Moreover, every mechanical operation increases the cost of the fibres due to the labour and energy involved in the process and decreases the fibre yield as fibre losses occur throughout the extraction. Especially during hackling these fibre losses can be significant, ranging between 35% and 45% [6,7]. Therefore, this paper investigates the effects on the mechanical properties of flax fibre composites when the extraction process is interrupted after the scutching step. More specifically, the effect of fibre fineness and residual non-fibrous material on the fibre properties and composite properties is examined. This will enable to check whether lower production cost flax fibres can be used to obtain better performing composites. If the properties remain stable or increase, significant cost savings may be expected.

4.2.2. Materials and methods

4.2.2.1. Flax fibres

Flax (*Linum usitatissium L.* , Vesta variety) was grown and retted in 2013 and 2014 at four different locations in France and Belgium, each location resulting in a different batch of fibres. All stems were dew retted on the field until they were deemed optimally suitable for scutching by the producer. Scutching for all fibres was performed with identical settings of the scutching turbines. These turbines, although installed at various locations, were considered identical as they were all constructed by the same manufacturer. Samples were collected immediately after the fibres exit from the scutching turbine. Prior to any operation or measurement, the fibres were conditioned at 21°C and 65% RH for at least 24 hours.

4.2.2.2. Matrix

A bisphenol A epoxy resin (Epikote 828LVEL) was mixed with 1,2 diaminocyclohexane in a 100:15.2 w/w ratio, to produce the epoxy matrix for the composite specimens.

4.2.2.3. Combing

To influence their fineness and purity, the fibres were repeatedly hackled with steel combs of decreasing pin spacing, shown in Figure 4-8. A first comb with a staple design was used to disentangle the fibres. The spacing between the staples was 20 mm to limit fibre breakage. For the second and third comb the staples were replaced by pins to ensure maximum fibre gripping. The pin spacing was 7 mm and 3.5 mm, respectively.

Batches of fibres that have undergone combing will be denoted by a suffix C followed by the number 1, 2 or 3 corresponding to the last comb number that was used to refine the batch. The number of times one comb passed through the fibre batch was fixed to 100.

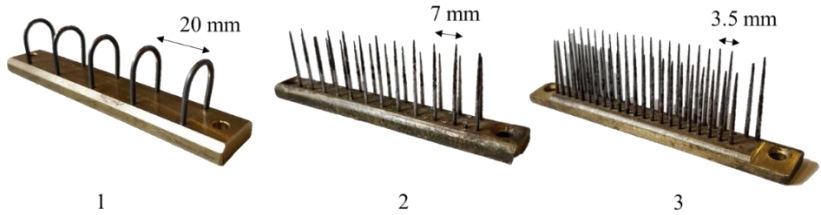

Figure 4-8: Different combs used to increase the fineness of the fibres.

4.2.2.4. Fineness measurements

Fibre fineness is a parameter that is indicative of the transverse size of the fibres. It is not unambiguously defined for natural fibres due to their irregular geometry, hence various methods exist to estimate this property [8].

In the micronaire method an airflow is sent through a standard amount or mass of fibres and the pressure drop is measured. From this pressure drop the specific surface can be calculated according to the ISO 2370 standard which can subsequently be converted to the International Fineness Standard (IFS) value. This value excludes the possible influence of the apparatus and operator on the measured results [9]. The air flowrate was set to 20 l/min. Each measurement was repeated four times.

In an alternative method, known as the gravimetric approach, the mass of a fibre is measured and an apparent average fibre diameter can be calculated assuming a certain geometric shape of the fibre cross section. As outlined in ASTM D 7025, the average fibre cross sectional area (A) can be calculated by dividing the mass of the fibres (m) by its density (ρ) and length (l) as shown in equation 1. The density of the used flax fibres is 1.44 g/cm³.

$$A = \frac{m}{\rho l} \tag{1}$$

Assuming a cylindrical cross section, an apparent diameter of the fibre can be calculated. A significant disadvantage of this method is the averaging of the

diameter along its length. Technical flax fibres, which consist of elementary fibre bundles, can split at certain locations reducing the local diameter. This phenomenon is not taken into account in the above method. Moreover, as every fibre needs to be weighed separately the method is very time consuming. For the gravimetric measurements at least 15 fibres measuring 15 cm in length were sampled. The mass of each fibre was measured with an analytical balance accurate to 10^{-5} g.

A third, newly proposed method uses optics combined with image processing to detect certain fibre features. In this automated image analysis, a number of fibres is randomly selected from a batch. A total number of 30 samples all 10 cm in length was collected. The fibre ends are glued to a contrasting background paper and are scanned with an optical flatbed scanner with a minimum resolution of 1200 dpi. An algorithm was developed that segments the fibres and separates them from the background. The algorithm computes the local mean intensity around each pixel (first-order statistics), using the *adaptthresh* function in MATLAB, in a specified region around that pixel. It subsequently calculates the threshold value based on the local mean intensity and considers the pixel to belong to the background when its intensity value is smaller than the threshold. Vice versa, if its value is larger, the pixel is marked as a foreground pixel. When the contrast between fibres and background is sufficient, the fibres will appear as a set of foreground pixels. In a subsequent step the axial centreline of the fibres is determined and for every pixel on this line the distance to the nearest background pixel is calculated as schematically illustrated in Figure 4-9. From this data the fibre diameter distribution is constructed. An inherent disadvantage of this technique is that it registers only projections of fibre shapes, the determined diameters are apparent as they do not fully take into account the three-dimensional nature of the fibre.

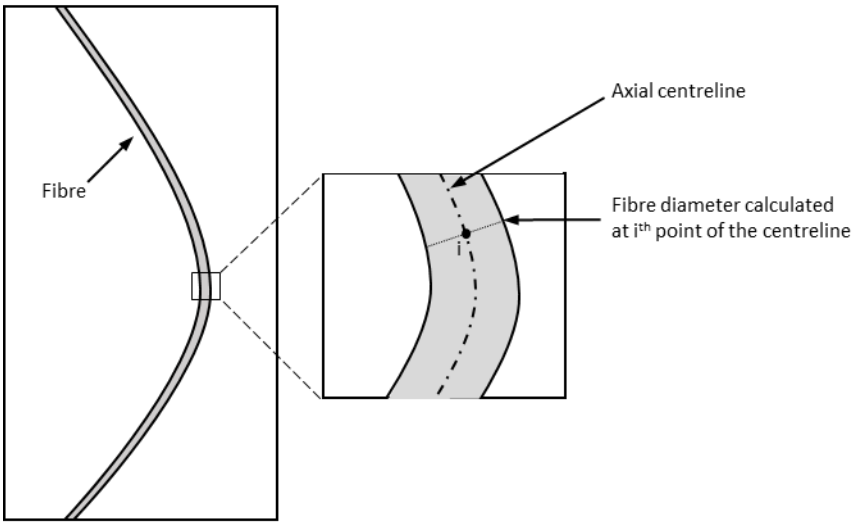

Figure 4-9: Schematic illustration of the fibre diameter algorithm. The diameter is calculated for every pixel found on the axial centerline of the fibre.

4.2.2.5. Technical fibre tensile tests

To determine the mechanical properties of a flax fibre it was glued onto abrasive paper (PS11A grain 1000, Klingspor) frame using a double-sided glue roller (Permanent Pritt glue roller, Henkel). The gauge length, i.e. fibre length was 50 mm. The frame facilitates sample mounting and fibre alignment in the grips, whereas the abrasive paper minimises fibre slippage during the test.
Tensile tests were performed on an Instron 5943 equipped with a 100 N load cell in a conditioned environment at 50% RH and 21°C. The frame was pneumatically gripped with a gripping force of 200 N. A pre-load of 0.01 N was applied to the fibre to straighten it. The upper grip is connected to the load cell with a ball joint which ensures the alignment of the fibre in the first stages of the test. The crosshead displacement rate was set equal to 1 mm/min. During data reduction, the modulus of the fibres was always calculated in the strain range between 0 and 0.1% strain.

4.2.2.6. Purity measurements

Impurities in flax fibre composites are mainly related to the presence of shives and dust. These porous structures have very low mechanical properties and are expected to cause stress concentrations during mechanical loading [10]. Hence, they are often considered unwanted in composites. Refining the fibres by combing removes shive and dust particles from the fibres simultaneously with the fibre parallelization. Another form of impurity may consist of pectin that is partially covering the elementary fibres (i.e. fibre cells) within the technical fibres. This

substance may hinder intimate contact between fibres and matrix during impregnation.

During the combing, some shorter fibres are pulled out from the batch rather than being refined, due to the limited clamping force applied to the fibres. These fibres are not considered impurities, thus they are separated and excluded from the impurities fraction. All the debris that is removed during combing is collected and submerged in water. The short fibres are separated from the shives by their difference in density as the density of water lies between that of the shives and the fibres. A gravimetric measurement of all fractions determines the final purity (P) of the fibres by equation 2. In this equation m_f is the mass of the fibres after the combing and separation procedure is completed and m_i is the mass of the fibres and impurities after executing step i.

$$P = \frac{m_f}{m_i} \tag{2}$$

4.2.2.7. Composite production

Prior to impregnation the flax fibres were dried in an oven at 60°C for 24 hours and subsequently dried under vacuum at 40°C for at least 1 hour prior to impregnation. Note that this does not imply that all of the moisture was removed from the fibres. From prior knowledge and non-destructive quality assessments, it is known that these steps suffice to prevent excessive moisture evaporation during impregnation and curing which could cause porosity in the composites.

Flax fibre - epoxy unidirectional composites were produced based on the procedure outlined in ISO 10618, adapted to natural fibres using compression molding [11]. A detailed outline of this procedure has been given by Bensadoun et al. [11]. The resin was degassed in a vacuum chamber prior to impregnation and curing of the resin was performed under atmospheric pressure at 80°C for 1 hour supplemented by a post-cure step at 150°C for 1 hour.

The fibre volume fraction (V_f) was set to 35% and the specimen thickness to 2 mm. All other dimensions were in accordance with ISO 10618 prescribing the dimensions to be used for unidirectional composite test specimens in tension.

ASTM D7264/D7264M prescribes the necessary sample dimensions for flexural testing of unidirectional composites. In deviation of ASTM D7264/D7264 M, the thickness-to-span ratio was altered to 1:16 instead of the advised 1:32. The decrease in ratio was necessary to guarantee the alignment of the fibres in the transverse specimens during production. Nevertheless, it was verified that the altered ratio did not influence the results as a control experiment using hackled flax fibres did not show significant differences in transverse properties. Therefore, the increase in shear stresses appear to be sufficiently low to not have a significant impact on the transverse behaviour of the composites.

4.2.2.8. Composite testing & calculation of the mechanical properties

a. Longitudinal properties

Longitudinal tensile tests were performed according to ISO10618, adapted to natural fibre composites [11]. An Instron 5567 tensile testing machine was equipped with a load cell of 30 kN and the crosshead displacement rate was set to 2 mm/min. As flax fibres are known to exhibit non-linear behaviour, the modulus of the composites (E_c) was calculated in the region between 0 and 0.1% strain. To compare results between different batches of fibres, a back-calculation to the fibre stiffness (E_f) and strength (σ_f) was performed using the inverse rules of mixtures in equations 3 and 4. Note that the calculation of the back-calculated fibre strength involves the failure strain of the composite (ε_c^*)

$$E_f = \frac{E_c - (1 - V_f)E_m}{V_f} \tag{3}$$

$$\sigma_f = \frac{\sigma_c - (1 - V_f)E_m \epsilon_c^*}{V_f} \tag{4}$$

All tests were performed under normal ambient conditions, on specimens that had been conditioned at 50%RH and 21°C for 7 days.

4.2.3. Transverse properties

Three-point flexural tests were performed following ASTM D7264/D7264 M. An Instron 5567 was equipped with a load cell of 1 kN and the crosshead displacement rate was set to 1 mm/min. All tests were performed under normal ambient conditions, on specimens that had been conditioned at 50%RH and 21°C for 7 days.

4.2.4. Results and discussion

4.2.4.1. Fibre fineness

The fibre fineness was measured for various batches of fibres with the methods described above. The batches differ in degree of retting, growth location, or both. For every batch the IFS values from airflow measurements and the average gravimetric fineness was determined.

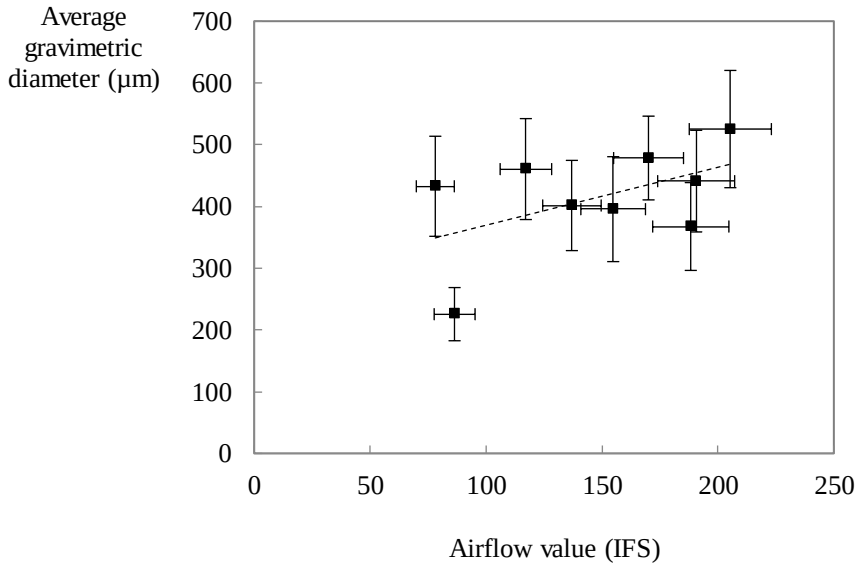

Figure 4-10: Correlation of fineness values obtained with the gravimetric method and airflow. (R^2=0.26)

As demonstrated in Figure 4-10 the correlation between the IFS values from airflow and gravimetric diameters is very poor (R^2=0.26). Although the airflow method allows for a fast identification of fineness, linking the IFS value to an average value of fibre size appears to be impossible. The lack of correlation between IFS value and gravimetric diameter can be due to the effect of fibre packing in the apparatus. Especially for coarser fibres such as flax, preferential airflow paths are created easily, even with high packing pressures, leading to biased measurements.

The above approach also exposes a significant disadvantage of the airflow technique. It does not provide any information on the distribution of fibre diameters. The relative frequency histogram of gravimetric fibre diameters in Figure 4-11 shows that even for the very limited amount of sampled fibres, there is a significant spread on the measured diameters. Hence, to fully characterize a batch of fibres, its diameter distribution should be determined.

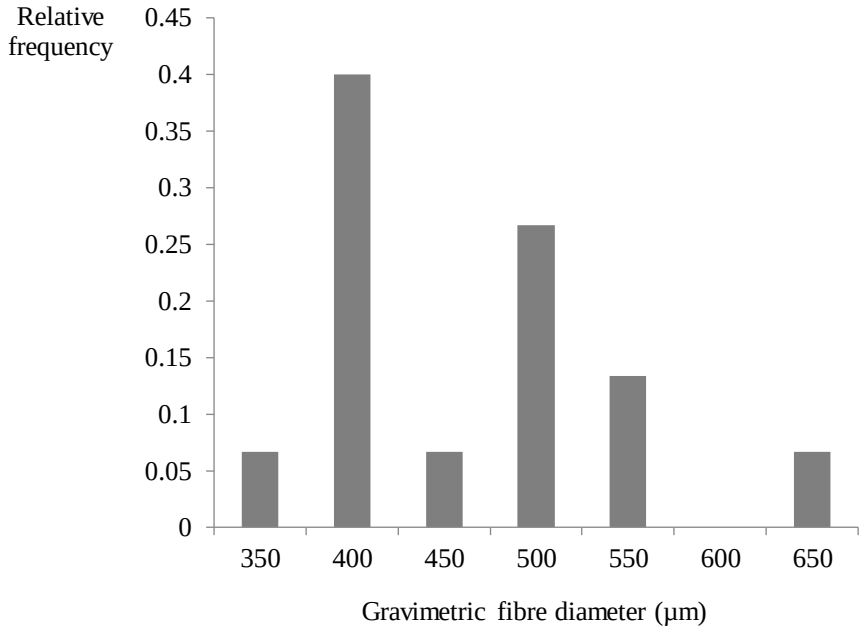

Figure 4-11: Relative frequency histogram of the gravimetric fibre diameters.

In theory it is possible to repeat the gravimetric analysis for several tens to hundreds of fibres to generate a more reliable distribution. However, the method assumes that sampled fibres are impenetrable structures with a well-defined geometry. This is clearly not the case for flax fibres, as seen in Figure 4-12 where technical fibre splitting is seen. Indeed, technical fibres consist of elementary fibres which may separate from each other due to the mechanical forces during scutching.

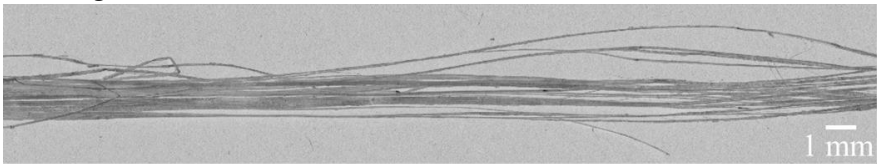

Figure 4-12: Technical flax fibre used in the automated image analysis showing fibre splitting and irregular geometry.

The above leads to the conclusion that it is impossible to accurately determine the diameter distribution from gravimetric analysis.

When a projection of the fibre is registered optically it is possible to extract a large number of fibre features. In the automated image analysis technique proposed in this work, the local fibre width is determined along the entire length of each fibre. This method is not hindered by the effect of technical fibre splitting at certain

locations along the length. To verify the ability of the optical method to return the fibre widths which are correlated to the actual fibre diameter, the optical fibre width and gravimetric fibre diameter were determined for several fibres from various batches and their values were compared. As shown in Figure 4-13, this correlation is indeed present, and for the data shown there appears to be a linear relation with a coefficient of determination of 0.93. In view of this correlation and for readability, the fibre width will be assumed to represent the fibre diameter.

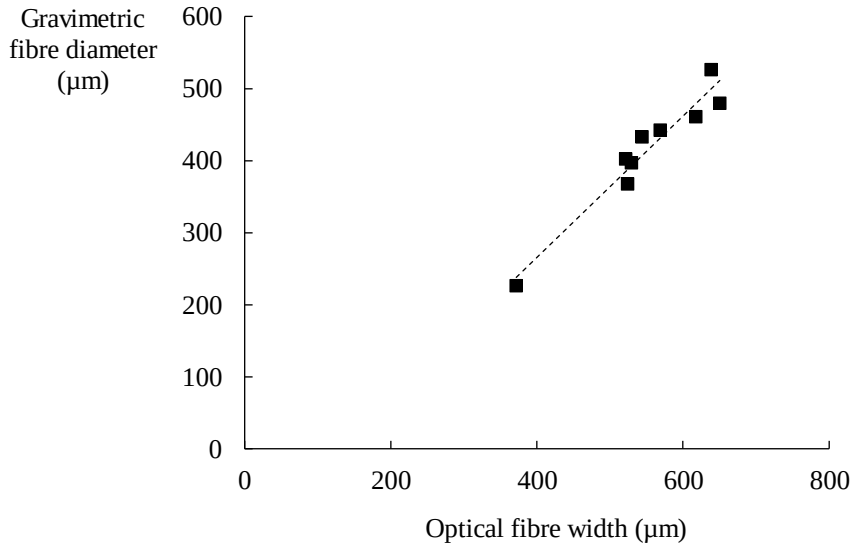

Figure 4-13: Relationship between the gravimetric fibre diameter and optical fibre width. (R^2=0.93)

Figure 4-14 shows the measured fineness using the optical method of a batch of scutched flax fibres. The diameters (d) follow a log-normal distribution ($p < 0.05$). Therefore, the distribution of each batch was fitted to the lognormal distribution with fitting parameters μ and σ, shown in equation 5.

$$\frac{1}{d\sigma\sqrt{2\pi}} e^{-\frac{(\ln(d)-\mu)^2}{2\sigma^2}} \tag{5}$$

As the batch is combed, the diameter distribution narrows and its heavy tail disappears. This indicates that large technical fibres split into smaller technical fibres. Larger technical fibres split into smaller fibres more readily as they usually are already split at certain locations, facilitating their full separation by the combs. The average values determined from the distribution fit, as well as their maximum values and the lognormal fitting parameters are listed in Table 4-7. Note that the maximum fibre diameter present in the batches is severely reduced with each

combing step. The results were verified on other batches which exhibited quasi-identical decreases in fibre diameter with each combing operation.

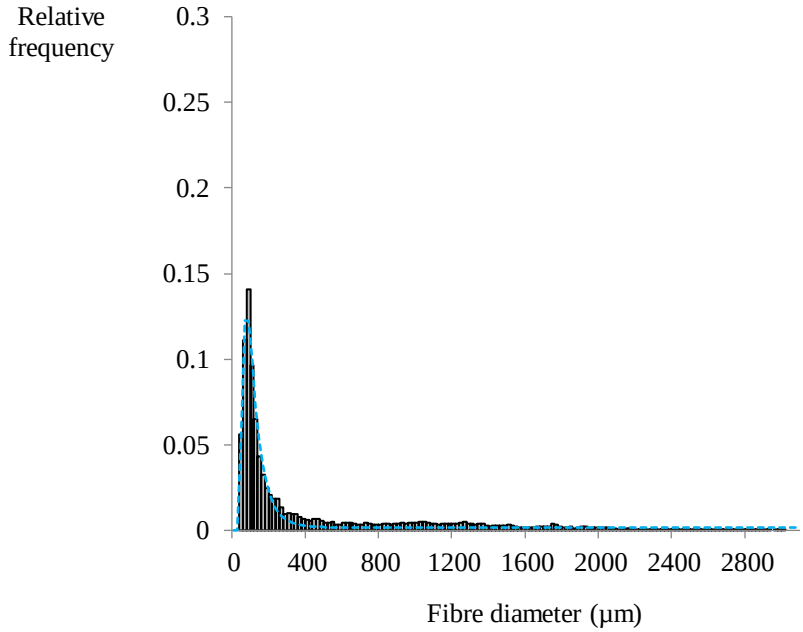

(a)

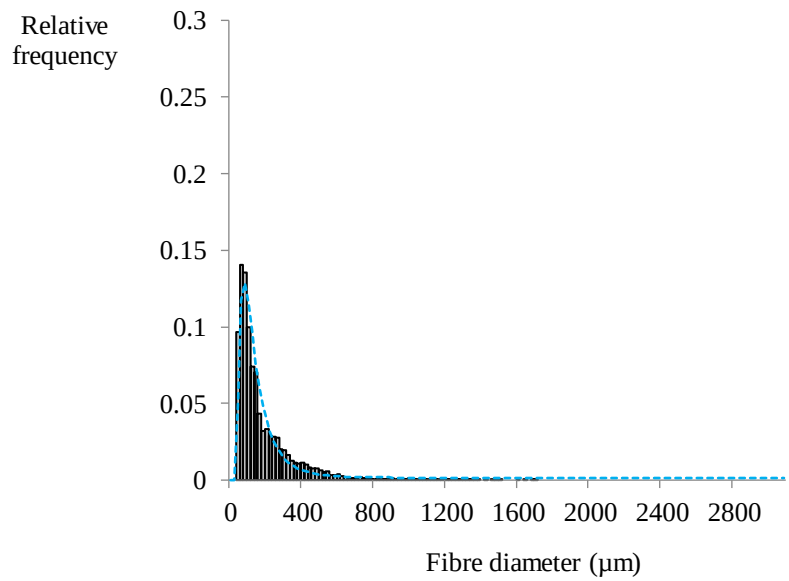

(b)

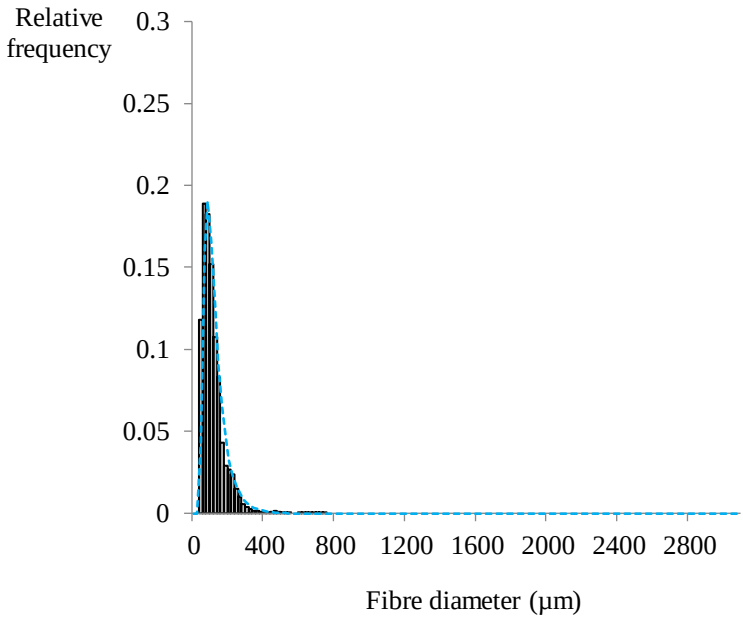

(c)

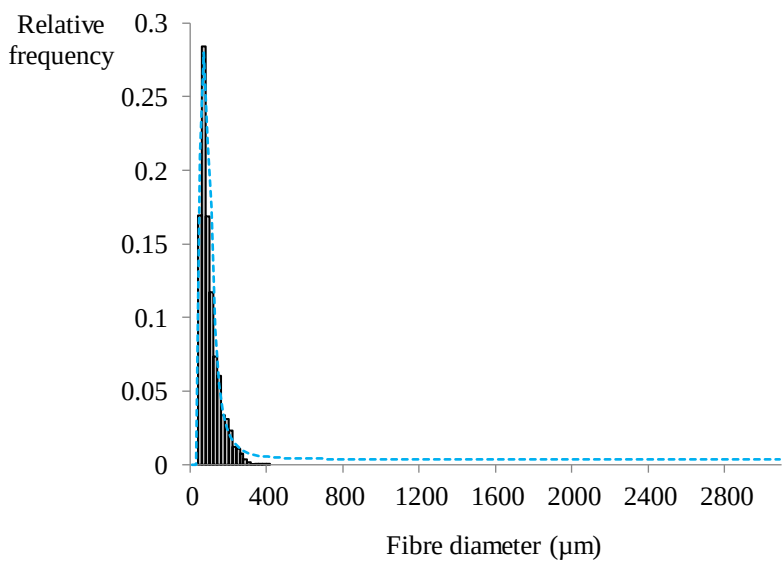

(d)

Figure 4-14: Fibre diameter distribution determined with the optical method for batches: (a) 4, (b) 4C1, (c) 4C2 and (d) 4C3. The data was fitted to the lognormal distribution.

Batch	Arithmetic average fibre diameter (µm)	95th percentile (µm)	µ	σ
4	429 ± 58	1744	76	0.664
4C1	169 ± 41	502	97	0.749
4C2	96 ± 30	214	83	0.610
4C3	81 ± 14	201	64	0.554

Table 4-7: Average (arithmetic) and 95th percentile values of the diameters of unrefined and refined fibres in the different batches. The parameters which provide the best fit of the lognormal distribution to the data are also shown.

4.2.4.2. Fibre tensile properties

Assessing the performance of single fibres can be done by performing single fibre tensile tests. Figure 4-15 displays the tensile behaviour of 47 scutched technical fibres (gauge length 50 mm) originating from batch 4 which was not further refined by combing. The average initial tensile modulus and strength were 37 ± 19 GPa and 615 ± 203 MPa, respectively. As can be seen from the large standard deviations and from the spread on the tensile behaviour in the figure, determining longitudinal fibre properties is often a challenging task due to the nature of the test preparation and procedure, and the intrinsic variability in fibre properties.

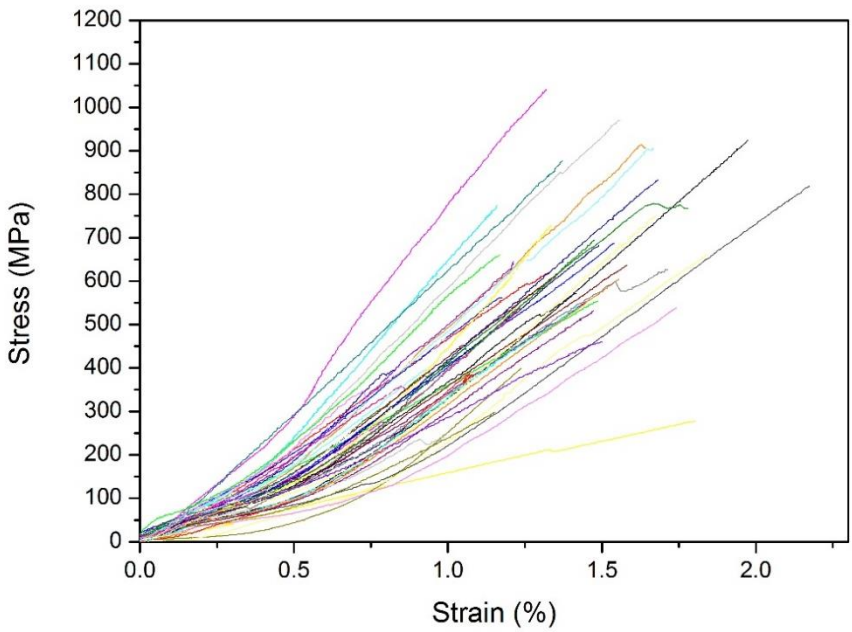

Figure 4-15: Stress-strain behaviour of 47 scutched technical fibres.

Firstly, it has been shown that appropriate strain measurement techniques should be used during the tests. Relying on clamp or crosshead displacement to calculate strain, even when corrected for slippage effects, may lead to severe underestimations of the fibre stiffness [12]. The authors developed a more accurate optical technique, presented in [12], eliminating the former effect and applied here to measure the elongation of the fibres.

Secondly, in a fibre tensile test, the fibre as a whole is assumed to be loaded uniformly. In some cases, however, the cohesion in technical fibres composed of smaller elementary fibres can be compromised due to damage to the middle lamellae. The extent of damage may vary from fibre to fibre. This is especially true for fibres which have been coarsely refined using mechanical processes such as breaking and scutching. The decreased load transferring capability and possible non-uniform loading of the technical fibre may lead to an unrealistic and low value of both strength and stiffness. Damage in the middle lamella could cause difficulties in stress transfer to the elementary fibres. Moreover, even when fibre cohesion is not compromised, the hierarchical nature of the fibre can lead to shear deformations in the middle lamellae. This is why the stiffness and strength of technical flax fibres is intrinsically lower than for elementary fibres. This additional deformation leads to a decrease in apparent stiffness [13,14].

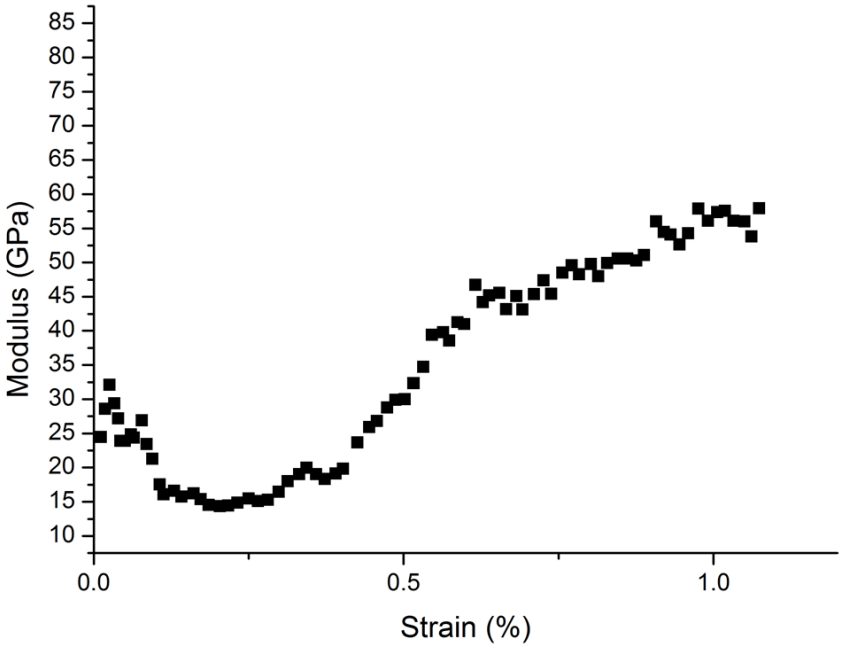

Figure 4-16: Evolution of the tangent modulus with increasing strain for a representative scutched technical fibre.

Although the spread on the tensile behaviour is large, even within the same batch, all fibres exhibit a similar evolution in their tangent modulus. When the tangent modulus is plotted as a function of strain, as is done in Figure 4-16, the modulus first decreases between 0.1% and 0.25% strain after which it steadily increases up to failure. This behaviour has also been observed for elementary fibres of flax and hemp fibres [15–18]. The decrease is likely due to shearing of the middle lamella or visco-plastic behaviour of the cell walls. This process is mainly dominated by the breaking of hydrogen bonds between the different biopolymer chains in the fibre [18]. After this initial decrease stage, amorphous regions of cellulose are prone to strain induced crystallization which will temper the rate of decrease [18]. Eventually, the microfibrils will start to reorient themselves with the loading direction, increasing the modulus until final failure of the fibre.

The unrefined batch 4 underwent combing with comb 1, decreasing the average diameter from 429 ± 58 µm to 169 ± 41 µm. The mechanical properties of 32 fibres of batch 4C1 were subsequently evaluated. The results are summarized in Table 4-8. No statistically significant differences could be detected between the two batches ($p < 0.05$). This could partly be due to the high standard deviations associated with the results. To reliably assess whether there are significant differences between the different batches, in particular for the tensile strength, the Weibull distributions need to be constructed. However, research shows that up to 500 tests are needed to reduce the coefficient of variation on the parameters of this distribution to values below 10% [19].

Batch	Initial tensile stiffness (GPa)	Tensile strength (MPa)
4	37 ± 19	615 ± 203
4C1	32 ± 15	754 ± 265

Table 4-8: Tensile modulus and strength of fibres originating from batches 4 and 4C1.

Apart from the statistically insignificant differences between the batches, fibre diameters appear to be correlated with the tensile strength. Testing fibres with larger diameters, thus larger volumes, would usually result in a lower measured strength as the probability of a defect occurring in that volume increases [20,21]. Figure 4-17 indeed shows that this relationship exists for the scutched fibres of

batch 4. A correlation coefficient of -0.71 was found between the fibre strength and fibre diameter.

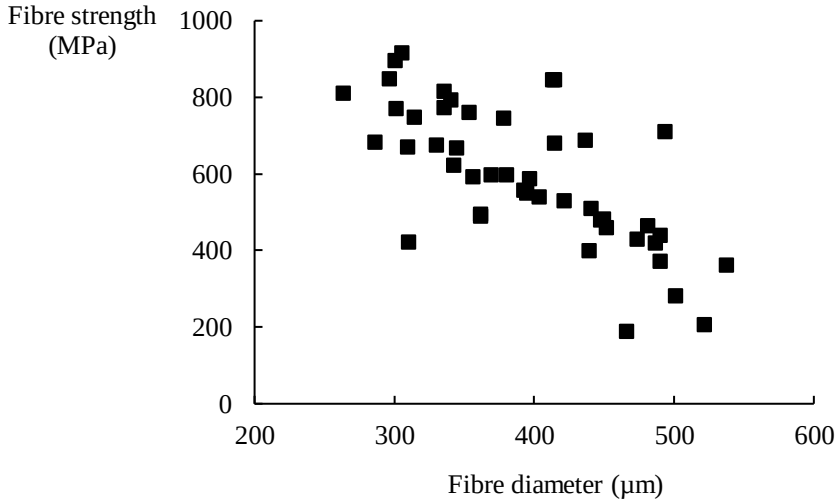

Figure 4-17: A negative correlation exists between fibre diameter and fibre strength for fibres of batch 4. (Correlation coefficient = -0.71)

Although the tensile behaviour of single technical fibres can be used to assess microstructural deformation mechanisms in the fibres, it cannot predict their composite performance due to several reasons. Firstly, the adhesion between the elementary fibres, essential for the strength of the technical fibre, could be of minor importance once they are embedded in a polymer matrix as it will fill the zones where the technical fibre has split and fully surrounds the elementary fibres. Secondly, the surrounding of the elementary fibres will change the stress transfer in the technical fibre. Instead of only clamping the elementary fibres at the end of the technical fibres, all elementary fibres which are in contact with the matrix are effectively loaded. This in turn restricts the relative movement of these elementary fibres, altering the deformation processes of the fibres in the composite [14]. Note that the previous discussion also implies that testing elementary fibres will not be representative of their behaviour in the composite. In a single fibre test the surface of the elementary fibres is unrestricted which imposes vastly different boundary conditions on its tensile response. Indeed, Charlet et al. have shown that the elementary fibre properties in tension were substantially higher than of the back-calculated properties obtained from testing composites reinforced with the technical fibres in which they are embedded [14,22,23].

In conclusion, single fibre tests require a high number of tests to reliably determine the parameters that characterize their mechanical properties, and they require meticulous test preparation and execution. In addition, for flax and other natural

fibres in general, the results are not predictive for their composite performance which limits the usability of the single fibre test method.

4.2.4.3. Longitudinal UD composite properties

In Figure 4-18, the resulting stress-strain curves of the tensile tests on six composite samples are shown. Comparing the data to Figure 4-15, it is seen that the mechanical response of the different composite samples is nearly identical, opposed to that of the fibres in the single fiber tests.

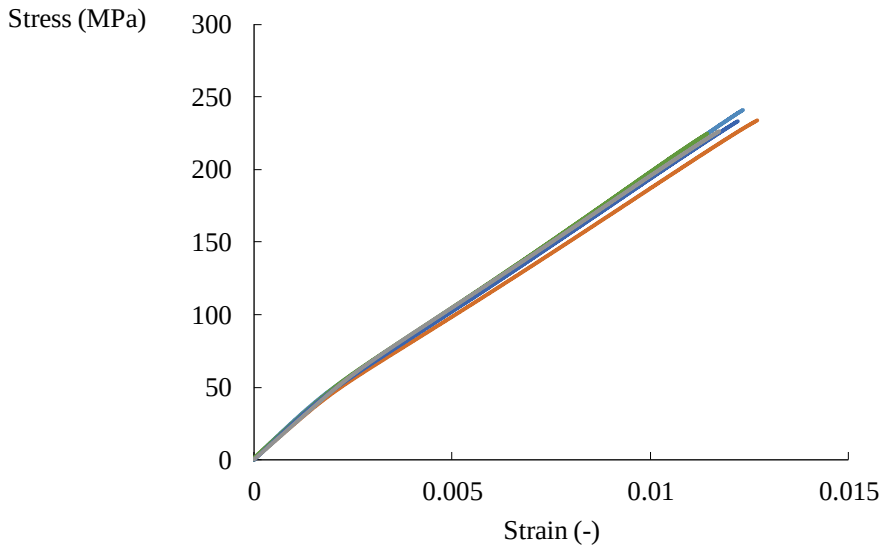

Figure 4-18: Stress-strain curves resulting from tensile tests on six composite samples

The fibre modulus and strength of all uncombed batches back-calculated from the composite tests were determined and are shown in Figure 4-19 a and b, respectively. As seen in Table 4-9, the spread on the results for six samples is far lower than on those of the single fibre tests. Indeed, during a tensile test on a composite sample the measured stiffness and strength effectively is an average on hundreds of technical and elementary fibres. Moreover, this “averaging” takes into account the real stress transfer mechanism between the matrix and the elementary fibre in the composite.

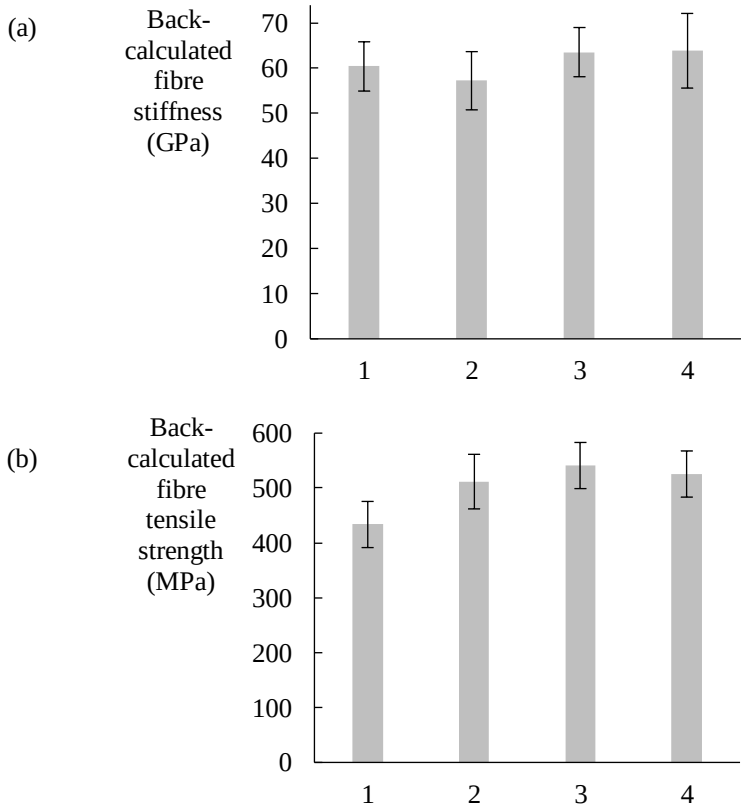

Figure 4-19: (a) Longitudinal back-calculated fibre modulus of the unidirectional composites calculated in the region between 0% and 0.1% strain. (b) Longitudinal back-calculated fibre strength of the unidirectional composites.

The differences in modulus between the batches are statistically insignificant ($p < 0.05$). This result is rather surprising as the batches of flax were grown in different years and at various locations. Furthermore, the stiffness values agreed very well with results obtained on hackled fibres [11,24]. The variability of flax fibre properties has always been a concern for their use in composites. Several studies in the past found evidence of mechanical properties that fluctuate from year to year [25,26]. However, in these studies, measurements were performed on elementary fibres. As discussed previously, fibre tests are only weakly predictive for their performance when embedded in a polymer matrix. The authors of these studies also acknowledge that significant dispersion on the results can be induced by the inaccurate determination of fibre diameters. The above results indicate that variability in longitudinal fibre properties may be of less importance than it is currently assumed to be. It is also noteworthy that the wider composite materials

community (i.e. the users of glass and carbon fibres) uses an impregnated fibre bundle test (ISO 10618) to test fibre properties.
One batch (batch 1) of fibres showed a significantly lower strength than the other batches ($p > 0.05$). This could be related to the fact that batch 1 was the only batch where shive particles were still visually present leading to stress concentrations in the composite.

Batch	Back-calculated fibre modulus (0-0.1%) (GPa)	Back-calculated fibre strength (MPa)
1	60 ± 5	434 ± 42
2	57 ± 6	512 ± 50
3	64 ± 5	541 ± 42
4	64 ± 8	525 ± 42

Table 4-9: Back-calculated longitudinal fibre properties for all batches of scutched and uncombed flax fibres.

To investigate the influence of fineness on the longitudinal performance of the fibres, batch 4 was gradually refined with the three combs and composite samples were produced. The results are summarized in Figure 4-20. No statistical differences were found between the unrefined fibres and the fibres which underwent combing nor between the various refined fibres ($p < 0.05$). One study found that flax fibre stiffness tends to increase as the fineness of the fibres increases [27]. However, the authors of this study used fibres from different varieties to evaluate the influence of fineness on the composite properties. As the variety which resulted in finer fibres after hackling also exhibited the highest modulus in elementary single fibre tests, the effects of variety and fineness cannot be distinguished. Furthermore, only if the fibres were extremely refined, i.e. when more than 93% of all elementary fibres had fully separated from the technical fibres, could this increase in stiffness be seen. Since the variety of all flax batches used in the present study was identical, this effect is excluded from influencing the results.
The absence of a change in stiffness when the fibre fineness increases leads to the conclusion that deformation processes in the fibre do not change significantly when their diameter is reduced.

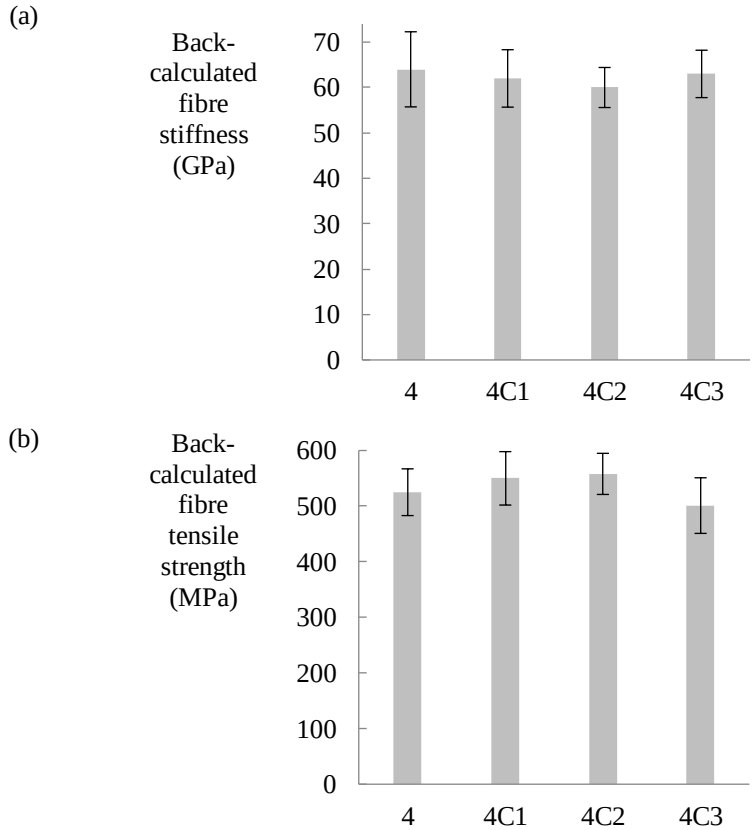

Figure 4-20: (a) Evolution of longitudinal back-calculated fibre modulus of the unidirectional composites, calculated in the region between 0% and 0.1% strain for decreasing fibre diameter, due to different levels of combing. (b) Evolution of longitudinal back-calculated fibre strength of the unidirectional composites for decreasing fibre diameter.

4.2.4.4. Transverse UD composite properties

In most applications, composites experience transverse loading conditions. It is therefore of vital importance to examine their behaviour under these loading conditions. In this study it was preferred to examine the transverse behaviour in flexion due to several reasons. Firstly, fibre alignment is intrinsically difficult to achieve with scutched flax fibres, hence the test span of samples (in the transverse direction) is limited. Secondly, the long test specimens required for tensile testing makes them prone to premature failure due to defects originating from the production process hence, potentially resulting in results which are lower than expected. On the other hand, testing in three-point flexion maximally loads only a limited region of the material leading to higher average results. Figure 4-21 shows the transverse flexural modulus and strength of all unrefined batches. The average

flexural modulus and flexural strength was 2.1 ± 0.3 GPa and 28 ± 3 MPa. In contrast to the longitudinal properties, both stiffness and strength values varied significantly more between the batches. To further investigate this influence, batch 4 which has the lowest transverse strength, was gradually refined, as described in the previous section and composite samples were produced.

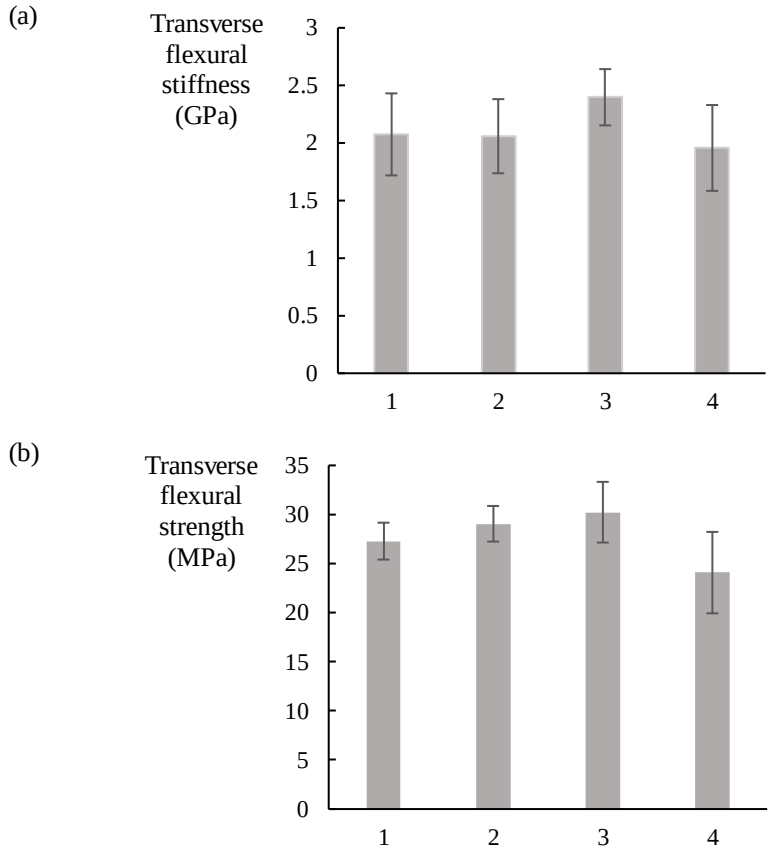

Figure 4-21: (a) Transverse flexural composite modulus of the unidirectional composites. (b) Transverse flexural composite strength of the unidirectional composites.

As seen in Figure 4-22, when the diameter of the flax fibres decreased, both transverse stiffness and strength of the composites increased. Transverse strength increased by as much as 31% when comparing unrefined fibres to the finest fibres while the respective increase in modulus reached 34%. Moreover, a 23% increase in strength and 20% increase in modulus is associated with the largest reduction in fibre diameter during the first, very coarse, combing step.

Increased strength in transverse loading was obtained by eliminating weaker areas in the composite. In the case of flax fibres, it has previously been shown that the middle lamella composed of pectin and hemicellulose is a weak spot in the

technical fibre, having both lower modulus and strength than the elementary fibres [13,28,29]. When loaded transversely, the middle lamella is loaded in tension. It is possible that these tensile forces may initiate and propagate cracks in this layer which eventually causes debonding between elementary fibres and the middle lamellae. This may be further facilitated by the presence of microdefects induced by the breaking and scutching operations. From a biological point of view, fibres in the flax plant would never experience this loading condition as their arrangement in the stem makes this type of failure unlikely to occur. In composites, when the diameter of the fibre is reduced, the total volume of middle lamellae is simultaneously reduced and more elementary fibres are able to make contact with the matrix. Moreover, it can be assumed that fibre refinement is achieved by a weakest link mechanism. This causes separation to occur first at the weakest middle lamellae leaving behind stronger and stiffer ones attributing to the increase of strength and stiffness, respectively.

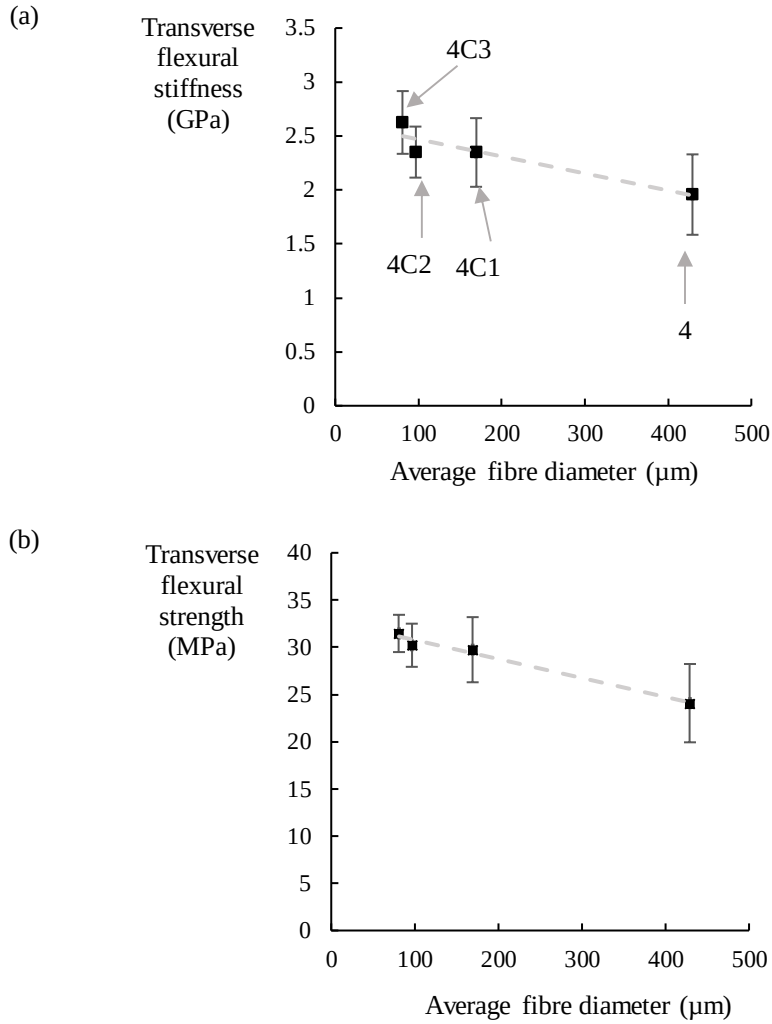

Figure 4-22: (a) Evolution of transverse composite modulus for decreasing fibre diameter (R^2 = 0.86). (b) Evolution of transverse composite strength for decreasing fibre diameter (R^2 = 0.98).

4.2.4.5. Influence of fibre purity

Fibre purity and fibre fineness are intrinsically coupled to each other. Combing a batch to reduce the fibre diameter will increase its purity. Therefore, separating these two variables is not straightforward. Table 4-10 shows that the purity of the batch increased by 20% after three combing operations. In the case of batch 4, the correlation coefficient of the two variables was -0.85, highlighting their strong mutual dependence. However, it is observed that the correlation coefficient between the average fibre diameter and transverse flexural strength was -0.99 and

only 0.84 between the fibre purity and transverse flexural strength. This provides an indication that the fibre diameter is the main factor contributing to the increase in transverse mechanical properties. There is a connection between the average fibre diameter and the “amount” of middle lamellae which is present. Decreasing the fibre diameter increases the specific surface area of the fibres which is in direct contact with the matrix. It is hypothesized that it is the elimination of these weak spots, which leads to the increase in transverse strength.

Batch	Purity (%)
4	79 ± 3
4C1	84 ± 4
4C2	93 ± 3
4C3	100*

Table 4-10: Evolution of the fibre purity with each combing operation (decreasing fibre diameter). *The purity of the batch after the last combing operation was assumed to be 100%. Hence, no standard deviation on the result can be provided.

4.2.5. Conclusions

This study investigated the effect of scutched flax fibre fineness and purity on the mechanical properties of the fibres and their composites.

First, a reliable method was presented to determine the fineness of the fibres based on optical image analysis. The advantage of this technique, in contrast to airflow or gravimetric methods, is that it can analyse a large number of samples rapidly and accurately, resulting in a fibre diameter distribution histogram. Furthermore, the obtained fibre widths, though not identical to the gravimetric fibre diameters, are strongly correlated with them.

Single fibre tensile tests were deemed unable to prove whether fibre fineness significantly affects the mechanical properties. This was attributed to several difficulties with the test method itself. Firstly, it was shown that the spread on the tensile properties was extremely high, exhibiting a coefficient of variation of approximately 50%. Moreover, part of this variation could be due to the difficult test set-up, requiring meticulous sample preparation, used in this procedure. Secondly, during a single fibre test, the stress transfer to the elementary fibres was found to not be representative of the transfer mechanism in a composite. This shows the method is not suited to be used as a reliable predictor of composite properties, at least for flax fibres. Finally, the spread on the composite properties was much lower than that of the individual fibres, exhibiting no significant differences between batches. This is a strong indication that variability in mechanical properties is of less importance than it is currently believed to be in literature.

Composite testing also revealed that longitudinal composite properties were not significantly affected by the fineness or purity of the fibres, reaching E-modulus

values close to what has been reported in the scientific literature for hackled fibre-based composites. In contrast, transverse properties were greatly affected by fibre fineness. The latter was attributed to the presence of the weak and possibly damaged middle lamellae, between the elementary fibres in a technical fibre. A coarse combing operation greatly improved transverse performance by approximately 20%, both in stiffness and strength, by adequately removing the weak spots in the middle lamella. Subsequent combing operations further reduce the fineness and improve the transverse strength, but the property gain is smaller than the increase in costs.

The correlation between fibre purity and transverse composite properties was weaker, leading to the conclusion that this is only of secondary importance for scutched fibres, given the high correlation between purity and fineness

Further research on the processability of scutched fibres is necessary as they may pose challenging, albeit technical, issues to spin into yarns and produce weaves from them. More fundamental investigations on other mechanical properties such as fatigue and toughness behaviour are advised as they are of vital importance to the composite industry.

References

[1] Van de Weyenberg I, Ivens J, De Coster a., Kino B, Baetens E, Verpoest I. Influence of processing and chemical treatment of flax fibres on their composites. Compos Sci Technol 2003;63:1241–6. doi:10.1016/S0266-3538(03)00093-9.

[2] Summerscales J, Dissanayake NPJ, Virk AS, Hall W. A review of bast fibres and their composites. Part 1 – Fibres as reinforcements. Compos Part A Appl Sci Manuf 2010;41:1329–35. doi:10.1016/j.compositesa.2010.06.001.

[3] Akin DE. Linen Most Useful: Perspectives on Structure, Chemistry, and Enzymes for Retting Flax. ISRN Biotechnol 2013;2013:1–23. doi:10.5402/2013/186534.

[4] Djemiel C, Grec S, Hawkins S. Characterization of Bacterial and Fungal Community Dynamics by High-Throughput Sequencing (HTS) Metabarcoding during Flax Dew-Retting. Front Microbiol 2017;8. doi:10.3389/fmicb.2017.02052.

[5] Depoortere NV. Trommel voor zwingelturbine. 2007/0318, 2009.

[6] Dimmock JPRE, Bennett SJ, Wright D, Edwards-Jones G, Harris IM. Agronomic evaluation and performance of flax varieties for industrial fibre production. J Agric Sci 2005;143:299. doi:10.1017/S0021859605005277.

[7] Easson DL, Molloy RM. A study of the plant, fibre and seed development in flax and linseed (Linum usitatissimum) grown at a range of seed rates. J Agric Sci 2000;135:S0021859699008400. doi:10.1017/S0021859699008400.

[8] Grishanov S a., Harwood RJ, Booth I. A method of estimating the single flax fibre fineness using data from the LaserScan system. Ind Crops Prod 2006;23:273–87. doi:10.1016/j.indcrop.2005.08.003.

[9] Van Den Oever MJA, Bas N, Van Soest LJM, Melis C, Van Dam JEG. Improved method for fibre content and quality analysis and their application to flax genetic diversity investigations. Ind Crops Prod 2003;18:231–43. doi:10.1016/S0926-6690(03)00063-3.

[10] Foulk JA, Chao WY, Akin DE, Dodd RB, Layton PA. Enzyme-Retted Flax Fiber and Recycled Polyethylene Composites. J Polym Environ 2004;12:165–71. doi:10.1023/B:JOOE.0000038548.73494.59.

[11] Bensadoun F, Verpoest I, Baets J, Müssig J, Graupner N, Davies P, et al. Impregnated fibre bundle test for natural fibres used in composites. J Reinf Plast Compos 2017;36:942–57. doi:10.1177/0731684417695461.

[12] Depuydt D, Hendrickx K, Biesmans W, Ivens J, Van Vuure AW. Digital image correlation as a strain measurement technique for fibre tensile tests. Compos Part A Appl Sci Manuf 2017. doi:10.1016/j.compositesa.2017.03.035.

[13] Charlet K, Béakou A. Mechanical properties of interfaces within a flax bundle – Part I: Experimental analysis. Int J Adhes Adhes 2011;31:875–81. doi:10.1016/j.ijadhadh.2011.08.008.

[14] Shah DU, Nag RK, Clifford MJ. Why do we observe significant differences between measured and 'back-calculated' properties of natural fibres? Cellulose 2016;23:1481–90. doi:10.1007/s10570-016-0926-x.

[15] Bensadoun F, Vallons KAM, Lessard LB, Verpoest I, Van Vuure AW. Fatigue behaviour assessment of flax-epoxy composites. Compos Part A Appl Sci Manuf 2016;82:253–66. doi:10.1016/j.compositesa.2015.11.003.

[16] Baley C. Analysis of the flax fibres tensile behaviour and analysis of the tensile stiffness increase. Compos Part A Appl Sci Manuf 2002;33:939–48.

doi:10.1016/S1359-835X(02)00040-4.

[17] Baley C, Le Duigou A, Bourmaud A, Davies P. Influence of drying on the mechanical behaviour of flax fibres and their unidirectional composites. Compos Part A Appl Sci Manuf 2012;43:1226–33. doi:10.1016/j.compositesa.2012.03.005.

[18] Placet V, Cissé O, Lamine Boubakar M. Nonlinear tensile behaviour of elementary hemp fibres. Part I: Investigation of the possible origins using repeated progressive loading with in situ microscopic observations. Compos Part A Appl Sci Manuf 2014;56:319–27. doi:10.1016/j.compositesa.2012.11.019.

[19] Swolfs Y, Verpoest I, Gorbatikh L. Issues in strength models for unidirectional fibre-reinforced composites related to Weibull distributions, fibre packings and boundary effects. Compos Sci Technol 2015;114:42–9. doi:10.1016/j.compscitech.2015.04.002.

[20] GURVICH MR, DiBENEDETTO AT, RANADE S V. A new statistical distribution for characterizing the random strength of brittle materials. J Mater Sci 1997;32:2559–64. doi:10.1023/A:1018594215963.

[21] Dhakal H, Zhang Z, Richardson M. Effect of water absorption on the mechanical properties of hemp fibre reinforced unsaturated polyester composites. Compos Sci Technol 2007;67:1674–83. doi:10.1016/j.compscitech.2006.06.019.

[22] Charlet K, Baley C, Morvan C, Jernot JP, Gomina M, Bréard J. Characteristics of Hermès flax fibres as a function of their location in the stem and properties of the derived unidirectional composites. Compos Part A Appl Sci Manuf 2007;38:1912–21. doi:10.1016/j.compositesa.2007.03.006.

[23] Charlet K, Jernot J-P, Gomina M, Bizet L, Breard J. Mechanical Properties of Flax Fibers and of the Derived Unidirectional Composites. J Compos Mater 2010;44:2887–96. doi:10.1177/0021998310369579.

[24] Khalfallah M, Abbès B, Abbès F, Guo YQ, Marcel V, Duval a., et al. Innovative flax tapes reinforced Acrodur biocomposites: A new alternative for automotive applications. Mater Des 2014;64:116–26. doi:10.1016/j.matdes.2014.07.029.

[25] Lefeuvre A, Bourmaud A, Lebrun L, Morvan C, Baley C. A study of the yearly reproducibility of flax fiber tensile properties. Ind Crops Prod 2013;50:400–7. doi:10.1016/j.indcrop.2013.07.035.

[26] Aslan M, Chinga-Carrasco G, Sørensen BF, Madsen B. Strength variability of single flax fibres. J Mater Sci 2011;46:6344–54. doi:10.1007/s10853-011-5581-x.

[27] Coroller G, Lefeuvre A, Le Duigou A, Bourmaud A, Ausias G, Gaudry T, et al. Effect of flax fibres individualisation on tensile failure of flax/epoxy unidirectional composite. Compos Part A Appl Sci Manuf 2013;51:62–70. doi:10.1016/j.compositesa.2013.03.018.

[28] Beakou A, Charlet K. Mechanical properties of interfaces within a flax bundle—Part II: Numerical analysis. Int J Adhes Adhes 2013;43:54–9. doi:10.1016/j.ijadhadh.2013.01.013.

[29] Perremans D, Hendrickx K, Verpoest I, Van Vuure AW. Effect of chemical treatments on the mechanical properties of technical flax fibres with emphasis on stiffness improvement. Compos Sci Technol 2018;160. doi:10.1016/j.compscitech.2018.03.030.

4.3. Influence of flax fibre variety, retting conditions and processing on the composite properties

Kevin Hendrickx, Wim Thielemans, Aart Willem Van Vuure, Jan Ivens

4.3.1. Introduction

Commercially available textiles of flax fibres for technical and non-technical applications are usually created with fibres sourced from various growing locations, varieties, and even different years. All this is done to guarantee a constant product quality of the produced textiles. Indeed, the variety determines the maturation time of the flax, their resistance to certain diseases, the maximum fibre yield, and the intrinsic quality of the fibres [1]. The stated quality aspect historically relates to the suitability of the fibres to be incorporated into non-technical textile applications. For instance, coloring and color homogeneity of flax fibres and textiles traditionally requires a very high degree of fineness of the fibre bundles or technical fibres, extracted from the plant, for which certain varieties may be more suitable. This is also the main reason for the hackling step, as it increases fibre fineness to a level that is acceptable for further processing. On the other hand, growth locations and time determine the environmental conditions (temperature, rain and humidity, sunshine) to which the plant is exposed during its growth and the extent of retting afterwards.

This entire process, from the variety selection to the extent of retting and fibre processing, is largely based on tradition and experience-based assessments by the flax fibre producer. As non-technical textiles are still the main market for flax fibres, the process is fully adapted to fit the requirements of this industry, i.e. mainly spinning companies. However, the requirements imposed on fibres to be incorporated in technical textiles, more specifically for composites, can be significantly different. For instance, in a previous study the authors have investigated the effect of fibre fineness on the longitudinal and transverse performance of unidirectional composites [Section 4.2]. It was established that fineness did not significantly influence the longitudinal behaviour of the composites. However, transverse properties were adversely affected by coarser fibres but could be improved significantly by a limited combing process. This illustrates the differences that exist between the requirements for non-technical textiles and technical textiles. Presently however, no method exists that directly relates the mechanical fibre properties to the corresponding property of the composite for natural fibres such as flax, making it difficult to even subjectively assess the “composite quality” of the fibres based on their appearance. This is due to the hierarchical nature of natural fibres which leads to entirely different load transfer mechanisms when the fibres are embedded in a polymer opposed to when they are not [2]. The only reliable method to accurately assess the behaviour of the fibres in a composite is through composite testing [3].

From the previous discussion it is clear that there is a need to rethink the entire selection and extraction process of the fibres to optimize it for composite reinforcement rather than for non-technical textile manufacturing. The best fibres for spinning may not be the best fibres to use in composites and vice versa.

Very few studies have examined the influence of variety, retting, and other processing conditions on the performance of the fibres in composites. Baley and Bourmaud investigated the effect of growing conditions and flax variety on the mechanical properties of elementary flax fibres by combining data over an 18 year period [4]. Surprisingly, no statistically significant relation was found between cultivation conditions nor variety and their mechanical properties. This was later confirmed by Thuault et al. in a separate study on 7 flax fibre varieties [5]. In contrast, Lefeuvre et al. found that flax variety significantly influenced the mechanical performance of the elementary fibres [6]. They also showed in two separate studies that despite drought or excess rainfall during growth, reproducible properties of flax fibres for the same variety, *Marilyn*, were obtained from year to year [7,8]. These authors also suggested that an increase in the extent of retting augments the strength of the fibres [7]. It has to be mentioned that this effect could be severely confounded with a variation in scutching parameters the authors used in the experiment. In contrast, Haag et al., who examined the influence of variety and year to year variability on final composite properties did show a significant influence of growing conditions and to a lesser extent of the variety on the composite stiffness and strength [9]. Furthermore, the shape of the stress-strain curve for elementary fibres in a tensile test appears to be related to the amount of structuring polysaccharides such as pectin [6]. It is known that these polysaccharides are degraded during retting, indicating a possible influence of the retting process on the overall mechanical performance of the fibres [10–12]. In general, the knowledge of the influence of variety and the degree of retting of the fibres on composite performance is insufficient to reliably draw conclusions regarding possible relations between these parameters and the mechanical properties.

In the traditional extraction process, mechanical operations on the fibres are performed after the retting stage. First, the xylem tissues of the stem are broken between serrated rollers to produce what is henceforth called the shives. The process also partly separates the soft tissue from the fibres. Immediately following the breaking, scutching is performed in a turbine where the fibres are beaten repeatedly by blunt blades to remove most of the shive particles from the fibres. Of course, although not intended, the process severely stresses the fibres to the point where they might develop microstructural defects, such as kink bands. Kink bands are regions where the orientation of the crystalline cellulose microfibrils is severely distorted. Thygesen and Asgharipour showed that kink bands are intrinsically present in flax fibres, formed during their growth [13]. In another study, Thygesen et al. artificially damaged the fibres by passing them through

intermeshing cogwheels. As the number of passings through these cogwheels increased, the defect count per unit length steadily increased until a saturation level was reached after which the defect density did not increase further [14]. Numerous studies have reported a negative influence of these defects on both stiffness and strength of the elementary fibres [15–17]. Furthermore it has been suggested by Hughes et al. that these kink bands may act as initiation sites for microcracks in composites due to elevated stresses around the defect [18]. Finally, Gourier et al. showed that during compounding of flax fibres the preferential fragmentation sites during the process are likely the kink bands [19]. Interestingly, to date it has not been established whether these kink bands influence the properties of the composites on a macroscopic scale. Moreover, Placet et al. have shown that not all kink bands are permanent as they witnessed the gradual disappearance of them during tensile loading of elementary hemp fibres [20]. If this would also occur for flax fibres in composites, the influence on the mechanical properties could be limited.

The aim of this study is threefold:

- The influence of variety on the composite properties is evaluated. Literature on the subject has been inconclusive up to now and there is a need for additional data.
- The effect of retting conditions of the stems on the composite properties is examined. Although studies indicate a relation between tensile strength and the extent of retting, the evidence is largely based on fibre testing which is a poor predictor of composite properties.
- The effect of the fibre processing on the microstructure of the fibre and its relationship with the composite properties is revealed. Currently, no data exist which explicitly relate the presence of defects to the properties of composites.

4.3.2. Materials and methods

4.3.2.1. Flax fibres

Flax (*Linum usitatissium L.*, Vesta and Amina varieties) was grown and retted in 2014 at different locations in Belgium. All stems were dew retted on the field approximately 3, 4 and 5 weeks, resulting in 6 different batches. Scutching for all fibres was performed with identical settings of the scutching turbines. These turbines, although installed at various locations, were considered identical as they were all constructed by the same manufacturer. Samples were collected immediately after the fibres exit from the scutching turbine. Prior to any operation or measurement, the fibres were conditioned at 21°C and 50% RH for at least 24 hours.

4.3.2.2. Matrix

A bisphenol A epoxy resin (Epikote 828LVEL) was mixed with 1,2 diaminocyclohexane in a 100:15.2 w/w ratio, to produce the epoxy matrix for the composite specimens.

4.3.2.3. Fineness measurements

Automated image analysis was used for the fineness measurements. This method was developed in a previous study from the authors [Section 4.2]. The projected diameters of the fibres are registered optically along the entire length of the fibre.

4.3.2.4. Composite production

Prior to impregnation the flax fibres were dried in an oven at 60°C for 24 hours and subsequently dried under vacuum at 40°C for at least 1 hour prior to impregnation. Note that this does not imply that all of the moisture was removed from the fibres. From prior knowledge and non-destructive quality assessments, it is known that these steps suffice to prevent excessive moisture evaporation during impregnation and curing which could cause porosity in the composites.

Flax fibre - epoxy unidirectional composites were produced based on the procedure outlined in ISO 10618, adapted to natural fibres [3]. The fibre volume fraction (V_f) was set to 35% and the specimen thickness to 2 mm. All other dimensions were in accordance with ISO 10618 prescribing the dimensions to be used for unidirectional composite test specimens in tension.

ASTM D7264/D7264M prescribes the necessary sample dimensions for flexural testing of unidirectional composites. In deviation of ASTM D7264/D7264 M, the thickness-to-span ratio was altered to 1:16 instead of the advised 1:32. The decrease in ratio was necessary to guarantee the alignment of the fibres in the transverse specimens during production. Nevertheless, it was verified that the altered ratio did not influence the results as a control experiment using hackled flax fibres did not show significant differences in transverse properties. Therefore, the increase in shear stresses appear to be sufficiently low to not have a significant impact on the transverse behaviour of the composites.

The resin was degassed in a vacuum chamber prior to impregnation and curing of the resin was performed under atmospheric pressure at 80°C for 1 hour supplemented by a post-cure step at 150°C for 1 hour.

4.3.2.5. Composite testing & calculation of the mechanical properties

a. Longitudinal properties

Longitudinal tensile tests were performed according to ISO10618, adapted to natural fibre composites [3]. An Instron 5567 tensile testing machine was equipped with a load cell of 30 kN and the crosshead displacement rate was set to 2 mm/min. As flax fibres are known to exhibit non-linear behaviour, the modulus of the composites (E_c) was calculated in the region between 0 and 0.1% strain. To

compare results between different batches of fibres, a back-calculation to the fibre stiffness (E_f) and strength (σ_f) was performed using the inverse rules of mixtures in equations 1 and 2. Note that the calculation of the back-calculated fibre strength involves the failure strain of the composite (ε_c^*)

$$E_f = \frac{E_c - (1 - V_f)E_m}{V_f} \quad (1)$$

$$\sigma_f = \frac{\sigma_c - (1 - V_f)E_m \epsilon_c^*}{V_f} \quad (2)$$

b. Transverse properties

Three-point flexural tests were performed following ASTM D7264/D7264 M. An Instron 5567 was equipped with a load cell of 1 kN and the crosshead displacement rate was set to 1 mm/min. All tests were performed under normal ambient conditions, on specimens that had been conditioned at 50%RH and 21°C for 7 days.

4.3.3. Results and discussion

4.3.3.1. Influence of flax fibre variety

Varietal influence on the mechanical properties of composites was studied here by evaluating the longitudinal performance of the fibres in a composite. Although also the transverse properties could be affected by the variety, this influence is difficult to evaluate as it is confounded with the effect of fineness, which the variety influences as well. Indeed, in a previous study, the authors showed that transverse properties are significantly influenced by the fibre fineness [Section 4.2]. To illustrate the above issue, Figure 4-23 gives the distribution of fibre fineness for scutched Amina and Vesta flax fibres. The average measured fibre diameters for Amina fibres was 209 µm while the Vesta fibres were noticeably coarser with an average diameter of 271 µm.

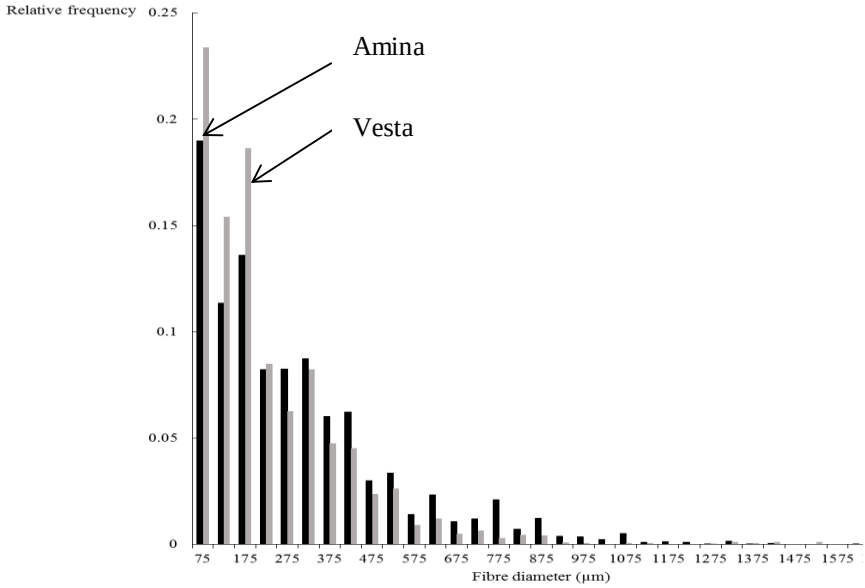

Figure 4-23: Relative frequency histogram of fibre fineness for scutched Amina and Vesta flax fibres.

The longitudinal stiffness and strength of both varieties is shown in Table 4-11. The two-sided student's t-test did not reveal significant differences for the strength or the stiffness at the 5% confidence level ($p = 0.27$, $p = 0.11$, $p = 0.32$) between both varieties.

Variety	Back-calculated fibre modulus E_{f1} (GPa)	Back-calculated fibre stiffness E_{f2} (GPa)	Back-calculated fibre strength (MPa)
Amina	65 ± 4	43 ± 4	515 ± 41
Vesta	62 ± 5	39 ± 4	542 ± 52

Table 4-11: Longitudinal stiffness and strength of the Amina and Vesta fibres in the composite.

In hindsight the obtained results for the fibre stiffness are not surprising. There are only two ways in which the stiffness of flax fibres can be increased: First, the crystalline cellulose content determines the final stiffness of the fibre. A detailed analysis of the crystallinity content in different varieties of flax fibres was performed by Thuault et al. [21]. The crystalline cellulose content ranged from 78.1% for Hermès fibres to 81.0% for the Drakkar variety. Furthermore, the stiffness of crystalline cellulose was estimated to be 134-138 GPa [22,23] where hemicellulose only attained 0.2 GPa in ambient conditions [24]. This shows that the differences occurring between the varieties are almost negligible. Indeed, in the cell wall of flax fibres, microfibrils of crystalline cellulose are oriented under

a certain angle with respect to the fibre axis and follow a helical path in this cell wall. This angle is usually denoted as the microfibrillar angle (MFA). Hence, in essence, the cell wall can be considered a unidirectional composite of crystalline cellulose microfibrils in a matrix of mainly hemicellulose, curled up in the shape of a hollow cylinder. Using a linear rule of mixture for the stiffness and assuming the ratio of cellulose microfibril stiffness to hemicellulose matrix stiffness is 136/0.2, it may be derived that a variation in volume fraction of crystalline cellulose of 78.1% to 81.0% corresponds to a variation in stiffness of maximum 3.6%.

Second, the MFA can strongly influence the stiffness of a fibre [25,26]. Bourmaud et al. investigated the MFA for 3 different textile flax fibre varieties [26]. They report a minimum MFA of 8.6° for Hermès fibres and a maximum MFA of 9.3° for Agatha fibres. Using classical laminate theory, it may be derived that for small values of the MFA (< 10°) the relative increase or decrease in stiffness, ΔE_{rel}, due to a change in MFA is given by Equation 3. The increase in MFA between Hermès and Agatha fibres of 8.6° to 9.3° can thus maximally induce a rise of 0.8% in the stiffness of the fibres.

$$\Delta E_{rel} \approx \frac{\cos(MFA_1)^4 - \cos(MFA_2)^4}{\cos(MFA_2)^4} \quad (3)$$

From the discussion above it can be concluded that although variations in stiffness of flax fibres due to variety can exist, they are restricted to the limited variations in crystalline cellulose content and MFA. Although more work is needed to corroborate these findings, future studies which address this influence and find significant differences, should therefore clearly show whether the changes are induced by a difference in crystallinity, MFA, or both.

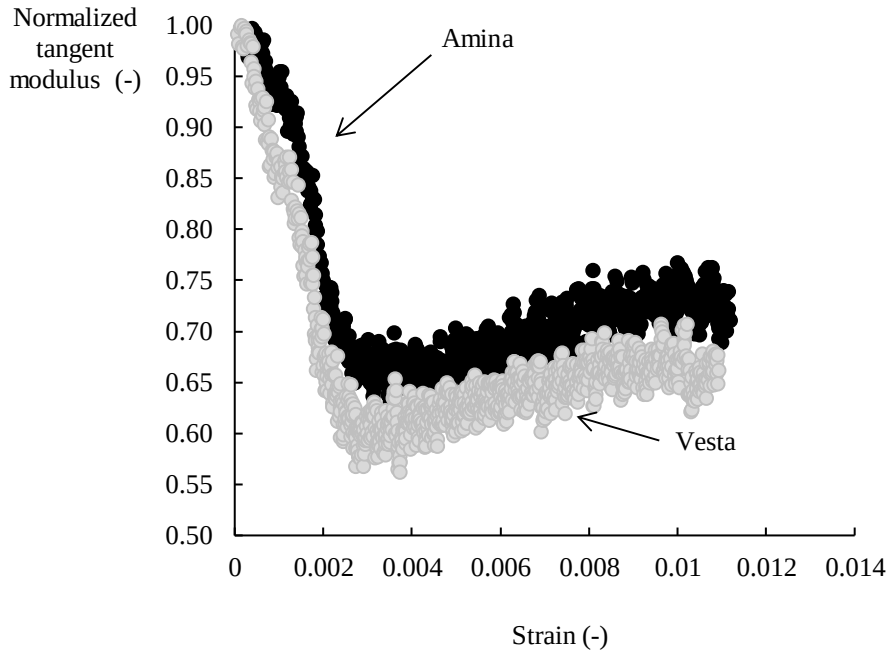

Figure 4-24: Normalized tangent modulus of Amina and Vesta fibres in the composites as a function of strain.

Observing the tangent modulus evolution of the fibres in the composite (Figure 4-24) one can see that both varieties show very similar behavior throughout their tensile loading. Both varieties show approximately identical drops in stiffness in the initial region up to 0.2% strain. In the region between 0.3% and 0.5% strain, the average modulus of the Vesta fibres decreased by 38% whereas the Amina fibres exhibited a decrease of 34% compared to their initial modulus value in the region determined between 0% and 0.1% strain. Statistically these differences were found to be insignificant due to the spread on the results. This is also true for the recovery of the modulus towards the end of the stress-strain curve.

In contrast to stiffness, strength values can be influenced by the variety as strength is a defect-sensitive property. Although not evidenced in this study, a weaker or damaged middle lamella, which is known to exist in certain varieties, could lower the strength of the composite [27]. However, it must be noted that most of these intrinsic differences related to strength might be overshadowed by subsequent processing steps such as retting, scutching, and hackling.

4.3.3.2. The effect of extent of retting

To evaluate the effect of fibre retting on composite properties, the Amina flax fibres were considered in four different states: Stems were collected immediately after pulling them out of the field, after incomplete retting (UR) (±3 weeks), after complete retting (DR) (±4 weeks), and after retting for what would be considered

too long (OR) (±5 weeks). Figure 4-25a shows the back-calculated stiffness of green fibres and fibres that underwent the three different retting degrees. In terms of the initial stiffness E_{f1}, no significant differences were observed. However, the E_{f2} value decreased with increased retting time. Indeed, green fibres preserved their modulus as the average difference between E_{f1} and E_{f2} is a mere 7%, compared to 16%, 31% and 44% for the UR, DR and OR fibres, respectively. Moreover, the difference found for green fibres could not be proven to be statistically significant at the 95% confidence level ($p = 0.07$). The effect of retting on the fibre fineness was also pronounced. With increasing degree of retting, the average diameter of the fibres decreased from 489 µm over 376 µm to 209 µm and finally 130 µm.

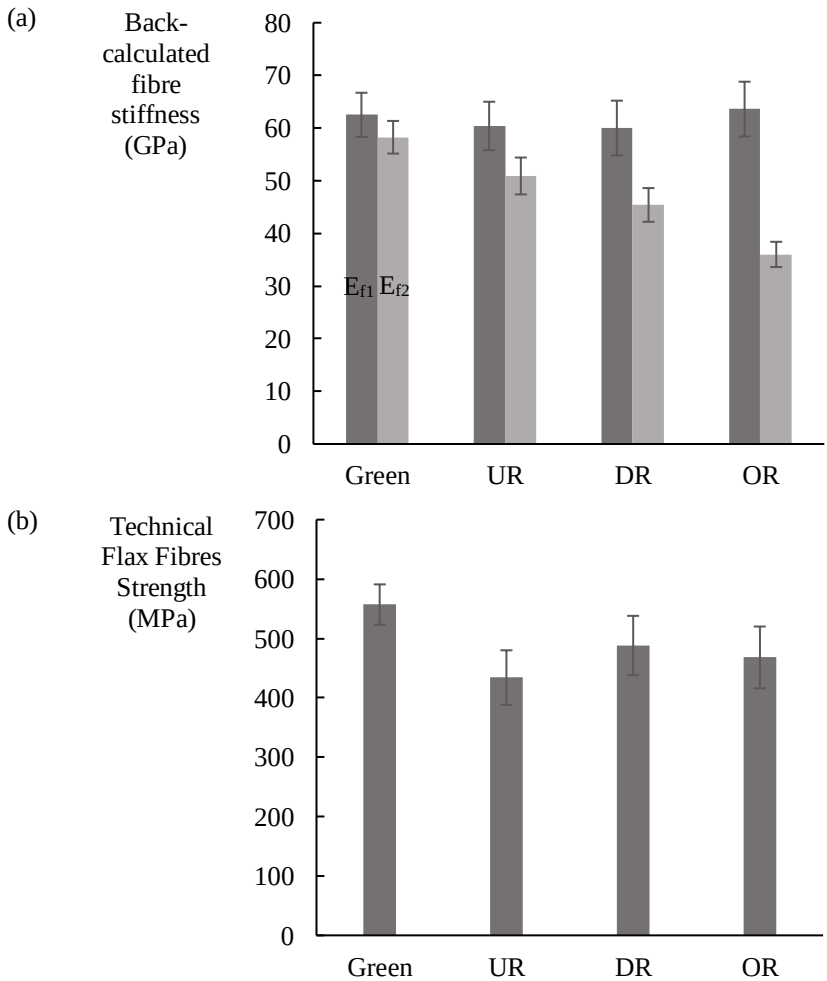

Figure 4-25: Back-calculated fibre (a) stiffness and (b) strength from the composites containing scutched fibres with different degrees of retting.

Lefeuvre et al. established that elementary fibres follow three distinct types of tensile behaviour as shown in Figure 4-26 [6], as had previously been observed for hemp fibres by several authors [20,28,29]. Type I (TI) fibres exhibit a nearly linear stress-strain curve, whereas Type II (TII) fibres are characterized by two linear regions with a decreasing slope in the second region. Type III (TIII) fibres behave more complexly with an initial linear region, followed by a decrease in modulus, and finally a recovery region where the modulus increases again. They showed that higher numbers of type III fibres are positively correlated with fibre stiffness and strength. Furthermore, they found a relation between the chemical composition of the fibres and the occurrence of type III behaviour. Aslan et al. showed that green (i.e. not retted) elementary flax fibres exclusively exhibited quasi-linear behaviour, closely agreeing with the Type I behaviour shown in Figure 4-26 [30].

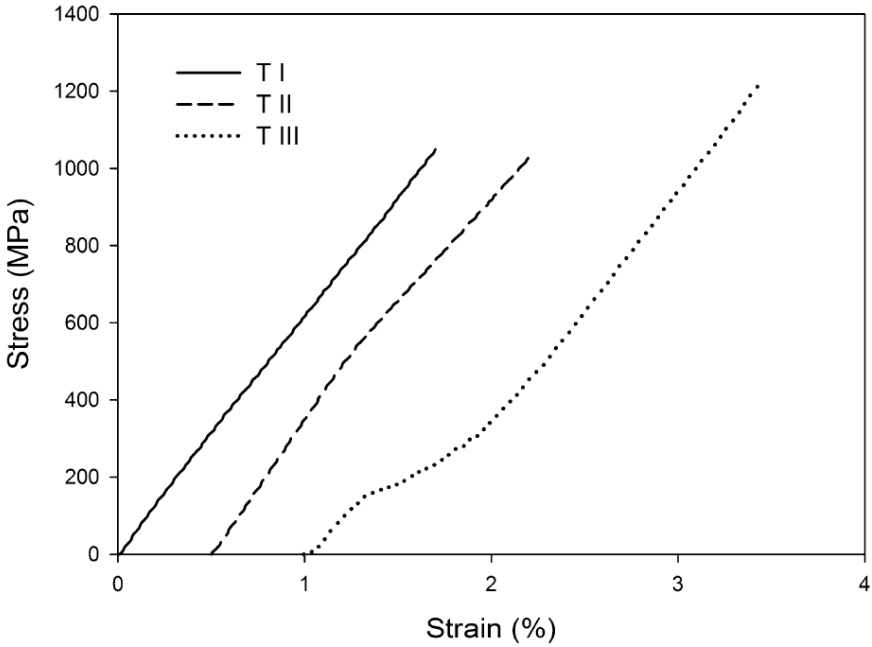

Figure 4-26: Three distinct types of tensile behaviour displayed by elementary flax fibres. (Reprinted from [6] with permission from Elsevier.)

For unidirectional flax fibre composites non-linear behaviour is consistently observed with a very short initial linear elastic region followed by a decrease in modulus and finally a limited recovery of the modulus [2,31]. Although this behaviour closely resembled the above-mentioned type III behaviour of elementary fibres, there exist large differences between both.

Firstly, the difference between the initial modulus and its minimum value for elementary fibres reached almost 50% [6]. In contrast, as shown in Figure 4-27,

this maximum decrease in modulus for the tested composites was only 44%. It has been suggested that this decrease is caused by the shearing of structuring hemicelluloses connecting the cellulose microfibrils [6,32]. Moreover, shearing in the middle lamella can contribute to this decrease as well. Important to note is that this process is accommodated by the reorientation of the microfibrils from the beginning of the deformation, as Keckes et al. proved for wood fibres [33]. The MFA decreased linearly with applied strain, although in composites this internal reorientation in the elementary fibres is likely to be restricted by the surrounding matrix. The reorientation would lead to stiffening, limiting the decrease in modulus due to the shearing of the hemicelluloses, but it appears the latter effect is dominant, as was also expected and illustrated by equation 1.

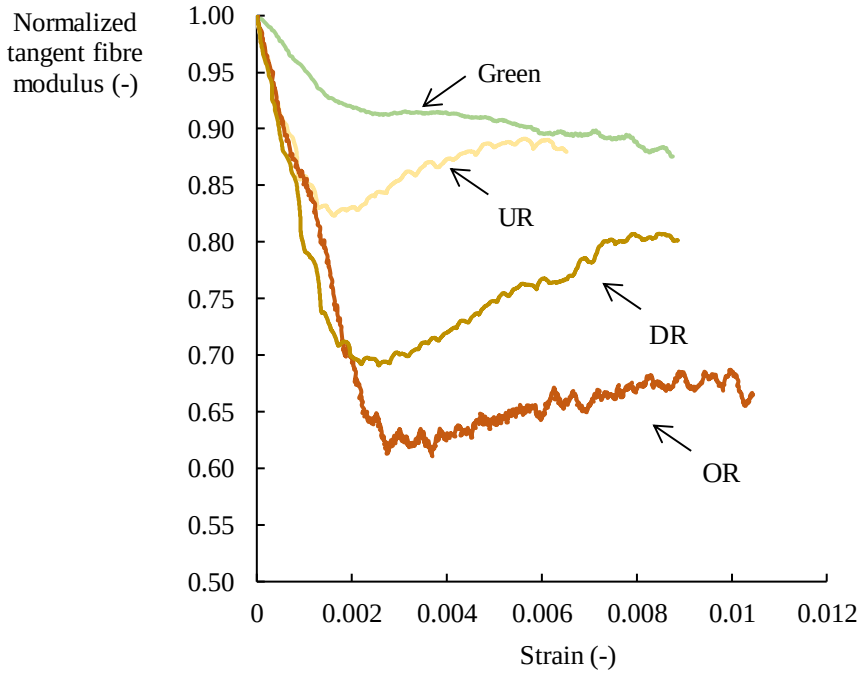

Figure 4-27: Evolution of normalized tangent modulus of the Amina flax fibre composites with tensile strain.

Secondly, the recovery of the modulus which starts after reaching the minimum value is limited and, in this study, ranged between 5% and 10%. The recovery rate in elementary fibres was far greater, ranging between 23% and 34% in the study of Lefeuvre et al., and rising above the initial modulus in some cases [6]. This is linked to the reorientation of the microfibrils and stress induced recrystallization of amorphous cellulose which is hampered by the restricting effect of the polymer matrix. It was established that stress induced recrystallization of amorphous cellulose contributes significantly to the recovery of elementary fibres. The decreased chain mobility due to the presence of the polymer matrix appear to

drastically cut down on the amount of amorphous cellulose which is able to recrystallize during deformation. The shearing deformation of the structuring hemicelluloses will become more difficult as it is hindered by the polymer matrix. The As the stress in the microfibrils increases, stress concentrations will arise in the cell wall and middle lamella. This process is unavoidable, as certain regions in the middle lamella and fibre-matrix interface are intrinsically weaker than others due to compositional variations. Eventually, these stress concentrations will lead to damage and subsequent failure of the composite. Hence, the modulus recovery in the composite will be severely limited.

The previously described tensile behaviour has also been observed here for the different retting degrees except for green fibres. The modulus of green fibres continuously decreased with tensile strain, although the relative decrease was smaller than for the retted fibres, as stated above. Furthermore, as the extent of retting increased the decrease in modulus was more severe. It is hypothesized that this trend is a direct result of the impact retting has on the stiffness of the structuring hemicelluloses and pectins. During retting, hemicellulase and pectinase enzymes will lower the degree of polymerization of hemicellulose and pectin in the fibre. It is hypothesized that this lowers the tensile and shear stiffness of a polymer, resulting in increased shear straining capacity and postponing the full loading of the microfibrils to slightly higher strain values [34]. The absence of a recovery region in the green fibres can be explained by a much higher modulus of the microfibril encrusting polymers, which will not allow extensive shearing nor extensive reorientation of the microfibrils. Simultaneously, the matrix system will also surround elementary fibres which are only loosely attached to their parent technical fibre. The initial modulus which appears to be independent from the degree of retting indicates that the degraded hemicellulose still possesses some resistance to shearing at very low stress levels. Hence, a threshold exists after which this shearing occurs. This could explain why there is no decrease observed in E_{f1} while there is for E_{f2}.

The strength of the composite and hence the fibres is not directly related to the extent of retting as seen in Figure 4-25b. One-way ANOVA showed that the only significant difference was found for incompletely retted fibers which was lower than for all other fibres. Important to highlight here is the difference in extraction method between the green and retted fibres. While the green fibres were peeled off the stem manually, resulting in a separation between the fibres and the xylem, the retted fibres were extracted mechanically through scutching, thus impurities may be left behind on the fibres and the fibre treatment was more aggressive. The reason for the latter is that the xylem itself is connected to the fibre by components which are degraded during retting. The lower the degree of retting, the less xylem is removed during scutching and the lower the final strength of the composite will be. This could explain why the strength of the incompletely retted fibre composites was lower, although this remains a hypothesis.

The former paragraph also illustrates the close relationship between retting and further processing steps such as scutching and hackling. Indeed, when fibres are retted insufficiently long, the subsequent processing will be adversely affected as the amount of impurities in the fibres will be high and the refinement of the fibres will be difficult; harsher machine settings will be needed to achieve sufficient purity and fineness, reducing fibre yield and potentially creating more damage. On the other hand, if the fibres are retted too long, the integrity of the technical fibres will be compromised, and more technical fibres will "break" during extraction, equally lowering the overall yield of long fibres.

To conclude, the previous discussion raises the question whether green, i.e. unretted, fibres could be used in composites. In principle, the previous results do not oppose this idea. However, the difficulty lies in the further processing of these fibres. The absence of retting makes the fibres much more difficult to extract in subsequent mechanical processing and will result in significantly lower yields. Therefore, a trade off will continue to exist between degree of retting and extractability. Nonetheless, it illustrates that retting is not a critical parameter as such when the composite properties of the fibres are considered.

4.3.3.3. The influence of fibre processing

During the traditional extraction of flax fibres, fibre damage is usually not treated as a main concern. Nonetheless, Hänninen et al. have shown that artificial processing of hemp fibres does increase the number of kink bands per unit length [14]. Moreover, they showed that formation of kink bands was not associated with scission of the cellulose chains but that they merely disrupt the alignment of the cellulose microfibrils in the affected regions.

In this study, fibres were sampled after each mechanical operation i.e. breaking, scutching, and hackling. After each step the longitudinal composite properties were measured. Note that the processing steps were sequential. For example, hackled fibres were broken and scutched first before they could be hackled.

As seen in Figure 4-28, the mechanical properties were not significantly affected by the processing conditions. This is a rather surprising result as it is commonly believed that further processing of natural fibres negatively affects the properties of the composites. As stated previously, this misconception in the literature is based mainly on fibre testing where fibre defects are considered to be detrimental to the fibre properties. It has been shown that kink bands in hemp fibres can indeed give rise to stress concentration factors of ≈ 1.4 when embedded in a matrix. However, there was no evidence that the additional kink bands formed through fibre processing lowered the mechanical properties of the composite. Since kink bands are already present in green flax fibres, it could be that a critical number of kink bands has already been accumulated during their growth leading to a "saturation" of damage. This apparent saturation can originate from three distinct phenomena. Firstly, it is possible that additional kink bands are not formed upon

further mechanical loading during processing. Secondly, as mentioned previously, upon loading, kink bands may gradually disappear leading [20]. It could be that the rate of disappearance of these bands is linked to their density in which they are present in a fibre. Finally, the presence of these bands could lead to a critical cluster forming in the composite. Once kink bands are present in a sufficient density to create such a cluster, additional kink bands would then have no further impact on tensile strength. The difference between E_{f1} and E_{f2} was approximately 20% and remained constant with further processing, except for the green fibres. The latter is due to the encrusting polymers of the microfibrils not being degraded by retting. Also, there were no discrepancies observed in the overall tensile behavior.

The difference in fibre strength is mainly attributed to the fibre purity rather than processing conditions, as described in the previous section. This is the likely reason that hackled fibres exhibited a slightly higher tensile strength. Moreover, the strength could have been augmented as well by the elimination of weaker structures such as the middle lamella during hackling.

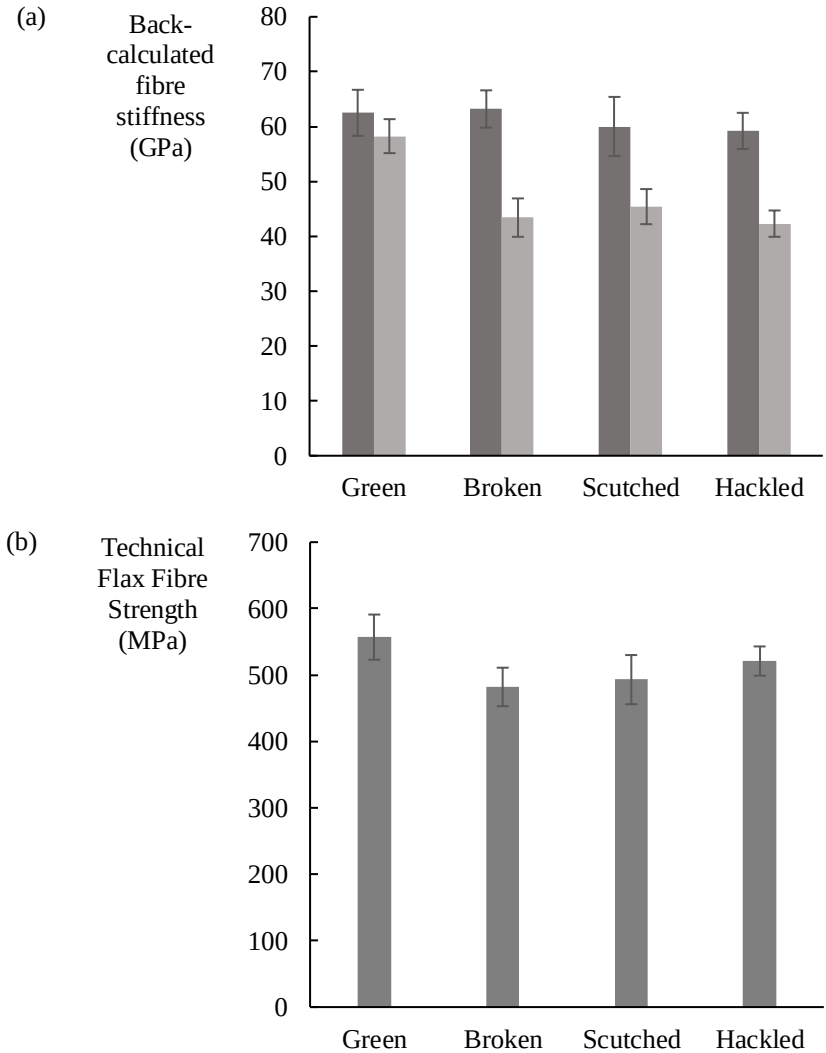

Figure 4-28: Back-calculated fibre (a) stiffness and (b) strength from the composites containing Amina flax fibres that underwent different processing steps. The broken, scutched and hackled fibres were dew retted.

4.3.4. Conclusions

This study evaluated the influence of flax fibre variety, degree of retting, and processing conditions on the properties of flax fibre composites.
The following conclusions can be made:

- No difference in mechanical properties nor shape of the stress-strain curve was observed between the Amina and Vesta varieties. Although only two varieties were considered here, this could be indicative that

current flax fibre varieties do not significantly differ in mechanical properties. Indeed, both the crystalline cellulose content and MFA were found to be very similar for various varieties in previous studies.

- The degree of retting clearly impacted the tensile response of the fibres. E_{f1} does not depend on the retting history of the fibres as it is the initial elastic response of the cellulose microfibrils to the applied loading below the shearing threshold that exists for the weaker hemicellulose and pectin. In contrast, E_{f2} decreased with increasing degree of retting. It is hypothesized that this effect is coupled with the decrease in degree of polymerisation of the structuring polysaccharides, promoting the extent of shearing that occurs when the microfibrils start to reorient.
- Composite properties were not significantly affected by the processing history of the fibres. Broken, scutched, and hackled fibres all performed quasi identically in terms of stiffness and strength. The authors believe that a damage saturation level exists which prevents a further decrease in strength and that this saturation level is already reached during the growth of the flax plant.

References

[1] SALMON-MINOTTE J, FRANCK RR. Flax. Bast Other Plant Fibres 2005:94–175. doi:10.1533/9781845690618.94.

[2] Shah DU, Nag RK, Clifford MJ. Why do we observe significant differences between measured and 'back-calculated' properties of natural fibres? Cellulose 2016;23:1481–90. doi:10.1007/s10570-016-0926-x.

[3] Bensadoun F, Verpoest I, Baets J, Müssig J, Graupner N, Davies P, et al. Impregnated fibre bundle test for natural fibres used in composites. J Reinf Plast Compos 2017;36:942–57. doi:10.1177/0731684417695461.

[4] Baley C, Bourmaud A. Average tensile properties of French elementary flax fibers. Mater Lett 2014;122:159–61. doi:10.1016/j.matlet.2014.02.030.

[5] Thuault A, Eve S, Jouannot-Chesney P, Bréard J, Gomina M. Interrelation Between the Variety and the Mechanical Properties of Flax Fibres. J Biobased Mater Bioenergy 2013;7:609–18. doi:10.1166/jbmb.2013.1396.

[6] Lefeuvre A, Bourmaud A, Morvan C, Baley C. Elementary flax fibre tensile properties: Correlation between stress-strain behaviour and fibre composition. Ind Crops Prod 2014;52:762–9. doi:10.1016/j.indcrop.2013.11.043.

[7] Lefeuvre A, Bourmaud A, Lebrun L, Morvan C, Baley C. A study of the yearly reproducibility of flax fiber tensile properties. Ind Crops Prod 2013;50:400–7. doi:10.1016/j.indcrop.2013.07.035.

[8] Lefeuvre A, Bourmaud A, Morvan C, Baley C. Tensile properties of elementary fibres of flax and glass: Analysis of reproducibility and scattering. Mater Lett 2014;130:289–91. doi:10.1016/J.MATLET.2014.05.115.

[9] Haag K, Padovani J, Fita S, Trouvé J-P, Pineau C, Hawkins S, et al. Influence of flax fibre variety and year-to-year variability on composite properties. Ind Crops Prod 2017;98:1–9. doi:10.1016/j.indcrop.2016.12.028.

[10] Sharma HSS. Enzymatic degradation of residual non-cellulosic polysaccharides present on dew-retted flax fibres. Appl Microbiol Biotechnol 1987;26:358–62. doi:10.1007/BF00256669.

[11] Akin DE, Henriksson G, Evans JD, Adamsen APS, Foulk JA, Dodd RB. Progress in Enzyme-Retting of Flax. J Nat Fibers 2004;1:21–47. doi:10.1300/J395v01n01_03.

[12] Foulk J a., Akin DE, Dodd RB. Processability of flax plant stalks into functional bast fibers. Compos Interfaces 2008;15:147–68. doi:10.1163/156855408783810902.

[13] Thygesen LG, Asgharipour MR. The effects of growth and storage conditions on dislocations in hemp fibres. J Mater Sci 2008;43:3670–3. doi:10.1007/s10853-008-2587-0.

[14] Hänninen T, Thygesen A, Mehmood S, Madsen B, Hughes M. Mechanical processing of bast fibres: The occurrence of damage and its effect on fibre structure. Ind Crops Prod 2012;39:7–11. doi:10.1016/j.indcrop.2012.01.025.

[15] Hernandez-Estrada A, Gusovius H-J, Müssig J, Hughes M. Assessing the susceptibility of hemp fibre to the formation of dislocations during processing. Ind Crops Prod 2016;85:382–8. doi:10.1016/J.INDCROP.2016.01.006.

[16] Norton AJ, Bennett SJ, Hughes M, Dimmock JPRE, Wright D, Newman G, et al. Determining the physical properties of flax fibre for industrial applications: the influence of agronomic practice. Ann Appl Biol 2006;149:15–25.

doi:10.1111/j.1744-7348.2006.00066.x.

[17] Andersons J, Poriķe E, Spārniņš E. The effect of mechanical defects on the strength distribution of elementary flax fibres. Compos Sci Technol 2009;69:2152–7. doi:10.1016/J.COMPSCITECH.2009.05.010.

[18] Hughes M, Sèbe G, Hague J, Hill C, Spear M, Mott L. An investigation into the effects of micro-compressive defects on interphase behaviour in hemp-epoxy composites using half-fringe photoelasticity. Compos Interfaces 2000;7:13–29. doi:10.1163/156855400300183551.

[19] Gourier C, Bourmaud A, Le Duigou A, Baley C. Influence of PA11 and PP thermoplastic polymers on recycling stability of unidirectional flax fibre reinforced biocomposites. Polym Degrad Stab 2017;136:1–9. doi:10.1016/J.POLYMDEGRADSTAB.2016.12.003.

[20] Placet V, Cissé O, Lamine Boubakar M. Nonlinear tensile behaviour of elementary hemp fibres. Part I: Investigation of the possible origins using repeated progressive loading with in situ microscopic observations. Compos Part A Appl Sci Manuf 2014;56:319–27. doi:10.1016/j.compositesa.2012.11.019.

[21] Thuault A, Eve S, Jouannot-Chesney P, Bréard J, Gomina M. Interrelation Between the Variety and the Mechanical Properties of Flax Fibres. J Biobased Mater Bioenergy 2013;7:609–18. doi:10.1166/jbmb.2013.1396.

[22] Bledzki AK, Jaszkiewicz A. Mechanical performance of biocomposites based on PLA and PHBV reinforced with natural fibres – A comparative study to PP. Compos Sci Technol 2010;70:1687–96. doi:10.1016/J.COMPSCITECH.2010.06.005.

[23] Nishino T, Takano K, Nakamae K. Elastic modulus of the crystalline regions of cellulose polymorphs. J Polym Sci Part B Polym Phys 1995;33:1647–51. doi:10.1002/polb.1995.090331110.

[24] Bourmaud A, Beaugrand J, Shah DU, Placet V, Baley C. Towards the design of high-performance plant fibre composites. Prog Mater Sci 2018;97:347–408. doi:10.1016/J.PMATSCI.2018.05.005.

[25] Bourmaud A, Beaugrand J, Shah DU, Placet V, Baley C. Towards the design of high-performance plant fibre composites. Prog Mater Sci 2018;97:347–408. doi:10.1016/J.PMATSCI.2018.05.005.

[26] Bourmaud A, Morvan C, Bouali A, Placet V, Perré P, Baley C. Relationships between micro-fibrillar angle, mechanical properties and biochemical composition of flax fibers. Ind Crops Prod 2013;44:343–51. doi:10.1016/j.indcrop.2012.11.031.

[27] Perremans D, Hendrickx K, Verpoest I, Van Vuure AW. Effect of chemical treatments on the mechanical properties of technical flax fibres with emphasis on stiffness improvement. Compos Sci Technol 2018;160:216–23. doi:10.1016/J.COMPSCITECH.2018.03.030.

[28] Duval A, Bourmaud A, Augier L, Baley C. Influence of the sampling area of the stem on the mechanical properties of hemp fibers. Mater Lett 2011;65:797–800. doi:10.1016/J.MATLET.2010.11.053.

[29] Pickering KL, Beckermann GW, Alam SN, Foreman NJ. Optimising industrial hemp fibre for composites. Compos Part A Appl Sci Manuf 2007;38:461–8. doi:10.1016/J.COMPOSITESA.2006.02.020.

[30] Aslan M, Chinga-Carrasco G, Sørensen BF, Madsen B. Strength variability of

single flax fibres. J Mater Sci 2011;46:6344–54. doi:10.1007/s10853-011-5581-x.

[31] Baets J, Plastria D, Ivens J, Verpoest I. Determination of the optimal flax fibre preparation for use in unidirectional flax–epoxy composites. J Reinf Plast Compos 2014;33:493–502. doi:10.1177/0731684413518620.

[32] Nilsson T, Gustafsson PJ. Influence of dislocations and plasticity on the tensile behaviour of flax and hemp fibres. Compos Part A Appl Sci Manuf 2007;38:1722–8. doi:10.1016/j.compositesa.2007.01.018.

[33] Keckes J, Burgert I, Frühmann K, Müller M, Kölln K, Hamilton M, et al. Cell-wall recovery after irreversible deformation of wood. Nat Mater 2003;2:810–4. doi:10.1038/nmat1019.

[34] Shlieout G, Arnold K, Müller G. Powder and mechanical properties of microcrystalline cellulose with different degrees of polymerization. AAPS PharmSciTech 2002;3:45–54. doi:10.1208/pt030211.

Chapter 5

The behaviour of flax fibres and their composites in humid environments

Chapter 5 The behaviour of flax fibres and their composites in humid environments

5.1. Kinetic and equilibrium hygroscopic behaviour of flax fibres and their composites

Kevin Hendrickx, Wim Thielemans, Aart Willem Van Vuure, Jan Ivens

5.1.1. Introduction

In 1975, Shen and Springer expressed their concerns on the effects moisture absorption could have in polymeric composite materials [1]. In the following years it was proven these concerns were justified. Indeed, it has been established in literature that moisture can severely degrade the properties of composites on several levels. The interfacial shear strength (IFSS) of carbon fibre/epoxy decreases by 22% when it is saturated with water compared to dry conditions while its 0° tensile strength decreases by 16% [2]. This decrease in IFSS contributes to observed decreases between 10 and 50% in transverse strength in unidirectional composites [3–5]. Interlaminar fracture toughness is also influenced by the moisture content. G_{IC} values of unidirectional carbon fibre/PEEK composites increased with increasing moisture content of the composite due to the increased plasticity of the matrix. Simultaneously, G_{IIC} values decreased, as expected due to the decrease in IFSS [6,7]. On the other hand, properties such as 0° tensile strength and stiffness were found not to be significantly affected by the moisture content while the compressive strength decreases by as much as 54% at maximum moisture content [8,9]. To date the effects of moisture in these synthetic fibre composites is still a topic of ongoing research [10–15].

Most synthetic fibres do not absorb moisture which implies the above-mentioned effects are mainly related to the matrix and fibre-matrix interactions. However, with the introduction of aramid fibres in the composite industry, moisture became a parameter that was to be closely monitored throughout the lifetime of the composite. Aramid fibres can, in contrast to glass and carbon fibres, absorb moisture themselves, leading to additional difficulties such as excessive interfacial stresses and intrinsic degradation of the fibre's mechanical properties [16–18]. Hence, characterizing the moisture absorption process in terms of diffusion coefficients, temperature dependence and maximum moisture content became vital to assess their behaviour in structural parts [19,20].

Over the past two decades, the use of natural fibres such as flax has increased significantly [21]. For example, in France the segment of biobased composites is

increasing at 15%/year in volume. By 2020 it would represent more than 12% of the total market volume of composites produced in this country [21]. Due to their chemical structure, natural fibres are inherently sensitive to moisture absorption [22]. Therefore, it is expected that they suffer from the same moisture effects as aramid fibre composites, possibly even worse. Indeed, research has shown that also for these composites the properties are degraded [23–29]. However, literature data is severely scattered and moisture effects can be obscured by various factors such as fibre quality, impregnation quality, impurities and many more. Two recent review articles on the hygroscopic behaviour of plant fibres were unable to reach conclusions regarding the impact of moisture on the mechanical properties of fibres and composites [22,26]. Moreover, unlike aramid fibres, flax fibres are multi-scale composites themselves, further complicating the understanding of moisture ingression [30]. Although some attempts to characterize the moisture absorption process in flax fibres have been performed in literature, most of the studies are limited to the determination of the diffusion coefficient and maximum moisture content of the composites in contact with liquid water. The authors believe that this does not reflect the in-service behaviour of most flax fibre composites as contact with liquids in structural applications is uncommon. Instead, research should rather focus on the absorption behaviour at different levels of the relative humidity. Data on the kinetic and equilibrium sorption behaviour in these conditions is extremely scarce and when it is present, the variation of the results is high. For example, the value of the diffusion coefficient of flax fibres was reported to range between values of $\sim 10^{-7}$ and $\sim 10^{-10}$ m²/s at 80%RH and ~20°C [31–33]. As a final remark, to the best of the authors knowledge, no data exists in literature on the diffusion coefficient during moisture desorption of flax fibres and composites.

This study provides a thorough investigation on the kinetic parameters of the diffusion process. Not only are diffusion coefficients determined for the first time in literature for the elementary and technical fibres, also their relationship to the composite diffusion coefficient is established. Furthermore, the equilibrium moisture content (EMC) of the fibres and composites are determined. Finally, the influence of the moisture on the mechanical properties of the composites is evaluated. In conclusion, this study tries to create a reliable data set of the kinetic and equilibrium parameters of the moisture absorption process.

5.1.2. Materials and methods

5.1.2.1. Flax fibres

Flax fibres were sourced from a commercially available, unidirectional preform FlaxTape 200 supplied by Lineo SA (France). The fibres in this preform underwent scutching and hackling prior to stabilization with water to dissolve part of the pectins and precipitate them at the surface of the tape.

a. Technical fibres

Technical fibres were directly sourced from the preform. For equilibrium and kinetic moisture behaviour measurements, the fibres were cut to a length of 100 mm. Optical microscopy was used to measure their diameter.

b. Elementary fibres

Elementary fibres were sampled from the technical fibres by manual extraction. The fibres were peeled off the technical fibres using fine tweezers without the use of solvents. This method was preferred over the use of solvents as they could leach components from the fibre altering their moisture absorption and desorption behaviour.

5.1.2.2. Matrix system

Epikote 828LVEL, a bisphenol A resin, was crosslinked using 1,4-diaminocyclohexane in a 100 to 15.2 w/w ratio to produce the epoxy matrix for the composites.

5.1.2.3. Dynamic vapour sorption (DVS)

DVS measurements were performed using a DVS Advantage-1 (Surface Measurement Systems). Fibres are placed in a balance with an accuracy of 10^{-7} g. The total mass of each batch is approximately 8 mg. Before the absorption process is started, the fibres are conditioned in the apparatus to a relative humidity (RH) of 0.1% at 20°C. Every 60 s the device registers the mass of the fibres. It is assumed that equilibrium is reached, i.e. fully dry fibres, once the relative difference between two consecutive mass measurements is lower than or equal to 0.002%.

Next, the target RH increases in 10% increments maintaining the data sampling rate and equilibrium condition of the previous paragraph. This process continues until the sample reaches its equilibrium condition at 90%RH after which the desorption process begins. The target RH is then reduced in 10% increments until equilibrium is reached at 0.1%, which ends the measurement.

The moisture content (MC) of the samples, expressed as a mass percentage relative to the dry mass of the fibre, was calculated from equation 1 where M(t) is the mass of the fibre at time t and M_0 is the mass of a fibre in equilibrium with 0.1% RH at 20°C.

$$MC = \frac{M(t) - M_0}{M_0} \quad (1)$$

The final result is called an isotherm which shows the moisture content of a fibre with respect to the relative humidity at a constant temperature, during absorption or desorption.

5.1.2.4. Fluorescence microscopy

A batch of green flax fibre plants (*Linum Usitatissimum L., var. Amina*), grown in Belgium in 2014 was examined using fluorescence microscopy. A part of the middle section of the stems was embedded in an epoxy resin and polished. An aqueous solution of rhodamine 6G was used as the fluorophore. A 532 nm laser was used to excite the rhodamine 6G in the samples.

5.1.2.5. Composite production

Prior to any form of impregnation flax fibres were dried in an oven at 60°C for 24 hours.
Flax fibre-epoxy unidirectional composite plates were produced with vacuum assisted resin infusion. In addition to the above-mentioned drying step, the fibres were dried under full vacuum at 40°C for 1h. The fibre volume fraction was set to 35% and the specimen thickness to 2 mm. Resin injection was performed at 40°C and curing of the resin was achieved under vacuum at 80°C for 1 hour, supplemented by a post-cure step at 150°C for 1 hour. The samples were then cut to the required dimensions using a water-cooled diamond saw. All of these dimensions are in accordance with ASTM D3039/D3039M and ASTM D7264/D7264M prescribing the dimensions to be used for unidirectional composite test specimens in tension and flexion, respectively.

5.1.2.6. Moisture saturation and mass gain/loss measurements of composite specimens

Composite specimens were conditioned to a specified RH value and temperature from their oven dry state in a Weiss WKL 64/40 climate chamber. The initial oven dry state was reached by drying the samples at least 7 days in an oven at 80°C. During saturation the mass of the samples was registered at regular time intervals. In their oven dry state, the mass was denoted as M_0 and equation 1 was used to calculate the moisture content at each time interval. Samples were considered to be equilibrium when the difference in mass between two consecutive measurements was lower than 0.1%/h.

5.1.2.7. Mechanical testing

Prior to any mechanical test, samples were conditioned at 80°C in an oven for at least 7 days to reach the oven dry state. Saturated samples were obtained by to a specified RH level at 80°C for at least 7 days. Testing was performed at 20°C immediately after removing the samples from the climate chamber.

a. Tensile tests

An Instron 5567, equipped with a 30 kN load cell, was used to test the composite samples in tension. Again, as prescribed by ASTM D3039/D3039M, the span length of the sample was set to 150 mm. Strain was registered using an

extensometer with a 50 mm gauge length. Emery cloth prevented slippage of the sample in the clamps. The crosshead displacement rate was set to 1 mm/min.
Due to the non-linear tensile behaviour of flax fibres, the stiffness is calculated between 0 and 0.1% strain, in deviation of the advised standard strain range between 0.1 and 0.3% [5].

b. Flexural tests

Flexural tests were performed following ASTM D7264/D7264 M every other cycle. The crosshead displacement rate was set to 1 mm/min. An Instron 5567 was equipped with a load cell of 1 kN and the crosshead displacement rate was set to 1 mm/min. All tests were done on specimens with a span length of 64 mm with a total sample length of 80 mm.

5.1.3. Results and discussion

5.1.3.1. Absorption behaviour of flax fibres

a. Elementary fibres

When water vapour comes into contact with an unsaturated flax fibre, the water will be absorbed and retained until an equilibrium moisture concentration (EMC) is reached. Higher water vapour concentrations, i.e. higher relative humidity of the environment, will increase the fibre's EMC and vice versa. If the fibre is in an oven dry state, liquid water will not form when the fibre saturation point is not reached. Instead, all water must, by default, be located inside the cell wall matrix and the middle lamella of the technical fibre. This increases both the mass of the cell walls and their volume, causing the cell walls to swell resulting in a macroscopic expansion of the fibres. Upon the introduction of additional water, the cell wall matrix will eventually reach its maximum absorption capacity. When this occurs, the cells cease to swell and the additional water is stored as liquid water in the fibre voids, such as the lumen as it was established in literature for wood fibres [34].
The length of elementary flax fibres is situated between 20 mm to 50 mm while their diameter varies between 10 µm and 30 µm [35–38]. Hence their aspect ratio is estimated to be 700-5000. In the first instance, elementary fibres may be assumed to be cylindrical, having nearly circular cross sections. For infinitely long, perfect cylinders an analytical solution to Fick's second law exists. Let r be the radius of the fibre, D its radial diffusion coefficient, and α_n the roots of the modified Bessel function, $J_0(rx)$, of the first kind and zeroth order, then the analytical solution to this diffusion problem is given in equation 1 [39].

$$MC = M_{sat}\left(1 - \sum_{n=1}^{\infty} \frac{4}{r^2\alpha_n^2}\exp(-D\alpha_n^2 t)\right) \quad (1)$$

α_n are the roots of $J_0(rx) = 0$

Microscopy on 25 elementary fibres revealed their average diameter to be 22 ± 3 µm. Inserting this value in equation 1 and using non-linear least squares fitting with the trust-region approach, enabled us to determine D and M_{sat} from the absorption data.

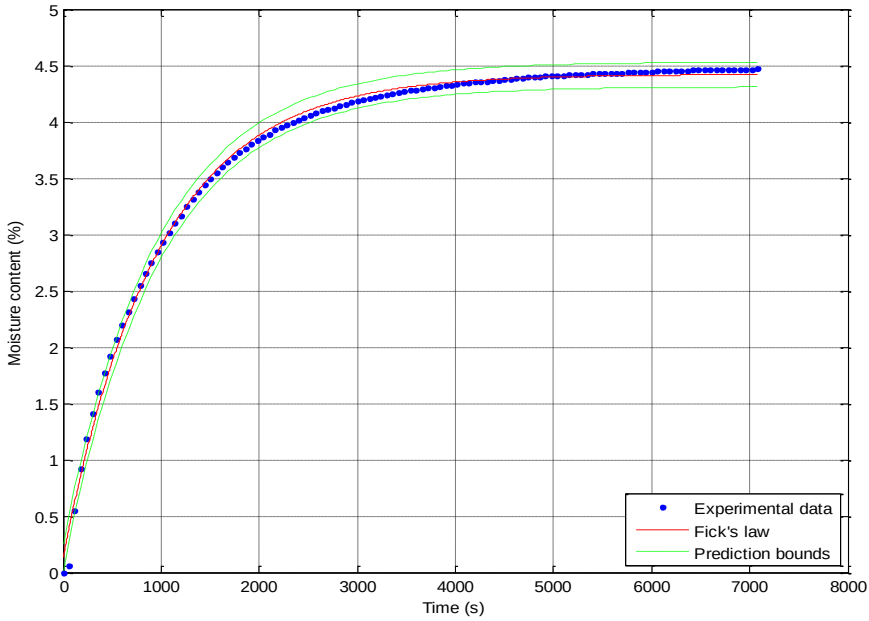

Figure 5-1: Moisture content of an initially dry elementary flax fibre as a function of time when brought into contact with an atmosphere at 20°C and 40% RH measured using DVS. The data was fitted using the analytical solution to Fick's second law for perfect, infinitely long cylinders ($\bar{R}^2$=99.9%).

Figure 5-1 shows a typical absorption curve of dry elementary flax fibres at 20°C when they were instantaneously exposed to a relative humidity of 40%. The process is entirely Fickian, as seen from the adjusted coefficient of determination associated with the fit to Fick's second law, exceeding 99.9 %. Table 5-1 shows the diffusion coefficients and maximum moisture content of the elementary flax fibres at different RH levels. The latter agree well with previous studies on the moisture content of flax fibres at the targeted humidity levels [24,40].

RH level	D (mm^2/s) x 10^6	EMC (%)
10	0.23 ± 0.03	2.00 ± 0.08
20	0.42 ± 0.04	2.86 ± 0.07
30	0.55 ± 0.03	3.56 ± 0.10
40	0.61 ± 0.06	4.48 ± 0.09
50	0.65 ± 0.05	5.29 ± 0.14
60	0.69 ± 0.05	6.66 ± 0.12
70	0.64 ± 0.06	8.19 ± 0.11
80	0.57 ± 0.04	10.43 ± 0.18
90	0.48 ± 0.08	14.07 ± 0.23

Table 5-1: Evolution of the diffusion coefficient and EMC for each RH increment of elementary flax fibres during DVS.

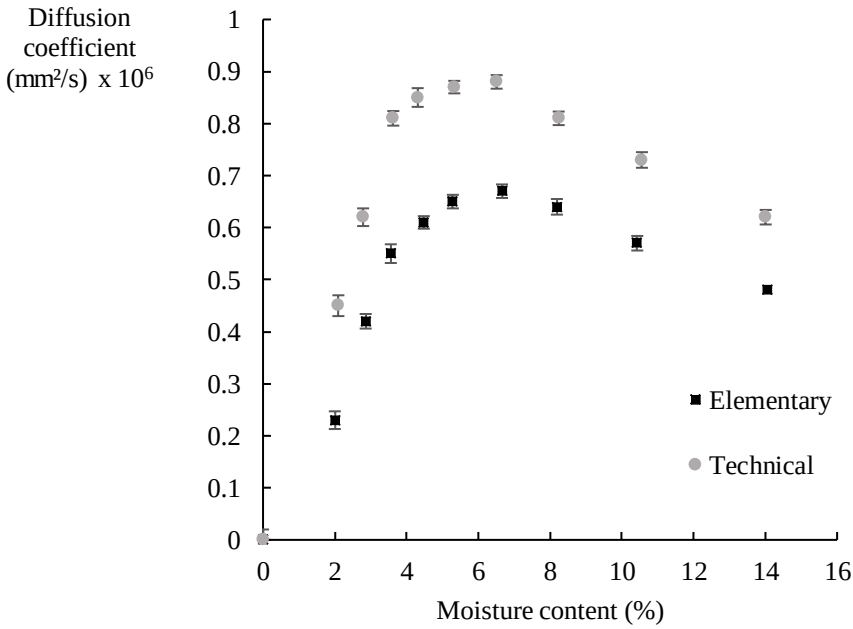

Figure 5-2: Diffusion coefficient as a function of moisture content in the elementary and technical fibres as measured by DVS.

With increasing moisture content in the fibres, the diffusion coefficient first increased significantly, followed by a gradual decrease at higher moisture contents (Figure 5-2). Numerous studies have observed this behaviour for flax and other hygroscopic materials such as keratin, polyamide, epoxies, and numerous other polymers [28,29,41–46]. This implies that the diffusion coefficient cannot be considered to be constant over the entire relative humidity range as it will

dependent on the local moisture concentration. Hence, Fick's second law gains additional complexity and without knowing the dependence of the diffusion coefficient on the concentration, this results in equation 2. This partial differential equation can only be solved by assuming a concentration dependence of D. Often, exponential or power laws are used to enable numerical solutions to this equation [39,47]. However, when considering diffusion calculations involving only small variations in moisture content of the fibres in the 5-10% moisture content range, assuming an average constant diffusion coefficient could provide an elegant alternative.

$$\frac{\partial C}{\partial t} = \frac{\partial}{\partial x}\left(D\frac{\partial C}{\partial x}\right) \tag{2}$$

Here, the origin of the concentration dependent diffusion coefficient is hypothesized to be coupled to the microstructure of flax fibres. Flax fibres consist of regions of crystalline and amorphous cellulose, hemicellulose, pectin and lignin [30,33,48–52]. The latter three are amorphous polymers by definition. All these amorphous polymers can interact with water molecules via hydrogen bonds as they have hydroxyl groups built into their chemical structure. The exception being crystalline cellulose as the crystals are impenetrable to moisture and can only interact with their surface groups [22,53]. Moreover, pectin is partly carboxylated, hence, these groups can also interact with water [30,46].

At low relative humidity (0 < RH < 30) the number of water molecules in the fibre will be low compared to the number of interaction sites provided by the hydroxyl groups of the biopolymers. Some of the hydroxyl groups may be interacting with each other at this stage since there are too few water molecules to occupy each interaction site (schematic Figure 5-3a). In this configuration it is particularly difficult for the water molecules to diffuse further into the fibre as the probability of being "captured" by one of the hydroxyl groups near the fibre surface is high, especially when these groups are mutually interacting with each other. Once a water molecule is interacting with a hydroxyl group, it is immobilized and therefore no longer participates in the diffusion. Due to molecular vibrations however, the water molecules may become mobile again and on longer time scales, this mobilization leads to diffusion. The immobilization time of the water molecules causes the diffusion coefficient within the fibre to be low. In the zone where this mechanism dominates, the process resembles Langmuirian adsorption and for this reason is called Langmuir sorption [45].

With increasing RH (30 < RH < 70), more water molecules will enter the fibre, occupying interaction sites and breaking hydrogen bonds of the mutually interacting hydroxyl groups on the chains. This will effectively result in the formation of an immobile zone (IZ) where water molecules are closely interacting with the hydroxyl groups and a mobile zone in which water molecules are free to move as depicted in Figure 5-3b. Most likely, the strict delineation of mobile to immobile is a simplification, as studies have shown that there is a gradual

transition in these polymers and the water molecules exist in a mobility continuum stretching from completely immobile to completely mobile [54,55]. In this stage of the absorption process, the influence of the interaction sites will diminish as the abundance of water molecules in the mobile zone will start to dominate the process. In the mobile zone, the water molecules are shielded from the influence of the hydroxyl groups and therefore do not experience any significant interactions other than the interaction with neighbouring water molecules. The diffusion coefficient starts to reach a maximum value.

At high RH (RH > 70), the concentration of water in the fibre exceeds a critical point where aggregation of water molecules becomes possible. Water molecules form clusters of larger sizes as indicated by the box in Figure 5-3c [46,56]. It is well known that the diffusion of larger structures progresses slower than those of smaller molecules hence lowering the overall diffusion coefficient again.

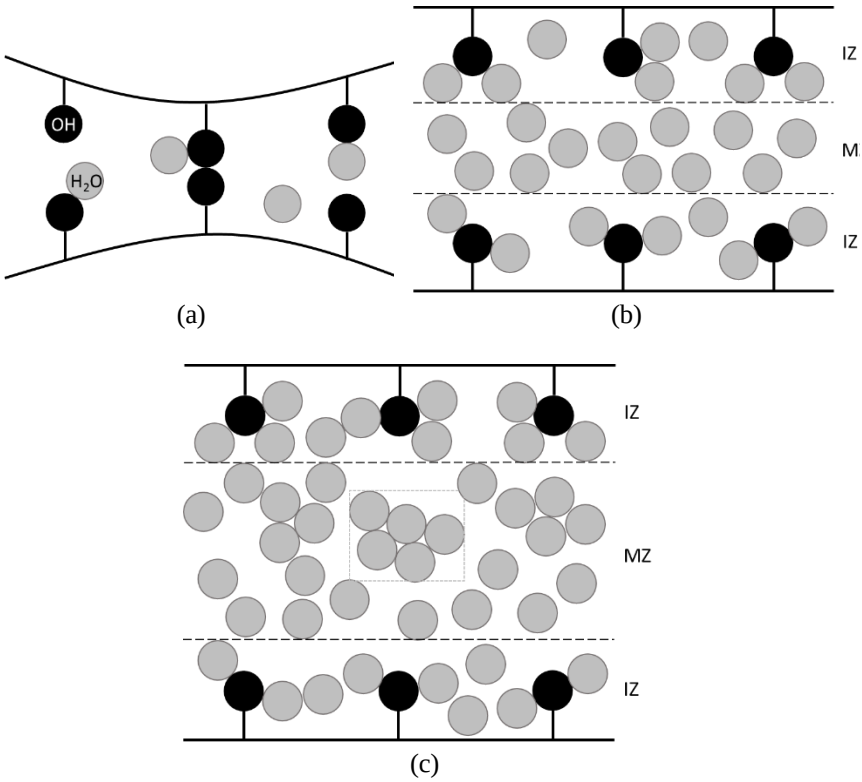

Figure 5-3: Schematic representation of the absorption process at (a) low and (b) intermediate and (c) high relative humidity. Water molecules interact with the hydroxyl functional groups of the biopolymers in the fibre. IZ = immobile zone, MZ = mobile zone; at high water content, water molecules start to aggregate.

b. Technical fibres

Technical fibres are composed of several elementary fibres. The plant ensures the cohesion of this bundle by producing pectin, more specifically rhamnogalacturonan type I, during its growth [30,48]. Pectin will form in between the elementary fibres and create what is commonly known as the middle lamella. This could influence the apparent diffusion coefficient of the technical fibre compared to the elementary fibre if the diffusion coefficient of water were to be significantly different in the interlayer. Furthermore, the EMC could be hypothesized to be different when the EMC of the middle lamella differs from the EMC of the elementary fibres.

The isotherms of elementary and technical fibres, shown in Figure 5-4, are not significantly different. In both type of fibres absorption and desorption of moisture resulted in identical EMCs for all RH conditions. This could indicate that the EMC of the middle lamella is not significantly different from that of the bulk of the fibre or that the pectin content is too low to have a significant effect on the equilibrium conditions. Indeed, several studies report that pectin content in flax fibres accounts for only 1-2% of the total fibre mass [25,57,58]. Further verification by extraction of the pectin and constructing the isotherms fell beyond the scope of this study and was not performed.

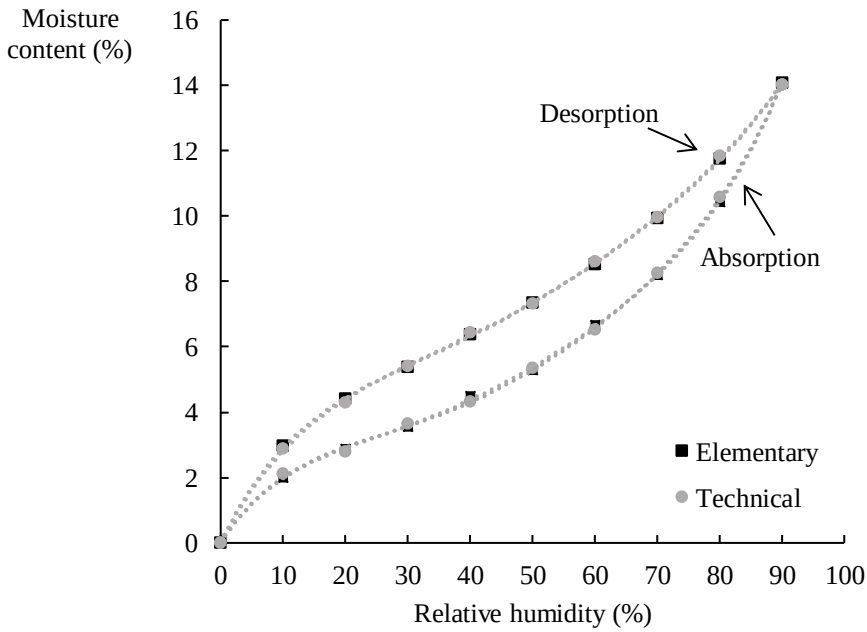

Figure 5-4: Absorption and desorption isotherms for elementary and technical flax fibres. The isotherms of elementary and technical fibres are nearly identical both in absorption and desorption.

The lack of influence on equilibrium conditions, does not exclude an influence on the rate of moisture absorption, as the kinetics and thermodynamics of moisture diffusion processes are generally not directly related. An apparent diameter of 78 ± 5 µm was measured for the technical flax fibres [Section 4.2]. Note that the shape of a technical fibre can differ significantly from a perfect cylinder; it was nonetheless assumed that the analytical solution to Fick's law as given by equation 1 is a sufficiently good approximation.

Comparing the data of the diffusion coefficients of elementary and technical fibres in Figure 5-2, one can see a significant increase in the diffusion coefficient of the technical fibres. As the only difference between the two fibres is the presence of a middle lamella, it must be responsible for the increase. A new mechanism is proposed here for the diffusion in technical flax fibres based on this observation where the middle lamella are proposed to offer a route through which accelerated diffusion can occur. The proposed mechanism is schematized in Figure 5-5. Upon initial contact with humidity in the atmosphere, water molecules starts diffusing into the middle lamellae in a fast diffusion step. Secondly and simultaneously, diffusion of moisture will begin into the cell wall matrix of the elementary fibres. However, this step is hypothesized to occur at a much slower rate than the first as the cell walls contain regions of crystalline cellulose, impermeable to the water molecules and according to the mechanisms described in § 3.1.1. Therefore, the absorption rate of the technical fibres is increased significantly resulting in a higher apparent diffusion coefficient, as it was assumed that the technical fibres behave as solid cylinders in the analytical solution to Fick's law.

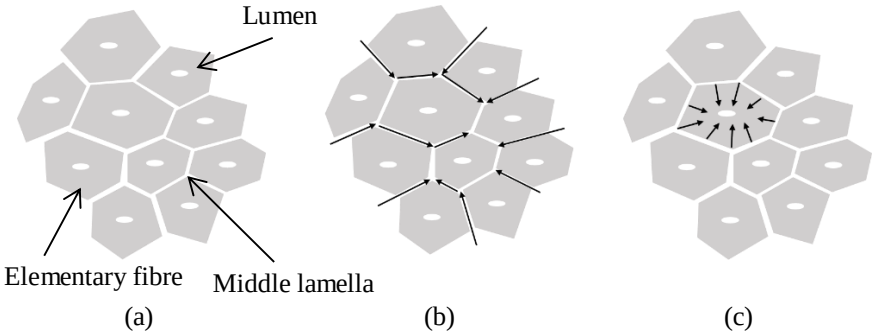

Figure 5-5: Schematic of the proposed diffusion process in technical flax fibres. (a) A technical flax fibre which has not reached its equilibrium moisture content. (b) Fast diffusion step, with water molecules diffusing mainly along the middle lamellae. (c) Slow diffusion step, with water diffusing into the cell wall matrix of the elementary fibres. The arrows indicate the main pathways for moisture diffusion.

This peculiar absorption process becomes highly relevant when the fibres are embedded in composite materials. Neglecting the middle lamella in transient analyses of moisture diffusion in these materials could potentially lead to

inaccurate results, especially when local stress states around the fibre need to be predicted.

5.1.3.2. Desorption behaviour of flax fibres

The absorption of moisture in flax fibres is entirely Fickian in the RH ranges recorded in this study, as discussed above, be it with a diffusion coefficient which is dependent on the moisture concentration in the fibre. When moisture is desorbed, however, anomalous diffusion at low RH levels has been found in this study. Figure 5-6a shows the moisture loss of an elementary flax fibre initially saturated at 30% RH and 20°C which is, subsequently, dried at 0% RH. Comparing the time required to reach saturation and the fully dry state in Figure 5-1 and Figure 5-6a, respectively, it can be seen that reaching the fully dry state takes significantly longer than to reach saturation. In this particular case, the fibre was in fact never able to achieve true equilibrium according to the preset condition ($\Delta M < 0.0002$). This inability to achieve equilibrium was systematically observed for the final drying stage, independent from the initial moisture content of the fibres. As can be seen in Figure 5-4, a hysteresis effect was present between the absorption and desorption equilibrium states at identical RH values. This effect has been observed for other natural fibres such as jute, flax, coir, cotton, hemp, and wood as well [40]. Different theories have been proposed to explain hysteresis in wood, however, no physically consistent model of sorption hysteresis has been put forward to date [59]. Nonetheless, it is clear that more water is retained in the fibre during desorption, implying some form of increased interaction involving water molecules inside the fibre that was not present in absorption.

(a)

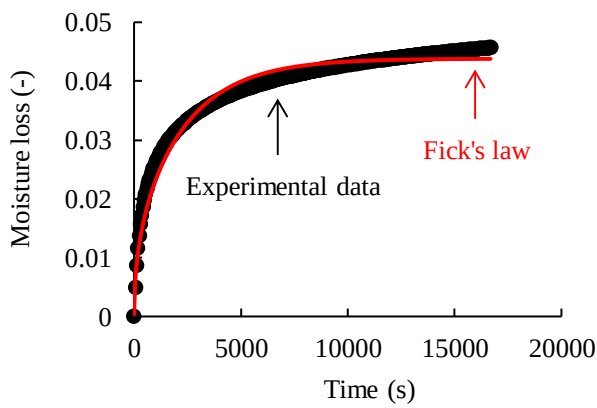

(b)

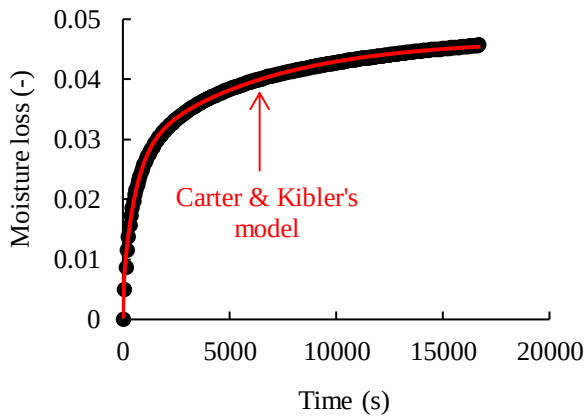

Figure 5-6: Moisture loss of an initially saturated elementary flax fibre at 20°C and 30% RH as a function of time when brought into contact with an atmosphere of 20°C and 0% RH. The data was fitted (a) using the analytical solution to Fick's second law for perfect, infinitely long cylinders ($\bar{R}^2$=86%) and (b) using the model according to Carter and Kibler ($\bar{R}^2$=99.9%) [60].

Diffusion of water molecules in the fibre can provide more details on their mobility throughout the process. Fitting the experimental data in Figure 5-6a to the analytical solution of Fick's law shows that desorption in flax fibres is not always a fully Fickian process. Célino et al. have reported similar, deviating absorption behavior of flax fibres in immersion tests [32]. Note that when the fibres are immersed, the nature of the diffusion process changes drastically and phenomena may occur which are beyond the scope of this study. However, the authors proposed a model, based on Langmuir theory and modified by Carter and Kibler to fit their differing results [32,60].

The former model considers two "types" of water; free water and bound water. When water enters the fibre, it may start interacting with the biopolymer chains in the fibre and become immobile. When this occurs, it is considered as bound. Bound water can become mobile or free again and proceed with its diffusion path. Carter and Kibler assumed this process is repeated indefinitely and assigned fixed probabilities to the mobilization and immobilization of the water. Moreover, only mobile water molecules are assumed to have a diffusion coefficient, D_γ. The model is described by the system of partial differential equations in equation 3.

$$\begin{cases} \dfrac{\partial n}{\partial t} = D_\gamma \left(\dfrac{\partial^2 n}{\partial r^2} + \dfrac{1}{r}\dfrac{\partial n}{\partial r} \right) + \dfrac{\partial N}{\partial t} \\ \dfrac{\partial N}{\partial t} = \gamma n - \beta N \\ \gamma n_\infty = \beta N_\infty \end{cases} \tag{3}$$

where n is the number of mobile molecules per unit volume, N is the number of bound molecules per unit volume, γ is the probability of a mobile water molecule

becoming immobile per unit time, and β is the probability of an immobile water molecule becoming mobile per unit time. Additionally, it is enforced that when equilibrium is reached, an identical number of water molecules shift states from bound to free as there are water molecules shifting from free to bound.

Figure 6b shows the fit of the data to this improved model for moisture diffusion. The adjusted coefficient of determination is increased from 86% to 99.9% with the new model. Note that the increase in adjusted coefficient of determination eliminates the possibility that a better fit was only obtained by the addition of 4 additional fitting parameters. Table 5-2 summarizes the fitting parameters obtained through Fick's law and the model of Carter and Kibler. In Carter and Kibler's model, the diffusion coefficient is about twice the value of its Fickian counterpart. Indeed, the value of D_γ only takes into account the diffusion coefficient of the mobile water molecules, while in Fick's law, the immobilized water molecules are assumed to partake equally in the diffusion process.

Model	Parameter	Value
Fick	D (mm²/s) x 10^6	0.34
	Moisture loss (%)	4.5
Carter and Kibler	D_γ (mm²/s) x 10^6	0.78
	γ (s^{-1})	9.42 x 10^{-5}
	β (s^{-1})	1.75 x 10^{-4}
	Moisture loss (%)	4.6

Table 5-2: Kinetic parameters determined via Fick's law and the Carter and Kibler model for the desorption of elementary flax fibres when dried from saturation at 40%RH to their fully dry state at 20°C.

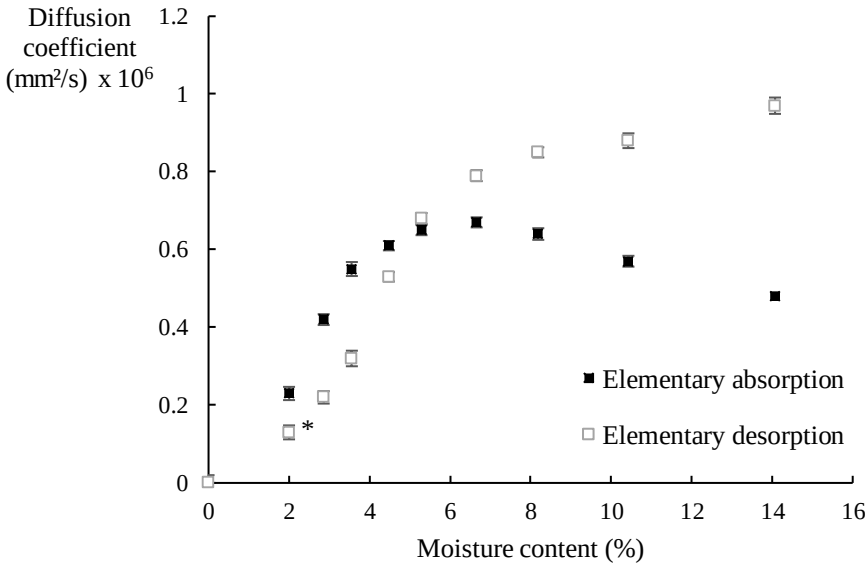

Figure 5-7: Diffusion coefficient as a function of moisture content in the elementary fibres for both absorption and desorption calculated using Fick's law. (*Fitted value according to Fick's law with R^2<0.9)

When the desorption diffusion coefficients are calculated for the entire humidity range it becomes evident that their values evolve differently with respect to the moisture content (Figure 5-7). Note that in this figure the final desorption was also fitted using Fick's law for illustrative purposes. The goodness of fit value is lower than 0.9 indicating the Carter & Kibler model is more appropriate to fit the final desorption stage. In principle the Carter & Kibler model can fit all the aborption and desorption data, however, the data would not be intuitive to interpret due to the additional parameters β and γ. When the fibre is saturated at 90%RH, moisture close to the surface of the fibre will be desorbed very fast as most of the water molecules do not interact with the biopolymer chains of the fibre, with a very strong initial dependence on moisture content. As the fibre continues to lose

moisture, the functional groups of the biopolymer chain are drawn closer together, increasing the possibility of hydrogen bonding between them. It is hypothesized that there is a critical moisture content where the formation rate of these hydrogen bonds increases significantly. This could be attributed to the disappearance of the mobile zone, as proposed in Figure 5-3b. The zone in which this critical moisture content is reached takes the form of a cylindrical shell and is subject to Langmuir sorption. The size of the latter increases as the moisture content decreases, effectively trapping the residual moisture in the core of the fibre, as shown in Figure 5-8. Residual moisture can only diffuse through this layer which requires much more time if no mobile zone is present.

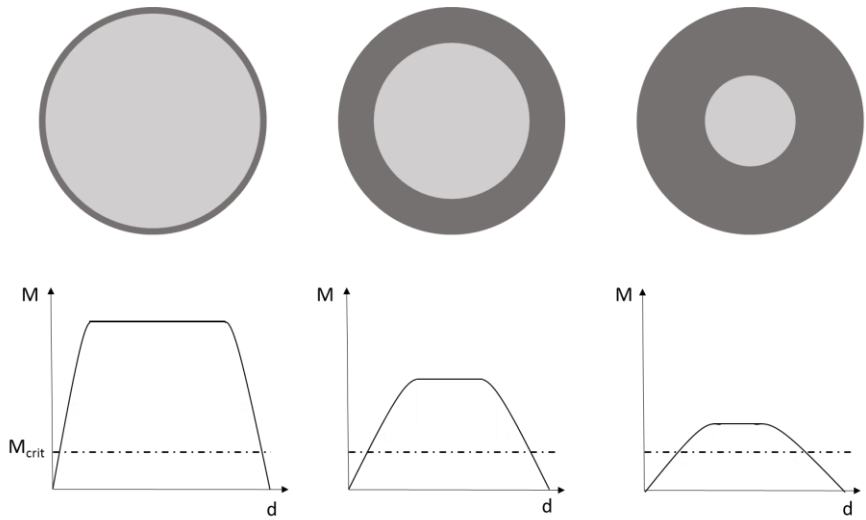

Figure 5-8: Schematic of the stages in the desorption process. The zone where Langmuir diffusion occurs in the fibre is shown in dark grey. This type of diffusion is initiated when the moisture concentration in that zone drops below a critical moisture content (M_{crit}). As the zone expands, the diffusion coefficient lowers significantly. (M=moisture content of the fibre, d=distance from the fibre centre)

It is hypothesized that the mobile zone disappears when the overall moisture content in the fibre reaches 6.5% due to the onset of a sharp decrease in the diffusion coefficient. Note that this value does not equal the value of M_{crit} in Figure 5-8. Conclusive evidence of this hypothesis could potentially be provided using nuclear magnetic resonance spectroscopy to detect the ratio of free to bound water. However, this was not within the scope of this study.

5.1.3.3. Spatial distribution of moisture in flax fibres during diffusion

Two main techniques exist to visualize diffusion paths in natural materials. Neutron radiography can detect water due to the ability of water to attenuate a neutron beam. Deuterium oxide can be used as a contrasting agent to highlight

liquid water flows [61–63]. Alternatively, magnetic resonance imaging (MRI) or nuclear magnetic resonance (NMR) imaging, relies on the non-zero spin of hydrogen atoms to visualize moisture [64–66]. Both techniques have several disadvantages; firstly, neutron beams can only be generated in a synchrotron facility. Secondly, the most advanced neutron radiography and MRI imaging can barely achieve sub-millimeter resolution making it unsuitable for water transport in smaller micron-dimensioned structures such as flax fibres.

At nanoscale level, techniques such as NMR have provided sufficient data to establish that water molecules associate with hydroxyl and, to a lesser extent, carboxyl groups on the cellulose, pectin and hemicellulose chains via hydrogen bonds. It was found for instance that only the 3-hydroxyl groups of amorphous cellulose are involved in water sorption and that hydroxyl groups can interact with multiple water molecules at a time [54].

From the previous two paragraphs it becomes clear that there is a knowledge gap involving moisture diffusion processes at the mesoscale. Therefore, in this study the diffusion path of liquid water in flax fibres was visualized using fluorescence microscopy. The advantages of this technique are its very high resolution and contrast when combined with fluorescent markers. Of course, the technique can only detect liquid water wherein the marker is dissolved, and it is mainly limited to 2D images. Another assumption of the technique is that the marker and the water will follow similar diffusion paths. Hence, two requirements of such a marker are its molecular size and ability to interact with hydroxyl groups. One of the smallest positively charged and commercially available dyes is rhodamine 6G, which was selected for this study. Its chemical structure is shown in Figure 5-9.

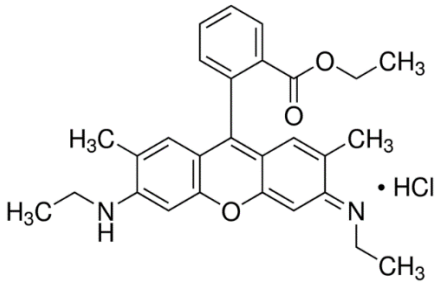

Figure 5-9: Chemical structure of the fluorescent dye, rhodamine 6G.

(a)

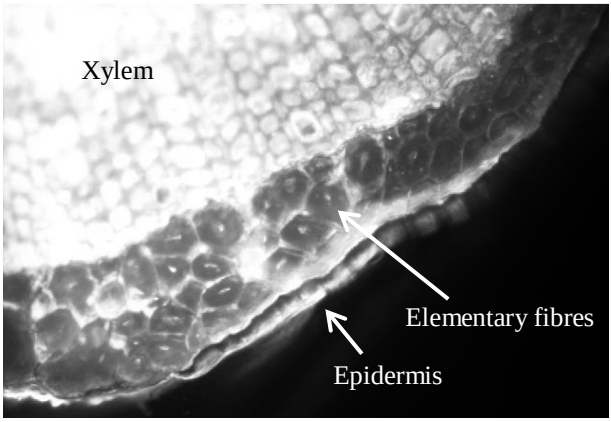

(b)

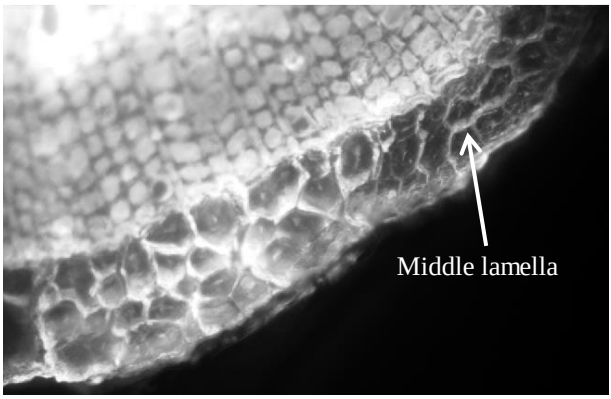

(c)

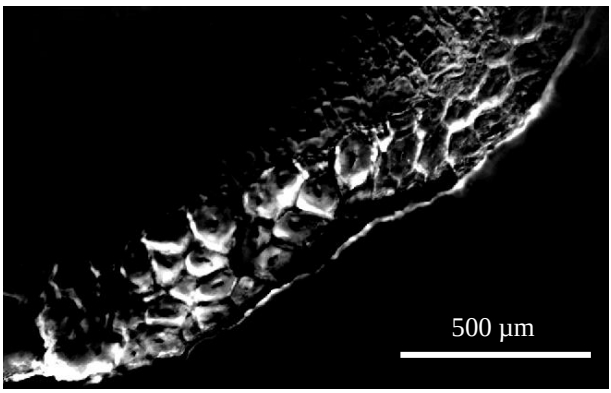

Figure 5-10: Fluorescence microscopy on a flax stem brought into contact with water containing rhodamine 6G (a) immediately after application of the drop, (b) after 20 s has passed and (c) image subtraction of (a) and (b).

A dry flax stem was embedded in an epoxy resin and brought into contact with a drop of liquid water containing 0.03 wt% rhodamine 6G. The flax fibres can be

seen in Figure 5-10a surrounding the xylem tissue and they themselves are surrounded by the epidermis. Weak autofluorescence is already visible in the dry state, in particular for the xylem. It is well known that lignin content in xylem tissue can reach 15 - 20 wt% [67,68]. As most aromatic molecules, lignin is able to fluoresce at different excitation wavelengths [69,70].

A droplet of the water containing the fluorophore was placed on the xylem. The xylem cells took up the liquid by capillary action and diffusion towards the fibre bundles started. After 1 s a first image was taken (Figure 5-10a) showing the filled capillaries of the xylem and the lumen of the elementary fibres. Surprisingly, the middle lamella between the elementary fibres fluoresced as well indicating water uptake. After another 19 s, the image in Figure 5-10b was taken. Here, the ingress of the fluorophore in the middle lamella was even more obvious and the fluorophore also started to diffuse into the elementary fibres. Figure 5-10c is the result of the subtraction of images b and a, where the increased fluorescence intensity in the middle lamella can be seen, indicating increased fluorophore concentration.

These observations corroborate the hypothesis formulated in section 5.1.3.1.b. Nevertheless, a few considerations must be taken into account: As mentioned before, the size and charge of the dye could result in a discrepancy between the diffusion behavior of water molecules and the dye. Its size might prevent it from accessing denser regions while its charge might increase or decrease the interaction with certain functional groups, possibly resulting in different diffusion paths. Also, this experiment was conducted using liquid water. Other diffusion processes can be triggered here compared to the diffusion of water vapor.

To conclude, strong indications exist that the middle lamellae play a crucial role in the early stages of moisture diffusion in technical fibres by acting as preferential diffusion paths.

5.1.3.4. Absorption and desorption in unidirectional flax fibre composites

Figure 5-11 shows the difference in the EMC of flax fibres at 20°C at different relative humidity levels in direct contact with the humidified environment and embedded in an epoxy matrix. The moisture content of the fibres was calculated by subtracting the moisture in the matrix, measured by producing a “composite sample” containing no fibres, from that in the composite at each RH value. A relative decrease in moisture content of 7% and 6% for the 60% and 80% RH level, respectively, was observed for the embedded fibres compared to the fibres that were not embedded during absorption. There are two phenomena that could explain this decreased EMC of the fibres in a composite. Firstly, the epoxide groups of the resin can react with the hydroxyl groups at the surface of the fibres generating crosslinks and eliminating a number of hydroxyl groups which would otherwise be responsible for part of the moisture uptake. A second effect could

involve the constriction of the fibres by the matrix, preventing it from swelling. Indeed, theories have been proposed that couple moisture uptake of the fibres to the radial expansion of the fibres. If one of these is prevented, the other one is also prevented from occurring. In desorption significant differences were found as well for the 60% and 80% RH level, with a relative decrease of 6% and 4% compared to not embedded fibres, respectively. Finally, the hysteresis effect seen in the absorption-desorption isotherm of elementary and technical flax fibres persists when they are embedded in a matrix.

Although, the differences in moisture content exist and are significant, the values are similar. Hence, it must be concluded that the equilibrium condition of the fibres both in and out of the composite is comparable, at least at the considered temperature.

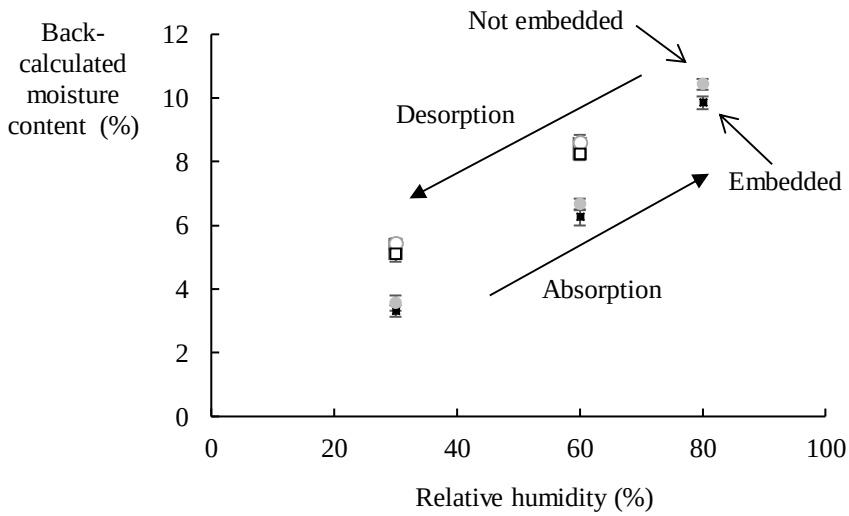

Figure 5-11: Back-calculated moisture content of the flax fibres in a unidirectional composite as a function of the relative humidity. Both absorption and desorption processes are shown.

The cross-sectional diffusion coefficients of the composite specimens were calculated using equation 3, where h is the thickness of the composite specimen concerned and t is the absorption or desorption time [39].

$$MC(t) = M_{sat}\left(1 - \frac{8}{\pi^2}\sum_{n=0}^{\infty}\frac{1}{(2n+1)^2}\exp\left(-\frac{D(2n+1)^2\pi^2 t}{h^2}\right)\right) \qquad (3)$$

In Table 5-3 the diffusion coefficients for the composites are shown for the different RH levels after several stepwise 30%RH increases (0% to 30%, 30% to 60% and 60% to 90%RH). Identically to what was observed for the fibres, the composites exhibit Fickian behaviour in both absorption and desorption. The final desorption step where composites were fully dried at 0% RH were not investigated

in this study. Possibly, this final desorption stage is subject to anomalous diffusion, but this remains to be verified.

To verify the calculated diffusion coefficients, they are compared to what is predicted by a rule of mixtures. Knowing the diffusion coefficient of fibre and matrix, it is possible to estimate the diffusion coefficient of the resulting unidirectional composites. Using the thermal-mass diffusivity analogy, Springer and Tsai were able to provide an analytical expression for the transverse diffusion coefficient of a unidirectional composite of cylindrical fibres with square packing, D_{22}, given in equation 4. D_m, D_f are the diffusion coefficients of matrix and fibre, respectively and V_f is the fibre volume fraction of the composite. Note that D_f is the transverse diffusion coefficient of the fibre and that the fibre is considered to be transversely isotropic.

$$D_{22} = \left(1 - 2\sqrt{\frac{V_f}{\pi}}\right) D_m + \frac{D_m}{K}\left[\pi - \frac{4}{\sqrt{1 - \frac{K^2 V_f}{\pi}}} \tan^{-1}\left(\frac{\sqrt{1 - \frac{K^2 V_f}{\pi}}}{1 + \sqrt{\left(\frac{K^2 V_f}{\pi}\right)}}\right)\right] \qquad (4)$$

$$K = 2\left(\frac{D_m}{D_f} - 1\right)$$

However, the equation is only valid for values of $K^2 V_f / \pi < 1$. Here, the diffusion coefficient of fibres and matrix do not satisfy this condition. Moreover, studies show that this model does not agree very well with experimentally measured data [71,72]. Alternatively, Hashin provided an assembled cylinder model which predicts the coefficient by using equation 5 [73].

$$D_{22} = D_m \frac{D_m(1 - V_f) + D_f(1 + V_f)}{D_m(1 + V_f) + D_f(1 - V_f)} \qquad (5)$$

Table 5-3 summarizes the values obtained using Hashin's approximation and the experimental data. In this study the values correspond remarkably well, though the predicted values of Hashin were always lower than what is observed experimentally. Indeed, it can be shown that equation 5 forms a lower bound on the diffusion coefficient.

RH (%)	Absorption		Desorption	
	D_{22} (experimental) x 10^6 (mm²/s)	D_{22} (predicted) x 10^6 (mm²/s)	D_{22} (experimental) x 10^6 (mm²/s)	D_{22} (predicted) x 10^6 (mm²/s)
30	2.15	2.03	2.01	1.90
60	2.29	2.19	2.28	2.21
90	2.19	2.16	2.40	2.34

Table 5-3: Experimentally observed through the thickness diffusion coefficients for the different RH levels, after several stepwise 30%RH increases (0% to 30%, 30% to 60% and 60% to 90%RH) Also, the predicted values using Hashin's formula based on the measured values of D_f (technical fibre) and D_m are given

In conclusion, the kinetic and equilibrium parameters of moisture diffusion in unidirectional composites can be predicted when these parameters are known for fibres and matrix. It was also found that the diffusion behaviour obeys Fick's law for the RH and temperature values considered here.

5.1.3.5. Influence of absorbed moisture on composite properties

In as-produced condition (0% RH) the back-calculated longitudinal modulus and strength of the flax fibres were 74 ± 1 GPa and 449 ± 28 MPa, respectively. When the moisture content of the composite increased its stiffness rapidly decreased as shown in Figure 5-12a. Stiffness at 80% RH was 46% lower than for the as-produced condition. Several studies have shown similar decreases in stiffness [23,74]. For instance, Berges et al. showed that the stiffness of composite samples conditioned at 70°C and 85% RH was 36% lower than when it was conditioned at 21°C and 50% RH [23]. They hypothesized that this was related to a plasticization effect of water which increased the mobility of the biopolymer chains in the fibre, reducing its stiffness.

The longitudinal strength increased with moisture content of the composite initially and then stabilized at higher moisture content. A similar trend was shown for elementary flax fibres by Thuault et al. [75]. This increase in strength was also attributed to the plasticizing effect of water. Indeed, the failure strain of the composite increased from 0.8% in oven dry condition to 1.8% at 80% RH, showing reduced brittleness (and hence defect sensitivity) due to plasticization effects.

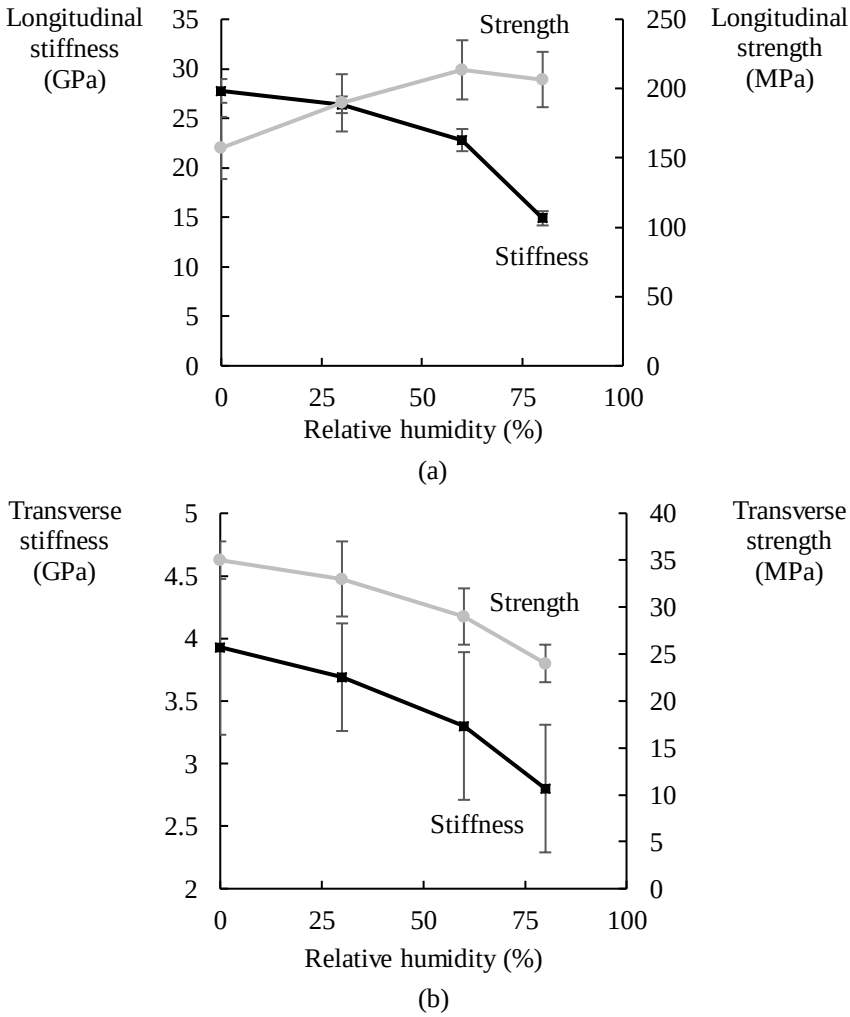

Figure 5-12: Evolution of unidirectional composite modulus and strength with relative humidity for (a) longitudinal and (b) transverse loading conditions.

Finally, the transverse flexural properties of the composites were investigated. Figure 5-12b showed a decrease in both transverse modulus and strength with increasing moisture content. It is well known that epoxy resins are sensitive to moisture, decreasing both properties [6,76]. Moreover, the transverse stiffness of the fibre will, analogous to its longitudinal stiffness, also reduce, contributing to an even greater loss of transverse stiffness of the composite.

The drop in transverse stiffness approached 32% at 80%RH when compared to as-produced samples. This reduction is in close agreement with the 27% decrease reported by Lin and Chen for a similar epoxy system [77]. Note that the flax fibres may also contribute to the decrease in stiffness by their plasticization. Secondly,

the hygroscopic expansion of the fibres may generate significant stresses at the fibre-matrix interface. In turn, these stresses could lead to an earlier development of damage. It is unclear at this moment if or when this damage would develop during the absorption process and what the effect on the mechanical properties would be.

5.1.4. Conclusions

This study evaluated the kinetic and equilibrium parameters of moisture absorption in flax fibres.

The EMC and diffusion coefficients of elementary and technical fibres were measured both in absorption and desorption at various RH levels. It was shown that the diffusion coefficient of both elementary and technical fibres depends on the moisture content of the fibre. The evolution of the coefficient was linked to the existence of mobile and immobile water molecules throughout the diffusion process. Furthermore, the diffusion coefficients were correlated with the values of the unidirectional composites through Hashin's model.

Secondly, a theory was outlined which describes the diffusion process in technical flax fibres. The role of the middle lamella in this process was highlighted as it was hypothesized to provide a path through which accelerated diffusion is possible. This was corroborated by fluorescence microscopy, which shows preferential diffusion occurs along the middle lamella.

Thirdly, the absorption and desorption process in the elementary and technical fibres follows a Fickian behaviour at all RH values, except for the final desorption stage to fully dry condition. Here, the Carter and Kibler model provided a better fit to the experimental data.

Finally, the influence of moisture on the longitudinal and transverse composite properties was measured. Both transverse stiffness and strength and longitudinal stiffness continuously decrease with increasing moisture content while the longitudinal strength reaches a minimum value in dry condition. The latter was linked to the plasticizing effect of water in flax fibres.

References

[1] Shen C-H, Springer GS. Moisture Absorption and Desorption of Composite Materials. J Compos Mater 1976;10:2–20.

[2] Bradley WL, Grant TS. The effect of the moisture absorption on the interfacial strength of polymeric matrix composites. J Mater Sci 1995;30:5537–42. doi:10.1007/BF00351570.

[3] Pomies F, Carlsson LA. Analysis of Modulus and Strength of Dry and Wet Thermoset and Thermoplastic Composites Loaded in Transverse Tension. J Compos Mater 1994;28:22–35. doi:10.1177/002199839402800102.

[4] Garg AC. Effect of moisture and temperature on fracture behavior of graphite-epoxy laminates. Eng Fract Mech 1988;29:127–49. doi:10.1016/0013-7944(88)90042-2.

[5] Rege SK, Lakkad SC. Effect of salt water on mechanical properties of fibre reinforced plastics. Fibre Sci Technol 1983;19:317–24. doi:10.1016/0015-0568(83)90017-9.

[6] Selzer R, Friedrich K. Mechanical properties and failure behaviour of carbon fibre-reinforced polymer composites under the influence of moisture. Compos Part A Appl Sci Manuf 1997;28:595–604. doi:10.1016/S1359-835X(96)00154-6.

[7] Todo M, Nakamura T, Takahashi K. Effects of Moisture Absorption on the Dynamic Interlaminar Fracture Toughness of Carbon/Epoxy Composites. J Compos Mater 2000;34:630–48. doi:10.1177/002199830003400801.

[8] Assarar M, Scida D, El Mahi a., Poilâne C, Ayad R. Influence of water ageing on mechanical properties and damage events of two reinforced composite materials: Flax–fibres and glass–fibres. Mater Des 2011;32:788–95. doi:10.1016/j.matdes.2010.07.024.

[9] Soutis C, Turkmen D. Moisture and Temperature Effects of the Compressive Failure of CFRP Unidirectional Laminates. J Compos Mater 1997;31:832–49. doi:10.1177/002199839703100805.

[10] Genna S, Trovalusci F, Tagliaferri V. Indentation test to study the moisture absorption effect on CFRP composite. Compos Part B Eng 2017;124:1–8. doi:10.1016/J.COMPOSITESB.2017.05.053.

[11] Huo Z, Anandan S, Xu M, Chandrashekhara K. Investigation of three-dimensional moisture diffusion modeling and mechanical degradation of carbon/bismaleimide composites under seawater conditioning. J Compos Mater 2018;52:1339–51. doi:10.1177/0021998317725159.

[12] Cysne Barbosa AP, P. Fulco AP, S.S. Guerra E, K. Arakaki F, Tosatto M, B. Costa MC, et al. Accelerated aging effects on carbon fiber/epoxy composites. Compos Part B Eng 2017;110:298–306. doi:10.1016/J.COMPOSITESB.2016.11.004.

[13] Yao X, Gao X, Jiang J, Xu C, Deng C, Wang J. Comparison of carbon nanotubes and graphene oxide coated carbon fiber for improving the interfacial properties of carbon fiber/epoxy composites. Compos Part B Eng 2018;132:170–7. doi:10.1016/J.COMPOSITESB.2017.09.012.

[14] Gargano A, Pingkarawat K, Pickerd V, Delaney T, Das R, Mouritz AP. Effect of seawater immersion on the explosive blast response of a carbon fibre-polymer laminate. Compos Part A Appl Sci Manuf 2018;109:382–91. doi:10.1016/J.COMPOSITESA.2018.03.027.

[15] Kim D, Centea T, Nutt SR. Modelling and monitoring of out-time and moisture

absorption effects on cure kinetics and viscosity for an out-of-autoclave (OoA) prepreg. Compos Sci Technol 2017;138:201–8. doi:10.1016/J.COMPSCITECH.2016.11.023.

[16] Hahn HT, Kim KS. Hygroscopic Effects in Aramid Fiber/Epoxy Composite. J Eng Mater Technol 1988;110:153. doi:10.1115/1.3226024.

[17] Cervenka AJ, Bannister DJ, Young RJ. Moisture absorption and interfacial failure in aramid/epoxy composites. Compos Part A Appl Sci Manuf 1998;29:1137–44. doi:10.1016/S1359-835X(98)00012-8.

[18] Allred RE, Roylance DK. Transverse moisture sensitivity of aramid/epoxy composites. J Mater Sci 1983;18:652–6. doi:10.1007/BF00745562.

[19] Verpoest I, Springer GS. Moisture Absorption Characteristics of Aramid-Epoxy Composites. J Reinf Plast Compos 1988;7:2–22. doi:10.1177/073168448800700101.

[20] Varelidis P., Papakostopoulos D., Pandazis C., Papaspyrides C. Polyamide coated Kevlar™ fabric in epoxy resin: mechanical properties and moisture absorption studies. Compos Part A Appl Sci Manuf 2000;31:549–58. doi:10.1016/S1359-835X(99)00101-3.

[21] JEC Group. Overview of the global composites market, at the crossroads. Paris: JEC Group; 2017.

[22] Célino A, Fréour S, Jacquemin F, Casari P. The hygroscopic behavior of plant fibers: a review. Front Chem 2013;1:43. doi:10.3389/fchem.2013.00043.

[23] Berges M, Léger R, Placet V, Person V, Corn S, Gabrion X, et al. Influence of moisture uptake on the static, cyclic and dynamic behaviour of unidirectional flax fibre-reinforced epoxy laminates. Compos Part A Appl Sci Manuf 2016;88:165–77. doi:10.1016/j.compositesa.2016.05.029.

[24] Masseteau B, Michaud F, Irle M, Roy A, Alise G. An evaluation of the effects of moisture content on the modulus of elasticity of a unidirectional flax fiber composite. Compos Part A Appl Sci Manuf 2014;60:32–7. doi:10.1016/j.compositesa.2014.01.011.

[25] Dittenber DB, Gangarao HVS. Critical review of recent publications on use of natural composites in infrastructure. Compos Part A Appl Sci Manuf 2012;43:1419–29. doi:10.1016/j.compositesa.2011.11.019.

[26] Mokhothu TH, John MJ. Review on hygroscopic aging of cellulose fibres and their biocomposites. Carbohydr Polym 2015;131:337–54. doi:10.1016/j.carbpol.2015.06.027.

[27] Regazzi A, Léger R, Corn S, Ienny P. Modeling of hydrothermal aging of short flax fiber reinforced composites. Compos Part A Appl Sci Manuf 2016;90:559–66. doi:10.1016/j.compositesa.2016.08.011.

[28] Stamboulis A. Environmental durability of flax fibres and their composites based on polypropylene matrix. Appl Compos Mater 2000;7:273–94. doi:10.1023/A:1026581922221.

[29] Alix S, Philippe E, Bessadok A, Lebrun L, Morvan C, Marais S. Effect of chemical treatments on water sorption and mechanical properties of flax fibres. Bioresour Technol 2009;100:4742–9. doi:10.1016/j.biortech.2009.04.067.

[30] Morvan C, Andème-Onzighi C, Girault R, Himmelsbach DS, Driouich A, Akin DE. Building flax fibres: more than one brick in the walls. Plant Physiol Biochem 2003;41:935–44. doi:10.1016/j.plaphy.2003.07.001.

[31] Gouanvé F, Marais S, Bessadok A, Langevin D, Morvan C, Métayer M. Study of water sorption in modified flax fibers. J Appl Polym Sci 2006;101:4281–9. doi:10.1002/app.23661.

[32] Célino A, Fréour S, Jacquemin F, Casari P. Characterization and modeling of the moisture diffusion behavior of natural fibers. J Appl Polym Sci 2013;130:297–306. doi:10.1002/app.39148.

[33] Alix S, Lebrun L, Marais S, Philippe E, Bourmaud A, Baley C, et al. Pectinase treatments on technical fibres of flax: Effects on water sorption and mechanical properties. Carbohydr Polym 2012;87:177–85. doi:10.1016/j.carbpol.2011.07.035.

[34] Mohr BJ, Nanko H, Kurtis KE. Durability of kraft pulp fiber–cement composites to wet/dry cycling. Cem Concr Compos 2005;27:435–48. doi:10.1016/J.CEMCONCOMP.2004.07.006.

[35] Charlet K, Baley C, Morvan C, Jernot JP, Gomina M, Bréard J. Characteristics of Hermès flax fibres as a function of their location in the stem and properties of the derived unidirectional composites. Compos Part A Appl Sci Manuf 2007;38:1912–21. doi:10.1016/j.compositesa.2007.03.006.

[36] Charlet K, Jernot JP, Eve S, Gomina M, Bréard J. Multi-scale morphological characterisation of flax: From the stem to the fibrils. Carbohydr Polym 2010;82:54–61. doi:10.1016/j.carbpol.2010.04.022.

[37] Bos HL, Van Den Oever MJA, Peters OCJJ. Tensile and compressive properties of flax fibres for natural fibre reinforced composites. J Mater Sci 2002;37:1683–92. doi:10.1023/A:1014925621252.

[38] Bos HL, Donald AM. In situ ESEM study of the deformation of elementary flax fibres. J Mater Sci 1999;34:3029–34. doi:10.1023/A:1004650126890.

[39] Crank J. The mathematics of diffusion. vol. 1. 2nd ed. Uxbridge: Clarendon Press, Oxford; 1975. doi:10.1016/0306-4549(77)90072-X.

[40] Hill CAS, Norton A, Newman G. The water vapor sorption behavior of natural fibers. J Appl Polym Sci 2009;112:1524–37. doi:10.1002/app.29725.

[41] Rouse PE. Diffusion of Vapors in Films. J Am Chem Soc 1947;69:1068–73. doi:10.1021/ja01197a029.

[42] King G. Permeability of keratin membranes to water vapour. Trans Faraday Soc 1945;41:479. doi:10.1039/tf9454100479.

[43] Joannès S, Mazé L, Bunsell AR. A concentration-dependent diffusion coefficient model for water sorption in composite. Compos Struct 2014;108:111–8. doi:10.1016/J.COMPSTRUCT.2013.09.007.

[44] George SC, Thomas S. Transport phenomena through polymeric systems. Prog Polym Sci 2001;26:985–1017. doi:10.1016/S0079-6700(00)00036-8.

[45] Gouanvé F, Marais S, Bessadok a., Langevin D, Métayer M. Kinetics of water sorption in flax and PET fibers. Eur Polym J 2007;43:586–98. doi:10.1016/j.eurpolymj.2006.10.023.

[46] Célino A, Gonçalves O, Jacquemin F, Fréour S. Qualitative and quantitative assessment of water sorption in natural fibres using ATR-FTIR spectroscopy. Carbohydr Polym 2014;101:163–70. doi:10.1016/j.carbpol.2013.09.023.

[47] Joannès S, Mazé L, Bunsell AR. A concentration-dependent diffusion coefficient model for water sorption in composite. Compos Struct 2014;108:111–8. doi:10.1016/J.COMPSTRUCT.2013.09.007.

[48] Bédouet L, Denys E, Courtois B, Courtois J. Changes in esterified pectins during development in the flax stems and leaves. Carbohydr Polym 2006;65:165–73. doi:10.1016/j.carbpol.2005.12.041.

[49] Akin DE. Linen Most Useful: Perspectives on Structure, Chemistry, and Enzymes for Retting Flax. ISRN Biotechnol 2013;2013:1–23. doi:10.5402/2013/186534.

[50] Kabir MM, Wang H, Lau KT, Cardona F. Chemical treatments on plant-based natural fibre reinforced polymer composites: An overview. Compos Part B Eng 2012;43:2883–92. doi:10.1016/j.compositesb.2012.04.053.

[51] van Hazendonk JM, Reinerik EJM, de Waard P, van Dam JEG. Structural analysis of acetylated hemicellulose polysaccharides from fibre flax (Linum usitatissimum L.). Carbohydr Res 1996;291:141–54. doi:10.1016/S0008-6215(96)00160-7.

[52] Girault R, Bert F, Rihouey C, Jauneau A, Morvan C, Jarvis M. Galactans and cellulose in flax fibres: putative contributions to the tensile strength. Int J Biol Macromol 1997;21:179–88. doi:10.1016/S0141-8130(97)00059-7.

[53] Nelson RA. The determination of moisture transitions in cellulosic materials using differential scanning calorimetry. J Appl Polym Sci 1977;21:645–54. doi:10.1002/app.1977.070210306.

[54] Nakamura K, Hatakeyama T, Hatakeyama H. Studies on Bound Water of Cellulose by Differential Scanning Calorimetry. Text Res J 1981;51:607–13. doi:10.1177/004051758105100909.

[55] Popineau S, Rondeau-Mouro C, Sulpice-Gaillet C, Shanahan MER. Free/bound water absorption in an epoxy adhesive. Polymer (Guildf) 2005;46:10733–40. doi:10.1016/J.POLYMER.2005.09.008.

[56] Rouse PE. Diffusion of Vapors in Films. J Am Chem Soc 1947;69:1068–73. doi:10.1021/ja01197a029.

[57] Yan L, Chouw N, Jayaraman K. Flax fibre and its composites – A review. Compos Part B Eng 2014;56:296–317. doi:10.1016/j.compositesb.2013.08.014.

[58] Hughes M. Defects in natural fibres: their origin, characteristics and implications for natural fibre-reinforced composites. J Mater Sci 2012;47:599–609. doi:10.1007/s10853-011-6025-3.

[59] Engelund ET, Thygesen LG, Svensson S, Hill CAS. A critical discussion of the physics of wood–water interactions. Wood Sci Technol 2013;47:141–61. doi:10.1007/s00226-012-0514-7.

[60] Carter HG, Kibler KG. Langmuir-Type Model for Anomalous Moisture Diffusion In Composite Resins. J Compos Mater 1978;12:118–31. doi:10.1177/002199837801200201.

[61] Warren JM, Bilheux H, Kang M, Voisin S, Cheng C-L, Horita J, et al. Neutron imaging reveals internal plant water dynamics n.d. doi:10.1007/s11104-012-1579-7.

[62] Zarebanadkouki M, Kim YX, Carminati A. Where do roots take up water? Neutron radiography of water flow into the roots of transpiring plants growing in soil. New Phytol 2013;199:1034–44. doi:10.1111/nph.12330.

[63] Defraeye T, Derome D, Aregawi W, Hartmann S, Lehmann E, Carmeliet J, et al. Quantitative neutron imaging of water distribution, venation network ans sap flow in leaves. Planta 2014;240:423–36.

[64] WINDT CW, VERGELDT FJ, DE JAGER PA, VAN AS H. MRI of long-distance water transport: a comparison of the phloem and xylem flow characteristics and

dynamics in poplar, castor bean, tomato and tobacco. Plant, Cell Environ 2006;29:1715–29. doi:10.1111/j.1365-3040.2006.01544.x.

[65] Van As H, van Duynhoven J. MRI of plants and foods. J Magn Reson 2013;229:25–34. doi:10.1016/J.JMR.2012.12.019.

[66] Zhou M, Caré S, Courtier-Murias D, Faure P, Rodts S, Coussot P. Magnetic resonance imaging evidences of the impact of water sorption on hardwood capillary imbibition dynamics. Wood Sci Technol 2018;52:929–55. doi:10.1007/s00226-018-1017-y.

[67] Kotelnikova NE, Panarin EF, Serimaa R, Paakkari T, Sukhanova TE, Gribanov AV. Study of flax fibre structure by WAXS, IR and 13C NMR spectroscopy, and SEM. Cellul Pulps, Fibres Mater 2000:169–79. doi:10.1533/9781845698546.169.

[68] Gorshkova T. Composition and Distribution of Cell Wall Phenolic Compounds in Flax (Linum usitatissimum L.) Stem Tissues. Ann Bot 2000;85:477–86. doi:10.1006/anbo.1999.1091.

[69] Albinsson B, Li S, Lundquist K, Stomberg R. The origin of lignin fluorescence. J Mol Struct 1999;508:19–27. doi:10.1016/S0022-2860(98)00913-2.

[70] DONALDSON LA, RADOTIC K. Fluorescence lifetime imaging of lignin autofluorescence in normal and compression wood. J Microsc 2013;251:178–87. doi:10.1111/jmi.12059.

[71] Venetis J, Sideridis E, Venetis J, Sideridis E. The Thermal Conductivities of Periodic Fibrous Composites as Defined by a Mathematical Model. Fibers 2017;5:30. doi:10.3390/fib5030030.

[72] Rolfes R, Hammerschmidt U. Transverse thermal conductivity of CFRP laminates: A numerical and experimental validation of approximation formulae. Compos Sci Technol 1995;54:45–54. doi:10.1016/0266-3538(95)00036-4.

[73] Hashin Z. Analysis of Properties of Fiber Composites With Anisotropic Constituents. J Appl Mech 1979;46:543. doi:10.1115/1.3424603.

[74] Stamboulis A. Environmental durability of flax fibres and their composites based on polypropylene matrix. Appl Compos Mater 2000;7:273–94. doi:10.1023/A:1026581922221.

[75] Thuault A, Eve S, Blond D, Breard J, Gomina M. Effects of the hygrothermal environment on the mechanical properties of flax fibres. J Compos Mater 2013;48:1699–707. doi:10.1177/0021998313490217.

[76] Maslinda AB, Abdul Majid MS, Ridzuan MJM, Afendi M, Gibson AG. Effect of water absorption on the mechanical properties of hybrid interwoven cellulosic-cellulosic fibre reinforced epoxy composites. Compos Struct 2017;167:227–37. doi:10.1016/J.COMPSTRUCT.2017.02.023.

[77] Lin YC, Chen X. Moisture sorption–desorption–resorption characteristics and its effect on the mechanical behavior of the epoxy system. Polymer (Guildf) 2005;46:11994–2003. doi:10.1016/J.POLYMER.2005.10.002.

5.2. Decreasing the moisture sensitivity of flax fibres through crosslinking treatments

Kevin Hendrickx, Wim Thielemans, Aart Willem Van Vuure, Jan Ivens

5.2.1. Introduction

Numerous studies show that flax fibres and their composites deform non-linearly upon tensile loading [1–5]. In the literature it is currently hypothesized that structuring polysaccharides between the cellulose microfibrils, reorientation of these fibrils, and crystallization of amorphous cellulose play a major role in this behaviour [6]. As these mechanisms occur at the nanoscale in a heterogeneous material, they are extremely difficult to verify, especially considering these mechanisms have to be monitored *in-situ* during a mechanical test.

It has also been shown that moisture significantly lowers the tensile stiffness of flax fibres [7]. For example, the stiffness of short flax fibre (30wt%) reinforced/polylactic acid (PLA) composites decreased by approximately 70% in saturated condition after water immersion [8,9]. The plasticizing effect of water molecules is intrinsically connected to the chemical composition of flax fibres [10]. This is because the hydroxyl functionalities are responsible for the interactions between the polysaccharide chains as well as the interaction with moisture.

In a previous study by some of the authors, it was shown that aldehydes are able to greatly influence the mechanical behaviour of technical flax fibres [11]. Treatment with ethanedial increased technical fibre stiffness and reduced the tensile strain to failure of the resulting composites. It was hypothesized that ethanedial acted as a crosslinker, reacting with the hydroxyl groups of the different biopolymer chains in the fibre. Indeed, in the presence of an acid catalyst, ethanedial readily reacts with these groups to form hemi-acetals. Upon the evaporation of excess water, stable acetal bonds are formed. When such crosslinks are formed between structuring polysaccharide chains in the fibre, the mechanical behaviour is altered as the chains' ability to move relatively to each other is decreased. This was evidenced by an extension of the linear elastic region seen in the tensile stress-strain behaviour for the ethanedial treated fibres as it was hypothesized that the decrease in tangent modulus is caused by shearing of the structuring polysaccharides [12].

As ethanedial is a dialdehyde, two acetal bonds can be formed, involving four distinct hydroxyl groups in the reaction. Although not reported in the previous study, the effective decrease in hydroxyl functionalities may decrease the interaction of the fibre with moisture. Moreover, the formed crosslinks could also limit the plasticizing effect of water in the fibres [9,13–15]. However, when fibres were treated with an aqueous solution of 15 wt% glyoxal, the strength of the

composites was reduced by almost 70%. This considerable decrease is a significant disadvantage for this treatment.
In a first instance this study investigates whether the crosslinking could also be exploited to reduce moisture sensitivity of flax fibre composites by maximal retention of the stiffness under humid conditions. Secondly, the crosslinking treatments that are performed could reveal information on the non-linear deformation mechanism of the fibres as the treatments would alter their non-linear behaviour by modifying the molecular interactions between the polysaccharide chains.

5.2.2. Materials & Methods

5.2.2.1. Flax fibres

All flax fibres used in this study originated from a unidirectional preform of hackled flax fibres, FlaxTape 200, with an areal density of 200 g/m², supplied by Lineo SA (France). No information concerning the variety, growing or retting conditions was given.

5.2.3. Matrix material

The matrix system was a bisphenol A epoxy resin, Epikote 828LVEL (Hexion) mixed with 1,2-diaminocyclohexane hardener. A mass ratio of resin to hardener of 100/15.2 was used. The mechanical properties of the resin are provided in Table 5-4, as previously reported in the literature [16].

Stiffness (GPa)	Strength (MPa)	Failure strain (%)
2.9	75	4

Table 5-4: Mechanical properties of the matrix system.

5.2.3.1. Chemical treatments

a. Treatment with 1,5-pentanedial, benzaldehyde, and benzene-1,4-dicarboxaldehyde

To treat the fibres, solutions of the reactant were made in tetrahydrofuran (THF). Their concentration was adapted to reach a stoichiometric ratio with the hydroxyl groups of the fibre, as explained in section 5.2.3.2. The reaction with a hydroxyl group requires an acid catalyst to give the desired acetals. As THF is an aprotic solvent and does not readily accept protons, 1 vol% of water was added to the solution. Acetic acid was used as the acid catalyst in a concentration of 0.5 vol%. It is debatable whether the addition of water is essential for the reaction to occur because, although the fibres are dried before being submerged, some moisture will be retained.
Next, the unidirectional flax fibre layer was submerged into the reagent solution for 10 minutes at room temperature while the solution was agitated continuously.

After reaction, excess water in the fibre was removed by drying in an oven at 80°C for at least 4 hours. Finally, to make sure all unreacted products are removed, the dry fibres were thoroughly rinsed in THF for 5 minutes.

b. Treatment with 1,2,7,8-diepoxyoctane (DEO)

DEO differs from the previous treatments as the product is largely inactivated upon contact with water. In acidic aqueous solutions, DEO hydrolyses to the corresponding diol. Water was thus not added to the solution and 0.5 mol% of sulfuric acid was dissolved to act as the acid catalyst which is able to directly protonate THF. Subsequent steps were identical to the treatment procedure of the other reagents.

5.2.3.2. Concentration of the reagents

Instead of arbitrarily defining a concentration of the reagents, the authors based these concentrations on the number of hydroxyl groups that are present in the mass of the treated fibres. It was assumed that flax fibres were entirely composed of repeating anhydroglucose units. Each unit has three hydroxyl groups that were assumed to be equally reactive towards the reagents. This means that 18.2 mmol of hydroxyl groups are present per gram of fibre. From this number, the necessary stoichiometric quantity was derived to, theoretically, allow the reaction with each hydroxyl group of the fibre.

Assuming the fibre is entirely composed of anhydroglucose units is a rough approximation, as pectins and hemicellulose account for almost 30% of the fibre mass [17,18]. However, quantification of the monosaccharides that were present in these polymers was not performed. A second approximation was that all of the hydroxyl groups are equally reactive which is not always true [19,20]. Primary and secondary hydroxyl groups may exhibit different affinities for the reagents and most of the hydroxyl groups in crystalline cellulose will not react.

5.2.3.3. Dynamic vapor sorption (DVS) and determination of the radial fibre diffusion coefficient

DVS measurements were performed using a DVS Advantage-1 (Surface Measurement Systems). Fibres were placed on a balance with an accuracy of 10^{-7} g. The total mass of each batch was approximately 8 µg. Before the absorption process was started, the fibres were conditioned in the apparatus to a relative humidity (RH) of 0.1% at 20°C. Every 60 s the device registered the mass of the fibres. It was assumed that equilibrium was reached, i.e. fully dry fibres, once the relative difference between two consecutive mass measurements was not more than 0.002%.

Next, the target RH was increased in 10% increments maintaining the data sampling rate and equilibrium condition of lower than or equal to 0.002% between two consecutive measurements. This process continued until the sample reached its equilibrium condition at 90% after which the desorption process was initiated.

The target RH was then reduced in 10% increments until equilibrium was reached at 0.1%, at which point the measurement was stopped.
The moisture content (MC) of the samples, expressed as a mass percentage relative to the dry mass of the fibre, was calculated from equation 1 where M(t) is the mass of the fibre at time t and M_0 is the mass of the fibre in equilibrium with 0.1% RH at 20°C.

$$MC = \frac{M(t) - M_0}{M_0} \tag{1}$$

To extract the radial fibre diffusion coefficient, technical flax fibres were assumed to have solid cylindrical cross-sections with constant diameter. The average diameter of the used flax fibres was determined to be 78 ± 5 µm. These assumptions enable the fit of the absorption data to the analytical solution of Fick's second law for solid cylinders: Let M_{sat} be the equilibrium moisture content of the fibres at a given relative humidity level, r the radius of the fibre, D its radial diffusion coefficient, and α_n the roots of the modified Bessel function, $J_0(rx)$, of the first kind and zeroth order, then the analytical solution to this diffusion problem is given by equation 2 [21].

$$MC = M_{sat}\left(1 - \sum_{n=1}^{\infty} \frac{4}{r^2\alpha_n^2}\exp(-D\alpha_n^2 t)\right) \tag{2}$$

α_n are the roots of $J_0(rx) = 0$

5.2.3.4. Composite production and sample preparation

Unidirectional composite plates were produced by vacuum assisted resin infusion. Prior to impregnation, the fibres were dried in an oven for 24 hours at 60°C followed by 1 hour under vacuum at 40°C.; The resin was degassed in a vacuum chamber. The fibre volume fraction was set to 35% by ensuring a plate thickness of 2 mm. Curing was performed at 70°C for 1 hour followed by a post-curing step at 150°C for 1 hour. The obtained average fibre volume fraction of the composite specimens after production was 38% ± 2%. Immediately after production, the samples were cut to a width of 12.7 mm and a length of 250 mm, as prescribed by ASTM D3039/D3039M.

5.2.3.5. Mechanical testing and stiffness calculation

Prior to testing, samples were conditioned at 80°C in an oven for at least 7 days to reach the oven dry state. Saturated samples were obtained by conditioning at 80°C and 80% RH for at least 7 days. The value of 80%RH was chosen as this represents the average outdoor condition in tepid sea climate, such as most of Western Europe.
An Instron 5567, equipped with a 30 kN load cell, was used to test the composite samples in tension. Again, as prescribed by ASTM D3039/D3039M, the span length of the sample was set to 150 mm. Strain was registered using an

extensometer with a 50 mm gauge length. Emery cloth prevented slippage of the sample in the clamps. The crosshead displacement rate was set to 1 mm/min.
Due to the non-linear tensile behaviour of flax fibres, the stiffness was calculated between 0 and 0.1% strain, in deviation of the advised standard strain range between 0.1 and 0.3% [5].

5.2.4. Results & Discussion

5.2.4.1. Selection of the treatments

Four separate treatments were selected, as shown in Figure 5-13.

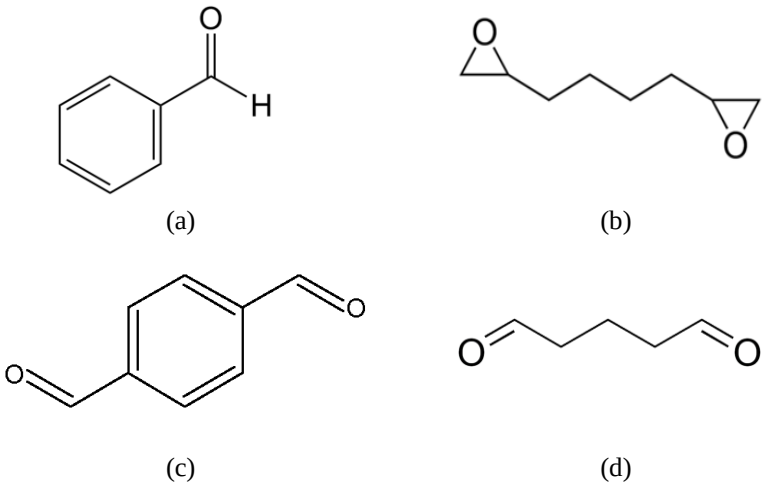

Figure 5-13: Chemical structure of the reagents used to treat the fibres: (a) benzaldehyde (BEN), (b) 1,2,7,8-diepoxyoctane (DEO), (c) benzene-1,4-dicarboxaldehyde (TER) and (d) 1,5-pentanedial (GLU).

First, 1,5-pentanedial or glutaraldehyde (GLU) was examined. It only differs from ethanedial by the length of its alkane chain. By increasing this chain length, it is hypothesized that the relative movement of the chains would increase, thereby increasing the strain to failure of the fibres.
As a second treatment, benzaldehyde (BEN) was proposed. This reactant is not able to crosslink chains as it contains only one aldehyde functionality. However, one molecule of benzaldehyde can theoretically react with two hydroxyl groups on the polysaccharide chain forming the acetal. Furthermore, the aromatic ring in the remainder is expected to increase the overall hydrophobicity of the fibre.
Benzaldehyde's dialdehyde analogue, benzene-1,4-dicarboxaldehyde or terephtalaldehyde (TER), was also examined to compare its effect to the non-crosslinking benzaldehyde and to the effect of 1,5-pentanedial to assess the influence of backbone aromaticity.

Finally, treating the fibres with 1,2,7,8-diepoxyoctane (DEO) should result in crosslinking without elimination of hydroxyl groups. An epoxide group will add to a hydroxyl group through an ether link and generate a primary hydroxyl group.

5.2.4.2. Fibre mass gain

Table 5-5 provides the relative increase in mass of the fibre layers, ΔM, for each treatment calculated with equation 3. M_0 and M_R are the fibre masses before and after the treatment, respectively.

$$\Delta M = \frac{M_R - M_0}{M_0} \tag{3}$$

Treatment	Molecular weight (MW) (g/mol)	Relative mass increase (%)	Yield (%)
THF (pure)	72.11	-0.06 ± 0.02	/
BEN	106.12	9.2 ± 0.3	11.6
GLU	100.12	4.1 ± 0.4	14.2
TER	134.13	4.2 ± 0.2	9.6
DEO	142.20	6.4 ± 0.3	13.4

Table 5-5: Relative mass increase of the fibres after the treatment and the yield of the reaction, assuming the fibre is composed entirely of anhydroglucose unit based polymers.

To verify that THF, which was used as a solvent, did not lead to excessive leaching of fibre components, the relative mass decrease due to the sole action of this substance was also registered. The mass loss of 0.06%, after 10 min of fibre immersion and subsequent drying, leads to the conclusion that THF did not significantly leach components from the fibres during THF exposure.
The relative mass increases of the treatments range between 4.1 and 9.2% and have no clear connection with the molecular weight of the reagents. The yields of the reactions are rather low, as it was assumed that all hydroxyl groups in the fibre were available for the reaction. From the discussion in section 5.2.3.2 it is clear that this was only an indication as the majority of the hydroxyl groups are arranged in impenetrable cellulose crystals.

5.2.4.3. Influence on the equilibrium moisture content (EMC) of technical fibres

In Figure 5-14a the absorption isotherms are shown for the different treatments. At first glance, the EMC of the treated fibres did not differ significantly from the untreated fibres (UNT). However, it is clear that the benzaldehyde treatment led to higher moisture absorption in the fibres. This result is counterintuitive as it was expected that benzaldehyde would increase the hydrophobicity of the fibres. The overall increase in EMC could be induced by the incorporation of the voluminous phenoxy group in the polysaccharide structure. When the distance between the chains increases slightly, it is less likely that neighbouring hydroxyl groups on

separate chains can interact through hydrogen bonding. In untreated fibres this chain separation occurs as well, albeit only under the influence of moisture sorption. This “bulking effect” benzaldehyde offers could therefore lead to increased EMC values at the same value of RH compared to untreated fibres. For the other treatments the EMC is slightly lower than for untreated fibres, except at relative humidities above 70%, where the difference increased. Again, this result was unexpected as the elimination of hydroxyl groups by the crosslinking treatments would normally lead to a global downwards shift of the isotherm. However, note that the previously mentioned bulking effect is also present here, which in turn leads to an increase in EMC by the initial increase in sorption sites, shifting the isotherm upwards. Under the reagent concentrations and conditions used in this study, the effects appear to cancel each other out by coincidence. It is hypothesized that this bulking effect and net elimination of hydroxyl groups are generally not related. Higher concentrations of the reagents may thus lead to lower EMC values, but this was not investigated here. Alternatively, the treatments might simply not eliminate a large enough number of hydroxyl groups to have a significant impact on the EMC.

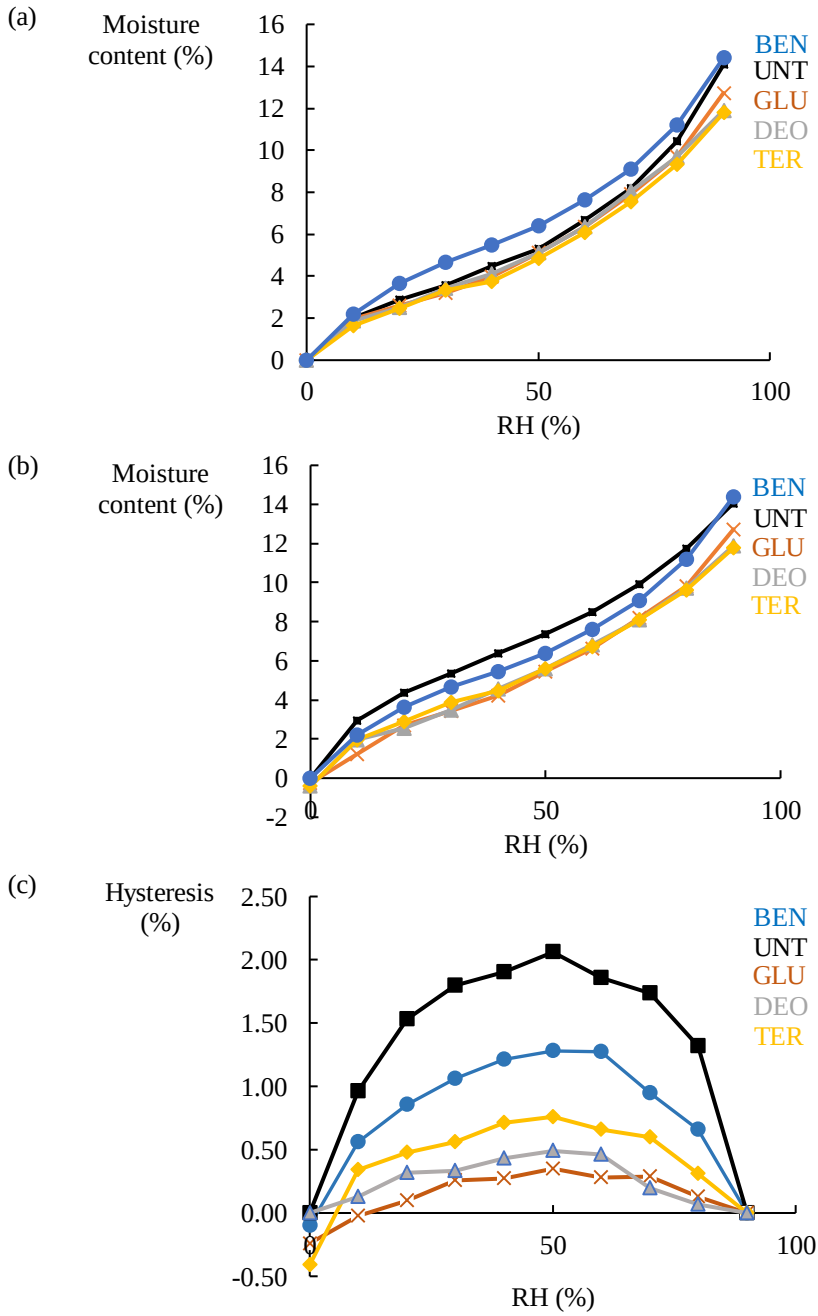

Figure 5-14: DVS isotherms of the untreated and treated flax fibres in (a) absorption and (b) desorption. (c) The hysteresis calculated as the difference of the absorption and desorption isotherms. The color codes are consistent throughout the text.

For wood, flax, and other natural fibres, a hysteresis is observed between their absorption and desorption curves [22]. The origin of the hysteresis is currently still a topic of debate and numerous theories exist. Some authors refer to the existence of a meniscus in cell wall microcapillaries [22,23]. During absorption, these capillaries are filled with water whereas during desorption evaporation above the meniscus governs the process, leading to a difference in EMC [24]. However, the concept of menisci appears to be rather problematic when considering that the size of the microcapillaries in these materials is only 2 to 4 nm [22]. Other theories include irregularly shaped microcapillaries and variations in mechanical constraints due to swelling [25,26]. More recently, Lu and Pignatello linked hysteresis in organic materials to the creation of new sorption sites during absorption due to swelling of the sorbent [27].

In a previous study, the authors hypothesized that the mechanism by which flax fibres absorb moisture is based on the availability of the hydroxyl groups and the existence of a mobile zone [Section Chapter 5]. For untreated fibres and at low relative humidities (< 30% RH), hydrogen bonding between the polysaccharide chains prevails and diffusion of moisture is hampered. This is because an energy barrier exists that will keep the chains together until water molecules are able to break these physical interactions and start interacting with the hydroxyl groups. As more water enters, a mobile zone will start to form in which water molecules can move more freely without too much interaction with the hydroxyl functionalities. At higher relative humidity (> 70%), water molecules start to form larger clusters which will again lower the diffusion coefficient. During desorption, the free volume of the sorbent will hence be greater and lead to different physical environments for the absorption and desorption processes [28,29]. This corresponds well with the proposed theory that the initial bulking effect caused by crosslinking exposes hydroxyl groups that would normally only be exposed later in the absorption process. The bulking effect is illustrated in Figure 5-15.

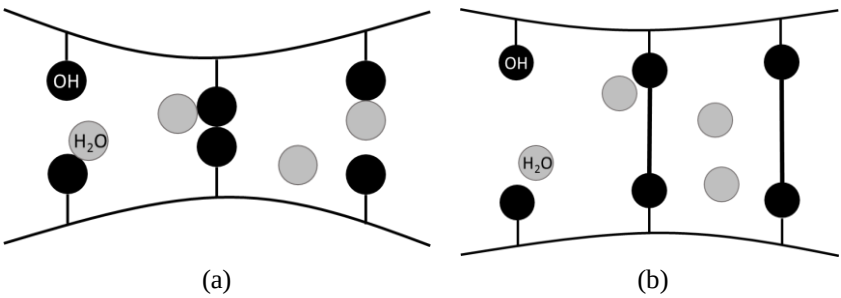

Figure 5-15: (a) Schematic representation of the absorption process at (a) low relative humidity in an untreated fibre and (b) at low relative humidity in a crosslinked fibre. In the latter case the crosslinks (solid line) force the backbone biopolymer chains further apart and prevent other hydroxyl groups from interacting.

The crosslinks subsequently restrain the polysaccharide chains during absorption, preventing the creation of new interaction sites. Simultaneously this also prevents the chains from reforming hydrogen bonds upon desorption of moisture as the chain separation is maintained. Hence, in theory these crosslinks should lead to a decrease in hysteresis if "inaccessible" sorption sites would play a role in hysteresis. This is precisely what is observed in Figure 5-14b and c. The desorption isotherm of untreated fibres is situated well above the isotherms of all the treated fibres. Benzaldehyde can offer only steric hindrance through its aromatic ring to neighboring polysaccharide chains that approach the steric hindrance. Therefore, the reduction in hysteresis is expected to be smaller than for the crosslinking treatments. Indeed, for the GLU fibres, the maximum reduction in hysteresis was 84% compared to the UNT fibres and was reached at 50% RH. At that same RH level, BEN fibres exhibited a 38% decrease in hysteresis.

After completing the desorption of moisture in the BEN, GLU, and TER fibres, some mass loss was observed. The loss was 0.10%, 0.24% and 0.41%, for the respective treatments. Acetal bonds are stable in the absence of water and an acid catalyst. However, during absorption excess moisture is introduced in the fibre structure. It is evident from these results that some acid catalyst was retained in the fibres, as the acetals can be hydrolysed in their presence.

5.2.4.4. Influence on the diffusion behavior of the fibres

The treatments performed here had a profound effect on the kinetic absorption behavior. All the fibres, untreated or treated, obeyed Fick's second law at each absorption stage but, as seen in Figure 5-16, the diffusion coefficients of the treated fibres at lower relative humidities were higher. This behavior is indicative of the bulking behavior of the treatments. The more voluminous the backbone structure of the reagent, the larger the initial separation of the chains. Clearly, the GLU treatment with shorter backbone did not increase the diffusion coefficient to the same extent as the DEO treatment did. The separation reduces chain interactions, lessening the resistance to moisture entering the fibre hence, increasing the diffusion coefficient. Nonetheless, some interactions still exist as the diffusion coefficients still increase with increasing relative humidity.

Focusing on higher relative humidities (>70%), the diffusion coefficients of the treated fibres converged to the value of the untreated fibres. Apparently, the clustering of water molecules becomes a dominant mechanism which solely determines the diffusion coefficient.

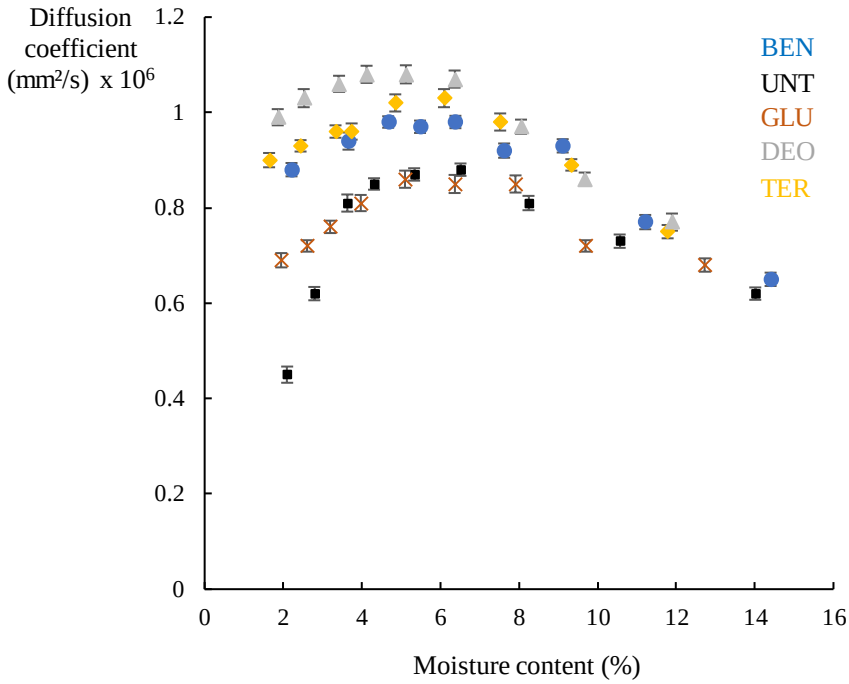

Figure 5-16: Diffusion coefficients as a function of moisture content in the untreated and treated fibres.

5.2.4.5. Influence on the mechanical properties before and after moisture sorption

To evaluate the effect of the treatments on the mechanical properties, the back-calculated fibre stiffness and strength were determined by performing tensile tests on unidirectional composites in their dry state and after saturation at 80°C and 80% RH. Figure 5-17a summarizes the stiffness of the fibres in the composite. No statistical differences were found between the untreated and treated fibres in dry conditions. However, for the saturated composites, the stiffness of the GLU, TER, and DEO fibres were all higher than for the untreated fibres. Indeed, as the moisture content of the untreated fibres increased, their stiffness dropped by 55% compared to the dry state, while GLU, TER, and DEO fibres only exhibited a 31%, 38% and 42% drop respectively. The stiffness of BEN fibres decreased by 56%.

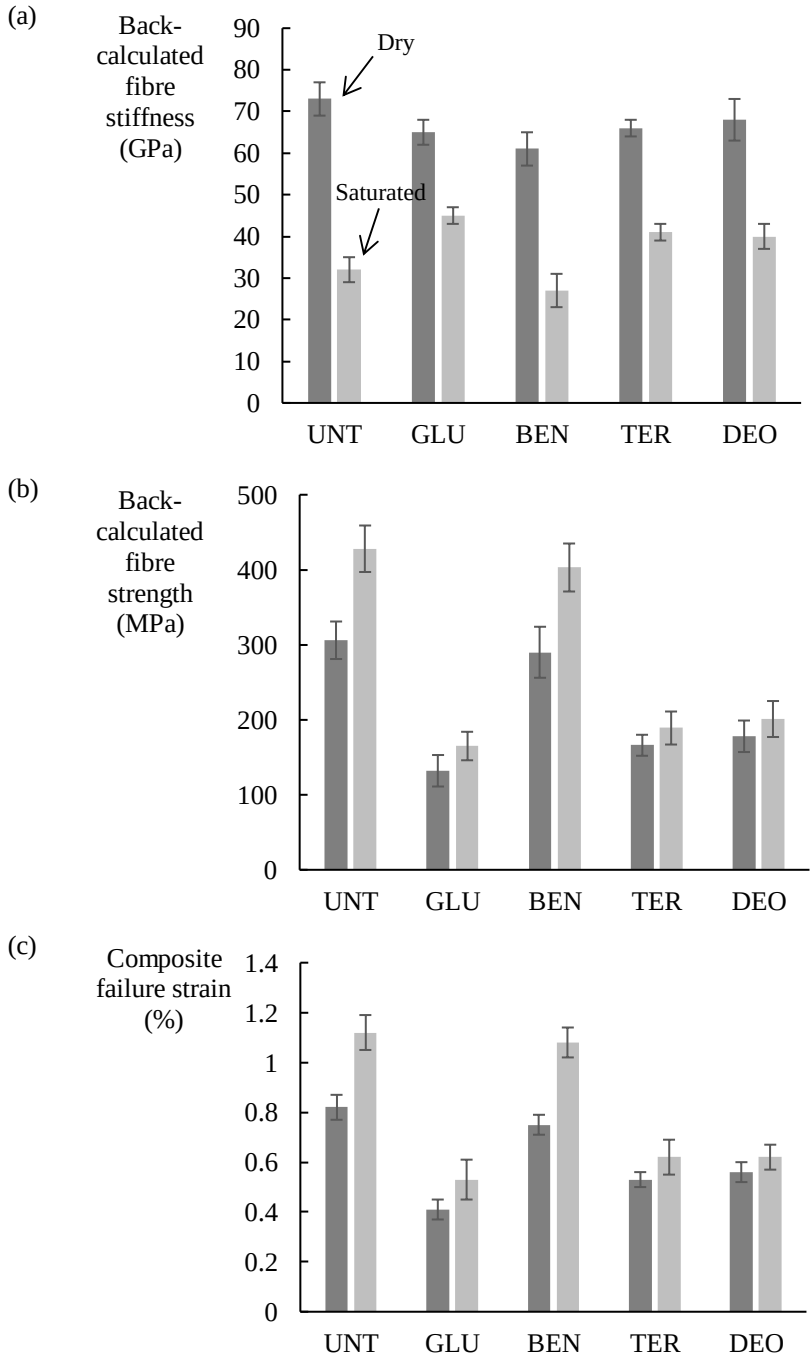

Figure 5-17: Back-calculated fibre (a) stiffness and (b) strength from tensile tests performed on the composites for the different treatments. (c) The failure strain of the composites.

It is known that water acts as a plasticizer when it is absorbed by the fibres thereby lowering their stiffness [30–32]. This effect is thought to be closely associated with the shearing of polysaccharides that interconnect the cellulose microfibrils and connects them to the surrounding matrix, also known as structuring polysaccharides as explained previously in sections 4.3 and Chapter 5. Under dry conditions it is apparent that there is sufficient interaction present through hydrogen bonding between these specific polysaccharides to guarantee a certain resistance to internal shearing. However, when moisture is present, much of these hydrogen bonds are broken by the water molecules and resistance to shear decreases. When crosslinks are present, the initial hydrogen bonds between the chains are replaced by covalent bonds which greatly enhance the resistance to shear. This could be the reason why the decrease in stiffness was smaller for the crosslinked fibres than for the untreated ones. Finally, comparing the effect of water plasticization with the effect of retting described in section 4.3, it is clear that water has a much more pronounced effect on E_{f1}. It is hypothesized that water lowers the threshold for shearing to occur whereas retting does not.

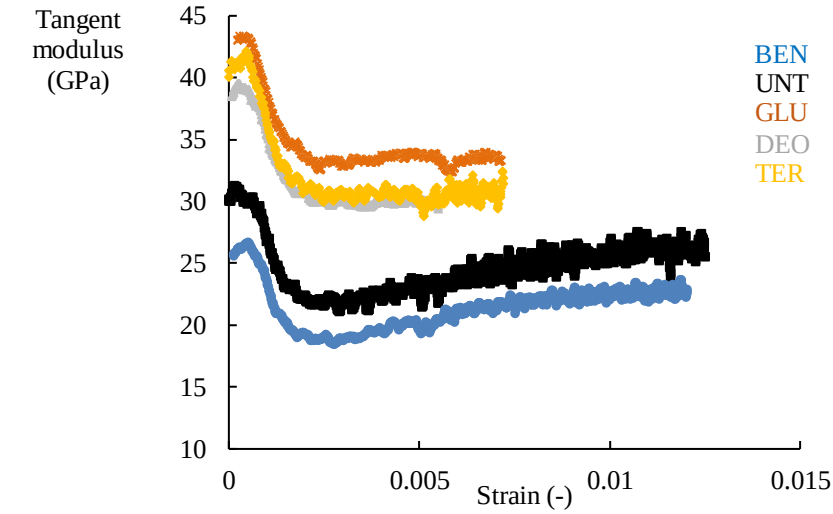

(a)

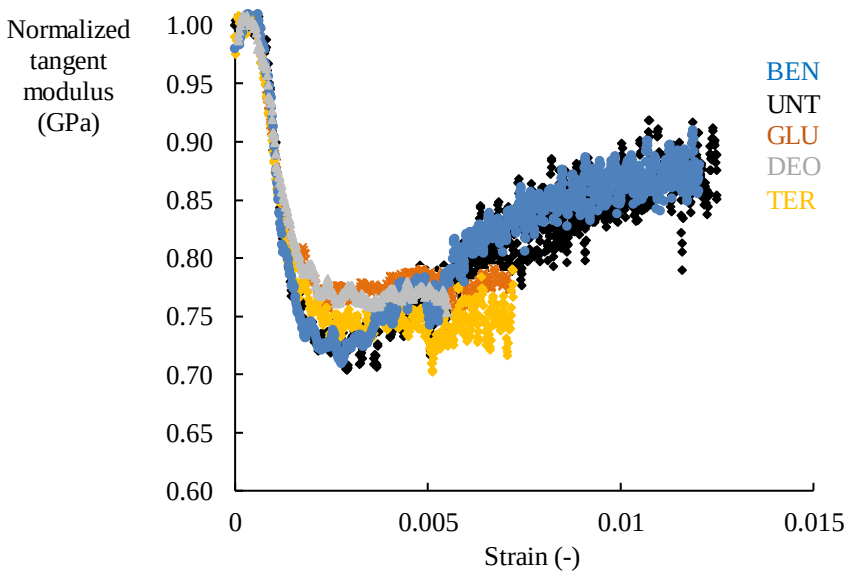

(b)

Figure 5-18: (a) Evolution of the back-calculated fibre tangent modulus at saturation and (b) evolution of this tangent modulus by normalizing to the initial stiffness.

Examining the evolution of the tangential stiffness of untreated fibre and treated fibre composites at saturation (Figure 5-18a), the most remarkable difference is that the stiffness recovery mechanism that was observed for UNT fibres was entirely absent in the fibres treated with crosslinking agents (GLU, TER and

DEO). The recovery region is usually attributed to the alignment of the cellulose microfibrils with the loading direction and crystallization of amorphous cellulose. The first mechanism could be inhibited by the increased stiffness of the matrix that surrounds the microfibrils. When crosslinks are formed between amorphous cellulose chains, the ability of this component to crystallize is largely inhibited and depends of the degree of crosslinking.

When the initial back-calculated fibre stiffness was used as a normalization factor, Figure 5-18b is obtained. Up to 0.1% strain, the relative decrease in stiffness was approximately equal for all fibres. Combining this insight with Figure 5-18a and assuming the decrease is associated with shearing of certain components in the fibres, it can be concluded that crosslinking treatments augment the threshold stress that is needed to induce shearing. However, it is apparent that after reaching this threshold, the mechanism by which the shearing occurs remains unaltered by the treatments. This hypothesis remains to be verified in future studies.

Finally, crosslinking treatments adversely affected the composite strength as they embrittle the fibres as seen in Figure 5-17b and c. As mentioned above, the plasticization effect of water which lowers the fibre stiffness simultaneously increases their failure strain by facilitating microfibril reorientation. In crosslinked fibres the plasticization is decreased as the covalent bonds do not allow extensive sliding of the amorphous biopolymer chains in the cell walls. When the rotation of the microfibrils is inhibited, partially or fully, stress concentrations will arise in the fibres between the microfibrils and the surrounding matrix. These will eventually lead to premature failure of the fibres and hence, the composite.

5.2.5. Conclusions

This study investigated the effect of crosslinking treatments on the moisture behaviour of flax fibre composites. It was observed that crosslinking affected the moisture content of the fibres during desorption of moisture but not during moisture absorption. At identical RH levels, the moisture content of the treated fibres was lower during desorption than for untreated fibres. The treatments therefore reduce the hysteresis. It is hypothesized that desorption of moisture in the crosslinked fibres is facilitated by the increase in free volume between the polysaccharide chains by incorporation of the reagents.

Increased diffusion coefficients at low relative humidity after crosslinking support this hypothesis. Indeed, the number of hydroxyl groups on neighbouring polysaccharide chains interacting with each other would be lower due to the increased free volume as a result of the introduction of the crosslinking agents, leaving more sites available for interaction with water.

Finally, the relative decrease in composite stiffness under saturated conditions compared to dry conditions was lower for the crosslinked fibres than for the untreated fibres. This was linked to an increased shear threshold of the matrix polysaccharides in the fibre. Simultaneously, the increased stiffness of the matrix

prevents the cellulose microfibrils from reorienting, inhibiting stiffness recovery. The resulting stress concentrations around the fibrils led to a lower composite strength for the crosslinked fibre composites.

References

[1] Keryvin V, Lan M, Bourmaud A, Parenteau T, Charleux L, Baley C. Analysis of flax fibres viscoelastic behaviour at micro and nano scales. Compos Part A Appl Sci Manuf 2014. doi:10.1016/j.compositesa.2014.10.006.

[2] Baley C. Analysis of the flax fibres tensile behaviour and analysis of the tensile stiffness increase. Compos Part A Appl Sci Manuf 2002;33:939–48. doi:10.1016/S1359-835X(02)00040-4.

[3] Charlet K, Eve S, Jernot JP, Gomina M, Breard J. Tensile deformation of a flax fiber. Procedia Eng 2009;1:233–6. doi:10.1016/j.proeng.2009.06.055.

[4] Perremans D, Verpoest I, Dupont-Gillain C, Van Vuure AW. Investigation of the tensile behavior of treated flax fibre bio-composites at ambient humidity. Compos Sci Technol 2018;159:119–26. doi:10.1016/J.COMPSCITECH.2018.02.038.

[5] Bensadoun F, Verpoest I, Baets J, Müssig J, Graupner N, Davies P, et al. Impregnated fibre bundle test for natural fibres used in composites. J Reinf Plast Compos 2017;36:942–57. doi:10.1177/0731684417695461.

[6] Placet V, Cissé O, Lamine Boubakar M. Nonlinear tensile behaviour of elementary hemp fibres. Part I: Investigation of the possible origins using repeated progressive loading with in situ microscopic observations. Compos Part A Appl Sci Manuf 2014;56:319–27. doi:10.1016/j.compositesa.2012.11.019.

[7] Perremans D, Verpoest I, Dupont-Gillain C, Van Vuure AW. Investigation of the tensile behavior of treated flax fibre bio-composites at ambient humidity. Compos Sci Technol 2018;159:119–26. doi:10.1016/J.COMPSCITECH.2018.02.038.

[8] Le Duigou A, Davies P, Baley C. Seawater ageing of flax/poly(lactic acid) biocomposites. Polym Degrad Stab 2009;94:1151–62. doi:10.1016/j.polymdegradstab.2009.03.025.

[9] Le Duigou A, Bourmaud A, Davies P, Baley C. Long term immersion in natural seawater of Flax/PLA biocomposite. Ocean Eng 2014:1–9. doi:10.1016/j.oceaneng.2014.07.021.

[10] Azwa ZN, Yousif BF, Manalo AC, Karunasena W. A review on the degradability of polymeric composites based on natural fibres. Mater Des 2013;47:424–42. doi:10.1016/j.matdes.2012.11.025.

[11] Perremans D, Hendrickx K, Verpoest I, Van Vuure AW. Effect of chemical treatments on the mechanical properties of technical flax fibres with emphasis on stiffness improvement. Compos Sci Technol 2018;160. doi:10.1016/j.compscitech.2018.03.030.

[12] Hendrickx K, Perremans D, Baets J, Ivens J, Dupont-Gillain C, Verpoest I, et al. Extending the linear elastic response region of flax fibre reinforced polymers using chemical treatments. Proc. 2nd Int. Conf. Nat. Fibres, 2015.

[13] Baley C, Morvan C, Grohens Y. Influence of the Absorbed Water on the Tensile Strength of Flax Fibers. Macromol Symp 2005;222:195–202. doi:10.1002/masy.200550425.

[14] Joffe R, Andersons J, Wallström L. Strength and adhesion characteristics of elementary flax fibres with different surface treatments. Compos Part A Appl Sci Manuf 2003;34:603–12. doi:10.1016/S1359-835X(03)00099-X.

[15] Alix S, Lebrun L, Marais S, Philippe E, Bourmaud A, Baley C, et al. Pectinase treatments on technical fibres of flax: Effects on water sorption and mechanical properties. Carbohydr Polym 2012;87:177–85.

doi:10.1016/j.carbpol.2011.07.035.

[16] Callens MG, Gorbatikh L, Verpoest I. Ductile steel fibre composites with brittle and ductile matrices. Compos Part A Appl Sci Manuf 2014;61:235–44. doi:10.1016/j.compositesa.2014.02.006.

[17] Bledzki A. Composites reinforced with cellulose based fibres. Prog Polym Sci 1999;24:221–74. doi:10.1016/S0079-6700(98)00018-5.

[18] Placet V, Trivaudey F, Cisse O, Gucheret-Retel V, Boubakar ML. Diameter dependence of the apparent tensile modulus of hemp fibres: A morphological, structural or ultrastructural effect? Compos Part A Appl Sci Manuf 2012;43:275–87. doi:10.1016/J.COMPOSITESA.2011.10.019.

[19] He L, Li X, Li W, Yuan J, Zhou H. A method for determining reactive hydroxyl groups in natural fibers: application to ramie fiber and its modification. Carbohydr Res 2012;348:95–8. doi:10.1016/j.carres.2011.10.035.

[20] Fedorova AF, Rogovin ZA. A study of the relative reactivity of the hydroxyl groups of cellulose in esterification in an acidic medium. Polym Sci USSR 1963;4:1189–94. doi:10.1016/0032-3950(63)90350-2.

[21] Crank J. The mathematics of diffusion. vol. 1. 2nd ed. Uxbridge: Clarendon Press, Oxford; 1975. doi:10.1016/0306-4549(77)90072-X.

[22] Hill CAS, Norton A, Newman G. The water vapor sorption behavior of natural fibers. J Appl Polym Sci 2009;112:1524–37. doi:10.1002/app.29725.

[23] Hill CAS, Papadopoulos AN. A review of methods used to determine the size of the cell wall microvoids of wood. J Inst Wood Sci 2001;15.

[24] Stamm A. Wood and cellulose science. New York: Ronald Press Co.; 1964.

[25] Cassie ABD. Absorption of water by wool. Trans Faraday Soc 1945;41:458–64.

[26] Koch P. Utilization of the Southern Pines. Agric Handb 1972;1:1–734.

[27] Lu Y, Pignatello JJ. History-Dependent Sorption in Humic Acids and a Lignite in the Context of a Polymer Model for Natural Organic Matter †. Environ Sci Technol 2004;38:5853–62. doi:10.1021/es049774w.

[28] Sander M, Lu Y, Pignatello JJ. A Thermodynamically Based Method to Quantify True Sorption Hysteresis. J Environ Qual 2005;34:1063. doi:10.2134/jeq2004.0301.

[29] Xie Y, Hill CAS, Xiao Z, Mai C, Militz H. Dynamic water vapour sorption properties of wood treated with glutaraldehyde. Wood Sci Technol 2011;45:49–61. doi:10.1007/s00226-010-0311-0.

[30] Stamboulis A. Environmental durability of flax fibres and their composites based on polypropylene matrix. Appl Compos Mater 2000;7:273–94. doi:10.1023/A:1026581922221.

[31] Berges M, Léger R, Placet V, Person V, Corn S, Gabrion X, et al. Influence of moisture uptake on the static, cyclic and dynamic behaviour of unidirectional flax fibre-reinforced epoxy laminates. Compos Part A Appl Sci Manuf 2016;88:165–77. doi:10.1016/j.compositesa.2016.05.029.

[32] Thuault A, Eve S, Blond D, Breard J, Gomina M. Effects of the hygrothermal environment on the mechanical properties of flax fibres. J Compos Mater 2013;48:1699–707. doi:10.1177/0021998313490217.

Chapter 6

Impact of cyclic humidity variations on the composite properties

Chapter 6 Impact of cyclic humidity variations on the composite properties

6.1. Development and progression of damage in flax fibre reinforced composites under cyclic hygroscopic loading

Kevin Hendrickx, Rein Vranken, Wim Thielemans, Aart Willem Van Vuure, Jan Ivens

6.1.1. Introduction

Flax fibres can absorb moisture from the environment due to the hygroscopic nature of their constituent polymers. A higher moisture content in flax fibres is associated with a decrease in stiffness of the fibres and a dimensional change of the fibres due to swelling [1,2].

The latter will generate significant hygroscopic stresses when the fibres are embedded in a polymer matrix which inevitably leads to the formation of damage over time. Although several publications investigated the effect of wetting and drying on the composite properties, moisturization of the composites is usually performed using liquid water to reduce cycling times. This can lead to leaching of certain components from the fibres and generally does not represent the effective in-service behaviour of a flax fibre composite. Moreover, the internal microstructural damage and its progression have not been visualized to this date [3–7].

When microscopic defects develop, the diffusion rate accelerates due to increased accessibility of the composite to moisture [8]. In turn, increased diffusion coefficients promote the rate at which damage develops as this leads to faster fibre swelling. Also, the EMC can increase significantly in subsequent wetting cycles. This phenomenon is associated with the lower vapour pressure of water in capillaries such as microvoids, a process known as capillary condensation [8].

Quantifying the swelling behaviour of the fibres is important as it enables the prediction of the interfacial stresses that occur in composite materials. However, up to now, only a single study exists which has measured the hygroscopic expansion coefficient of flax fibres. Further experimental data are thus needed to corroborate this work [2].

This manuscript sets out to examine the effects of moisture absorption in unidirectional flax fibre composites by exposing them to an environment with a predetermined relative humidity, avoiding interaction of the material with liquid water. The damage that develops over several wetting and drying cycles is linked to the diffusion coefficients and EMC of the composite materials. The extent of damage was quantitatively assessed by analysing the void content of the composites in oven dry state and its impact on the mechanical properties was

evaluated by transverse flexural tests. To conclude, the hygroscopic expansion coefficients of the fibres were determined.

6.1.2. Materials & Methods

6.1.2.1. Fibres & matrix systems

Unidirectional hackled flax fibre tape (Flaxtape 200, Lineo SA) with an areal density of 200 g/m² was used to produce the composites. No further details on growing, retting, and processing conditions, nor on the fibre variety were given.
A bisphenol A epoxy resin (Epikote 828LVEL) was mixed with 1,2 diaminocyclohexane to produce the epoxy matrix for thermoset composite specimens. Polypropylene (PP) films (Propex GmbH) with a thickness of 20 µm were used as matrix material for the remainder of the specimens.

6.1.2.2. Composite production

Prior to any form of impregnation, the flax fibres were dried in an oven at 60°C for 24 hours. Flax fibre-epoxy unidirectional composite plates were produced with vacuum assisted resin infusion. In addition to the above-mentioned drying step, the fibres were dried under full vacuum at 40°C for 1h. The fibre volume fraction was set to 35% and the specimen thickness to 2 mm. Resin injection was performed at 40°C and curing of the resin was achieved under vacuum at 80°C for 1 hour, supplemented by a post-cure step at 150°C for 1 hour. The samples were then cut to the required dimensions using a water-cooled diamond saw. All the dimensions were in accordance with ASTM D3039/D3039M and ASTM D7264/D7264M prescribing the dimensions to be used for unidirectional composite test specimens in tension and flexion, respectively. Samples for damage inspection were cut using a low speed diamond saw without using water as this could interfere with the nature of the cyclic measurements.
Unidirectional flax fibres were impregnated with PP by stacking fibre layers with PP films followed by compression moulding at 170°C and 20 bar for 10 minutes after which the plates were cooled to room temperature. The fibre volume fraction was set to 35% and the specimen thickness to 2 mm. Specimen width of 12.7 mm and lengths were in accordance with ASTM 3039/3039M and ASTM D7264/D7264M.
Specimens used for damage inspection with micro computed tomography were randomly sampled from the produced plates and cut to a width of 2 mm and a length of 50 mm.

6.1.2.3. Hygroscopic loading

Immediately after production the composite samples were transferred to an oven at 80°C with no relative humidity (RH) control. However, since the air entering the oven has a quasi-constant RH of 50% at 20°C, the RH in the oven was reduced to less than 1.2%. The samples remained here until the loading cycles began.

Hygroscopic loading was achieved by placing the samples in a climatic chamber (Weiss WKL 64) at 80°C and 80% RH. The mass of the samples was measured initially in the oven dry state and subsequently at regular intervals after hygroscopic loading had started. Once saturated, the samples underwent the reverse process and were dried again in the oven following the scheme in figure 1. After the drying was completed, one cycle had finished. This process was repeated for a total number of 10 cycles.

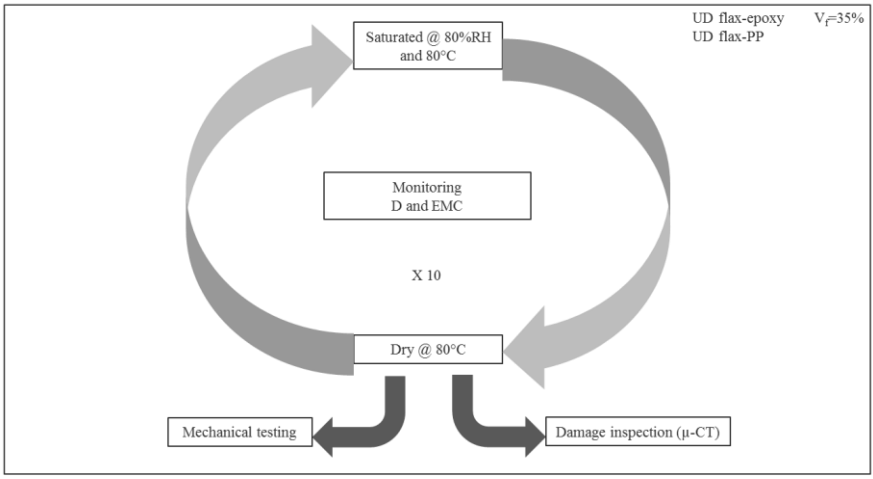

Figure 6-1: Scheme of the hygroscopic cycle, repeated ten times. The diffusion coefficient and EMC were monitored at regular intervals during each cycle. Damage inspection and mechanical testing was performed every other cycle.

6.1.2.4. Calculation of the moisture content

The moisture content at time t, M_t, is calculated using equation 1, where W_t is the mass of the sample at time t and W_i is the oven dry mass of the sample before hygroscopic loading.

$$M_t = \frac{W_t - W_i}{W_i} \tag{1}$$

A sample is considered to be saturated when the change in moisture content after at least 1 hour is less than 0.01%.

6.1.2.5. Calculation of the diffusion coefficient

In most hygroscopic loading cases, flax fibre composites exhibit Fickian diffusion behavior [4,9,10]. For a transversely isotropic specimen with sealed edges the moisture concentration in the composite, c, obeys equation 2. Herein, D_z is the through-the-thickness diffusion coefficient of the composite.

$$\frac{\partial c}{\partial t} = D_z \frac{\partial^2 c}{\partial z^2} \tag{2}$$

However, edge sealing is particularly difficult for composites where the fibres themselves provide significant pathways for moisture entering the material. Hence, unsealed specimens were chosen and equation 2 expands to equation 3, where D_x represents the diffusion coefficient in the fibre direction. Moreover, it was assumed that the diffusion coefficient perpendicular to the fibres is equal to D_z.

$$\frac{\partial c}{\partial t} = D_x \frac{\partial^2 c}{\partial x^2} + D_z \left(\frac{\partial^2 c}{\partial y^2} + \frac{\partial^2 c}{\partial z^2} \right) \tag{3}$$

The global diffusion coefficients of the composite specimens were calculated using equation 4, where h is the thickness of the composite specimen concerned and t is the absorption or desorption time [11].

$$M_t = M_{sat} \left(1 - \frac{8}{\pi^2} \sum_{n=0}^{\infty} \frac{1}{(2n+1)^2} \exp\left(-\frac{D(2n+1)^2 \pi^2 t}{h^2} \right) \right) \tag{4}$$

This global diffusion coefficient is related to the directional diffusion coefficients by equation 5, which takes into account the entry of moisture from all sides of the specimen [12]. Here, w is the dimension of the sample in the direction perpendicular to and in the plane of the fibres and l is the sample dimension in the direction of the fibres.

$$D = D_z \left(1 + \frac{h}{w} + \frac{h}{l} \sqrt{\frac{D_x}{D_z}} \right)^2 \tag{5}$$

By choosing two samples for which at least one of the sample dimensions is different, the directional diffusion coefficients can both be determined.

6.1.2.6. Damage inspection

A Phoenix Nanotom 180 was used to collect X-ray projections of specimens after every other cycle in the dry state, starting from the initial material immediately after production. All scans were performed using a molybdenum target. The X-ray tube acceleration voltage was set to 53 kV and the current level to 265 µA creating a spot size of 0.84 µm on the detector (2400 pixels x 2400 pixels). After reconstruction the resulting voxel size of the 3D volume was 1.4 µm³.

6.1.2.7. Damage content

In this study, “damage” is defined as the occurrence of regions in the composite which do not contain fibres nor matrix material, effectively appearing as voids in the µ-CT scans. For example, a crack is considered to be damage as it will create a void like region which will become filled with gasses and vapors in contact with

the sample. In X-ray imaging these regions will contrast significantly with the fibres and the matrix materials. To determine the volumetric abundance of the damage, further called the "damage content", the scanned sample volumes were segmented manually based on voxel grey value and overlaid with the original image. The numeric value of the threshold was chosen so that all the visible damage was distinguished from the original images.
Segmentation inevitably leads to voxel isolation by local fluctuations in grey value. To eliminate voxels that belonged to the background but were retained by the thresholding as part of the damage, morphological opening was applied with a spherical kernel with a radius of 3 voxels. Next, morphological closing using an identical kernel size, ensured that voxels inside damaged areas, which were not recognized as foreground pixels, were correctly attributed as damage.

6.1.2.8. Mechanical testing

Prior to any mechanical test, samples were conditioned at 80°C in an oven for at least 7 days to reach the oven dry state. Saturated samples were obtained by conditioning at 80°C and 80% RH for at least 7 days.

a. Longitudinal tensile tests

An Instron 5567, equipped with a 30 kN load cell, was used to test the composite samples in tension. Again, as prescribed by ASTM D3039/D3039M, the span length of the sample was set to 150 mm. Strain was registered using an extensometer with a 50 mm gauge length. Emery cloth prevented slippage of the sample in the clamps. The crosshead displacement rate was set to 1 mm/min.
Due to the non-linear tensile behaviour of flax fibres, the stiffness was calculated between 0 and 0.1% strain, deviating from the advised standard strain range between 0.1 and 0.3% [5].

b. Transverse flexural tests

Flexural tests were performed following ASTM D7264/D7264 M every other cycle. The crosshead displacement rate was set to 1 mm/min. An Instron 5567 was equipped with a load cell of 1 kN. All tests were done on oven dry specimens, unless further specified, with a span length of 64 mm and a total sample length of 80 mm.

6.1.2.9. Hygroscopic strain and hygroscopic expansion coefficient (CHE)

After drying the unidirectional composite samples for at least 7 days in an oven at 80°C, a speckle pattern was applied to the surface of each sample. Next, the samples were conditioned at the appropriated relative humidity according to the conditions outlined in section 6.1.2.3. For each sample the mass was determined with an analytical balance accurate to 10^{-5} g at regular time intervals. Simultaneously, the side of the sample with the speckle pattern applied to it was

scanned with an optical flatbed scanner (Epson Perfection V700) at a resolution of 4800 dpi at room temperature, hence excluding temperature effects.
From the resulting image sequence, the full field hygroscopic strain was calculated using digital image correlation software (VIC 2D, Correlated Solutions GmbH). Next, the field was averaged, and the average transverse and longitudinal strain was obtained. Finally, the hygroscopic expansion coefficient (β), defined by equation 6, was determined in transverse and longitudinal directions by calculating the slope of the linear regression line constructed by plotting the hygroscopic strain (ε_h) as a function of the moisture content in the samples.

$$\beta = \frac{\Delta\epsilon_h}{\Delta M} \tag{6}$$

6.1.3. Results & Discussion

6.1.3.1. EMC

The EMC of the composite specimens is shown in figure 3. For flax-epoxy samples the average EMC throughout the cycles was 4.3% while flax-PP absorbed only 3.4% of moisture. Indeed, the flax-epoxy samples had a higher EMC than the flax-PP samples as the neat epoxy matrix itself absorbed 1.3% of moisture. At first sight, the EMC values can be seen to fluctuate but there is no statistical evidence to conclude the EMC values rise or fall throughout the cycles (student t-test on slope of linear regression line, p=0.25 for flax-epoxy and p=0.15 for flax-PP). Indeed, as leaching or deposition of matter is impossible and the chemical composition of the fibres and matrix remains unchanged, the EMC of the samples is not expected to change. This is a strong advantage compared to similar studies where the samples are conditioned in contact with liquid water. The absorption process will then also involve leaching of fibre components and the induced damage cannot be extrapolated to environments where liquid water is absent.
The previous result is also an important indication that during cycling capillary condensation does not occur. Inside a microcapillary, the saturation vapor pressure of water is decreased, which could lead to the formation of liquid water, according to Kelvin's law. When this type of condensation occurs, the EMC of the samples would increase significantly, which is not observed here.
Nonetheless, fluctuations in EMC can occur when the samples are given insufficient time to fully saturate. This could indicate that the criterion to decide when a sample was fully saturated was not entirely adequate in this case.

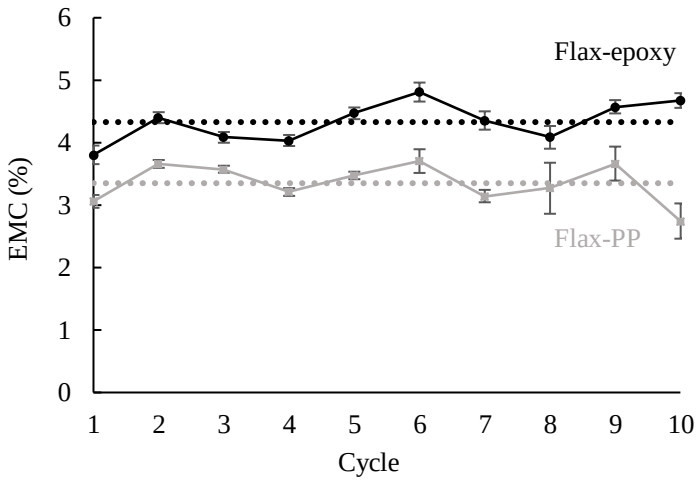

Figure 6-2: EMC of the composites throughout the cycles, after each absorption half-cycle. Dotted lines indicate the average EMC value throughout the cycles.

6.1.3.2. Damage development

a. Damage visualization

Figure 6-3 shows some representative cross-sections of flax-epoxy samples before and after cycling. In the reference state (a), which shows the situation immediately after production, no damage is visible. This either means that there is no damage present or that it is too small to be observed. However, assuming some form of damage would be present, this should be reflected in the transverse properties of the composites which are extremely sensitive to damage. As will be discussed in 6.1.3.3, the transverse strength closely agrees with data found in the literature. Hence, there is no reason to assume that damage would already be present immediately after production. The lumen, which is an intrinsic part of elementary flax fibres, is not considered to be damage in our analysis. These lumens can however be seen clearly as somewhat circular or elliptical voids in the cross sections.

Surprisingly, after the first cycle, in the dry state, the first damage appeared in the form of extensive fibre-matrix debonding. Note that debonding was initially concentrated near the edges of the samples. Indeed, the edges experienced the largest moisture gradients during absorption and desorption. However, after several cycles, internal damage in the samples becomes evident which is not related to the edge effect. The effect is aggravated by fibres which were exposed directly to the environment causing them to swell quasi-instantaneously. The onset of damage was therefore not captured exactly in this study, as it is possible that the first damage occurred during absorption rather than during desorption by generation of tensile stresses in the matrix. Alternatively, the sample could be scanned after 0.5 cycles, i.e. in saturated condition to verify whether fibre swelling

initiated the damage. However, during scanning, the samples absorbed part of the x-ray radiation which led to a rise in temperature of the specimen and accelerated moisture desorption. In turn, this caused the sample to shrink, distorting the reconstructed 3D volume. To enable scanning the samples at saturation, the environment around the sample would need to be conditioned or the scanning time needs to be reduced significantly to eliminate shrinkage. The latter condition can be satisfied using monochromatic x-rays in a synchrotron facility.

Figure 6-4 provides a detailed view of the developed internal damage in the flax-epoxy and flax-PP samples after 10 cycles compared to the reference state immediately after production. As said previously, the epoxy composite shows evidence of fibre-matrix debonding. This means that the generated hygroscopic stresses must have exceeded the interfacial strength at some locations. For the PP composite, fibre-matrix debonding is also present which is to be expected due to the very weak interface between the hydrophobic PP matrix and hydrophilic flax fibres [16].

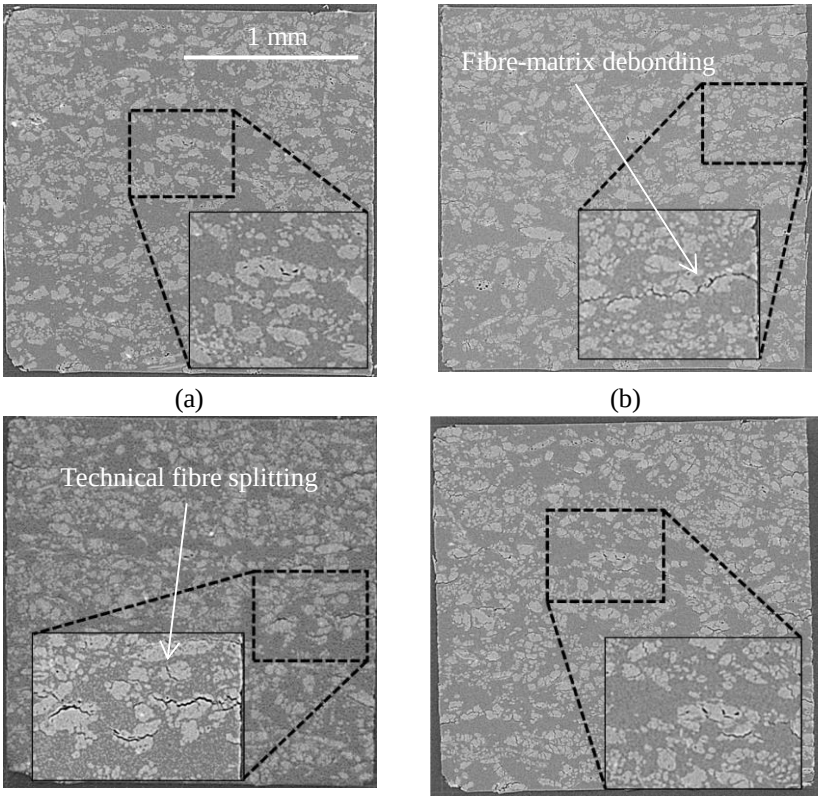

(a) (b) (c) (d)

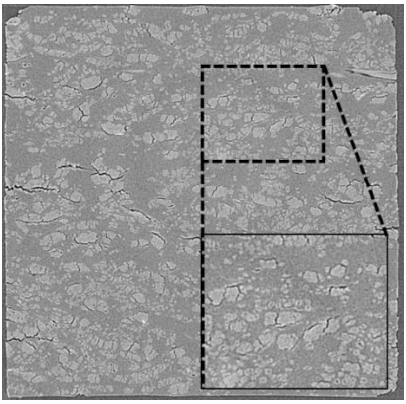

(e)

Figure 6-3: Representative cross-sections captured using µ-CT after 0, 1, 3, 5 and 10 hygroscopic cycles, shown in (a), (b), (c), (d) and (e), respectively. All samples are scanned in oven dry condition. To increase clarity, certain parts of the image were enlarged.

In addition, the flax-epoxy composite also suffered from technical fibre splitting. The elementary flax fibres in a technical fibre are glued together by a relatively weak pectin-based interphase [17–19]. When tensile and shear stresses are generated within such a fibre the interphase fails and this leads to internal decohesion. For this phenomenon to occur the fibre-matrix interface must be strong enough to develop a critical stress state in the fibre itself. This is the reason why flax-epoxy composites suffered from this effect and flax-PP composites did not. The interphase in flax-PP composites is simply too weak to allow significant stresses to develop inside the technical fibres.

Once the fibre-fibre internal crack is initiated the stresses generated during the subsequent cycle will cause it to grow. As the distance over which the debonding region can grow is very limited, it will reach the fibre-matrix interface over the next few cycles. When this occurs, significant stress concentrations will arise at this point which facilitate the initiation of fibre-matrix debonding or matrix cracking, leading to more extensive damage and hence, lower mechanical properties.

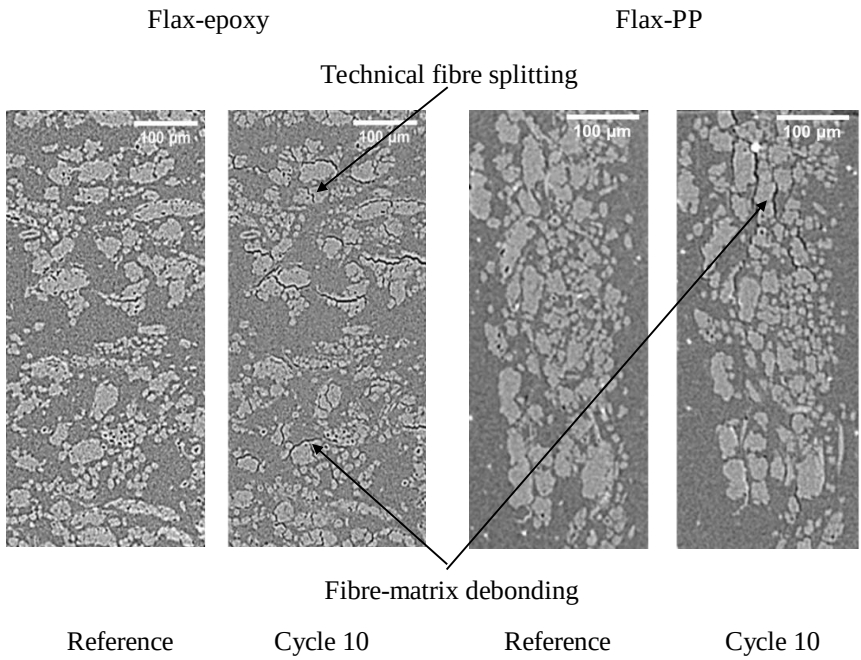

Figure 6-4: µ-CT damage visualization of two composite specimens with a different polymer matrix. After 10 cycles both fibre-fibre debonding and fibre-matrix debonding has developed in the epoxy composite. In contrast, the flax-PP sample only shows fibre-matrix debonding.

b. Damage content & impact on the diffusion coefficient

Damage content of the composites increased linearly with increasing cycle number, representing the extent of technical fibre splitting and/or fibre-matrix debonding. As can be seen in Figure 6-5a, the damage content increased faster for flax-PP which is due to the weak fibre-matrix interface.

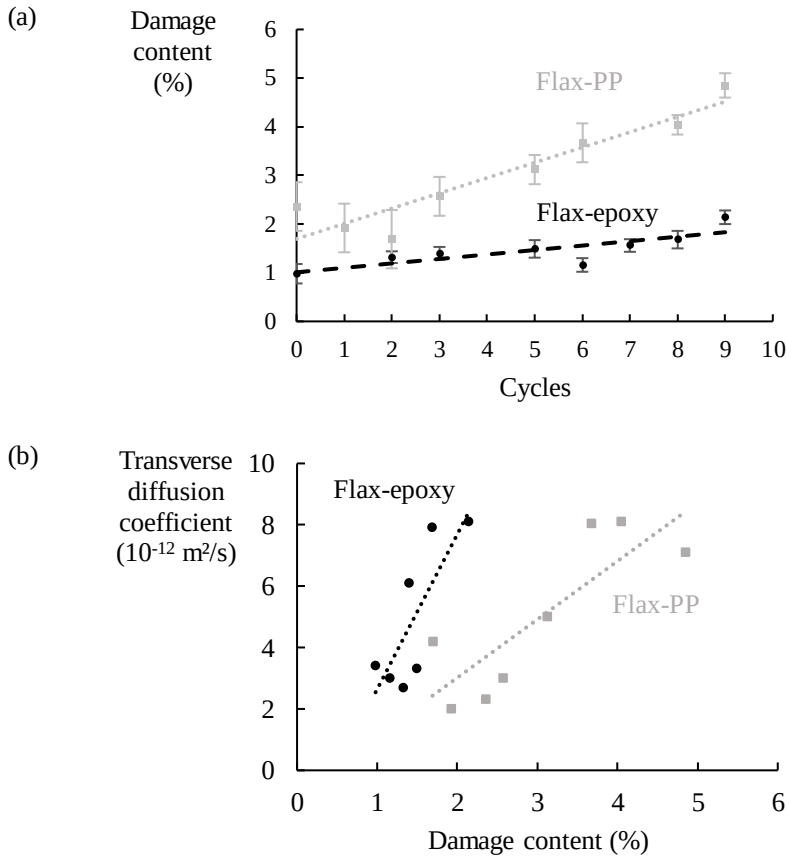

Figure 6-5: (a) Increase of void content with increasing cycle number for the composites. (b) Impact of void content on the transverse diffusion coefficient. The dotted regression lines are only added to highlight the upward trend and do not necessarily reflect the effective relationship between damage content and diffusion coefficient.

The increasing damage content has a direct impact on the transverse diffusion coefficient of the composite, shown in Figure 6-5b. Over the entire cycle range, the diffusion coefficient increased by a factor 2.4 for flax-epoxy and by a factor 3.5 for flax-PP. When debonding occurs, the created defect in the material acts as a diffusion accelerator around that location as the water molecules can diffuse much faster in this confined space, thereby increasing the total diffusivity of the material. Indeed, the inter-diffusivity of gasses is several orders of magnitudes larger than the diffusion in solids. The longitudinal diffusion coefficient in both composites remained constant at 2.4 x 10^{-10} m²/s as the diffusion in this direction is dominated by the fibres. This result also indicates that debonded regions do not form a percolated network through which moisture can diffuse much more rapidly, even after 10 cycles.

6.1.3.3. Mechanical properties

Damage development had a significant effect on the mechanical properties of the composites especially in the transverse direction. In figure 5a and b, a decrease in stiffness and strength can be seen for PP composites already after the first cycle. In this study, a decrease in transverse stiffness can only be caused by a loss in stress transfer capability between matrix and fibres. Hence, fibre-matrix debonding must play a crucial role in the degradation.

Flax-epoxy composites showed greater resistance to hygroscopic stresses. Stiffness and strength declined gradually over the cycles. After 5 cycles, both stiffness and strength remained constant indicating that a critical amount of damage had been accumulated. Further debonding did not lead to a further decrease in mechanical properties. Comparing the values after cycle 9 with the as-produced material the decrease in stiffness reached approximately 45% for both composites whereas strength values were reduced by 55% and 16% for flax-epoxy and flax-PP, respectively. The smaller decrease for flax-PP composites is related to the inherently lower interfacial strength in these composites.

The similar decrease in transverse stiffness for flax-epoxy and flax-PP samples combined with the observation of damage, mainly taking the form of fibre-matrix debonding in the first cycles, lets us conclude that fibre-matrix debonding is the main mechanism that contributed to the degradation of transverse stiffness of the composite. Technical fibre splitting would then only play a secondary role in the degradation process.

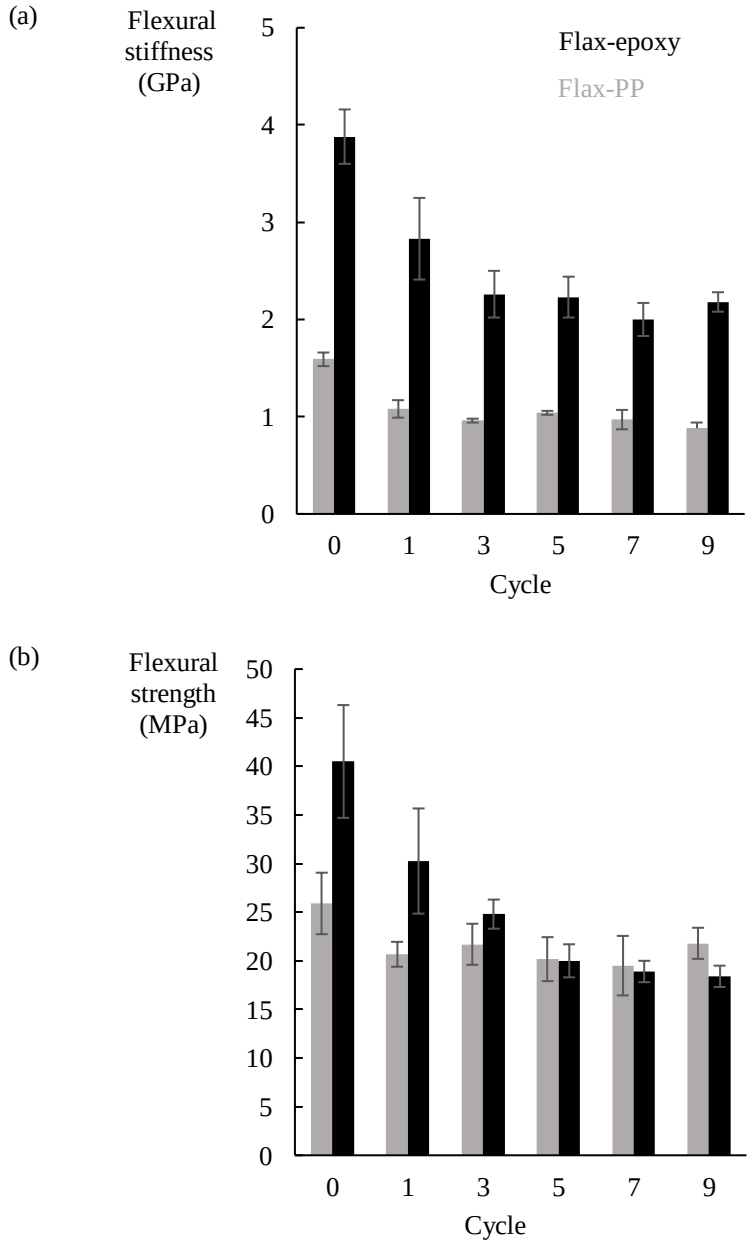

Figure 6-6: (a) Transverse flexural stiffness and (b) transverse flexural strength of the composites with increasing cycle number. (cycle 0 = reference oven-dry state)

In tension, the decrease in composite longitudinal stiffness was less pronounced. This is because the longitudinal stiffness is rather insensitive to defect density. Therefore, no statistically significant evidence was found that the tensile stiffness varied with the number of hygroscopic cycles.

The tensile strength of the composites, however, showed a distinct decrease. After 10 cycles, the relative decrease in strength of flax-epoxy and flax-PP samples was 40% and 35%, respectively. Note that this evolution is different from what was observed in the transverse direction where the strength decreased only up to the fifth cycle (for flax-epoxy) after which it stabilized. The reason for this should be sought in the test set-up itself. In transverse flexion, tensile stresses are generated at the fibre-matrix interface. When fibre-matrix debonding is present in the volume where these stresses are at their highest, the probability that the stress concentration around this debonding will initiate a matrix crack is high as the stress concentration around a hole is larger than when the fibre is bonded to the matrix. Once such a crack is formed, the energy required to propagate the crack in the brittle epoxy matrix is rather small, leading to final failure. It theoretically requires only one debonded region to generate final failure of a composite specimen. Hence, when a certain number of debonded areas are already present in the loaded volume, any additional debonds will not cause the strength to decrease further. Indeed, the probability of having a defect in the highly stressed region does not increase significantly.

In contrast, in longitudinal tension, the interface is not loaded in tension, hence allowing the debonding to propagate along the interface before initiating a fibre break at a weak spot. Subsequently, this fibre break can initiat e a matrix crack, which can then grow through the matrix but only until it meets another fibre-matrix interface. Hence, more energy is dissipated in this process and composite failure will be postponed until a critical number of fibre breaks have accumulated. The more debonded sections that are already present, the faster this critical number will be reached. On the other hand, debonding also lowers the stress concentrations around neighboring fibres by crack tip blunting.

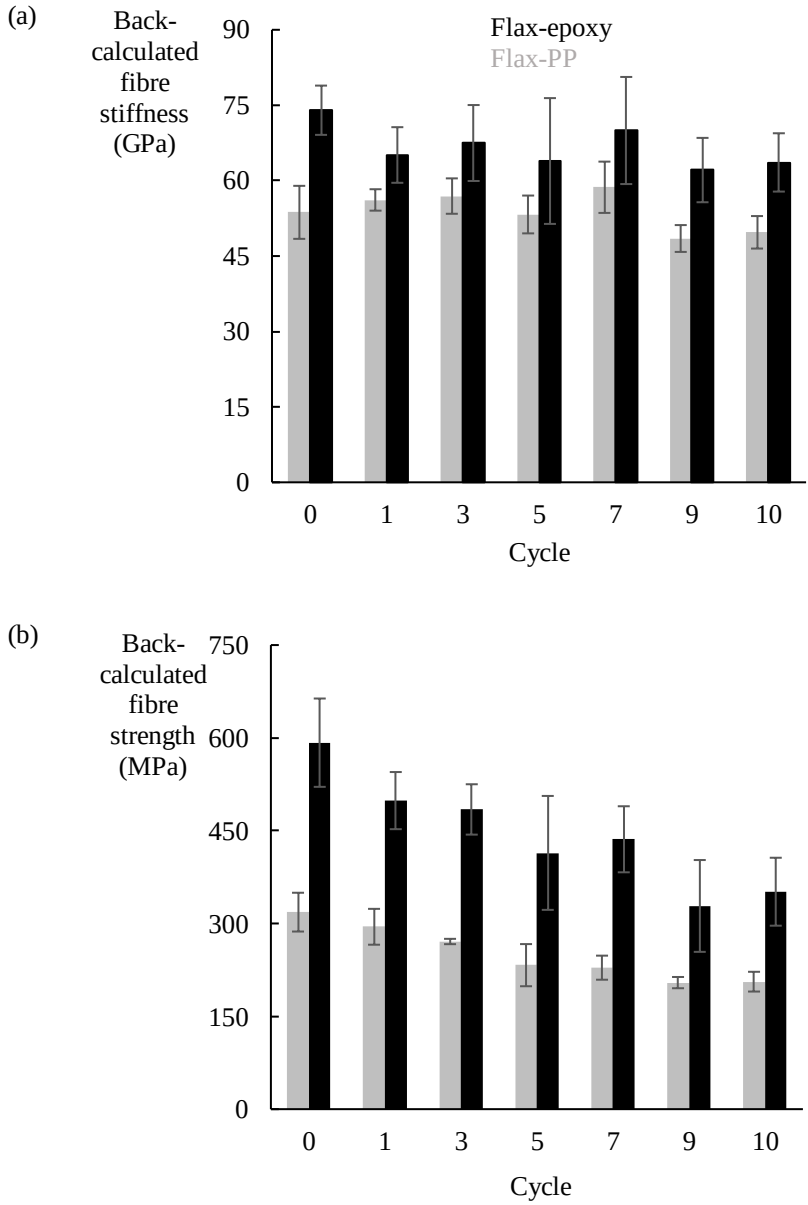

Figure 6-7: (a) Back-calculated longitudinal tensile stiffness and (b) back-calculated longitudinal tensile strength of the composites with increasing cycle number. (cycle 0 = reference oven-dry state)

6.1.3.4. Determination of the fibre's CHE

As described in section 6.1.2.9, hygroscopic swelling of the composites was registered using DIC at the surface of unidirectional composite specimens. When measuring hygroscopic strain in this manner, care should be taken that the

measured strain represents the bulk strain experienced by the entire composite. Figure 6-8 shows the normalized moisture content and hygroscopic strain as a function of the absorption time. Their maximal values were used as the normalization factor. It is apparent that the hygroscopic strain and the moisture content curve approximately overlap. With the former representing a surface property and the latter one a bulk property it must be concluded that the surface hygroscopic strain is a good representation of the bulk hygroscopic strain. Note that although both curves closely agree, they do not overlap entirely. This is because moisture will enter via the surface of the composite resulting in a higher local moisture content compared to the average moisture content in the specimen, hence producing higher surface strains. Furthermore, and more importantly, the overall shape of the curves is also nearly identical, guaranteeing a correct estimation of the CHE.

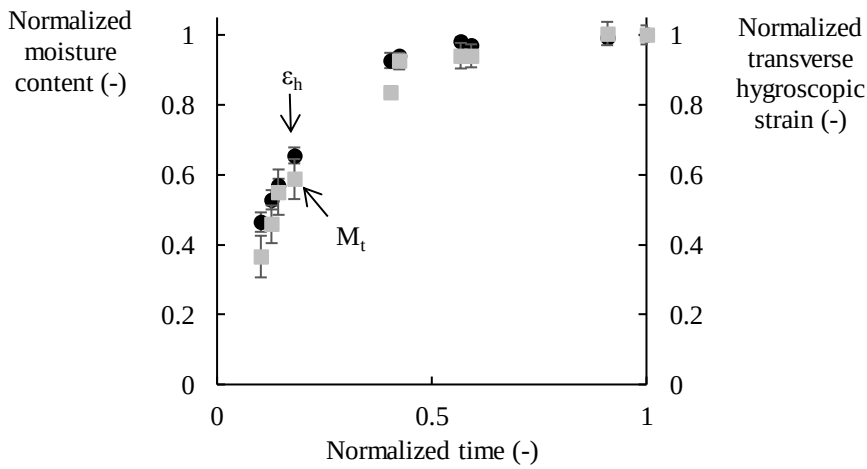

Figure 6-8: Normalized moisture content and hygroscopic strain during moisture sorption of a unidirectional composite specimen as a function of the absorption time.

The hygroscopic strain fields at saturation for pure epoxy and a unidirectional epoxy composite are shown in Figure 6-9a and b, respectively. Neat epoxy exhibited a uniform strain field as it is exposed to a high humidity environment. Upon the addition of flax fibres a peculiar pattern developed that appears to be linked to the orientation of the fibres. Some regions experienced smaller strains while others experienced larger strains. Hypothetically, resin rich zones could experience smaller strains compared to fibre rich zones. However, it was verified that these variations did not correlate with the locations of the fibres that were visible immediately underneath the surface epoxy layer.

Alternatively, a non-flat surface can also result in erroneous strain patterns. The surface roughness of the sample was measured, and the maximum height difference was found to be 8 µm, i.e. too small to have a noticeable effect on the

strain pattern. As a comparison the neat epoxy showed a maximum height difference of 12 µm.

The origin of this pattern remains unclear. Possibly, the strain pattern on the surface is influenced by the volumetric distribution and orientation of fibres in the composite up to a certain depth.

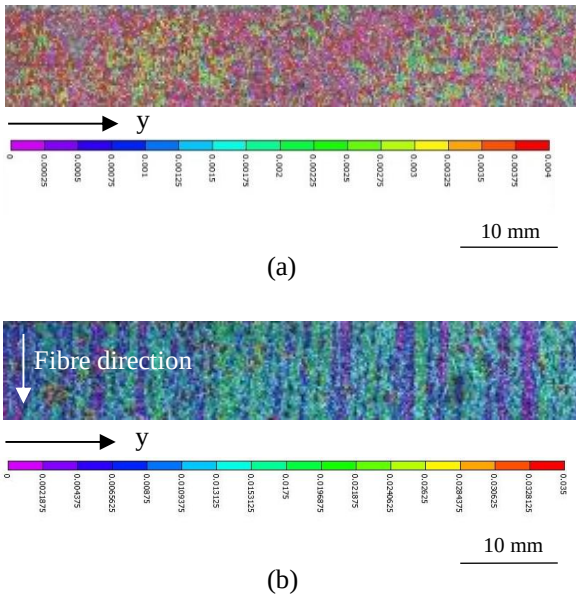

Figure 6-9: Full field strain map in the y-direction of (a) the neat epoxy resin and (b) of a unidirectional flax-epoxy sample.

The discussion in the previous paragraphs does not affect the overall hygroscopic surface strain which is obtained after averaging the full field strain. Therefore, the hygroscopic expansion coefficients of the samples can be calculated with great accuracy. The expansion coefficients of the neat epoxy resin and unidirectional composites, in longitudinal (β_L) and transverse (β_T) direction, can be found in Figure 6-10a and b, respectively. CHE values for the neat resin are lower compared to literature data on similar systems where values between 0.3 and 0.6 are obtained [20–23]. However, every epoxy system reacts differently to moisture, depending on the chemical structure of resin and hardener, and the degree of crosslinking.

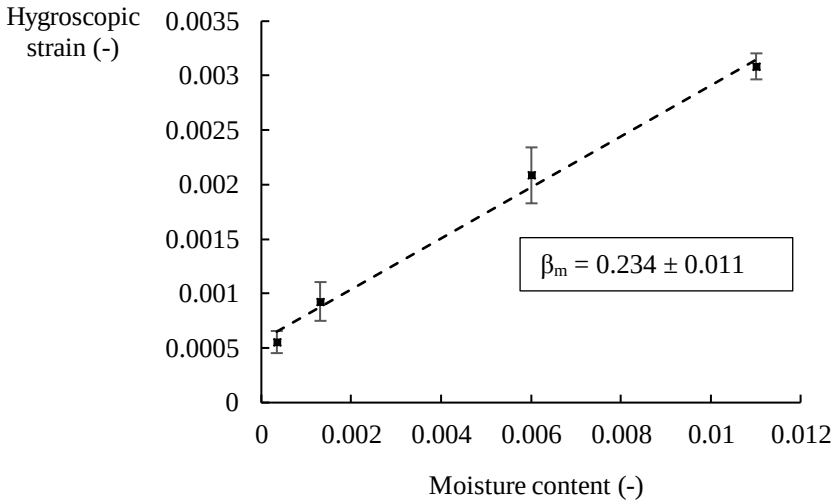

(a)

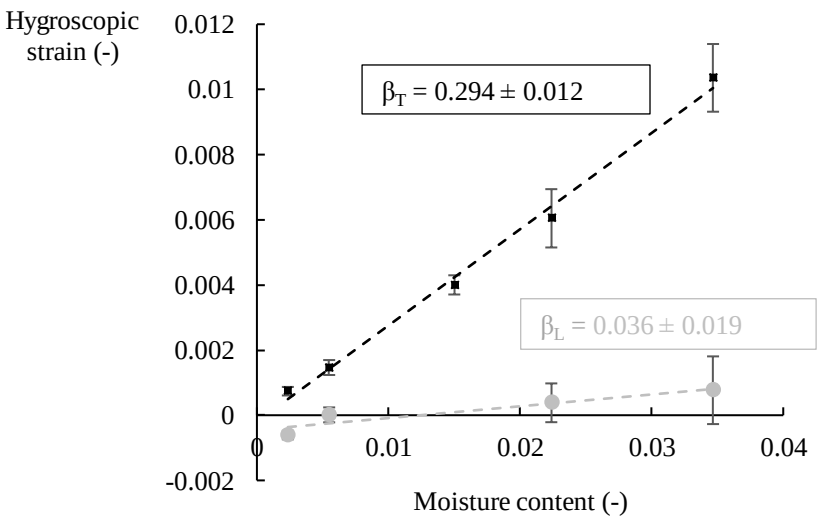

(b)

Figure 6-10: Determination of the CHE of (a) neat epoxy and (b) the unidirectional composite (R^2=0.993, R^2=0.994, R^2=0.874 for β_m, β_T and β_L fits respectively)

According to Springer and Hahn, equation (7) and (8) relate the CHEs of the composite and matrix to the CHE of the fibres [24]. In Table 6-1 the necessary parameters are found in order to perform the back-calculation of the fibre's CHE. Furthermore, the concentration ratio of moisture in the fibre to that in the matrix, c_{fm}, was assumed to be constant and equal to the value at saturation. This ratio can be calculated using equation 9. Density and stiffness variations due to the

absorption of moisture were not considered here. Their values were assumed to be identical to the value at 50% RH and 21°C.

$$\beta_L = \frac{V_f E_{f,L} c_{fm} \beta_{f,L} + V_m E_m \beta_m}{\left(V_f E_{f,T} + V_m E_m\right)\left(V_m \rho_m + V_f \rho_f c_{fm}\right)} \rho_c \tag{7}$$

$$\beta_T = \frac{V_f\left(1 + \nu_{f,TT}\right) c_{fm} \beta_{f,T} + V_m (1 + \nu_m) \beta_m}{V_m \rho_m + V_f \rho_f c_{fm}} \rho_c - \left(V_f \nu_{f,LT} + V_m \nu_m\right) \beta_L \tag{8}$$

$$M_{fm} = \frac{M_{f,\infty}}{M_{m,\infty}} = \frac{M_{c,\infty} \rho_c - V_m M_{m,\infty} \rho_m}{V_f \rho_f M_{m,\infty}} \tag{9}$$

Parameter	Description	Value	
$E_{f,L}$	Fibre modulus in longitudinal direction	59.8 GPa	[25]
$E_{f,T}$	Fibre modulus in transverse direction	5.9 GPa	[26]
E_m	Matrix modulus	2.87 GPa	[27]
V_f	Fibre volume fraction	0.35	This study
V_m	Matrix volume fraction	$1 - V_f$	No voids (lumens are not considered)
c_{fm}	Concentration ratio of moisture in fibre to matrix	6.83	This study
β_m	Matrix CHE	0.234	This study
ρ_c	Composite density	$\rho_c = V_f\rho_f + V_m\rho_m$	
ρ_f	Fibre density	1.4 g/cm³	[25]
ρ_m	Matrix density	1.13 g/cm³	This study
$\nu_{f,TT}$	Transverse poisson coefficient of fibre	0.2	[28]
$\nu_{f,LT}$	Longitudinal poisson coefficient of fibre	0.16	[29]
ν_m	Matrix poisson coefficient	0.3	Estimated
$EMC_m = M_{m,\infty}$	Matrix equilibrium moisture content	0.0129	This study
$EMC_c = M_{c,\infty}$	Composite equilibrium moisture content	0.0430	This study

Table 6-1: Input parameters, necessary for back-calculation of the fibre's CHE.

Back-calculating the CHE of the flax fibres results in a longitudinal CHE, β_{fL}, of 0.0018 and a transverse CHE, β_{fT}, of 0.275. These values correspond well with data found in the literature on the CHE of different wood species [30–32]. For example, European oak (*Quercus Robur*) is characterized by a tangential CHE of 0.28. This is not surprising as the chemical composition of wood is very similar to that of natural fibres such as flax.

Le Duigou *et al.* examined the swelling of elementary flax fibres in an environmental scanning electron microscope [2]. A transverse CHE of 1.14 was obtained for the fibres, which is significantly higher than what is obtained in this

study. The difference may arise for several reasons. Firstly, the experiments by Le Duigou *et al* were performed on elementary fibres whereas the fibres embedded in the composite are technical fibres. However, if this would be the main factor, then the middle lamella would have to severely restrict the swelling of the elementary fibres which is unlikely in view of their low mechanical properties. Secondly, the swelling could be restricted when the fibres are embedded in a matrix material. Joffre *et al.* provided evidence for this in the case of a wood polymer composite, where the CHE of the fibres halved when they were embedded in a polymer when compared to their free state [13]. Nonetheless, additional data on the CHE of elementary and technical flax fibres are needed to verify whether they experience a similar effect.

Finally, the CHE of the epoxy and the unidirectional composites were also determined in desorption. Identical to the absorption case, the hygroscopic strains were linearly dependent on the moisture content of the material. However, both for the epoxy and the composites, the CHE in desorption is smaller than it is in absorption. This hysteretic behavior is unexpected as it is not observed for other natural materials such as wood [33]. Its existence implies that residual strain must be present in the composite throughout the desorption of moisture. One reason that could explain this observation is the fact that hygroscopic strains were measured continuously rather than after equilibrating the samples at a certain moisture content (via RH control) followed by a stepwise reduction in the moisture content. When measuring in a continuous fashion, viscoelastic effects can be present which could prevent the composite from immediately returning to its original state. Hence, the data presented here should be interpreted with caution when comparing with data resulting from stepwise experiments.

6.1.4. Conclusions

Unidirectional flax fibre composites were hygroscopically loaded in cycles in a humid environment in the absence of liquid water. The development of damage, EMC, diffusion coefficients and mechanical properties were monitored for both thermoset (epoxy) and thermoplastic (PP) composites.

EMC measurements confirmed that liquid water was not formed during the cycling of the samples. µ-CT images of the cycled samples showed that fibre-matrix debonding was a dominant mechanism in damage development. For flax-epoxy composites, the higher interfacial adhesion between epoxy and flax fibres led to technical fibres splitting whereas this did not occur for flax-PP composites. As the extent of damage, represented by the void content in the material, rose, the transverse diffusion coefficient of the composites increased and the longitudinal diffusion coefficient remained constant.

The longitudinal stiffness was not influenced significantly by the hygroscopically induced damage which could be expected as the sensitivity of this property to

defects is low. Longitudinal strength decreased gradually over the cycles reaching a value around 60% of the initial strength after 10 cycles.

Transverse mechanical properties exhibited a drastic decrease after a few cycles. After merely 5 cycles the flexural strength of epoxy composites decreased with 60% compared to the value measured immediately after production after which a saturation value is reached. This was attributed to extensive debonding between fibres and matrix.

Finally, the longitudinal and transverse CHE of flax fibre epoxy composites was measured using digital image correlation. From these values an estimation of the fibre's longitudinal and transverse CHE was calculated. It was found that the longitudinal CHE approximated 0 and the transverse CHE was similar to that of most wood species, around 0.28.

References

[1] Scida D, Assarar M, Poilâne C, Ayad R. Influence of hygrothermal ageing on the damage mechanisms of flax-fibre reinforced epoxy composite. Compos Part B Eng 2013;48:51–8. doi:10.1016/j.compositesb.2012.12.010.

[2] le Duigou A, Merotte J, Bourmaud A, Davies P, Belhouli K, Baley C. Hygroscopic expansion: A key point to describe natural fibre/polymer matrix interface bond strength. Compos Sci Technol 2017;151:228–33. doi:10.1016/J.COMPSCITECH.2017.08.028.

[3] Newman RH. Auto-accelerative water damage in an epoxy composite reinforced with plain-weave flax fabric. Compos Part A Appl Sci Manuf 2009;40:1615–20. doi:10.1016/j.compositesa.2009.07.010.

[4] Assarar M, Scida D, El Mahi a., Poilâne C, Ayad R. Influence of water ageing on mechanical properties and damage events of two reinforced composite materials: Flax–fibres and glass–fibres. Mater Des 2011;32:788–95. doi:10.1016/j.matdes.2010.07.024.

[5] Le Duigou A, Davies P, Baley C. Seawater ageing of flax/poly(lactic acid) biocomposites. Polym Degrad Stab 2009;94:1151–62. doi:10.1016/j.polymdegradstab.2009.03.025.

[6] Le Duigou A, Bourmaud A, Davies P, Baley C. Long term immersion in natural seawater of Flax/PLA biocomposite. Ocean Eng 2014:1–9. doi:10.1016/j.oceaneng.2014.07.021.

[7] Le Duigou A, Davies P, Baley C. Exploring durability of interfaces in flax fibre/epoxy micro-composites. Compos Part A Appl Sci Manuf 2013;48:121–8. doi:10.1016/j.compositesa.2013.01.010.

[8] Halpin JC. The Role of the Matrix in Fibrous Composite Structures. Role Polym. Matrix Process. Struct. Prop. Compos. Mater., Boston, MA: Springer US; 1983, p. 3–17. doi:10.1007/978-1-4615-9293-8_2.

[9] Berges M, Léger R, Placet V, Person V, Corn S, Gabrion X, et al. Influence of moisture uptake on the static, cyclic and dynamic behaviour of unidirectional flax fibre-reinforced epoxy laminates. Compos Part A Appl Sci Manuf 2016;88:165–77. doi:10.1016/j.compositesa.2016.05.029.

[10] Summerscales J, Dissanayake N, Virk A, Hall W. A review of bast fibres and their composites. Part 2 – Composites. Compos Part A Appl Sci Manuf 2010;41:1336–44. doi:10.1016/j.compositesa.2010.05.020.

[11] Crank J. The mathematics of diffusion. vol. 1. 2nd ed. Uxbridge: Clarendon Press, Oxford; 1975. doi:10.1016/0306-4549(77)90072-X.

[12] Shen C-H, Springer GS. Moisture Absorption and Desorption of Composite Materials. J Compos Mater 1976;10:2–20.

[13] Joffre T, Wernersson ELG, Miettinen A, Luengo Hendriks CL, Gamstedt EK. Swelling of cellulose fibres in composite materials: Constraint effects of the surrounding matrix. Compos Sci Technol 2013;74:52–9. doi:10.1016/J.COMPSCITECH.2012.10.006.

[14] Hahn HT, Kim KS. Hygroscopic Effects in Aramid Fiber/Epoxy Composite. J Eng Mater Technol 1988;110:153. doi:10.1115/1.3226024.

[15] Hashin Z. Analysis of Properties of Fiber Composites With Anisotropic Constituents. J Appl Mech 1979;46:543. doi:10.1115/1.3424603.

[16] Bledzki AK. The effects of acetylation on properties of flax fibre and its

polypropylene composites. EXPRESS Polym Lett 2008;2:413–22. doi:10.3144/expresspolymlett.2008.50.

[17] Charlet K, Beakou A. Interfaces within flax fibre bundle: Experimental characterization and numerical modelling. J Compos Mater 2013;48:3263–9. doi:10.1177/0021998313508871.

[18] Charlet K, Béakou A. Mechanical properties of interfaces within a flax bundle – Part I: Experimental analysis. Int J Adhes Adhes 2011;31:875–81. doi:10.1016/j.ijadhadh.2011.08.008.

[19] Beakou A, Charlet K. Mechanical properties of interfaces within a flax bundle—Part II: Numerical analysis. Int J Adhes Adhes 2013;43:54–9. doi:10.1016/j.ijadhadh.2013.01.013.

[20] Tsai SW. Composite Design. 3rd ed. Dayton: Think Composites; 1987.

[21] Jacquemin F, Freour S, Guillen R. A Hygroelastic Self-consistent Model for Fiber-reinforced Composites. J Reinf Plast Compos 2005;24:485–502. doi:10.1177/0731684405045014.

[22] Wang S, Choi I. Boundary-Layer Hygroscopic Stresses in Angle-Ply Composite Laminates. AIAA J 1982;20:1592–8. doi:10.2514/3.51223.

[23] Abot JL, Yasmin A, Daniel IM. Hygroscopic Behavior of Woven Fabric Carbon-Epoxy Composites n.d. doi:10.1177/0731684405043548.

[24] Tsai SW, Hahn HT. Introduction to composite materials. 1st ed. Westport: Technomic Pub; 1980.

[25] Bensadoun F, Verpoest I, Baets J, Müssig J, Graupner N, Davies P, et al. Impregnated fibre bundle test for natural fibres used in composites. J Reinf Plast Compos 2017;36:942–57. doi:10.1177/0731684417695461.

[26] Bensadoun F. In-service behaviour of flax fibre reinforced composites for high performance applications. KU Leuven, 2016.

[27] Callens MG, Gorbatikh L, Verpoest I. Ductile steel fibre composites with brittle and ductile matrices. Compos Part A Appl Sci Manuf 2014;61:235–44. doi:10.1016/j.compositesa.2014.02.006.

[28] Salmén L, de Ruvo A. A model for the prediction of fiber elasticity. Wood Fiber Sci 1985;17:336–50.

[29] Baley C. Analysis of the flax fibres tensile behaviour and analysis of the tensile stiffness increase. Compos Part A Appl Sci Manuf 2002;33:939–48. doi:10.1016/S1359-835X(02)00040-4.

[30] Patera A, Derome D, Griffa M, Carmeliet J. Hysteresis in swelling and in sorption of wood tissue. J Struct Biol 2013;182:226–34. doi:10.1016/J.JSB.2013.03.003.

[31] García Esteban L, Gril J, De Palacios De Palacios P, Guindeo Casasús A. Reduction of wood hygroscopicity and associated dimensional response by repeated humidity cycles. Ann For Sci 2005;62:275–84. doi:10.1051/forest:2005020.

[32] Noack D, Schwab E, Bartz A. Characteristics for a judgment of the sorption and swelling behavior of wood. Wood Sci Technol 1973;7:218–36. doi:10.1007/BF00355552.

[33] Patera A, Derome D, Griffa M, Carmeliet J. Hysteresis in swelling and in sorption of wood tissue. J Struct Biol 2013;182:226–34. doi:10.1016/J.JSB.2013.03.003.

Chapter 7

General conclusions

Chapter 7 General conclusions

This dissertation investigated and discussed two main issues responsible for the difficult market penetration of flax fibres in the composite industry. The first is related to the cost of the fibres and can partly be attributed to a costly extraction process oriented towards the production of non-technical textiles. The influence of several extraction processes on the physical and mechanical properties of flax fibres and their composites were therefore studied. In particular, the effect of fibre scutching, hackling, retting, and flax variety on the composite mechanical behaviour was thoroughly investigated. A second problem impeding the full potential of flax fibres is their moisture sensitivity and its effect on their mechanical performance. By gaining knowledge on the diffusion behaviour of moisture in fibres and composites both in single and multi-cycle absorption and desorption, properties were gathered which will allow for predictive modelling of the composite behaviour in humid environments. Two main research objectives were defined:

- to understand the impact of the fibre extraction operations on the physical and mechanical properties of the fibres and of their composites, and
- to characterize the moisture absorption and desorption behaviour both under static and cyclic relative humidity levels, and to establish the influence of moisture on the mechanical properties of the composites.

The following paragraphs summarize the results related to these objectives.

7.1. Fineness and purity

In the first part the effect of fineness and purity of the fibres on the composite properties was discussed. Data on the impact of these properties on the composite behaviour were very scarce in the literature, emphasizing the need to establish reliable data. The effect of fineness and purity was evaluated through single fibre testing and longitudinal and transverse composite tests on unidirectional material. First, a reliable and optimized method was developed for the testing of single fibres. Currently many studies still calculate the fibre strain from the clamp displacement. Although corrections are applied to account for system compliance, it has been shown that this method leads to significant error on the measured fibre modulus. Therefore, a direct strain measurement method was developed to eliminate this issue. Direct strain measurement based on digital image correlation eliminates the effect of slippage because the deformation of the fibre is registered optically. Moreover, compared to traditional single fibre testing, the newly developed method significantly reduces the number of samples needed to obtain a

reliable modulus value. This method was therefore used in the analysis of flax fibre fineness on the properties of the technical fibres.

Next, a fast, automated image analysis method was proposed to determine the projected diameters of the fibres. This diameter then represents the fineness of the fibres. A clear advantage of this technique is that it generates a distribution of the fineness in contrast to techniques such as the airflow method which result in a single fineness number.

Single fibre tensile tests on scutched flax fibres resulted in inconclusive results regarding the effect of fineness on the fibre tensile properties. This is due to the fact that hundreds of tensile tests still need to be performed to obtain a low spread on the resulting modulus, as indicated by other studies. With 50 tests performed, the coefficient of variation of the E-modulus was still more than 50%. Another downside of single fibre tests on technical flax fibres is that the stress transfer to the composing elementary fibres is entirely different from the loading inside a composite material. Hence, it was concluded that single fibre tests do not provide a good estimate of the fibre modulus as it would behave in a composite material. Impregnated fibre bundle tests (IFBT) are preferred; the fibre E-modulus is calculated from the composite properties.

The influence of fineness was however, clearly visible in mechanical tests performed on composite materials. They revealed that longitudinal stiffness and strength of unidirectional composites were not significantly influenced by the fibre fineness. Moreover, it was seen that scutched fibre composites reached modulus values close to what has been observed in the literature on hackled fibre composites. The transverse composite strength was approximately 25% lower for scutched fibres compared to hackled material. Nonetheless, a mild combing operation could improve this property by 20%, again approaching the value of hackled flax fibres. The fibre fineness and transverse composite strength were highly correlated showing particularly negative effects for very coarse fibres. It was hypothesized that weak spots within the middle lamellae cause the strength to decrease in scutched material; the combing operation removes most of these weak spots and increases the strength again. In this way, the weaker spots are replaced by the stronger resin when the fibres are impregnated. This is a promising result as it indicates that mildly combed scutched fibres might perform as well as hackled fibres. Hackling is considered an energy intensive process, also involving some manual labour, and hence contributes considerably to the cost of the fibres. Eliminating this process is expected to lower the costs of the fibres, yarns, and textiles.

The correlation between fibre purity and transverse composite properties was weaker, leading to the conclusion that this is only of secondary importance for scutched fibres, given the high correlation between purity and fineness.

7.2. Variety and retting

If scutching would be retained as the main mechanical extraction process, the influence of variety and retting becomes more important. Indeed, increased impurities after scutching, for example due to incomplete retting, can be rectified by a more severe hackling operation in the traditional process, whereas if the extraction ends with scutching it cannot.

From examining in detail two varieties, Amina and Vesta, no differences could be observed in mechanical properties nor in shape of the stress-strain curve. This is indicative of the fact that current flax fibre varieties do not significantly differ in mechanical properties, a result which was also corroborated in the literature when testing elementary flax fibre from different varieties. Indeed, both the crystalline cellulose content and MFA were found to be very similar for various varieties in previous studies. These two factors are believed to mainly determine the stiffness of flax fibre composites.

The degree of retting impacts the tensile response of the unidirectional composites. The initial stiffness of the fibres is unaltered as this is related to the initial elastic response of the material. However, the tangential stiffness of the latter part of the stress-strain curve decreases with increased degree of retting of the fibres. It is hypothesized that this effect is coupled with the decrease in degree of polymerisation of the structuring polysaccharides, hemicellulose, and pectin, due to the retting, promoting the extent of shearing that occurs when the microfibrils start to reorient. The shearing could either be in the middle lamellae as well as inside the cell walls. This hypothesis is supported by the tensile behaviour of green fibre composites, which show virtually no decrease in tangential stiffness with increasing strain.

Finally, the processing history of the fibres did not influence the longitudinal composite properties significantly as broken, scotched, and hackled fibre all performed quasi-identically in terms of stiffness and strength. These results confirm that fineness did not influence these properties as these different operations resulted in a different fineness of the fibres.

7.3. Insights in moisture diffusion in flax fibres and their composites

A second hurdle for the penetration of flax fibres in composite markets is related to the inherent moisture sensitivity of the fibres. Therefore, a thorough analysis of the kinetic and equilibrium parameters of the moisture absorption and desorption was performed for both fibres and composites.

At the fibre level, it was shown that the diffusion coefficient of both elementary and technical fibres depends on the moisture content of the fibre. The coefficient increased in absorption with increasing moisture content in the fibres up to a certain moisture content (± 7%) and decreased again afterwards. During desorption, the diffusion coefficients continuously decreased with decreasing

moisture content. This evolution was linked to the existence of mobile and immobile water molecules throughout the diffusion process. Furthermore, the diffusion coefficients of the technical fibres corresponded well with the back-calculated values from unidirectional flax-epoxy composites predicted through Hashin's model. The absorption and desorption process in the elementary and technical fibres was shown to follow a Fickian behaviour at all RH values, except for the final desorption stage to fully dry condition. Here, the Carter and Kibler model provided a better fit to the experimental data.

Next, a theory was proposed which describes the diffusion process in technical flax fibres. The role of the middle lamella in this process was highlighted as it was hypothesized to provide a path through which accelerated diffusion is possible. This was corroborated by fluorescence microscopy, which shows preferential diffusion occurs along the middle lamella.

Moisture absorption in composite materials also leads to an intrinsic decrease in properties which was characterized in this study by evaluating the mechanical performance of unidirectional composites. Transverse stiffness and strength as well as longitudinal modulus continuously decreased with increasing moisture content while the longitudinal strength reached a minimum value in dry condition and continuously increased with increasing moisture content. The former was linked to the plasticization effect of water in flax fibres.

To influence the above-mentioned processes and to further deepen the understanding of these processes, crosslinking treatments were performed on the fibres which aimed at eliminating hydroxyl functionalities on the biopolymers by crosslinking them to neighbouring chains. This crosslinking affected the moisture content of the fibres during desorption of moisture, but this effect was absent during absorption. At identical RH levels, the moisture content of the treated fibres was lower during desorption than for untreated fibres. The treatments therefore reduced the hysteresis. It is hypothesized that desorption of moisture in the crosslinked fibres is facilitated by the increase in free volume between the polysaccharide chains by incorporation of the reagents. This was supported by an increase in diffusion coefficients at low relative humidity after crosslinking. Finally, these treatments also influenced the resulting mechanical performance of the composites. The relative decrease in composite stiffness under saturated conditions compared to the dry state was lower for the crosslinked fibres than for the untreated fibres. It was hypothesized that crosslinking leads to an increased stiffness of the hemicellulose and pectin surrounding the microfibrils, elevating their resistance to yielding. Simultaneously, the increased stiffness of the matrix prevents the cellulose microfibrils from reorienting, inhibiting stiffness recovery. The resulting stress concentrations around the fibrils also led to a lower composite strength for the crosslinked fibre composites.

7.4. Impact of hygroscopic fatigue on the composite properties

Whereas the previous part mainly focussed on single cycle moisture absorption or desorption, a more realistic scenario for a composite part is that where it is continuously absorbing and desorbing moisture throughout its lifetime. Therefore, unidirectional flax fibre-epoxy and -PP composites were loaded hygroscopically via cycling between high (80%) and low (0%) relative humidity at elevated temperature (80°C). Importantly, this was done in the absence of liquid water, as this can lead to the manifestation of component leaching and associated difficulties which significantly alter the diffusion process.

µ-CT images of the cycled samples showed that fibre-matrix debonding is a dominant mechanism in the damage development. This is due to significant stresses being generated in this interface region. For flax fibre-epoxy composites which typically exhibit high interfacial adhesion, technical fibre splitting appears as a second damage mechanism. Indeed, as interfacial adhesion between fibre and matrix increases, the internal interphases, i.e. the middle lamellae, are exposed to higher stresses. As it is known that this interphase is weak, technical fibre splitting is likely to occur by failure of the middle lamellae.

When the extent of damage, represented by the void content in the material, rises, the transverse diffusion coefficient of the composites increases while the longitudinal diffusion coefficient remains constant. This indicates that the created damage in the material does not form a percolating network.

Upon the evaluation of composite mechanical properties during cycling it was observed that longitudinal stiffness was not influenced by the number of cycles. Longitudinal strength, transverse strength, and transverse stiffness were however, severely affected. Whereas longitudinal strength decreased only gradually, the transverse properties fell by 40% after a mere 5 cycles. Indeed, during transverse loading the fibre-matrix interfaces are loaded in tension and, hence, play a crucial role in the composite performance.

From the expansion behavior of flax fibre-epoxy composites the hygroscopic expansion coefficients (CHE) of the fibres were derived. For the first time, accurate values for this property were measured. It was found that the longitudinal CHE approximated 0 and the transverse CHE was similar to that of most wood species (± 0.28).

7.5. Scientific and industrial impact of the research

When the knowledge of fineness, purity, and retting is linked to the parameters of the extraction process a large potential for innovations is seen.

A screening protocol to assess the quality of the fibres can be proposed. From the results, it appears that mainly the transverse composite properties are influenced by the fibre fineness. To assess the fibre quality of a batch of flax fibres, tests should be performed to determine this transverse property while also determining

their diameter distribution. Longitudinal testing is of lesser importance as it was seen that, certainly the initial response of the material is independent of variety, fineness, purity, and degree of retting. Nonetheless, it can be implemented as a continuous quality assurance parameter. It is believed that with a substantial amount of data, absolute correlations between fibre fineness and transverse strength should become apparent. Eventually, this could evolve into predictive models where only fibre diameters need to be determined to be able to judge whether a batch of fibres will meet a specific range of transverse properties.

As said previously it is advised to rethink the extraction process of flax fibres in view of their use in composites. However, the required changes very likely have minimal impact on the supply chain of flax fibres as it is established today. Flax fibre extraction in Europe has been severely delocalized over the past decades. All operations that are performed on the fibre, except hackling, are mainly performed in Western Europe. Hackling itself is currently done in low-wage countries due to the manual labour associated with it. Therefore, eliminating the hackling processes as advised in the previous paragraphs, would not disturb process continuity or feed rates, it merely implies a termination of further fibre processing after scutching. Of course, a mild combing and alignment operation remains necessary to produce ‘preforms’ which can be further spun in to yarns and processed further into textiles. However, this is a technical difficulty which can be easily overcome. Although a cost breakdown analysis falls out of the scope of this study, eliminating the hackling process will result in a profound lowering of the market price of flax fibres for composites.

In the second part of the thesis, the description of moisture diffusion in flax fibre composites and its influence on the composite properties also has its significance in terms of valorisation. Indirectly, these results provide a solid framework containing vital parameters to describe moisture diffusion in flax fibre composites. This is a first step in abating hesitance of the industry as they are able to predict both the weight increase in their part as well as its stiffness and strength.

The important role of the middle lamellae in diffusion could also have repercussions on the extraction process. Since the middle lamella form a highway for moisture diffusion, the diffusion coefficient of the composites might be lowered by using finer fibres. However, this again increases cost, resulting in another possible trade off between diffusion rate and fibre cost.

Chemical treatments that were carried out in the scope of this study show the potential of counteracting the intrinsic decrease in stiffness observed by flax fibres in humid environments. However, the use of these chemicals in an industrial setting would have a highly negative impact on the environmental performance of the fibres. Nevertheless, these treatments offer a starting point for alternative routes to increase fibre performance such as genetic modification or enzymatic treatments.

Finally, from the results of cyclic hygroscopic loading of flax fibre composites it is possible to formulate a practical advice. Fluctuations in moisture content of the fibres should be kept minimal. It must, however, be remarked that in longitudinal direction the composite properties are hardly affected by damage which develops in the composites. The main focus therefore should be the transverse properties. Limiting the fluctuations in moisture content can be done by integrating parts in environments with relatively constant humidity or, when this is not possible, by applying semi-impermeable coatings which slow down moisture diffusion significantly. The latter will result in an approximately constant moisture content of the fibres. This advice should be interpreted with caution as it is unsure whether less extreme conditions, for instance a higher minimum relative humidity through the cycles, would also result in damage.

7.6. Future outlook

Some of the results in this work have led to further questions which fell out of the scope of this thesis. Therefore, a selection of topics is presented here which require further investigations or new related topics are proposed that are worthwhile to investigate in the future.

When examining properties such as fineness, purity, and degree of retting of scutched flax, their effect on the unidirectional composite properties can be easily assessed as it requires not too much effort to produce such composites from semi-aligned fibres. However, processing the materials further into yarns and textiles will pose some technical challenges. It is necessary to assess whether these properties influence yarn processing and weaving. Indeed, difficulties in these processes might result in increased costs which would go against the original intention of the research. Next, once such architectures have been produced, the influence of the aforementioned parameters on their properties should be thoroughly investigated as well. Moreover, it was not assessed in this study whether these properties have an effect on the fatigue life, impact strength, shear strength, or other properties of the composites.

The two flax fibre varieties which were examined here were fibre flax varieties. Although much more varieties would need to be studied to produce conclusive evidence that these do not influence the mechanical properties of the fibres, it would be worthwhile to include oil flax varieties in the comparison as well. These fibres might be similar to fibre flax in terms of crystallinity and MFA. And oil flax would as side product from the linseed oil production have much lower price.

Throughout this dissertation, unidirectional composites were studied. Evidently, these systems are the simplest to study, especially when studying complex phenomena such as diffusion. However, this diffusion behaviour might also be affected when textile architectures are considered. For hygroscopic fibres, such as flax, percolation networks can be created in these composites which lead to accelerated diffusion rates.

The damage related to hygroscopic cycling of the composite materials could be severely influenced by the boundary conditions. When using other values of relative humidity and temperature it is not guaranteed that the same mechanisms and extent of damage will be present in the composites. This can only be resolved through experimental design to gather information on the impact of these conditions on the composite.

Finally, transient models should be developed which incorporate the diffusion of moisture in composite materials throughout time. When real fibre geometries, collected by µ-CT visualization, are combined with knowledge of the interdependence between mechanical properties and moisture content of fibres and matrix a leap can be made towards highly predictive models for the response of flax fibre composite structure to various hygroscopic loading conditions.

Curriculum vitae

Kevin Hendrickx
Born August 27, 1991 in Brasschaat, Belgium

Professional experience

2018 - present: INEOS Oxide, Zwijndrecht, Belgium
R&TD / TS&D Engineer

2016 - 2018: The European Confederation of Linen and Hemp (CELC), Paris, France
Technical Consultant and Member of the European Scientific Committee

Education

2014 - 2018: PhD in Engineering Technology
Thesis: Extraction optimisation for and hygroscopic behaviour of flax fibres in composite applications.

2012 - 2014: Master of Materials Engineering (magna cum laude)
Thesis: Investigation of the improvement in mechanical properties of flax fiber epoxy composites using a polymerization condensation reaction

2009 - 2012: Bachelor of Materials Engineering (cum laude)
Thesis: Development of a tensile testing methodology for unidirectional impregnated bamboo fibre bundles

Articles in international refereed journals

- Depuydt D., Vogeler F., Six W., Hendrickx K., Ivens J., Desplentere F., Ferraris E., Van Vuure AW., Printability of natural fibre reinforced polylactic acid (PLA) via fused filament fabrication and performance. (submitted)

- Depuydt D., Balthazar M., Hendrickx K., Six W., Ferraris E., Desplentere F., Ivens J.,Van Vuure, AW., Production and characterization of bamboo and flax fiber reinforced polylactic acid filaments for fused deposition modeling (FDM). Polymer Composites, Advance online publication, 2018.

- Perremans D., Hendrickx K., Verpoest I., Van Vuure AW., Effect of chemical treatments on the mechanical properties of technical flax fibres with emphasis on stiffness improvement. Composites Science and Technology, 160, 216-223, 2018.

- Depuydt D., Hendrickx K., Mehdikhani M., Petrov N., Lomov S., Seveno D., First steps in composite materials for schoolchildren: A STEM educational project. Composites A, Applied Science and Manufacturing, 109, 298-302, 2018.

- Depuydt D.*, Hendrickx K.*, Biesmans W., Ivens J., Van Vuure AW., Digital image correlation as a strain measurement technique for fibre tensile tests. Composites A, Applied Science and Manufacturing, 99, 76-83, 2017.

- Van Vuure AW., Baets, J., Wouters K., Hendrickx K., Compressive properties of natural fibre composites. Materials Letters, 149, 138-140, 2015.

- Hendrickx K., Sitohang R.D.R., Thielemans W., Van Vuure AW., Ivens J., The influence of flax fibre fineness and purity on the mechanical performance of the technical fibres and their composites. (prepared)

- Hendrickx K., Thielemans W., Van Vuure AW., Ivens J., Influence of flax fibre variety, retting conditions and processing on the composite properties. (prepared)

- Hendrickx K., Thielemans W., Van Vuure AW., Ivens J., Kinetic and equilibrium hygroscopic behaviour of flax fibres and their composites. (prepared)

- Hendrickx K., Thielemans W., Van Vuure AW., Ivens J., Decreasing the moisture sensitivity of flax fibre composites through crosslinking treatments. (prepared)

- Hendrickx K., Vranken R., Thielemans W., Van Vuure AW., Ivens J., Development and progression of damage in flax fibre reinforced composites under cyclic hygroscopic loading. (prepared)

Articles in international conference proceedings

- Hendrickx K., Vranken R., Van Vuure AW., Ivens J., Development and progression of damage in flax fibre reinforced composites under cyclic hygroscopic loading. In: Proceedings of the 18th European Conference on Composite Materials (ECCM). Athens, Greece, 24-28 Jun 2018.

- Hendrickx K., Thielemans W., Van Vuure AW., Ivens J., Kinetic characteristics of moisture diffusion in flax fibres and their composites. In: Proceedings of the 3rd International Conference on Natural Fibers (ICNF). Braga, Portugal, 21-23 Jun 2017.

- Hendrickx K., Depuydt D., Van Vuure AW., Ivens J., The relationship between the tensile properties of natural fibres and their UD composites. In: Proceedings of the 17th European Conference on Composite Materials (ECCM). Munich, Germany, 22-26 Jun 2016.

- Hendrickx K., Perremans D., Baets J., Ivens J., Dupont-Gillain C., Verpoest I., Van Vuure AW., Extending the linear elastic response region of flax fibre reinforced polymers using chemical treatments. In: Proceedings of the 2nd International Conference on Natural Fibers. Ponta Delgada (São Miguel), Azores, Portugal, 27-29 Apr 2015.

- Hendrickx K., Romian RD., Goedemé T., Van Vuure AW., Ivens J., Rapid and effective methods for the screening of flax fibres for composite applications. In: Proceedings of the 20th International Conferences on Composite Materials (ICCM). Copenhagen, Denmark, 19-24 Jul 2015.

- Van Vuure AW., Baets J., Wouters K., Hendrickx K., Compressive properties of natural fibre composites. In: Proceedings of the 20th International Conferences on Composite Materials (ICCM). Copenhagen, Denmark, 19-24 Jul 2015.

Abstracts in international conference proceedings

- Hendrickx K., Thielemans W., Van Vuure AW., Ivens J. (2016). Understanding moisture induced degradation in flax fiber composites by innovative and targeted treatments. Presented at the International symposium on Bioplastics, Biocomposites and Biorefining (ISBBB), Guelph, Ontario, Canada, 31 May-03 Jun 2016.

Other contributions

- Hendrickx K., Biosourcing: What are the available reinforcements on the market?. In: Flax & Hemp Fiber Composites, a market reality (pp. 33-44), Paris: JEC Group, 2018.

- Hendrickx K., How do we reliably characterize the mechanical properties of flax & hemp fibers?. In: Flax and Hemp Fiber Composites, a market reality (pp. 47-51), Paris: JEC Group, 2018.

- Hendrickx K., Ziegmann G., Composite manufacturing processes and applications on the market: a combination of knowhow, from producers to manufacturers, to finished product. In: Flax & Hemp Fiber Composites, a market reality (pp. 67-85), Paris: JEC Group, 2018.